Natural and CRISPR-induced genetic variation for plant immunity

Baptiste CASTEL

Thesis submitted to the University of East Anglia for the degree of

Doctor in Philosophy

The Sainsbury Laboratory

February 2019

Abstract

Our understanding of the genetic basis of a trait primarily relies on analysing heritable phenotypic diversity.

For instance, different accessions of *Arabidopsis thaliana* (Arabidopsis) can either be resistant or susceptible to a given strain of *Albugo candida*, an oomycete that causes the white rust disease. The virulent *Albugo candida* race Exeter1 (AcEx1) can grow on most Arabidopsis accessions. Using the resistant Arabidopsis Oy-0, I mapped and cloned the gene responsible for AcEx1 resistance: *White Rust Resistance 4A* (*WRR4A*). Arabidopsis Col-0 also contains *WRR4A* but does not resist AcEx1. I found that $WRR4A^{Col\text{-}0}$ has an early stop codon, which is responsible for the recognition specificity of some effector candidates from *Albugo candida*. This example illustrates how natural diversity can be used to identify *Resistance*-genes and reveal components of the plant immune system.

However, natural diversity is not always available. Clustered and regularly interspaces short palindromic repeats (CRISPR) from bacterial genomes defines an immune system, re-invented for genome editing. I optimized a CRISPR-Cas9 method to generate null alleles in Arabidopsis. Using this method, I produced a double mutant of two immunity-related gene candidates that are in tandem in the genome: *AtNRG1A* and *AtNRG1B*. I confirmed the 7-year-old hypothesis that *NRG1A* and *NRG1B* are redundantly required for signalling downstream of multiple *Resistance*-genes, mainly from the TIR-NLR immune receptor family. So far very few genes required for immunity upon Resistance-protein activation were defined. This second example illustrates that CRISPR can be used to generate variation to unravel redundant genetic pathways.

The widespread adoption of CRISPR tools is likely to lead to a better understanding of the plant immune system. Ultimately, it will result in solutions to deploy genetics-based resistance to protect our crops from disease, reducing the need for chemicals.

Table of contents

Acknowledgments

I feel very fortunate to have completed my PhD at The Sainsbury Laboratory with Professor Jonathan Jones. Jonathan has been a constant source of support, encouragement and novel ideas for the projects. He will remain an example and a source of inspiration for the rest of my scientific career.

I am also grateful for the team members he managed during my PhD. Particularly I would like to thank Dr Volkan Cevik, Dr Pingtao Ding and Dr Laurence Tomlinson for their valuable mentoring. Their professional and talented guidance helped me achieve rapid progress during my first years in the laboratory. Their enthusiasm for science largely contributed to develop my own.

I want to acknowledge all the Albugans for their help and for running such an enjoyable working team: Volkan Cevik, Oliver Furzer, Agathe Jouet, Amey Redkar, Sebastian Fairhead and Dae-Sung Kim. I also want to thank the CRISPRers: Laurence Tomlinson, Lila Grandgeorge, Federica Locci, Ying Yang, Oleg Raitskin and Nicola Patron; and the RRS1/RPS4 team including but not limited to Yan Ma, Pingtao Ding, Hannah Brown, Joanna Feehan, Panos Sarris, Panos Moschou, Sung Un Huh, Bruno Ngou, Zane Duxbury, Billy Taker-Brown, Hailong Guo, Hee-Kyung Ahn and Shanshan Wang.

I would like to thank my secondary supervisor Professor Cyril Zipfel, as well as the committee members Dr Volkan Cevik, Dr Nicola Patron and Professor Wendy Harwood. They have been a precious support for my PhD management.

The supportive team at TSL and JIC greatly facilitated my projects: the SL-JJ and JIC horticultural services, the administration team, the lab support team, the bioinformatics team, the IT support at TSL, the synthetic biology team and the tissue culture team.

Finally, I would like to thank all the people I met in Norwich including my numerous housemates (particularly Sylvain Capdevielle), my TSL, JIC, TGAC/EI, IFR/QIB, UEA mates, my climbing mates, my salsa mates, my couchsurfing mates, my cycling mates, my jiu-jitsu mates, my gym mates, my JIC Recreational Centre and pub mates.

To my family, my master cohort BFP, “Les Jozés” and all these people who made my PhD journey such a wonderful experience, thank you all again.

Major abbreviations

Ac	*Albugo candida*
Avr	Avirulence
c-terminal	Carboxyl-terminal
Cas	CRISPR-associated
CC	Coiled-coil
CDS	Coding sequence
CRISPR	Clustered and regularly inter-spaced palindromic repeat
DSB	Double-strand break
DNA	Deoxyribonucleic acid
Dpi/hpi	Day(s) / hour(s) post-inoculation
EDS1	Enhanced disease susceptibility 1
ETI	Effector-triggered immunity
ETS	Effector-triggered susceptibility
GFP	Green fluorescent protein
HDR	Homology-directed recombination
Hpa	*Hyaloperonospora arabidopsidis*
HR	Hypersensitive Response
KIB	Knock-in breeding
LRR	Leucine-rich repeat
N-terminal	Amino-terminal
NB	Nucleotide binding
NHEJ	Non-homologous end joining
NLR	NB and LRR
NRG1	N-requirement gene 1
OD	Optical density
PAMP	Pathogen-associated molecular pattern
PCR	Polymerase chain reaction
(RT-PCR	Reverse transcription PCR)
(RT-qPCR	Reverse transcription quantitative PCR)
PRR	Pattern recognition receptor
PTI	PAMP-triggered immunity
R	Resistance
RNA	Ribonucleic acid
ROS	Reactive oxygen species
RPP	Resistance to *Hyaloperonospora arabidopsidis*
RPW8	Resistance to powdery mildew 8
SA	Salicylic acid
TIR	Toll, interleukin-1 receptor and many R-proteins
WRR	White Rust Resistance
WT	Wild type

List of publications

Castel B, Ngou PM, Cevik V, Kim DS, Yang Y, Ding P, Jones JDG. 2018. Diverse NLR immune receptors activate defence via the RPW8-NLR NRG1. *New Phytologist*: 10.1111/nph.15659.

Castel B, Tomlinson L, Locci F, Yang Y, Jones JDG. 2019. Optimization of T-DNA architecture for Cas9-mediated mutagenesis in Arabidopsis. *PLoS ONE* **14**: e0204778.

Cevik V, Boutrot F, Apel W, Robert-Seilaniantz A, Furzer O, Redkar A, Castel B, Kover P, Prince D, Holub E, *et al.* 2019. Transgressive segregation reveals mechanisms of Arabidopsis immunity to Brassica-infecting races of white rust (*Albugo candida*). *Proceedings of the National Academy of Sciences* **116**: 2767-2773.

Chapter 1 : General Introduction

1.1 Molecular Plant-Microbe Interactions

1.1.1 The plant immune system

1.1.1.1 Two layers of plant defence

Plants can interact with micro-organisms including fungi, oomycetes, bacteria and viruses. Many are found at the plant surface, forming the phyllosphere in the shoots and the rhizosphere in the roots. Some can penetrate within the plant tissue. They form biological interactions from symbiotic to parasitic. Many cases of beneficial interactions have been reported, such as mycorrhiza and nitrogen fixing symbioses (Oldroyd, 2013). Micro-organisms can also negatively affect plant physiology to promote their own, in so-called pathogenic interactions.

The outcome of such interactions relies on a molecular dialogue between the pathogen and its host (Jones & Dangl, 2006). On the one hand, plants can recognize conserved microbial molecules resulting in pattern-triggered immunity (PTI). On the other hand, pathogens deliver virulence factors, known as effectors, to colonize the plant, feed, reproduce, counteract plant defences and enhance their fitness resulting in effector-triggered susceptibility (ETS). Plants have also evolved intracellular immune surveillance devices, called Resistance (R)-proteins, which recognise effectors, resulting in effector-triggered immunity (ETI). This three-component conceptual framework has been called the zig-zag-zig model (Jones & Dangl, 2006).

1.1.1.2 Pattern-triggered immunity (PTI)

Plants detect apoplastic elicitors via cell surface Pattern Recognition Receptors (PRRs) (Zipfel, 2008). PRRs can be Receptor-Kinases (RKs) or Receptor-like proteins (RLPs). Both harbour an extracellular domain involved in elicitor perception; RKs also have an intracellular kinase domain. Their cognate elicitors are in general conserved pathogen/microbe-associated molecular patterns (PAMPs/MAMPs), such as flagellin and elongation factor thermo unstable (EF-Tu) for bacteria, chitin for fungi or coat protein for viruses (Boutrot & Zipfel, 2017). Some PAMPs are even shared across microbial kingdoms, such as the "necrosis- and ethylene-inducing protein 1"-like proteins (NLPs) that are found

in oomycetes, bacteria and fungi and recognised by the PRR RLP23 (Albert *et al.*, 2015; Lenarčič *et al.*, 2017).

PRRs can also recognise endogenous compounds degraded during pathogen attack, called danger-associated molecular patterns (DAMPs). For instance, some pathogens use polygalacturonases to degrade the host cell wall and facilitate penetration. Polygalacturonases cleave homogalacturonan into oligogalacturonide, which are DAMPs recognised by the PRR WAK1 (Lorenzo *et al.*, 2011).

PRR activation induces ion fluxes, oxidative burst, mitogen-activated protein kinases (MAPKs) activation, changes in gene expression and in protein phosphorylation, receptor endocytosis and callose deposition, resulting in local and systemic resistance (Couto & Zipfel, 2016). In general, PTI is sufficient to prevent infection, but in some cases the pathogen produces effectors to overcome PTI resulting in Effector-Triggered Susceptibility (ETS).

1.1.1.3 Effector-triggered susceptibility (ETS)

Effectors are pathogen-produced molecules contributing to virulence (Cornelis & Van Gijsegem, 2000). Many are delivered inside the plant cell via the Type III Secretion System (T3SS) of bacteria or the haustorium of filamentous pathogens (Cornelis, 2006; Yoshida *et al.*, 2016). For instance, the effector AvrPphB is a bacterial T3SS effector from the bacteria *Pseudomonas syringae* that can cleave host kinases involved in PTI, such as BIK1, PBL1 and PBL2 (Zhang *et al.*, 2010). Some effectors are also delivered into the apoplast (Kamoun, 2006). The oomycete *Phytophthora sojae* can secrete glucanase inhibitors in the apoplast of soybean to block the action of the host glucanases EGaseA and EGaseB, which otherwise degrade the pathogen cell wall (Rose *et al.*, 2002). Beside inhibition of host defence, effectors can target nutritional pathways. One example is the transcriptional hijacking of the rice sugar transporter-encoding gene *SWEET11* by the transcriptional activator-like (TAL) effector PthXo1 from the bacteria *Xanthomonas oryzae* (Chen *et al.*, 2010). These examples illustrate the virulence function of effectors.

1.1.1.4 Effector-triggered immunity (ETI)

Effectors can be recognised by R-proteins, resulting in effector-triggered immunity (ETI). Most of the plant *R*-genes cloned to date belong to a class of immune receptors called NLR (nucleotide binding domain, leucine-rich repeat) (Jones *et al.*, 2016). NLR-encoding genes are also found in genomes of animals and fungi. In plants, their activation results in

induction of PR (Pathogenesis-Related) proteins, salicylic acid (SA) production, transcriptional reprogramming and often leads to cell death at infection sites. This cell death, called the Hypersensitive Response (HR) helps to stop the propagation of the pathogens.

Some effectors can be recognised by non-NLR type of R-proteins. For instance, the effector AvrBs3 from *Xanthomonas campestris* triggers HR in *Nicotiana benthamiana* in presence of the pepper flavin monooxygenases Bs3 (Römer *et al.*, 2013). Thus, Bs3 is an R-protein despite not being an NLR. The small non-NLR R-protein RPW8 is necessary and sufficient for resistance against powdery mildew fungi (Xiao *et al.*, 2001).

1.1.1.5 Beyond the model

Some pathogen elicitors/host protein pairs do not fall in one or the other category. For instance, the PRR Cf-2 from tomato recognises the effector Avr2 from the fungus *Cladosporium fulvum*. Thus, the categorization of this pair within PTI or ETI can be discussed. As Avr2 is an effector, it activates ETI; as Cf-2 is a PRR, it activates PTI. Some models have proposed to replace the dichotomy PTI/ETI by a continuum of immunogenic proteins (Thomma *et al.*, 2011; Cook *et al.*, 2015) or by a nine-category classification (Kourelis & Van Der Hoorn, 2018). The zig-zag-zig (*i.e.* PTI/ETS/ETI) model will be used as a conceptual framework for this thesis, focusing on the ETI mediated by NLRs.

1.1.2 NLRs: Structure

1.1.2.1 Evolution

Since the cloning of the first *R*-gene, Hm1 from Maize, 25 years ago (Johal & Briggs, 1992), 323 other immunity-activating protein have been described so far in plants (Kourelis & Van Der Hoorn, 2018). 191 of them (60.8 %) are NLRs (Kourelis & Van Der Hoorn, 2018). These immune receptors are also found in animals and fungi, although they emerged convergently (Jones *et al.*, 2016). In plants, NLRs emerged before the charophyte-embryophyte separation, *i.e.* before the colonization of the land (Gao *et al.*, 2018; Han, 2018).

Canonical plants NLRs are composed of three domains: (i) an N-terminal Toll, Interleukin 1 receptor, Resistance protein (TIR), Coiled-Coil (CC) or Resistance to Powdery Mildew 8 (RPW8) domain, (ii) a central Nucleotide-Binding adaptor shared by Apaf-1, certain *R*-gene products and CED-4 (NB-ARC) domain followed by a (iii) Leucine-rich repeats (LRR)

domain. Several NLRs show variations such as domain duplication, domain truncation and/or fusion of extra domain. Animal NLRs usually have a NAIP, CIITA, HET-E and TP1 (NACHT) central domain and a pyrin (PYD)) or a caspase recruitment (CARD) N-terminal domain (Jones *et al.*, 2016). Fungal NLRs harbour a central NACHT or NB-ARC domain bordered by variable N-terminal (HeLo-like, Goodbye-like, sesB-like, PNP_UDP or HET) and C-terminal (WD40, Ankyrin or tetratricopeptide repeats) domains. Unlike in animals and plants, none of the 5616 fungal NLRs reported carry LRRs (Dyrka *et al.*, 2014).

Based on their conserved central NB-ARC domain, there are three monophyletic classes of plant NLRs. Interestingly, each class is associated with TIR, CC or RPW8 N-terminal domain. The three classes are thus called TIR-NLRs, CC-NLR and RPW8-NLRs (Shao *et al.*, 2014). Each plant NLR can be assigned to a class based on its NB-ARC domain and independently of its N-terminal domain. For instance the NB-ARC domain of ADR1-L3 from Arabidopsis (*Arabidopsis thaliana*) enables to be classified as an RPW8-NLR although it lacks an RPW8 N-terminal domain (Bonardi *et al.*, 2011; Andolfo *et al.*, 2014). In general, RPW8-NLRs are conserved and low copy number in all angiosperms, TIR-NLRs are diverse and expanded in rosids and CC-NLRs are diverse and expanded in asterids and monocots (Shao *et al.*, 2016). TIR-NLRs are found in charophytes, bryophytes and in the basal angiosperm *Amborella trichopoda* but have been lost in monocots (Shao *et al.*, 2014; Gao *et al.*, 2018).

1.1.2.2 NB-ARC central domains

NLR activity can result in HR. Interestingly, there is homology between a specific region of plant NLRs and the cell death regulators CED-4 (from *Caenorhabditis elegans*) and Apaf-1 (from *Homo sapiens*). This related region is the NB-ARC domain (Van Der Biezen & Jones, 1998a). NB-ARC consists in three subdomains: NB, ARC1 and ARC2 (Takken *et al.*, 2006). Several sequences are highly conserved among NB-ARCs and are crucial in NLR function. These motifs are P-loop (or Walker A), RNBS-A, kinase-2 (or Walker B), RNBS-B, RNBS-C, GLPL, RNBS-D and MHD (Van Der Biezen & Jones, 1998a; Takken *et al.*, 2006; van Ooijen *et al.*, 2008; Shao *et al.*, 2016). For instance, mutations in the RNBS-A, Walker B or MHD motifs of the tomato NLR I-2 (S233F, D283E and D495V respectively) result in autoactive gain-of-function alleles (Tameling *et al.*, 2006). A K207R mutation in the P-loop of the tomato NLR I-2 results in a loss-of-function allele, which is epistatic to the RNBS-A, Walker B and MHD autoactive mutations (Tameling *et al.*, 2006).

1.1.2.3 LRR domain

LRR domains are found towards the C-terminus of NLRs, and additional domains can be found C-terminal to the LRRs. Each repeat consists of 20-29 amino acids including a consensus motif LxxLxLxxN/CxL. LRRs are involved in protein-protein interactions (Kobe & Kajava, 2001). In NLRs, LRRs are structurally irregular with varying repeat lengths and non-canonical LRR motifs (Takken & Goverse, 2012). Two LRR functions are proposed: (i) effector recognition and (ii) maintenance of NLR inactivation in the absence of pathogen (Takken & Goverse, 2012).

1.1.2.4 N-terminal domains

TIR domains

TIR domains are found in plant NLRs and in animal Toll, Toll-like and Interleukin-1 receptors. In both cases, they play a role in immunity; although this function is likely a convergence (Ausubel, 2005). In plants, TIR domains are thought be the signalling domain of TIR-NLRs because their overexpression often causes cell death (Nimma *et al.*, 2017). Dimerization is required for signalling. Structural analysis revealed that the TIR-TIR interaction of the Arabidopsis TIR-NLRs SNC1, RPP1 and RPS4 involves the α-helices A and E (AE interface) and the α-helix D and E (DE interface) (Zhang *et al.*, 2016a). At least for RRS1/RPS4, the integrity of both interfaces is required for cell death induction (Williams *et al.*, 2014; Zhang *et al.*, 2016a). Both AE and DE interfaces are required for signalling of RBA1, a plant TIR-only protein (Nishimura *et al.*, 2016). In animals, TIR-containing protein activation involves TIR-TIR interactions via different interfaces for different proteins (Akira & Takeda, 2004; Nimma *et al.*, 2017).

Since RBA1 is a TIR only protein, its TIR domain is necessarily involved in the direct or indirect recognition of its cognate effector HopBA1, from *P. syringae*. Moreover, the TIR domain of the tobacco NLR N is necessary and sufficient to interact with the p50 viral elicitor (Burch-Smith *et al.*, 2007). This indicates that TIR domains are not only involved in signalling but can also play a role in effector recognition.

The TIR domain of the mammalian protein SARM1 has intrinsic enzymatic activity (Essuman *et al.*, 2017). It directly degrades NAD (Nicotinamide adenine dinucleotide) resulting in axonal degeneration. The glutamic acid E642 is conserved between SARM1, other TIRs and other NADases and is required for SARM1 function. A glutamate at this position is required for function of RPS4 (Swiderski *et al.*, 2009; Sohn *et al.*, 2014). Bacterial

and archaeal TIR domains also have an NADase activity (Essuman *et al.*, 2018). Whether plant TIR domains have intrinsic enzymatic activity is not known.

CC domains

Coiled-coil domains are found in various proteins such as leucine zipper transcription factors, tropomyosin and plant R-proteins. They comprise two or three α-helixes folded to form a superhelix. One of their features is to be able to form homo- and hetero- dimers or oligomers (Lupas, 1996). For example, the CC domains of MLA10 from barley and ZAR1 from Arabidopsis can form homomultimers, an association required to trigger cell death (Maekawa *et al.*, 2011; Baudin *et al.*, 2017). The CC domain of the maize NLR Rp1 also induces cell death in *N. benthamiana* (Wang *et al.*, 2015a). Like the TIR domains, NLR CC domains can be involved in cell death signalling.

An EDVID motif has been identified in CC domains of NLRs (Rairdan *et al.*, 2008). At least in the CNL Rx from potato, the EDVID motif is involved in interaction with the NB-ARC domain. Correspondingly, the CC domain of Rp1 can interact with the NB-ARC domain, suppressing the CC-induced cell death (Wang *et al.*, 2015a).

In addition, some CC domains have been shown to interact with other proteins. For example, the CC domains of RPS5 from Arabidopsis can interact with its guardee PBS1 (Ade *et al.*, 2007) and the CC domain of MLA10 can interact with some WRKY transcription factors (Shen *et al.*, 2007). The CC domain of the wheat NLR Lr10 is under diversifying selection and therefore thought to be involved in effector recognition (Loutre *et al.*, 2009).

NLR CC domains can interact with themselves, other CC domains, other subdomains from the NLR, different endogenous proteins and perhaps with effectors. This suggests that there may be not a single model but several modes of signalling.

RPW8 domains

RPW8 was first characterised as a small *R*-gene involved in powdery mildew resistance (Xiao *et al.*, 2001). Arabidopsis accession Ms-0 contains two functional paralogs: *RPW8.1* and *RPW8.2*, absents in the susceptible accession Col-0. Instead, Col-0 contains four paralogs: *HR1*, *HR2*, *HR3* and *HR4*. They quantitatively contribute for a weak immune response to powdery mildew, although Col-0 remains largely susceptible (Berkey *et al.*, 2017). During infection, RPW8 is targeted to the extra-haustorial membrane, likely directed by a predicted signal anchor at its N-terminus (Wang *et al.*, 2009).

Some NLRs have an N-terminal domain that resembles RPW8. Although RPW8 may have a coiled-coil structure, the RPW8-NLR clade is not contained in, but sister to the CC-NLR clade (Xiao *et al.*, 2001; Shao *et al.*, 2014). RPW8 domains are also characterised by the absence of an EDVID motif in their N-terminal domain (Collier *et al.*, 2011). The most characteristic motifs of RPW8-NLRs are found in the NB-ARC domain. Their RNBS-B is often LV(T/V)SR, while it is often xxTTR in TIR- and CC-NLRs (Shao *et al.*, 2016).

Compared to the *TIR-NLRs* and *CC-NLRs*, the *RPW8-NLR* genes have not expanded intensively (Zhang *et al.*, 2016b). For instance, in Arabidopsis, only five genes encode a RPW8-NLR: *ADR1*, *ADR1-L1*, *ADR1-L2*, *NRG1A* and *NRG1B*.

1.1.3 NLRs: Activation

1.1.3.1 Effector recognition

NLR activation is initiated after direct or indirect effector recognition. For example, in Arabidopsis the recognition of ATR1 effector (from the oomycete *Hyaloperonospora arabidopsidis*, *Hpa*, the cause of downy mildew) was shown to be the consequence of a direct interaction with the TIR-NLR RPP1 (Krasileva *et al.*, 2010).

On the other hand, the 'guard model' explains how NLRs can recognise indirectly an effector (Van Der Biezen & Jones, 1998b; Dangl & Jones, 2001). For example, the CC-NLR ZAR1 from Arabidopsis can trigger ETI after recognition of the effectors AvrAC, HopF2a (both from *P. syringae*) or HopZ1a (from the bacteria *Xanthomonas campestris*) (Lewis *et al.*, 2013; Wang *et al.*, 2015b; Seto *et al.*, 2017). However, neither AvrAC nor HopZ1a can directly interact with ZAR1. In fact, ZAR1 'guards' intermediate Receptor-Like Cytoplasmic Kinases (RLCKs). HopZ1a can acetylate the RLCK ZED1, which activates ZAR1 (Lewis *et al.*, 2013). AvrAC can uridylylate PBL2 triggering its recruitment by a pre-complex formed by ZAR1 and the RLCK RKS1 (Wang *et al.*, 2015b). The RLCK ZRK3 is required for HopF2a recognition by ZAR1 (Seto *et al.*, 2017).

Avirulence factors such as AvrAC, HopZ1a and HopF2a are recognized and prevent infection. Unless they contribute to virulence in the absence of their cognate R-protein, they should be under negative selection pressure in pathogen genomes. Their conservation is consistent with the 'decoy hypothesis' (van der Hoorn & Kamoun, 2008). Decoys are host proteins that evolved, from an effector target or any host gene, to mimic an effector target, so that they can recognize an effector action and enable ETI. For

instance, PBL2 is a paralog of BIK1, which is uridylylated by AvrAC to suppress immunity. PBL2 mimics BIK1, acting as a decoy target of AvrAC to triggers immunity via ZAR1 (Wang *et al.*, 2015b). The decoy terminology implies (i) that recognized effector has a virulence function in the absence of cognate R-protein and (ii) that the decoy protein, unlike the authentic effector target, does not contribute to virulence (van der Hoorn & Kamoun, 2008). Since AvrAC promotes infection in the absence of ZAR1, PBL2 or RKS1 and PBL2 uridylylation does not contribute to virulence, PBL2 is a good example of a decoy in Arabidopsis. Another is Pto, which is guarded by the tomato NLR Prf and mimics the AvrPto target FLS2 (van der Hoorn & Kamoun, 2008).

1.1.3.2 Effector-independent activation

Gain-of-function NLR alleles have been characterized in Arabidopsis. They constitutively activate ETI responses such as cell death and *PR* gene activation. They enable to study NLR signalling without the use of an exogenous effector.

For instance, suppressor screens of *npr1* (which lacks expression of *PR* genes) revealed gain-of-function alleles of the TIR-NLR encoding genes *SSI4* and *SNC1* (Li *et al.*, 2001; Shirano *et al.*, 2002). Many NLR encoding genes were identified in an EMS mutagenesis screen for *chilling sensitive* (*chs*) mutants (Schneider *et al.*, 1995). These mutants grow normally at 22 °C but show ETI-like responses at 16 °C. *CHS1* encodes a TIR-NB protein, *CHS2* encodes the TIR-NLR RPP4 and *CHS3* encodes a non-canonical TIR-NLR having an extra C-terminal LIM domain (Huang *et al.*, 2010; Yang *et al.*, 2010; Wang *et al.*, 2013a). All three are gain-of-function mutations. The reason why some R-proteins are activated at cold temperature is unclear. *chs3-1* renders the plant more resistant to a freezing treatment (-6 °C for two to four hours) compared to wild type (Yang *et al.*, 2010). This suggest that NLRs can play a role in freezing tolerance, independently of their role in plant-pathogen interaction. A suppressor screen of *chs3-2D*, another gain-of-function allele of *CHS3*, identified the TIR-NLR CSA1 as required for CHS3 function (Xu *et al.*, 2015). Similarly, the activity of CHS1 requires the TIR-NLR SOC3 (Zhang *et al.*, 2016c). SOC3 and CHS1 are also known to guard the homeostasis of the E3 ligase SAUL1, which might be a pathogen target (Tong *et al.*, 2017). SOC3 pairs with CHS1 to guard the absence of SAUL1 function and pairs with TN2 to guard the over-activity of SAUL1 (Liang *et al.*, 2018b).

Autoimmune phenotypes have also been observed in crosses between wild type plants resulting in hybrid necrosis. For example, *DM1* (a wild type allele of the TIR-NLR *SSI4*) was identified as incompatible with *DM2d* (a wild type allele of the TIR-NLR *RPP1*) (Chae *et al.*,

2014). A cross between the accession Uk1 and Uk3 carrying one or the other of these alleles results in hybrid necrosis. The study of incompatible *R*-gene loci also revealed incompatibility between some alleles of RPW8 and some other alleles of the CC-NLR RPP7 (Chae *et al.*, 2014).

Characterization of autoimmune phenotype can be misleading. CAMTA3 is a transcription factor that can bind the promoter of some defence-related genes such as *EDS1* (Du *et al.*, 2009). Since the *camta3* mutant displays an autoimmune phenotype and many ETI marker genes are upregulated in the mutant, it was proposed that CAMTA3 is a transcriptional repressor of these ETI-related genes (Galon *et al.*, 2008; Prasad *et al.*, 2016). In fact, CAMTA3 activity is guarded by the TIR-NLRs DSC1 and DSC2. The phenotype and the gene activation observed are the result of the DSC1 and DSC2 activation rather than the loss of transcription activity of CAMTA3 (Lolle *et al.*, 2017).

1.1.3.3 NLR pairs

Several plant NLRs have been found to work in pairs, with both proteins required for signalling. For instance, SOC3 and CSA1 are required for the signalling of CHS1 and CHS3 (Xu *et al.*, 2015; Zhang *et al.*, 2016c). In Arabidopsis accession Ws-2, RRS1/RPS4 form another TIR-NLR pair required for the recognition of the effectors AvrRPS4 and PopP2, from the bacteria *Pseudomonas* and *Ralstonia* respectively (Narusaka *et al.*, 2009). Its paralog pair RRS1B/RPS4B also recognises AvrRPS4, but not PopP2 (Saucet *et al.*, 2015). Interestingly, the functional pairs CHS3/CSA1, CHS1/SOC3, RRS1/RPS4 and RRS1B/RPS4B also form physical pairs in the genome, linked in a head-to-head orientation (Narusaka *et al.*, 2009). There are other TIR-NLR pairs found in a head-to-head orientation in Arabidopsis, but they have not been functionally characterized. The TIR-NLR-paired encoding genes constitute two monophyletic groups (Andolfo *et al.*, 2014). This indicates that the current TIR-NLR pair repertoire is the result of duplication events from an original pair. Some CC-NLR genetic and functional pairs have also been described such as Pik-1/Pik-2 and RGA4/RGA5 in rice, involved in the recognition of AVR-Pik and AVR1-CO39 from the blast fungus *Magnaporthe oryzae* (Kanzaki *et al.*, 2012; Cesari *et al.*, 2013).

Some genes have been shown to function in pairs without being clustered in a head-to-head orientation. *RPP2A* and *RRP2B* encode two TIR-NLRs both required for resistance against *Hpa* race Cala2 and are clustered in a head-to-tail orientation (Sinapidou *et al.*, 2004). *RPW8* and the CC-NLR encoding cluster *RPP7*, as well as some *SSI4* and *RPP1* alleles, are involved in hybrid necrosis, indicating that they can induce immunity as a pair (Chae

et al., 2014). However, they are physically unlinked. The TIR-NLR N from tobacco confers resistance to TMV, and requires the RPW8-NLR NRG1 but their encoding genes are not linked in the tobacco genome (Peart *et al.*, 2005). Roq1 and RPP1 are unrelated TIR-NLRs that also require NRG1 to signal (Qi *et al.*, 2018). Similarly, the unrelated NRLs RPS2, RPP4, SNC1, UNI-1D, CHS3 and RPP1 require function of ADR1 to signal. ADR1s are RPW8-NLRs from the sister clade of NRG1 (Bonardi *et al.*, 2011; Dong *et al.*, 2016).

1.1.3.4 Sensor and helper NLRs

The requirement of an NLR by several NLRs is explained by the "sensor-helper" model (Bonardi *et al.*, 2012). Some diverse NLRs "sense" the infection and are "helped" by an NLR which executes the immune response. ADR1 and NRG1 are two examples of helper NLRs.

Similarly, NRC proteins are CC-NLR helpers in Solanaceae (Wu *et al.*, 2016). They redundantly contribute to the resistance mediated by the sensor NLRs Rpi-blb2, Mi-1.2, Sw5b, R8, R1, Prf, Rx and Bs2 (Wu *et al.*, 2017). Interestingly, all these NRC-dependent sensors are part of a monophyletic group that emerged over 100 Mya and is broadly distributed among Asterids. Since the NRC helper clade and the NRC-dependent sensor clade are monophyletic, they form a network expanded from a single sensor-executor pair. The sensor clade is more diversified than the NRC clade. Sensors have expanded to recognize effectors from many pathogens and helpers are more constrained as immune signalling nodes (Wu *et al.*, 2017).

In Arabidopsis, DM1 (an allele of SSI4 from Arabidopsis accession Uk-3) and DM2d (an allele of RPP1 from Arabidopsis accession Uk-1) can interact to trigger HR (Tran *et al.*, 2017). DM1- and DM2-related NLRs might constitute a local sensor-executor network within Arabidopsis.

1.1.4 NLRs: Signalling

1.1.4.1 Conformational change model

The NB-ARC domain belongs to the superfamily of nucleotide-binding domains signal transduction ATPases with numerous domains (STAND), which also includes NACHT from animal NLRs (Leipe *et al.*, 2004). The STAND protein MalT from *Escherichia coli* was used to describe the ADP/ATP switch model. MalT switches between an ADP-bound resting form and an ATP-bound active form that oligomerises. The ATPase activity of MalT is not

required for transcription activation. In fact, the Walker B hydrolyses ATP to ADP to reset MalT into its ADP-bound off state (Marquenet & Richet, 2007). It was proposed that this model could apply for all STAND proteins. Structural data of the NB-ARC protein Apaf-1 supports this model and indicate that the P-loop is involved in nucleotide binding (Cheng *et al.*, 2016). In plant NLRs, P-loop mutants are in general loss-of-function and Walker B mutants are in general autoactive (Zhang *et al.*, 2017). It supports the idea that P-loop is involved in ATP binding and required to switch to the active form, while Walker B is involved in ATP hydrolysis required to switch back from active to ADP-bound inactive form. So far there are no structural data available to confirm this model for plant NB-ARCs.

The effectors PopP2 and AvrRps4 interact with the C-terminal of the Arabidopsis NLR RRS1, resulting in activation of immunity (Ma *et al.*, 2018). Similarly, the C-terminal domain of the NLRs RPP1 (from Arabidopsis) and Roq1 (from *N. benthamiana*) physically interacts with the cognate effectors ATR1 (from *Hpa*) and XopQ (from *Xanthomonas*) to trigger immunity (Krasileva *et al.*, 2010; Qi *et al.*, 2018). On the other hand, TIR, CC and RPW8 domains are in general sufficient to activate an immune response on their own (Bernoux *et al.*, 2011; Collier *et al.*, 2011; Bai *et al.*, 2012). Thus it was proposed that, for plant NLRs, the C-terminal domain is involved in sensing, NB-ARC is involved in switching via conformational change and the N-terminal domain is involved in signalling (Collier & Moffett, 2009). For the Solanaceae NLRs N and Rx, elicitor sensing is regulated by the N-terminal domain (Burch-Smith *et al.*, 2007; Rairdan *et al.*, 2008), indicating that pathogen detection by NLRs is more complex than in this proposed model. The signalling role of the N-terminal domain is clearly established for all the mammalian NLRs described so far (*e.g.* NLRP1, NLRP3 and NLRC4) (Lechtenberg *et al.*, 2014; Broz & Dixit, 2016), the fungal NLR NWD2 and PLP-1 (Riek & Saupe, 2016; Heller *et al.*, 2018) and for many plant NLRs including RPS4, RPP1, At4g19530, NRG1, ADR1, MLA10, Rx and RPS5 (Ade *et al.*, 2007; Rairdan *et al.*, 2008; Swiderski *et al.*, 2009; Maekawa *et al.*, 2011; Collier *et al.*, 2011).

1.1.4.2 In animals and fungi

Animal NLRs

Animal NLRs can initiate an immune response often culminating in a form of regulated programmed cell death (PCD) called pyroptosis, which resembles the plant HR (Duxbury *et al.*, 2016).

Pyroptosis is driven by specific caspases (*e.g.* caspases 1, 4 and 5 in humans) and initiated by inflammasomes (Vande Walle & Lamkanfi, 2016). At least three NLRs can form

inflammasomes upon activation: NRLP1, NLRP3 and NLRC4. They exist as monomeric surveillance devices in the cytosol. After recognition of an effector from the bacteria *Bacillus anthracis* for NLRP1, a Type 3 Secretion System (T3SS) subunit or flagellin for NLRC4 (the stimulus of NLRP3 is not known), they oligomerize to form a ring-shape complex: the inflammasome (Broz & Dixit, 2016). The inflammasome activates inflammatory caspases, resulting in the cleavage of gasdermin D. The N-terminal fragments of gasdermin D oligomerize at the plasma membrane to form pores (Liu *et al.*, 2016b). This plasma membrane permeabilization characterises the pyroptosis but is also observed during necroptosis but not during apoptosis (Vande Walle & Lamkanfi, 2016). Similarly, Apaf-1 can oligomerize after cytochrome *c* activation to form a ring-shaped apoptosome (Zhou *et al.*, 2015).

Fungal NLRs

Fungi can recognise non-self during cell fusion between two genetically distinct individuals and respond with cell death. This rejection is called heterokaryon incompatibility and is genetically controlled by *het* (*heterokaryon incompatibility*) loci. Interestingly, some HET proteins (*e.g.* HET-D, HET-E, HET-R, NWD2) are NLRs with an N-terminal HET domain (Paoletti & Saupe, 2009).

The NWD2/HET-S system is one of the best-described incompatibility system in fungi (Daskalov & Saupe, 2015; Riek & Saupe, 2016). NWD2 is an NLR with an N-terminal HET domain, a central NACHT domain and a C-terminal WD-repeats domain. HET-S is a non-NLR two-domain protein with an N-terminal executor HeLo domain and a C-terminal prion forming domain. The prion-forming domain can adopt an amyloid β-solenoid fold (prion form) leading to a refolding of the HeLo domain which then acquires a toxic pore-forming activity at the plasma membrane. The amyloid templating of HET-S can be induced independently by [HET-s], an incompatible allele of HET-S that lacks the pore-forming activity, or the NLR NWD2. When activated by a specific ligand at the WD40 repeats region, NWD2 induces the prionisation of HET-S that leads to the pore-forming activity of its HeLo domain. This system illustrates the role of an NLR in a PCD-mediated defence strategy in fungi. Similarly, the fungal NLR PLP-1 triggers cell death upon recognition of SEC-9 alleles from incompatible strains (Heller *et al.*, 2018).

PNT1/HELLP is a *Chaetomium globosum* pair, homolog of NWD2/HET-S (Daskalov *et al.*, 2016). Like HET-S, HELLP has a HeLo N-terminal domain, can form amyloid fibrils, is membrane-targeted and has a cell death-inducing activity. The HeLo executor domain of

HELLP and HET-S shares sequence similarities with RPW8 and NRG1 from plants (Daskalov *et al.*, 2016). This suggests that RPW8 and/or RPW8-NLRs might trigger HR via a related pathway.

1.1.4.3 In plants: Downstream signalling

Plant NLR-mediated resistance requires many proteins and hormones. NDR1 and EDS1 are two important proteins acting downstream of NLRs (Glazebrook *et al.*, 1997). CC-NLR signalling is often dependent on NDR1 while TIR-NLR signalling is often dependent on EDS1 (Century *et al.*, 1995; Parker *et al.*, 1996). The apparent specific requirement of EDS1 by TIR-NLRs and NDR1 by CC-NLRs is not strict. For instance, EDS1 regulates RPP8- and RPS2-mediated immunity, redundantly with SID2 (Venugopal *et al.*, 2009).

EDS1 is a nucleocytoplasmic lipase-like protein, which interacts with its sequence-related partners PAD4 or SAG101 (Wagner *et al.*, 2013). The mechanism of EDS1 has not been fully solved yet. It can be required for ROS burst, HR, gene induction and SA accumulation (Wiermer *et al.*, 2005; Cui *et al.*, 2017, 2018). PAD4 and SAG101 interact with EDS1 at the same interface, suggesting co-existence of both EDS1-PAD4 and EDS1-SAG101 complexes (Wagner *et al.*, 2013).

NDR1 plays a role in the plasma membrane/cell wall adhesion during infection (Knepper *et al.*, 2011). It regulates expression of genes from *LEA* and *PIP* gene families. LEA and PIP proteins control fluid loss and entry, suggesting a role of NDR1 in electrolytes leakage during infection (Knepper *et al.*, 2011).

1.1.4.4 In plants: Phytohormone signalling

Some plant hormones, such as jasmonic acid (JA), Salicylic Acid (SA) and Ethylene (ET) are reported to regulate plant immunity (Bari & Jones, 2009). Typically, SA is associated with resistance against biotrophic / hemibiotrophic pathogens, whereas JA and ethylene are associated with resistance against necrotrophic pathogens (Buscaill & Rivas, 2014).

SA is a positive regulator of plant immunity. SA treatment in tobacco enhances resistance to TMV while overexpression of NahG, encoding a salicylate hydroxylase that catabolizes SA, compromises immunity (Durner *et al.*, 1997). SA accumulates at infection points but also contributes to systemic resistance. Accumulation in non-infected tissues mediates and enhances a long-lasting resistance to secondary pathogen challenge, called Systemic Acquired Resistance (SAR) (Durrant & Dong, 2004). NPR1 is the central protein required for SAR and its activity is regulated by SA (Yan & Dong, 2014). The related proteins NPR3

and NPR4 are also SA receptors. In high SA, NPR1 interacts with TGA transcription factors to activate SA-responsive genes, such as *PR1*. In low SA, NPR3/NPR4 play the opposite role by interacting with other TGAs to repress gene expression (Ding *et al.*, 2018). This SA regulation is described in Arabidopsis immunity but may not be generalised to all plants. In rice, the basal level of SA is higher than in Arabidopsis and defence gene activation by SA is not reported. However, NPR1 is present and regulates immunity in rice (Chern *et al.*, 2005). The roles of SA in rice immunity remain to be explored.

Jasmonate related metabolites, including the active form jasmonyl-isoleucine (JA-Ile), are lipid-derived compounds rapidly synthesized upon pathogen attack and leaf damage (Pieterse *et al.*, 2012). JAZ proteins, MYC2 and COI1 are central for JA-triggered immunity (Bari & Jones, 2009). JAZ proteins can bind to transcription factors, such as MYC2, 3 and 4 and EIN3/EIL1, to block their activities (Campos *et al.*, 2014). JA-Ile produced upon infection can bind COI1, resulting in JAZ protein degradation and de-repression of the transcription factors. Release of EIN3/EIL1 activates PDF1.2 expression (indirectly, through activation of intermediate transcription factors EFR1 and ORA59). Release of MYC2 directly activates transcription of VSP292. Typically, ERF1-activated genes are associated with necrotrophic resistance and MYC-activated genes are associated with resistance against herbivores (Pieterse *et al.*, 2012).

JA and SA pathways seem antagonistic: activation of one pathway leads to repression of the other (Bari & Jones, 2009). The hemibiotrophic bacterium *P. syringae* produces a JA analogue, called coronatine, to repress the SA/biotrophic resistance pathway (Zhao *et al.*, 2003). However, both SA and JA accumulate after activation of the Arabidopsis NLR RPS2, activated by AvrRpt2 from *P. syringae*. This suggests that JA and SA could interplay to maintain resistance against necrotrophic pathogens while building an effective defence against a biotrophic pathogen (Liu *et al.*, 2016a).

Hormones are also involved in priming. Priming occurs during infection to prepare plants for secondary pathogen challenge. Primed plants respond to infection faster and stronger than non-primed ones. Priming correlates with specific chromatin marks, *e.g.* on some promoters, which have been reported to be inherited to the next generation. SA, JA, pipecolic acid and azelaic acid are indispensable for priming (Conrath *et al.*, 2015; Mauch-Mani *et al.*, 2017).

1.2 *Albugo candida*, a plant pathogen oomycete

1.2.1 Taxonomy

A. candida causes white rust of Brassicaceae. It is a filamentous biotrophic pathogen. It can affect both wild and crop species such as Arabidopsis, cabbage (*Brassica oleracea*), radish (*Raphanus sativus*) and brown mustard (*Brassica juncea*) (Pidskalny & Rimmer, 1985; Holub *et al.*, 1995).

A. candida belongs to the oomycetes, a group of filamentous non-photosynthetic eukaryotes. Oomycetes used to be classified as fungi, but cladistic methods placed them as a monophyletic group, independent of fungi and more related to brown algae (Beakes *et al.*, 2012). Unlike fungi, oomycete hyphal walls contain cellulose and glucan but not chitin. Most of the oomycetes are marine organisms, obligate parasites of seaweeds, crustacea and nematodes. Others can be freshwater or soil saprophytes or insect, animal or plant parasites (Beakes & Sekimoto, 2008). Plant pathogen oomycetes includes the genera *Phytophthora*, *Hyaloperonospora* and *Albugo* (Kamoun *et al.*, 2015). Among oomycetes, *A. candida* belongs to an independent group called Albuginales, related to Peronosporales, the group of *Phytophthora* and *Hyaloperonospora* (Thines, 2014). Albuginales contain only one family, the Albuginaceae, that encompasses three genera: *Albugo*, *Pustula* and *Wilsoniana* (Choi *et al.*, 2009). At least 17 lineages have been defined within *A. candida*, each colonizing a specific range of host and having a distinct effector set (Jouet *et al.*, 2018). Despite their unique host range, there is evidence of recombination between lineages (McMullan *et al.*, 2015).

1.2.2 Life cycle

A. candida reproduces sexually by oospores and asexually by zoospores (Saharan *et al.*, 2014). During the sexual cycle, an antheridium (male gamete, multinucleate) delivers its nuclei to an ooplasm (female gamete, mononucleated). The ooplasm nucleus fuses to one of the nuclei released by the antheridium, forming an oospore. In favourable conditions, oospores can germinate in short germ tubes that produce 40 to 60 zoospores each. Similarly, zoospores can form germ tubes that penetrate the leaf through wound or stomata. Then hyphae develop in the host mesophyll and produce asexual zoosporangia, each containing ~5 zoospores. Pressure applied by numerous zoosporangia on the lower

epidermis results in symptomatic white pustules. Increases in pressure result in cracks that release zoosporangia out of the leaf (Holub *et al.*, 1995; Saharan *et al.*, 2014).

In crop fields, *A. candida* reproduces asexually on its host and sexually at the end of the host growing season. Indeed, oospores are thick-walled and can survive in the absence of host during winter.

1.2.3 Impact and management

A. candida sporangia production results in symptomatic white pustules on the lower surface of the leaf. Due to this symptom, the resulting disease is called white rust disease. All members of Albuginales (*i.e. Albugo*, *Pustula* and *Wilsoniana*) can cause white rust symptoms. *A. candida* is characterized by its specificity to infect Brassicaceae (Thines *et al.*, 2009), although it has been reported on some Cleomaceae and Capparaceae (Choi *et al.*, 2009). Some other *Albugo* species, such as *A. laibachii* and *A. koreana*, can also grow on Brassicaceae (Thines *et al.*, 2009). *A. candida* is distributed worldwide and can infect both wild species and crops including radish, cabbage, wasabi, indian mustard and turnip. 30-60 % of yield losses have been reported on rapeseed in Manitoba, Canada, 1971; 5-10 % in Australia, 1981; up to 89.8 % in an indian mustard, India, 1988 (Saharan *et al.*, 2014). Moreover, plants infected by white rust are often co-infected by other pathogens such as the oomycetes *Hpa* and *Phytophthora infestans*, increasing yield losses (Cooper *et al.*, 2008; Saharan *et al.*, 2014; Belhaj *et al.*, 2017; Prince *et al.*, 2017).

There is no specific fungicide for white rust disease control, but some broad-spectrum fungicides such as Metalaxil, Mancozeb and Blitox can reduce white rust development (Saharan *et al.*, 2014). Since *A. candida* grows ideally in cold and humid environments, keeping leaves away from moisture can also reduce white rust propagation (Saharan *et al.*, 2014).

1.2.4 Virulence

1.2.4.1 CCG effectors

As a biotrophic pathogen, *A. candida* requires living plant tissues to complete its life cycle. Its effectors must be particularly specialized to maintain host cells alive and, at the same time, enable its propagation within plant tissues. Natural selection that maximises parasite fitness on one host species might lead to specialisation and reduced host range

In fact, *A. candida* evolved races, each specialised to infect a distinct host range (McMullan *et al.*, 2015; Jouet *et al.*, 2018).

Genome analysis of several *A. candida* races and the closely related species *A. laibachii* revealed a set of secreted proteins (Kemen *et al.*, 2011; Links *et al.*, 2011). Based on comparison with previously identified secreted effector families, it has been shown that the *A. candida* secretome contains 13 glycosyl hydrolases, 3 chitinases, 9 elicitins or elicitin-like, one CBEL-like, 6 Crinklers and 26 proteins that carry an RxLR motif (Links *et al.*, 2011). Surprisingly, the extensively described RxLR effector family (Morgan & Kamoun, 2007) is not expanded in the *A. candida* secretome. They are 26 RxLRs in *A. candida* compared to 563 in *P. infestans* (Links *et al.*, 2011). On the other hand, a new family of secreted proteins was identified in *A. laibachii* (Kemen *et al.*, 2011) and observed as well in *A. candida* (Links *et al.*, 2011). They carry a conserved CxxCxxxxxG motif and are consequently called as "CCG" effector candidate proteins. There are ~100 CCGs in each *A. candida* race (Jouet *et al.*, 2018). Since CCGs are specific and abundant in *Albugo* species, they may be key effectors in white rust disease development. Currently, their function in virulence and avirulence is under investigation (Redkar *et al.*, in prep).

1.2.4.2 Immunosuppression

A. laibachii race Nc14 (an isolate of Acem1)-induced ETS not only facilitates its own colonisation, but also enables the growth of otherwise incompatible pathogens (Cooper *et al.*, 2008). Nc14 disrupts resistances against powdery mildew (via RPW8), *Hpa* races Cala2 (via RPP2) and Hiks1 (via RPP7) and the oomycete *Phytophthora infestans* (Cooper *et al.*, 2008; Belhaj *et al.*, 2017). In contrast, it does not affect the growth of already compatible pathogens such as the fungus *Colletotrichum higginsianum* (Cooper *et al.*, 2008).

A. laibachii imposes a reduction of tryptophan-derived antimicrobial metabolites in the host, which explains partially the immunosuppression (Prince *et al.*, 2017).

Despite the host specificity of each race, recombination has occurred between races (McMullan *et al.*, 2015). Immunosuppression by a compatible *A. candida* race could enable co-infection with an incompatible race, thus allowing sexual reproduction and emergence of a new race. Recombination of effectors in this new race could potentially facilitate the colonization of a new hosts (McMullan *et al.*, 2015).

1.2.5 *White Rust Resistance*-genes discovery

1.2.5.1 Using natural variation

White rust is a significant disease of *B. juncea*, a major crop in India. Although the cultivated lines Varuna, Pusa bold, Pusa jai kisan and Rohini are susceptible, some European lines such as Heera and Donskaja-IV are fully resistant. This variation was used to map and clone the CC-NLR encoding gene *BjuWRR1* from Donskaja-IV. *BjuWRR1* confers full resistance to white rust in Varuna, Pusa bold, Pusa jai kisan and Rohini (Arora *et al.*, 2019). However, the lack of genetic data for *B. juncea* impede the rapid cloning of *WRR*-genes from this species.

Most *A. candida* races will not colonize Arabidopsis, but if they do, they fail to grow on every Arabidopsis accession. This variation enables genetic analysis to identify *White Rust Resistance* (*WRR*)-genes in Arabidopsis, that could be transformed into crops.

The *Capsella bursa-pastoris*-infecting race AcEm2, the *Brassica juncea*–infecting race Ac2V and the *Brassica rapa*-infecting race Ac7V cannot grow on the Arabidopsis accession Col-0 but can trigger a weak chlorosis on cotyledons in Nd-1. Map-based cloning was used to clone the underlying resistance gene: the TIR-NLR WRR4A (Borhan *et al.*, 2008). The Col-0 allele of *WRR4A* confers resistance to a broad range of *A. candida* races including AcEm2, Ac2V, Ac7V and the *Brassica oleracea*-infecting race AcBoT. Arabidopsis *WRR4A* can be transformed into the brown mustard crop (*B. juncea*) providing full resistance to Ac2V (Borhan *et al.*, 2010).

Similarly, the race AcNc2 can grow on the Arabidopsis accession Ws-2 but not Col-0. A cross between Col-0 and Ws-2 highlighted the role of two *WRR* loci. One is the TIR-NLR pair WRR5A/WRR5B and the second is the atypical RPW8-NLR WRR7 (Cevik *et al.*, in prep).

Variation observed in white rust disease resistance among Arabidopsis accessions was successfully used to identify the broad-spectrum gene *WRR4A*. However, *WRR4A* resistance could theoretically be broken if deployed alone. Thus, it remains crucial to identify other WRR genes against the crop-infecting *A. candida* races.

1.2.5.2 Revealing novel WRR*-genes using transgressive segregation*

Genetic mapping of *WRR* genes is possible when both susceptible and resistant parents can be crossed. However, all the Arabidopsis accessions tested are resistant (at leaf stage) to Ac2V, Ac7V and AcBoT races (Cevik *et al.*, 2019). One reason could be the

presence of non-overlapping sets of resistance genes within each Arabidopsis accession. This hypothesis was tested using transgressive segregation. Multiparent Advanced Generation Inter-Cross (MAGIC) lines, deriving from 19 Arabidopsis parents (Kover *et al.*, 2009), were screened for susceptibility to Ac2V. Although all 19 parents are resistant to Ac2V, two MAGIC lines (MAGIC23 and MAGIC329) are susceptible to this race due to transgressive segregation of *WRR*-genes (Cevik *et al.*, 2019). These lines are also susceptible to Ac7V. However, they show weak or no susceptibility to AcBoT. Backcross of MAGIC329 and MAGIC23 with some of the MAGIC parents enabled to identify new *WRR*-genes. *WRR4B* from Ws-2 and Col-0, *WRR8* from Sf-2 and *WRR9* from Hi-0 are all TIR-NLR encoding genes that confer resistance to Ac2V.

An F2 population between MAGIC23 and MAGIC329 resulted in "Double-Magic" lines that are susceptible to AcBoT. Backcross of one AcBoT-susceptible "Double-Magic" line with the resistant parent MAGIC329 enabled the identification of a novel TIR-NLR involved in AcBoT resistance: WRR12 (Cevik *et al.*, 2019).

1.3 CRISPR for genome editing

1.3.1 CRISPR: a bacterial immune system

CRISPR genome editing methods derive from a bacterial immune system. Bacteria can be infected by viruses and carry an adaptive immune system to be "vaccinated" in case of secondary infection (Horvath & Barrangou, 2010). It is based on CRISPR (Clustered Regularly Inter-Spaced Palindrome Repeat) sequences and *Cas* (*CRISPR-associated*) genes. Cas proteins share similarities with various known proteins such as nucleases and polynucleotide-binding proteins. CRISPR loci comprise 23 to 47 bp repeats separated by highly polymorphic 21 to 72 bp spacer sequences. Spacers consist mostly of viral DNA fragments integrated after infection.

Several CRISPR immune systems (including Type I to Type VI) are reported in bacteria. They all function in three steps: (i) spacer acquisition, (ii) CRISPR component expression and (iii) cleavage of foreign nucleic acid (Karvelis *et al.*, 2013). Spacer acquisition consists in integration of foreign DNA (typically from a bacteriophage) in CRISPR loci by Cas1 and Cas2. Then, CRISPR sequences are transcribed in long pre-crRNAs (precursor CRISPR RNAs). pre-crRNAs are cleaved into short crRNAs containing a single spacer flanked by CRISPR repeats. In CRISPR Type I, III, IV, V and VI, the single crRNA directly binds it cognate

endonuclease. In CRISPR Type II, each mature crRNA hybridizes with a tracrRNA (trans-acting CRISPR RNA) at a ~25-nucleotide interface that has complementarity between both crRNA and tracrRNA (Deltcheva *et al.*, 2011). Each crRNA-tracrRNA forms a complex with a single protein from the Cas9 family. Complexed (Class I including Type I, III and IV) or individual (Class II including Type II, V and VI) ribonucleoproteins can cleave foreign DNA that shares complementarity with the crRNA spacer sequence (Makarova *et al.*, 2017a,b). To avoid cleavage of endogenous CRISPR sequences, ribonucleoproteins cleave spacer-similar DNA only when it is next to a specific PAM (protospacer adjacent motif), *e.g.* "NGG" for *Streptococcus pyogenes* Cas9 (SpyCas9, all occurrences of 'Cas9', unless otherwise stated, will refer to 'SpyCas9' in the rest of the text) (Sander & Joung, 2014). Since spacers integrated in endogenous CRISPR regions are not next to a PAM, they are not cleaved by ribonucleoproteins. The Type VI CRISPR protein Cas13 (previously C2c2) has the particularity to cleave RNA instead of DNA. As in Type II and Type V, Cas13 mediated cleavage is processed by individual ribonucleoproteins (Gootenberg *et al.*, 2017; Smargon *et al.*, 2017).

The CRISPR immune system illustrates how integration of viral DNA during a primary infection leads to homologous DNA or RNA cleavage and resistance during secondary infection. In 2012, two groups proposed the use of CRISPR for genome editing application (Gasiunas *et al.*, 2012; Jinek *et al.*, 2012). Indeed, cleaved DNA is processed *in vivo* by repair mechanisms, sometimes introducing short insertions of deletions (indels). This method, so-called CRISPR system, was successfully applied to induce targeted mutations *in vivo*, in animal cells (Cong *et al.*, 2013; Mali *et al.*, 2013) and in plant cells (Li *et al.*, 2013; Nekrasov *et al.*, 2013; Shan *et al.*, 2013).

1.3.2 CRISPR for genome editing

1.3.2.1 Targeted mutagenesis

Type II, Type V and Type VI single ribonucleoproteins can cleave nucleic acid *in vitro* (Gasiunas *et al.*, 2012; Jinek *et al.*, 2012; Zetsche *et al.*, 2015; Abudayyeh *et al.*, 2016). Type II-based systems, using the endonuclease Cas9, are the most commonly used. Cas9-mediated cleavage requires presence of DNA template and each of three components of the ribonucleoprotein: Cas9, tracrNRA and crRNA (Gasiunas *et al.*, 2012). They cause a DSB (double strand break) on a template DNA complementary to the crRNA if it is located at the 3' of a PAM. The DSB occurs three nucleotides before the PAM.

To simplify CRISPR system, Jinek *et al.* engineered a tracrRNA/crRNA fusion by adding a linker loop, forming a single guide RNA (sgRNA, hereafter gRNA) (Jinek *et al.*, 2012). They showed that the Cas9/gRNA complex is sufficient to induce DSB on targeted DNA template *in vitro*. In addition to the gRNA, the second central component of CRISPR system is Cas9, an endonuclease with two nuclease domains: RuvC and HNH. The crystal structure of Cas9 reveals a conformation in two lobes (Nishimasu *et al.*, 2014). The recognition lobe is involved in interaction with the gRNA. The nuclease lobe contains both RuvC and HNH domains and executes the DSB. It also contains a PAM-interacting domain. Mutations in this domain modify the PAM recognition from NGG to NGAA, NGAC, NGAT or NGAG for Cas9-VQR (Kleinstiver *et al.*, 2015) and to NG for xCas9 (Hu *et al.*, 2018) and Cas9-NG (Nishimasu *et al.*, 2018).

In vivo and particularly *in planta*, DSB are processed by two primary repair mechanisms: NHEJ (non-homologous end joining) and HDR (homology-directed recombination) (Puchta, 2005; Lieber, 2008). NHEJ can join two DNA ends, without homologous template and at any stage of the cell cycle. It is quick but error-prone, sometimes inducing small insertions or deletions (indels). The cNHEJ (classic NHEJ) is based on the KU70/KU80 complex, which binds and links two ends resulting from a DSB. More NHEJ pathways can take over in plants, including a-NHEJ (alternative -NHEJ), b-NHEJ (backup-NHEJ) and MMEJ (microhomology-mediated end joining) (Schmidt *et al.*, 2019). In mouse, a *polq-ku80* double mutant, *i.e.* impaired in the MMEJ and cNHEJ pathways, displays an increased frequency of HDR (Zelensky *et al.*, 2017). It indicates that MMEJ and cNHEJ are the two major NHEJ pathways in mouse.

HDR occurs during late S and G2 phases of cell cycle, because it requires an undamaged chromatid as template to repair DSB on sister chromatid. It is precise but occurs much less frequently than NHEJ (Steinert *et al.*, 2016).

NHEJ-induced indels can disrupt the coding DNA sequence (CDS) or *cis* regulatory elements. HDR can be used to insert a sequence through recombination between endogenous target and exogenous DNA donor template. CRISPR cleavage has been demonstrated *in vivo* in heterologous systems including human, mouse, frog, zebrafish, fruit fly, silkworm, bacteria, rice, tobacco and Arabidopsis (Sander & Joung, 2014).

1.3.2.2 Optimization in Arabidopsis

First reports

In 2013, CRISPR for genome editing was reported for the first time in Arabidopsis and *N. benthamiana* protoplasts (Li *et al.*, 2013), in wheat protoplasts and rice stable lines (Shan *et al.*, 2013) and *N. benthamiana* leaves (Nekrasov *et al.*, 2013). In protoplasts and rice stable lines, authors reported indels at a gRNA target and a 48-nucleotide deletion using two gRNA targets. Furthermore, they observed HDR-mediated gene replacement after CRISPR-induced DSB, in presence of a donor template (Li *et al.*, 2013; Shan *et al.*, 2013). Indels were also observed in *N. benthamiana* leaves after transient expression of Cas9 and gRNA (Nekrasov *et al.*, 2013).

Many biotechnological applications, including generation of knockout lines, require stable CRISPR-mediated genome editing, *i.e.* CRISPR events in germ cell line inherited to the progeny. In 2014, it was reported that, among the second generation of CRISPR-transformed Arabidopsis lines, some plants bear indels inherited from their parent (Feng *et al.*, 2014).

Variation in efficiency

In plant, CRISPR typically involves the transgenic expression of Cas9 and one or several gRNA(s). The expression of Cas9 is regulated by an RNA-Polymerase II-dependent promoter. The gRNA expression is regulated by a RNA-Polymerase III-dependent promoter to avoid post-transcriptional modifications, such as poly-adenylation and capping on the gRNA. Whereas Feng *et al.* reported 27.4% of inherited events in T2 using the *35S* (from *Cauliflower Mosaic Virus*) promoter to drive *Cas9* expression (Feng *et al.*, 2014), Fauser *et al.* obtained 8 to 70% of CRISPR-induced homozygous mutants in T2, from different T1 parents using *Ubi4-2* (from *Petroselinum crispum*) promoter (Fauser *et al.*, 2014). By using one gRNA targeting *FT* and *ICU2* promoter to drive *Cas9* expression, Hyun *et al.* recovered 1/34 heterozygous mutant among a T2 family (Hyun *et al.*, 2014). Xing *et al.* tried to knockout three genes in a single multiplex assay. They obtained 52.9% of triple mutants from five independent T2 populations. In their experiment, *Cas9* expression was driven by the *35S* promoter (Xing *et al.*, 2014). These methods for Arabidopsis reported contrasting efficiencies. One reason of such variability could be the use of different CRISPR components (Volpi e Silva & Patron, 2017).

Germline-specific promoters

Based on the hypothesis than Cas9 *cis*-regulation can result in variable CRISPR efficiency, Wang *et al.* and Mao *et al.* developed a germ line specific CRISPR system to increase inheritable events (Mao *et al.*, 2015; Wang *et al.*, 2015c). They expressed *Cas9* under the control of *EC1.1*, *EC1.2* or *SPL* promoters, specifically active in the female (*EC1.1* and *EC1.2*) or male (*SPL*) germ line. These systems trigger less somatic activity in T1 but stable CRISPR-induced mutations in T2. *Cas9* regulation by *EC1.2* promoter resulted in nine triple homozygous mutants out of 108 tested T1 lines tested (Wang *et al.*, 2015c). This system is the first to report stable CRISPR-induced mutations in the first generation after transformation with such efficiency. Interestingly in their experiment, *Cas9* terminator seems to influence the mutation rate. Higher mutation rate was observed when Cas9 expression was regulated by *E9* terminator (*rbcS E9* from *Pisum sativum*) compared to the *Nos* terminator (*Nopaline synthase* from *Agrobacterium tumefaciens*). The idea of using a germline specific promoter to drive *Cas9* expression has been further investigated. A high CRISPR activity has been reported using *SPL* (Mao *et al.*, 2015), *MGE1* (Eid *et al.*, 2016) and *YAO* (Yan *et al.*, 2015) promoters. Particularly, the *YAO* promoter can lead to 90.5% of somatic activity whereas, in the same conditions, the 35S promoter led to 4.3% of somatic activity. The *RPS5a* promoter is also shown to be extremely efficient to induce inheritable mutations (Tsutsui & Higashiyama, 2017).

gRNA transcription

The gRNA expression can also be crucial for CRISPR activity. Generally, the gRNA expressing cassette contains the *U6-26* promoter, one gRNA and a seven-thymine repeat that constitutes an RNA-polymerase III terminator. *U6-26* promoter is indeed the most active *U6* promoter, although *U6-1, U6-4, U6-5, U6-6* and *U6-29* are also effective in Arabidopsis (Li *et al.*, 2007). Nevertheless, RNA polymerase III-dependent promoters are not tissue specific and less diverse than RNA polymerase II-dependent ones. A strategy has been proposed to drive gRNA expression using RNA polymerase II, based on RNA self-cleavage. Hammerhead type and hepatitis delta virus ribozymes can be self-cleaved from RNA 5'- and 3'- ends respectively. Gao and Zhao proposed the use of RGR (ribozyme-gRNA-ribozyme) in CRISPR systems (Gao & Zhao, 2014). RGR can be transcribed by RNA polymerase II and the self-cleavage of ribozymes can release a desired gRNA. Similarly, the endogenous tRNA-processing system can cleave and release tRNA precursors. A tRNA-gRNA architecture enables the production of multiple gRNAs using a single promoter (Xie *et al.*, 2015). Csy4 is an RNase of *Pseudomonas aeruginosa* that has a specific

recognition site. A single transcript of gRNAs flanked by Csy4 recognition sites can produce multiple gRNAs using a single promoter (Tsai *et al.*, 2014). tRNA, RGR and Cys4 gRNA processing system can successfully trigger CRISPR-mediated disruption of targeted gene *in vivo* (Čermák *et al.*, 2017).

gRNA backbone

In addition to *Cas9* and gRNA expression regulations, the gRNA structure may enhance CRISPR activity (Jinek *et al.*, 2013). Most of the CRISPR systems reported so far are based on a crRNA-tracrRNA fusion (Jinek *et al.*, 2012). This gRNA coding sequence contains a succession of four thymines that can act as a terminator for RNA-polymerase III. Thus, *Chen et al.* proposed an improved version of this gRNA (Chen *et al.*, 2013). First, they broke the succession of four thymines by doing an A->T transversion and secondly, they added a five base-pair extension in the stem, since Cas9 binds gRNA through its duplex stem (Nishimasu *et al.*, 2014). As this gRNA has a nucleotide "flip" and an "extension", it is referred as gRNA-EF. It was used by Chen *et al.* to direct a dead version of Cas9 (dCas9, bearing a D10A mutation in RuvC domain and H840A mutation in HMH domain, rendering inactive both nuclease domains) fused to KRAB, a human transcription repressor, in human cells. dCas-KRAB was able to repress transcription two-fold more when led by gRNA-EF compared to the classic gRNA (Chen *et al.*, 2013). Three subsequent CRISPR assays conducted in mammals (Dang *et al.*, 2015; Peng *et al.*, 2015) and *Caenorhabditis elegans* (Ward, 2014) reported elevated mutation rates when gRNA-EF was used instead of classic gRNA.

gRNA spacer

Moreover, the spacer sequences of the gRNA may play a critical role in CRISPR efficiency. Three different gRNAs targeting *AtBRI1* triggered variable CRISPR activity, from 30% to 84.2%, when expressed in the same conditions and in same CRISPR system (Feng *et al.*, 2014). Based on the crystal structure of Cas9, recognition of gRNA spacer should be sequence independent although Arg71 may induce a preference to guanine in the four nucleotides at 3' end of the spacer sequence (Nishimasu *et al.*, 2014). Prediction of CRISPR efficiency based on gRNA spacer sequence remains largely empirical. A comparative study of 1841 gRNAs in mammal cells revealed that some nucleotides are statistically favoured or disfavoured at certain positions, especially at 3' end of the spacer sequence (Doench *et al.*, 2014). It is not known if these observations are valid in plants.

Influence of temperature on Cas9 activity

LeBlanc *et al.* used a different approach to optimise CRISPR in Arabidopsis. Cas9 is originally a protein from *S. pyogenes*; its enzymatic activity optimum is 37°C *in vitro*. In Arabidopsis, a series of 37°C treatments of plants expressing Cas9 results in elevated activity, as compared to plant grown at 22°C (Le Blanc *et al.*, 2017). The heat treatments not only increased the Cas9 activity but also gRNA expression.

1.3.2.4 Diversity of CRISPR endonucleases

Cas9 from *S. pyogenes* is widely used in CRISPR systems. However, other CRISPR endonucleases can be used.

Cas9 from *Staphylococcus aureus* (SaCas9) is smaller and equally or more efficient than SpyCas9 (Steinert *et al.*, 2015; Raitskin *et al.*, 2018; Wolter *et al.*, 2018). However, it has a more specific PAM: NNGGGT, which reduces the targeting range.

The Type V CRISPR endonuclease Cas12 (previously Cpf1) from *Lachnospiraceae bacterium* and *Acidaminococcus sp.* functions in human cells (Zetsche *et al.*, 2015). Instead of the dual crRNA-tracrRNA recognized by Cas9, Cas12 uses a single and shorter crRNA. Also, Cas12 recognizes a TTTV PAM located at the 5' of the target and releases fragments with a five-nucleotide overhang after cleavage, whereas Cas9 produces blunt ends. The Cas12 system has been successfully applied for targeted mutagenesis in rice and tobacco (Endo *et al.*, 2016; Hu *et al.*, 2017; Tang *et al.*, 2017).

Cas13a (previously C2c2), the endonuclease of CRISPR Type VI, has been discovered in 2015 and characterised in 2016 (Shmakov *et al.*, 2015; Abudayyeh *et al.*, 2016). Another CRISPR Type VI endonuclease, Cas13b, was characterized in 2017 (Smargon *et al.*, 2017). Unlike Cas9 and Cas12, Cas13 cleaves specifically RNA. Importantly, Cas13 can cleave collateral RNA molecules even if they do not share identity with the template crRNA-targeted RNA (Gootenberg *et al.*, 2017).

The addition of Cas12 and Cas13 in the genome editing toolbox has facilitated the development of novel CRISPR applications, beyond the generation of targeted random mutations (Murugan *et al.*, 2017; Schindele *et al.*, 2018)

1.3.2.5 Genome editing and beyond

NHEJ-mediated gene editing

The imprecise repair of Cas9-targeted DSB by the NHEJ have been extensively use to generate null alleles (Hsu *et al.*, 2014). It enabled recapitulation of key events of tomato

domestication in only few months (Li *et al.*, 2018; Zsögön *et al.*, 2018), generation of transgene-free powdery mildew resistant tomato plants (Nekrasov *et al.*, 2017) and correction of a heart genetic disease in mice during early postnatal stage (Xie *et al.*, 2016) and in human zygote (Ma *et al.*, 2017). The precise RNA-guided targeting of Cas proteins to nucleic acid can also lead to much diverse applications (Langner *et al.*, 2018; Schindele *et al.*, 2018).

Transcriptional regulation

RuvC and HNH, the two nucleases of Cas9, can be mutated to obtain a nuclease dead Cas9 (dCas9). A fusion of the demethylase TET1CD or the acetyltransferase p300 to dCas9 successfully up-regulated the transcription of targeted gene (Hilton *et al.*, 2015; Choudhury *et al.*, 2016). In addition, transcriptional repressors such as KRAB and the methyltransferase DNMT3A were fused to dCas9 to hypermethylate targeted gene promoters, resulting in transcriptional repression (Thakore *et al.*, 2015; Vojta *et al.*, 2016).

Base editing

In order to generate precise mutations at Cas9-binding site, two groups engineered a fusion of Cas9 with the human cytidine deaminases APOBEC or AID (Komor *et al.*, 2016; Nishida *et al.*, 2016). Such cytidine base editor (CBE) modules catalyse the deamination of cytosine, resulting in uracil which can be processed as thymine during replication. Following the same strategy, David Liu's laboratory generated an adenine base editor (ABE) using the adenine deaminase TadA (Gaudelli *et al.*, 2017). Deamination of adenosine results in inosine, which can be processed as guanosine during replication. The activity of ABE and CBE is very precise, occurring in a 7 bp frame (N3-N9 in N20-PAM) (Shan & Voytas, 2018). Base editors have proven to be efficient *in planta* (Zong *et al.*, 2017; Kang *et al.*, 2018).

Dynamic loci visualisation

dCas9 is also used as a fluorophore-carrier to highlight specific loci. Combined with high resolution microscopy, this system enabled to follow multiple loci in human cell (Chen *et al.*, 2013) or telomeres in plant cells (Dreissig *et al.*, 2017) during different stages of the cell cycle.

Cas13 applications

The specificity of Cas13 for RNA binding has open the doors to novel CRISPR applications (Wolter & Puchta, 2018). Targeting of mRNA enabled to knock down gene expression at similar level than RNAi (RNA interfering, a typical method to knockdown gene expression)

but with a higher specificity (Abudayyeh *et al.*, 2017). The transcriptional status of tested cell was otherwise normal, indicating that the collateral activity of Cas13 *in vitro* is not observed *in vivo*.

The *in vitro* collateral activity of Cas13 was used as an advantage to design the SHERLOCK (specific high-sensitivity Enzymatic Reporter unlocking) detection system (Gootenberg *et al.*, 2017). By adding a fluorescent reporter (quenched fluorescent RNA), collateral Cas13 activity results in fluorescence. Such collateral activity occurs only in presence of a template RNA identical to the crRNA in complex with Cas13. The system was able to detect *Zika virus* fragments with high sensitivity and specificity.

Cas13 was also used to defend against RNA virus, such as TuMV (*turnip mosaic virus*) in plants (Aman *et al.*, 2018). Transient expression of Cas13 and crRNA targeting TuMV reduced the proliferation of the virus by 50%. This is one example among many other CRISPR applications for plant disease resistance (Langner *et al.*, 2018).

1.3.3 CRISPR for plant immunity

1.3.3.1 Knocking-out Susceptibility-*genes*

R-genes are sufficient to confer resistance to a given pathogen. In contrast, some genes are required for susceptibility and are consequently called *Susceptibility*(*S*)-genes (Eckardt, 2002). Several examples of CRISPR-mediated *S*-gene disruption have resulted in resistant plants (Zaidi *et al.*, 2018). *MLO* is a dominant *S*-gene that confers broad spectrum susceptibility to powdery mildew in diverse plants from monocots to dicots. An Arabidopsis *mlo2-mlo6-mlo12* triple mutant is fully resistant to an Arabidopsis-compatible powdery mildew strain (Acevedo-Garcia *et al.*, 2014). CRISPR was used to knock-out *MLO* genes in wheat and tomato (Wang *et al.*, 2014; Nekrasov *et al.*, 2017). The edited plants were resistant to powdery mildew. This approach enables to generate resistant crops in few months, with mutation undistinguishable from naturally occurring mutation (Nekrasov *et al.*, 2013).

1.3.3.2 Knock-in breeding Resistance-*genes*

HDR-mediated repair of CRISPR-induced DSB can result in gene replacement or insertion in plant and animal (Li *et al.*, 2013; Mali *et al.*, 2013). Gene targeting via HDR occurs via homologous recombination between a template and genomic DNA at very low frequency. It is drastically enhanced when DSB occurs (Puchta & Fauser, 2013). Although

CRISPR-mediated gene targeting is a routine assay in animal, it remains currently a challenge in plant. Stable gene targeting was achieved in Arabidopsis and tomato in 6% to 25% of transformed plants (Dahan-Meir *et al.*, 2018; Wolter *et al.*, 2018; Vu *et al.*, 2019). Theoretically, CRISPR could be used to introgress an *R*-gene in a susceptible line quickly and with no other DNA introgression as compared to classic breeding. Currently it has not been demonstrated.

In only five years, CRISPR has been deployed to build significant resistance in plant via RNA virus targeting and *S*-gene knock-out. If gene targeting is one of the current challenges, we can expect to see much more CRISPR-derived applications in the next few years, for plant disease resistance and beyond.

Chapter 2 : Materials and methods

2.1 Material

2.1.1 Plant material

Arabidopsis thaliana (Arabidopsis) wild type lines used in this study are Col-0, Oy-0, Ler-0 and Ws-2. The Recombinant Inbred Line population between Oy-0 and Col-0 is the collection "27RV" from the "Versailles Arabidopsis Stock Centre". The MAGIC329 and MAGIC23 are from the MAGIC collection (Kover *et al.*, 2009). The mutant lines used in this study are Be-0_ADHR002 (NASC: N8102), Col-0_*wrr4-6* (NASC: N667351), Col-0_*adr1-adr1-l1-adr1-l2* (Bonardi *et al.*, 2011), Ws-2_*rrs1-rps4-rps4b* (Saucet *et al.*, 2015), Ws-2_*eds1-1* (Falk *et al.*, 1999), Col-0_*eds1-2* (Bartsch *et al.*, 2006), Col-0_*eds1-12* (Ordon *et al.*, 2017), and Col-0_*RPW8-S5* (Xiao *et al.*, 2003). *Camelina sativa* wild type used in this study is cultivar Celine. Seeds were sown directly on compost and plants were grown at 21 °C, with 10 hours of light and 14 hours of dark, 75 % humidity. For seed collection, 4- to 5-weeks old plants were transferred under long-day condition: 21 °C, with 16 hours of light and 8 hours of dark, 75 % humidity.

The Solanaceae plants used in this study were *Nicotiana benthamiana* and *Nicotiana tabacum* cultivar "Petit Gerard". Seeds were sown directly on compost and plants were grown at 21 °C, with 16 hours of light and 8 hours of dark, 55 % humidity.

2.1.2 Microbial material

2.1.2.1 Escherichia coli

Escherichia coli strain DH10B genotype F– mcrA Δ(mrr-hsdRMS-mcrBC) Φ80lacZΔM15 ΔlacX74 recA1 endA1 araD139 Δ(ara leu) 7697 galU galK rpsL nupG λ– was used for cloning purposes. They were grown at 37 °C overnight on LB media supplemented with antibiotic according to the plasmid-carried selectable marker.

2.1.2.2 Agrobacterium tumafaciens

Agrobacterium tumafaciens strains used in this study were GV3101, Agl-1 and GALLS (Hodges *et al.*, 2004). They were grown at 28 °C overnight for 48 hours on LB media

supplemented with gentamycin (GV3101 and GALLS) or carbenicillin (Agl-1) along with rifampicin and a third antibiotic according to the plasmid-carried selectable marker.

2.1.2.3 Pseudomonas spp.

Pseudomonas syringae pv tomato strain DC3000 (DC3000) and *Pseudomonas fluorescens* strain Pf0-1 (Pf0-1) engineered with a Type III Secretion System (Thomas *et al.*, 2009) were used in this study. They were grown at 28 °C for 48 hours on KB media supplemented with rifampicin and kanamycin (DC3000) or chloramphenicol, tetracycline and gentamycin (Pf0-1).

DC3000 strains were expressing the following constructs: *pVSP61* (empty vector), *pVSP61:: AvrRps4*, *pVSP61::AvrRps4-KRVYAAAA*, *pVSP61::PopP2*, *pVSP61::PopP2-C321A*, *pVSP61::AvrRpt2*, *pVSP61:AvrRpm1* or *pVSP61:AvrPphB* (Axtell & Staskawicz, 2003; Sohn *et al.*, 2009; Williams *et al.*, 2014).

Pf0-1 strains were expressing the following constructs: *pBBR1MCS-5::AvrRps4*, *pBBR1MCS-5::AvrRps4-KRVYAAAA*, *pEDV6::PopP2*, *pEDV6::PopP2_C321A* or *pEDV6::AvrRpt2* (Sohn *et al.*, 2007, 2014).

2.1.2.4 Oomycetes

The following *Albugo candida* races were used in this study: *the Brassica oleracea*-infecting race AcBoT, the *Brassica juncea*-infecting race Ac2V, the *Brassica rapa*-infecting race Ac7V, the *Capsella spp.*-infecting race AcEm2 and the *Arabidopsis spp.*-infecting races AcNc2 and AcEx1 (Liu & Rimmer, 1993; McMullan *et al.*, 2015; Prince *et al.*, 2017).

The following *Hyaloperonospora arabidopsidis* races were used in this study: Emoy2 and Cala2 (Parker *et al.*, 1996).

2.1.3 Media

All recipes are for scale of 1 litre.

2.1.3.1 Lysogeny Broth (LB)

10 g tryptone, 5 g yeast extract, 5 g NaCl, 1 g glucose, pH 7.0. For solid medium, 10 g agar was included.

2.1.3.2 Lennox (L)

10 g tryptone, 5 g yeast extract, 10 g NaCl, pH 7.0. For solid medium, 10 g agar was included.

2.1.3.3 King's B (KB)

20 g peptone, 10 ml glycerol, 1.6 g Potassium Hydrogen Phosphate, 10 ml glycerol. pH was adjusted to 5.8 with NaOH. For solid medium, 15g agar was included.

2.1.3.4 Murashige and Skoog ½ (MS ½)

2.2 g of Murashige and Skoog medium (micro and macro elements including vitamins), 30 g sucrose. pH was adjusted to 5.8 with NaOH. For solid medium, 10g agar was included.

2.1.4 Antibiotics

Stock solutions were stored at -20 °C, except for rifampicin, which was stored at 4 °C. Working concentrations indicate the final concentrations used in selective media.

Antibiotic	Stock concentration	Working concentration
Carbenicillin	100 mg/ml in H_2O	100 µg/ml
Chloramphenicol	10 mg/ml in H_2O	10 µg/ml
Gentamycin	10 mg/ml in H_2O	10 µg/ml
Kanamycin	150 mg/ml in H_2O	150 µg/ml
Rifampicin	10 mg/ml in methanol	10 µg/ml
Spectinomycin	100 mg/ml in H_2O	100 µg/ml
Tetracycline	5 mg/ml in ethanol	5 µg/ml

Table 2-1: Antibiotics used in this study

2.2 Methods

2.2.1 Molecular Biology

2.2.1.1 Genomic DNA isolation

For short-term storage of plant DNA (*e.g.* for genotyping by PCR), ~0.5cm² of leaf tissue was printed by mechanical pressing on a Whatman® FTA® card. Card was air dried and stored at room temperature. For PCR application, a 1.2mm diameter disc was extracted from the card-printed leaf with a Harris Uni-Core Punch and incubated for 2 hours at room

temperature with 50 µl FTA extraction buffer (10mM TrisHCl, 0.01 %v/v Tween 20, 2mM EDTA). The buffer was discarded and the disc was washed with 180 µl water before being used as PCR template.

For long term storage, tissue was ground and mixed with 700 µl CTAB extraction buffer (2 g CTAB, 2 g PVP MW 40,000, 28 ml NaCl 5 M, 4 ml EDTA 0.5M pH 8, 10 ml TrisHCl 1M pH 8 in water for a total volume of 100 ml) and placed at 65 °C for 2 hours. DNA was extracted with 500 µl Chloroform:Isoamylalcol, by mixing the sample by inversion and centrifuging for 10 minutes at 20,000 RCF. The upper phase was transferred in a new tube and DNA was precipitated with 2/3 volume of isopropanol for 5 minutes at room temperature. DNA was span down by centrifuging at 20,000 RCF. Supernatant was discarded. Pellet was washed with ethanol 76 %, air-dried, re-suspended in 300 µl water and stored at -20 °C.

2.2.1.2 Polymerase chain reaction

Standard PCR were performed using Taq DNA Polymerase (NEB). For cloning of PCR products (except for USER® cloning), Q5® High-Fidelity DNA Polymerase (NEB) was used. For cloning of PCR products via USER® cloning, KAPA HiFi HotStart Uracil+ ReadyMix (KAPABIOSYSTEM) was used. Reaction mix, annealing and extension temperature were defined following the manufacturer's instructions. PCR were carried out in a thermocycler.

To estimate PCR product size and quantity, gel electrophoresis was used. Gels were made with 1.5 % agarose, TAE buffer 1X and 0.01 µl/ml ethidium bromide. Gels were run at ~100-150 V and were visualized using UV light. Gel extractions were performed using the QIAquick Gel Extraction Kit (QIAGEN), following the manufacturer's instructions.

2.2.1.3 Golden Gate Cloning

The Golden Gate assembly enables a single-step assembly of multiple DNA fragments into a destination vector, utilising the activities of type II endonucleases BsaI and BpiI and DNA ligase T4 (Engler *et al.*, 2009; Weber *et al.*, 2011). For each assembly, a unique set of compatible 4 bp overhangs at the junction of each modules are designed to ensure the assembly in desired order. The overhang were chosen following the plant Golden Gate standards (Engler *et al.*, 2014). The modules were assembled in a single digestion and ligation reaction called diglig.

Digligs were done in the following conditions: 0.02 pmol of each module and the destination vector were mixed with 0.5 µl BsaI-HF® enzyme (20,000 units/ml, NEB) or

BpiI® enzyme (10,000 units/ml, ThermoFisher), 0.15 µl BSA 10X (2 mg/ml, NEB), 1 µl T4 DNA ligase (400,000 units/ml, NEB), 1.5 µl CutSmart® buffer (NEB) and water to a final volume of 15 µl. Digligs were carried out in a thermocycler with the following steps: initial digestion at 37 °C for 1 minute, 25 cycles of digestion at 37 °C for 3 minutes and ligation at 16 °C for 4 minutes, denaturation of enzymes at 50 °C for 5 minutes and 80 °C for 5 minutes.

2 to 4 µl were used for transformation in electro-competent *E. coli*.

2.2.1.4 USER cloning

The USER cloning assembly enables to integrate one or several PCR amplicons in a USER-compatible vector (Geu-Flores *et al.*, 2007). The procedure is based on the use of PCR primers that contain a single deoxyuridine near their 5' end. Treatment of the PCR products with deoxyuridine-excision enzyme generates long overhangs designed to specifically complement each other.

USER-compatible vector was pre-digested with PacI and Nt.BBvCI. USER ligation was conducted by mixing 0.02pmole of gel purified PCR product(s) with the pre-digested destination vector with 1 µL USER® enzyme (NEB), 1 µL Taq DNA Polymerase Buffer (NEB) and water in a total reaction volume of 10 µl. The mix was incubated at 37 °C for 15 minutes then 25 °C for 15 minutes.

2 to 4 µl were used for transformation in chemical-competent *E. coli*.

2.2.1.5 Gibson assembly

Gibson assembly enables to join multiple linear DNA fragments sharing identity at their extremity (Gibson *et al.*, 2009). It is based on the concerted action of a 5' exonuclease, a DNA polymerase and a DNA ligase. Two DNA fragment can be assembled if the ~20 nucleotides 5' end of one is identical to the 3' end of the other.

The reagents are the 5X ISO buffer (for 6 ml: 3 ml TrisHCl [1 M, pH 7.5], 150 µl $MgCl_2$ [2 M], 60 µl of dGTP [100 mM], 60 µl of dATP [100 mM], 60 µl of dTTP [100 mM], 60 µl of dCTP [100 mM], 300 µl DTT [1 M], 1.5 g PED-8000, 200 µl NAD [100 mM] and water) and the Gibson Assembly Mix (for 1.2 ml: 320 µl 5X ISO buffer, 0.64 µl T5 exonuclease [10,000 units/ml, NEB], 20 µl Phusion® High-Fidelity DNA Polymerase [2,000 units/ml, NEB], 160 µl Taq DNA ligase [10,000 units/ml, NEB] and water).

Two or more Gibson compatible linear DNA molecules (typically PCR products) were mixed in an equimolar amount with 15 µl Gibson Assembly Mix and water in a total volume of 20 µl. The mix was incubated at 50 °C for 1 hour.

2 to 4 µl were used for transformation in chemical-competent *E. coli*.

2.2.1.6 Transformation in E. coli and A. tumefaciens

Plasmid were transformed using ~5x10^8 cells in a 0.1cm cuvette and a micropulser (Bio-Rad) on settings recommended by the manufacturer. Bacteria were suspended in 300 µl of LB and incubated 1 hour at 37 °C (*E. coli*) or 2 hours at 28 °C (*A. tumefaciens*). 50 µl were spread on L plate with the appropriate antibiotic. For transformation of a Golden Gate cloning product, 10 µl of X-Gal (40mg/ml) was added on top of the plate for white/blue selection. The plate was incubated at 37 °C overnight (*E. coli*) or at 28 °C for 48 hours (*A. tumefaciens*).

2.2.1.7 Plasmid purification and confirmation

For plasmid purification, two white colonies were re-cultivated on liquid LB with the appropriate antibiotic and incubated overnight at 37 °C (*E. coli*) or at 28 °C (*A. tumefaciens*). The plasmid DNA was extracted using a QIAprep Spin Miniprep Kit (QIAGEB) following the manufacturer's instruction. The plasmid DNA was eluted in 50 µl water and stored at -20 °C.

Successful DNA insertions into the plasmid were checked by restriction enzyme analysis. Plasmids sequences were confirmed by Illumina sequencing using service provided by GATC Biotech. The sequencing data were analysed using CLC Main Workbench 7.7.1. Correctly transformed bacteria were stored as glycerol stock (1 ml of liquid culture from a single colony with 1 ml of 60 % glycerol) at -80 °C.

2.2.1.8 Gene expression measurement by RT-qPCR

For gene expression analysis, RNA was isolated from three biological replicates and used for subsequent reverse transcription quantitative PCR (RT-qPCR) analysis. Briefly, RNA was extracted using the RNeasy Plant Mini Kit (QIAgen) and treated with RNase-Free DNase Set (QIAgen). Reverse transcription was carried out using the SuperScript IV Reverse Transcriptase (ThermoFisher). qPCR was performed using CFX96 Touch™ Real-Time PCR Detection System. Data were analysed using the double delta Ct method (Livak & Schmittgen, 2001).

2.2.1.9 Protein extraction and Western Blot

Proteins were extracted from leaf tissue using TruPAGE™ LDS Sample Buffer (Sigma-Aldrich) following the manufacturer recommendations. They were separated by SDS-PAGE and analysed by immunoblotting. Tris-Glycine polyacrylamide (PAA) gels were prepared with 5 % polyacrylamide for the stacking gel, and 10 or 12 % polyacrylamide for resolving gels in this study. The pre-stained protein ladder (PageRuler, ThermoFisher) was used as molecular weight marker. Proteins were transferred to Immobilon-P PVDF membranes (Merck Millipore), using a semi-dry transfer apparatus supplied by Trans-Blot Turbo (Bio-Rad). Membranes were blocked for 1 h at room temperature or overnight at 4 °C in TBST (Tris-Buffered Saline with 0.1 % Tween) containing 5 % (w/v) non-fat dry milk. Membrane incubation with Horseradish Peroxidase (HRP) conjugated antibodies (AntiFLAG M2, 1:10000 dilution, Sigma; Anti-GFP, 1:10000 dilution, Santa Cruz Biotechnology) was carried out in TBST supplemented with 5 % milk by gentle agitation at room temperature for 1 h. The membrane was then rinsed 3 times in TBST (10 min), and once in TBS (Tris-Buffered Saline). Chemiluminescence detection for proteins of interest was carried out firstly by incubating the membrane with developing reagents (SuperSignal West Pico & West Femto), using ImageQuant LAS 4000 (Life Sciences).

2.2.2 Plant biology

2.2.2.1 Transient expression

A. tumefaciens strains were streaked on selective media and incubated at 28 °C for 48 hours. A single colony was transferred to liquid LB medium with appropriate antibiotic and incubated at 28 °C for 24 hours in a shaking incubator (200 rotations per minute). The resulting culture was centrifuged at 3000 rotations per minute for 5 minutes and resuspended in 2 ml of infiltration buffer (10mM MgCl2, 10mM MES, pH 5.6) at OD_{600}=0.5 ($2.5x10^8$ colony forming unit [cfu]/ml). For co-expression, each bacterial suspension was adjusted to OD_{600}=0.5 in the final mix. The abaxial surface of 5-weeks old *N. tobacco* or *N. benthamiana* were infiltrated with 1 ml needle-less syringe. Leaves were phenotyped for cell death at 3 to 7 dpi.

2.2.2.2 Stable transformation

A. tumefaciens mediated transformation of Arabidopsis was carried out using the floral dip method (Clough & Bent, 1998). Briefly, 6- to 8-weeks old plants were dipped in a solution of *A. tumefaciens* at OD_{600}=0.5 ($2.5x10^8$ cfu/ml).

Recovered seeds were selected with either herbicide (glufosinate sprayed three times on 1- to 3-weeks old plants at a concentration of 0.375g/l), antibiotic or fluorophore expression in seeds. The fluorescence in seeds is the result of the expression of RFP or GFP under the control of the seed-specific *AtOLEOSIN1* promoter, described as the FAST-Red/FAST-Green method (Shimada *et al.*, 2010). The seeds were manually selected using a fluorescence stereomicroscope.

2.2.2.4 CRISPR event characterization

Six to twelve independent transformants were tested for CRISPR activity. The loc(i)us containing the gRNA-target(s) was(were) amplified by PCR. The amplicon was either sent for sequencing or digested with a restriction enzyme having its recognition site at the gRNA target. The loss of restriction site was assessed on an electrophoresis gel. Transformants showing a high undigested *vs* digested ratio and/or a sequencing trace with elevated polymorphism at the gRNA target was considered as somatically CRISPR active lines. The progeny of the most CRISPR active line was screened for homozygous events, using the same method. Lines showing full resistance to digestion and/or a sequencing trace with a clear single indel were considered as putative homozygous mutant. Such lines were generally identified in T2 but in some cases, homozygous mutants were identified directly in T1.

Once a line was genotyped as putative homozygous mutant, its progeny was selected for the absence of T-DNA and screened by PCR and sequencing to confirm that the mutation was indeed inherited from the parent. The seeds of least one non-transgenic progeny carrying the CRISPR-induced homozygous mutation were collected and stored for further experiments.

For the characterization of CRISPR event at the *ADH1* locus specifically, plants were screened with allyl-alcohol. ~100 seeds were sterilized, immersed in water and incubated at 4 °C in the dark overnight. Then they were treated with 30mM allyl-alcohol (ALDRICH) at room temperature for 2 hours, shaken at 750 rpm. Then they were rinsed three times with water and sown on MS½ medium. After two weeks, the number of germinated and non-germinated seeds was monitored. The *adh1* mutation was confirmed by PCR and sequencing for up to six allyl-alcohol resistant lines per genotype. Sequencing results were compared to the Col-0 sequence of *ADH1* using CLC Main Workbench 7.7.1. *ADH1* genotypes were reported as WT (identical to Col-0), heterozygous (both Col-0 and single mutation detected), biallelic (two different mutations detected), homozygous (single

mutation detected) or somatic (more than two signals detected). For each T2 family, the CRISPR efficiency was defined as the ratio of homozygous and biallelic mutants compared to the total number of seeds sown.

2.2.3 Pathology assay

2.2.3.1 Albugo candida infection

For propagation of *A. candida*, zoospores were suspended in water (~10^5 spores/ml) and incubated on ice for 30 min. The spore suspension was then sprayed on plants using a Humbrol® spray gun (~700 µl/plant) and plants were incubated at 4 ˚C in the dark overnight. Infected plants were kept under 10 hours light (20 ˚C) and 14 hours dark (16 ˚C) cycles. Plants were scored as susceptible if a pathogen was capable of accomplishing its life cycle and sporulation was macroscopically visible within 3 weeks after plant inoculations.

2.2.3.2 *Hyaloperonospora arabidopsidis* infection

For propagation of *H. arabidopsidis* (*Hpa*), 1-week old Arabidopsis seedlings were sprayed with fresh *Hpa* spores at a concentration of 10^4 spores/ml using a Humbrol® spray gun (~700 µl/plant). Sprayed seedlings were covered with a plastic lid and were kept under 10 hours light (20 ˚C) and 14 hours dark (16 ˚C) cycles. Susceptibility was measured as the number of spores per plant. Approximately 80 plants were bulked in 2 ml of water and spores were counted using a haemocytometer. Results are expressed as the number of spores per plant.

2.2.3.3 Hypersensitive Response assay

Pseudomonas fluorescens (Pfo-1 EtHAn) or pVSP61:AvrPphB or *Pseudomonas syringae* (DC3000) carrying denoted constructs were grown on selective KB-medium agar plate for 48 hours at 28 ˚C. Bacteria were harvested from plate, re-suspended in 10 mM $MgCl_2$ and concentration was adjusted to OD_{600} = 0.2 (10^8 cfu/ml). The abaxial surface of 4- to 5-weeks old Arabidopsis leaves were hand-infiltrated with 1 ml needle-less syringe. Cell death was monitored qualitatively 12 to 24 hours after infiltration. For quantitative measurement of HR, electrolyte leakage assay was conducted. Leaf discs were taken with a cork borer from infiltrated leaves. Discs were dried, washed in deionized water for half an hour before being floated on deionized water (16 discs per sample, 3 samples per

biological replicate for 3 biological replicates). Electrolyte leakage was measured on a Horiba LAQUQtwin-EC-33 conductivity meter at indicated time points.

2.2.3.4 Bacterial growth assay

Pseudomonas syringae (DC3000) carrying denoted constructs were grown on selective KB-medium agar plate for 48 hours at 28 °C. Bacteria were harvested from plate, re-suspended in 10mM $MgCl_2$ and concentration was adjusted to OD_{600} = 0.001 ($5x10^5$ cfu/ml). The abaxial surface of 4- to 5-weeks old Arabidopsis leaves were hand-infiltrated with 1 ml needle-less syringe. For quantification, leaf sample were harvested with a 6 mm diameter cork borer, resulting in a ~0.283 cm^2-sized leaf disc. Two leaf discs per leaf were harvested and used as single sample. For each condition, four samples were collected just after infiltration and eight samples were collected 72 hours after infiltration. Samples were ground in 200 µl of 10mM $MgCl_2$, serially diluted (5, 50, 500, 5000 and 50000 times) and spotted (6 to 10 µl per spot) on selective KB-medium agar plate to grow 48 hours at 28 °C. The number of colonies (cfu per drop) was monitored and the bacterial growth was expressed in cfu/cm^2 of leaf tissue.

2.2.3.7 Salicylic acid measurement

Pseudomonas fluorescens (Pf0-1) (Thomas *et al.*, 2009) carrying denoted construct were grown on selective KB-medium agar plate for 48 hours at 28 °C. Bacteria were harvested from the plate, re-suspended in infiltration buffer (10mM $MgCl_2$, pH 5.6) and concentration was adjusted to OD_{600} = 0.05 ($2.5x10^7$ cfu/ml). The abaxial surface of 5-week old Arabidopsis leaves was hand-infiltrated with 1 ml needle-less syringe. Leaves were harvested 24 hours post inoculation and freeze dried. Salicylic acid was extracted from 10 mg of ground dry tissue with 400 µl of 10 % methanol and 1 % acetic acid in water on ice for 30 minutes. The solution was centrifuged at 13000 rpm for 10 minutes. A second extraction was carried out on the pellet in the same conditions and both supernatants were mixed. Samples were analysed on an Acquity UPLC attached to a TQS tandem mass spectrometer (both from Waters). Detection was by negative electrospray MS. Spray chamber conditions were 600 °C desolvation temperature, 900L.hr^{-1} desolvation gas, 150 L.hr^{-1} cone gas, and 7.0 bar nebulizer pressure. The spray voltage was 1.5 kV in negative mode.

2.2.3.6 Trypan Blue staining

Cell death and filamentous pathogen development were studied in leaf mounts stained with lactophenol-trypan blue. Whole leaves were boiled for 1 minute in stain solution (10 ml lactic acid, 10 ml glycerol, 10g phenol, 10mg trypan blue and water in a final volume of 10 ml) and then decolorized in chloral hydrate (2.5 g chloral hydrate and water in final volume of 1 ml) for several hours to several days. They were mounted in 60 % glycerol and examined on a microscope.

Chapter 3 : Allelic variation in the TIR-NLR WRR4 defines white rust resistance specificity

3.1 Introduction

Albugo candida is an oomycete causing white rust in Brassicaceae. There are many genetic races of *A. candida*, which are characterized by a strong host specificity (Jouet *et al.*, 2018). Sexual recombination has been reported between races, indicating that gene exchanges and emergence of new races are possible (McMullan *et al.*, 2015). Despite the host specificity, some crop-infecting races can grow in Arabidopsis. This compatibility has been exploited to map *White Rust Resistance* (*WRR*)-genes in Arabidopsis, to be cloned into crops. For instance, *WRR4A* and its paralog *WRR4B* from Arabidopsis Col-0 confer resistance to the *Brassica juncea*-infecting race Ac2V and to the *Brassica oleracea*-infecting race AcBoT (Borhan *et al.*, 2008; Cevik *et al.*, 2019). These resistances are effective in Arabidopsis and in crops (Borhan *et al.*, 2010; Cevik *et al.*, 2019).

Although *WRR4A* and *WRR4B* from Col-0 confer broad spectrum white rust resistance, *A. candida* race Exeter1 (AcEx1) can grow on Col-0 (Prince *et al.*, 2017). If *WRR4A* and *WRR4B* are deployed in Brassica crops, these resistances can conceivably be overcome. Moreover, AcEx1 can grow on the oil-producing crop *Camelina sativa*.

C. sativa has been engineered to produce a PUFA (polyunsaturated fatty acid)-rich oil. PUFA, particularly the long chain (LC-PUFA) such as eicosapentaenoic (EPA) and docosahexaenoic (DHA), are recognized for their health benefit. For example, they reduce the risk of coronary heart diseases (Sidhu, 2003). Land plants do not synthesise EPA and DHA. The main source for human consumption remains fish and seafood, which accumulate LC-PUFA from marine microalgae in the wild. In aquaculture, the main source of LC-PUFA is fish oil, which is an unsustainable practice (Tocher, 2015). *C. sativa* modified to express algal genes can produce fish-like oil containing 12% of DHA (Petrie *et al.*, 2014). This oil can effectively replace fish-oil from salmon feed, without affecting their nutritional quality for human consumption (Betancor *et al.*, 2015). The culture of transgenic *C. sativa* for fish oil-like production may increase in the next few years and cultures would be exposed to white rust, particularly the race AcEx1. *WRR* genes against AcEx1 from Arabidopsis could be used to protect *C. sativa* fields.

The Arabidopsis accessions Oy-0 and HR-5 resist AcEx1. Recombinant Inbred Lines (RILs) between Oy-0 and the AcEx1-compatible accession Col-0 were used to map and clone an AcEx1 *WRR* gene from Oy-0.

3.2 Results

3.2.1 Col-0 displays a weak WRR4A-dependent response to AcEx1

Although AcEx1 can achieve its life cycle on Col-0, a weak chlorotic response can be observed (

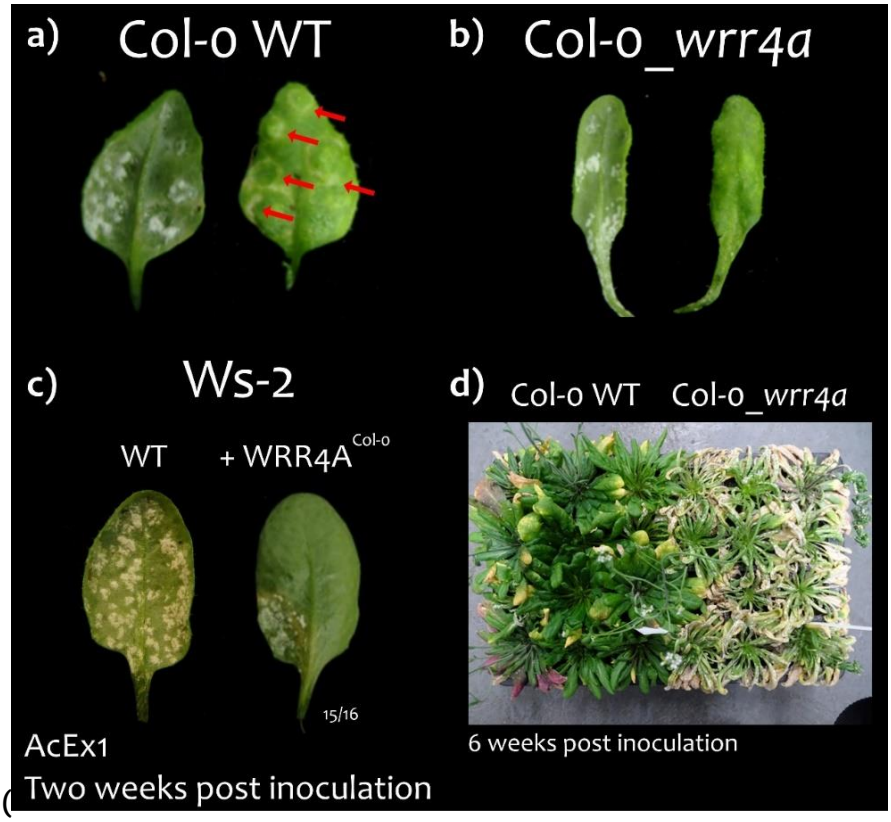

Figure 3-1**).** This chlorotic response is not seen in the fully susceptible accession Ws-2 or in a Col-0_*wrr4a* knock-out mutant. It indicates that WRR4A is activated upon AcEx1 infection but cannot trigger a sufficient immune response for pathogen growth arrest. Six weeks after inoculation, Col-0 WT (carrying *WRR4A*) shows less disease symptoms than Col-0_*wrr4a*. Ws-2 lines expressing *WRR4A* from Col-0 under the control of native 5' and 3' regulatory sequences are partially resistant. The resistance appears higher than in Col-0 WT likely due to elevated expression of the transgene compared to natural expression level. Since WRR4A response is weak and is not sufficient to arrest the pathogen propagation, Col-0 is considered as susceptible in this study.

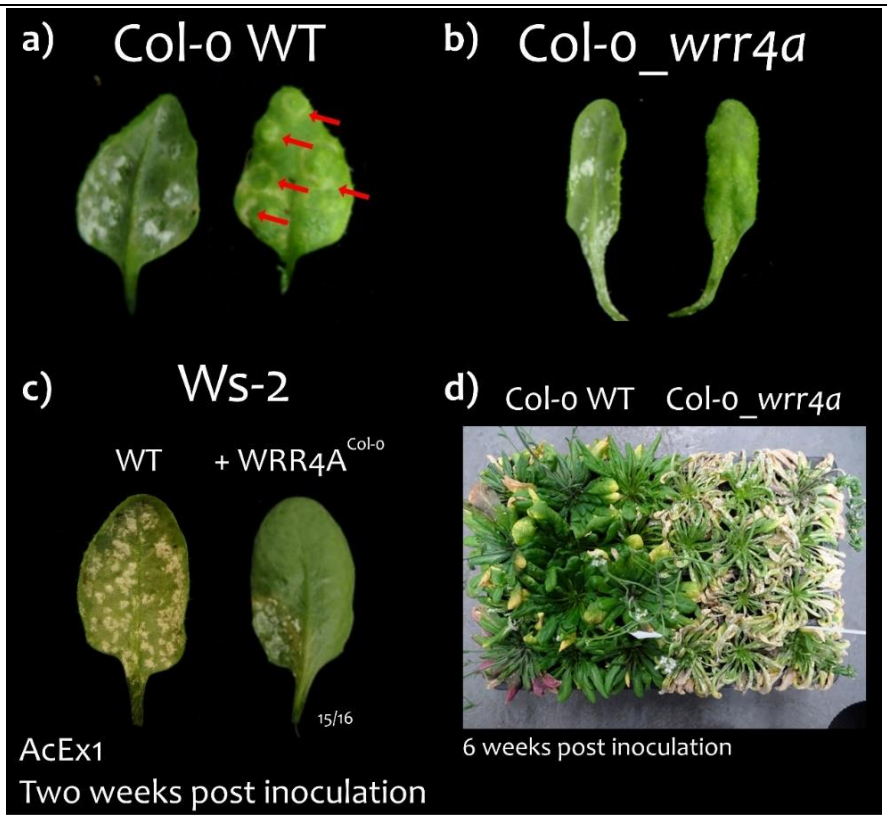

Figure 3-1: WRR4ACol-0 confers weak response to AcEx1 infection
Col-0, Col-0_*wrr4a*, Ws-2 and Ws-2_WRR4A^{Col-0} (expressing *WRR4A*$^{Col-0}$ under the control of native 5' and 3' regulatory sequences) were spray inoculated with AcEx1. **a.-c.** Pictures were taken 2 weeks post inoculation. **d.** Picture was taken six weeks post inoculation. **a.** Col-0 displays chlorotic response indicated by red arrows. **b.** Col-0_*wrr4a* is fully susceptible. **c.** Ws-2 WT is fully susceptible. Ws-2 turns partially resistant when expressing WRR4A from Col-0. This phenotype was observed in 15/16 lines from two independent transformants. One plant was fully resistant. **d.** Six-week post inoculation, Col-0_*wrr4a* plants developed more symptoms than Col-0 WT.

3.2.2 Oy-0 resists AcEx1 via two loci *WRR13* and *WRR11*

Volkan Cevik and Sebastian Fairhead previously conducted a Quantitative Trait Locus (QTL) analysis among RILs between a resistant parent Oy-0 and a susceptible parent Col-0. It indicates that two major loci are involved in AcEx1 resistance in Oy-0: the *WRR13* locus on chromosome 1 (20,384,267 - 22,181,333 bp) and the *WRR11* locus on chromosome 3 (17,282,622 - 19,628,061 bp). There is also a small QTL on chromosome 5, called *WRR15*. This QTL is below the LOD score threshold and was not further investigated.

RenSeq (*R*-gene enrichment sequencing) helps define the NLR repertoire of a sample (Jupe *et al.*, 2013). Oliver Furzer conducted RenSeq in Oy-0 and identified all the NLRs associated with *WRR13* and *WRR11*. The *WRR13* locus contains a cluster of TIR-NLRs, orthologous to the *WRR4* cluster in Col-0, and a CC-NLR cluster, orthologous to the *RPP7* cluster in Col-0. The organisation of the *WRR4* locus is different between Oy-0 and Col-0.

In Col-0 there are three genes referred as *WRR4A*, *WRR4B* and At1g56520 (*WRR4C*) (Cevik *et al.*, 2019). In Oy-0, *WRR4A* and *WRR4B* are presents, *WRR4C* is pseudogenised and a fourth paralog, called *WRR4D*, is present distal to *WRR4A*. The *WRR11* locus contains two TIR-NLR encoding genes, paired in a head-to-head orientation (At3g51560-At3g51570), the CC-NLR encoding gene *ZAR1*, the *RPW8* cluster and a CC-NLR encoding gene absent in Col-0.

3.2.3 Fine mapping of *WRR13*

Twelve RILs recombine within the *WRR13* locus. Based on their phenotype and on their genotype at *WRR11* and *WRR15* loci, three have the Col-0 allele of *WRR13*, three have the Oy-0 allele and six were not considered as they could be either **(Table 3-1)**.

Line	*WRR13*	*WRR11*	*WRR15*	Phenotype	If Col-0	If Oy-0	*WRR13* allele
506	recombinant	Col-0	Col-0	5	4 to 5	3 to 5	?
252	recombinant	Col-0	Col-0	4	4 to 5	3 to 5	?
315	recombinant	Col-0	Col-0	5	4 to 5	3 to 5	?
189	recombinant	Col-0	**Oy-0**	3	3 to 5	1 to 4	?
64	recombinant	Col-0	Col-0	5	4 to 5	3 to 5	?
103	recombinant	Col-0	Col-0	5	4 to 5	3 to 5	?
91	recombinant	**Oy-0**	**Oy-0**	3	3 to 4	0 to 2	Col-0
298	recombinant	**Oy-0**	**Oy-0**	3	3 to 4	0 to 2	Col-0
118	recombinant	**Oy-0**	**Oy-0**	3	3 to 4	0 to 2	Col-0
273	recombinant	Col-0	Col-0	3	4 to 5	3 to 5	Oy-0
19	recombinant	**Oy-0**	**Oy-0**	0	3 to 4	0 to 2	Oy-0
336	recombinant	**Oy-0**	**Oy-0**	2	3 to 4	0 to 2	Oy-0

Table 3-1: Phenotypes and genotypes of *WRR13* recombinant lines
The phenotype is scored on a scale from 0 (fully resistant) to 5 (as susceptible as Col-0). The "if Col-0" column indicates the phenotypic score range in RILs having the indicated genotype at *WRR11* and *WRR15* loci and being Col-0 at the *WRR13* locus. The "if Oy-0" column indicates the phenotypic score range in RILs having the indicated genotype at *WRR11* and *WRR15* loci and being Oy-0 at the *WRR13* locus. Oy-0 alleles are highlighted in bold. The score range matching the score of each line is underlined.

I identified a SNP (Single Nucleotide Polymorphism; C1_21,195) and a RFLP (Restriction Fragment Length Polymorphism; C1_21,691) marker within *WRR13*, between the *WRR4*

and *RPP7* clusters. These markers enabled fine mapping (

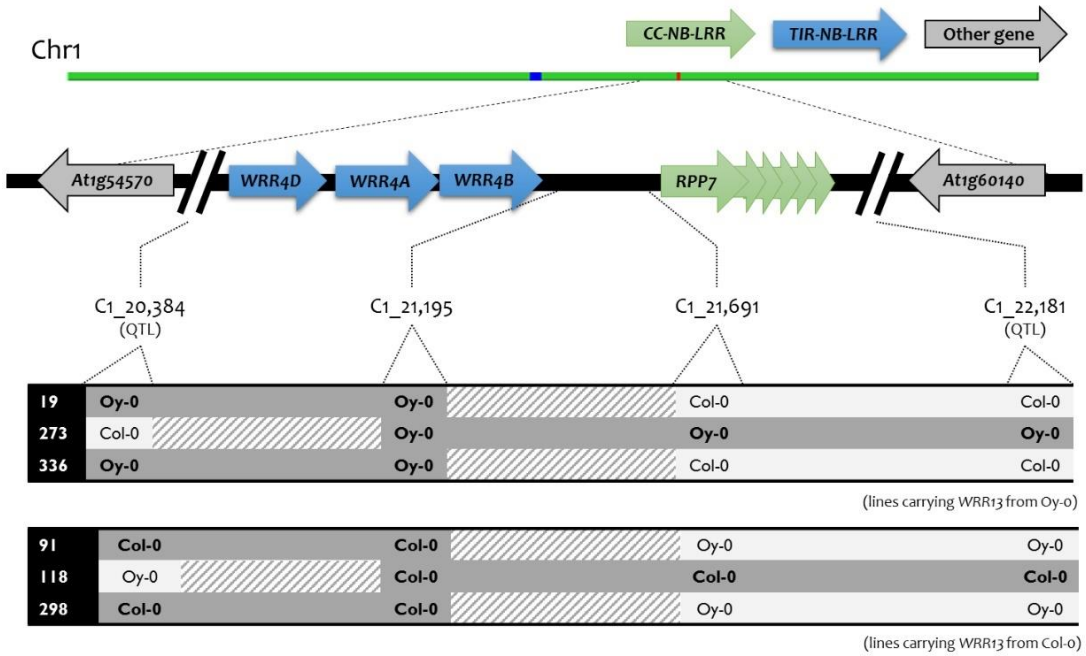

Figure 3-2**)**. Four lines eliminate the *RPP7* cluster from the *WRR13* QTL. None eliminates *WRR4*, indicating that *WRR13* resistance is mediated by one or several of the *WRR4* paralogs or by a non NLR-encoding gene in the vicinity.

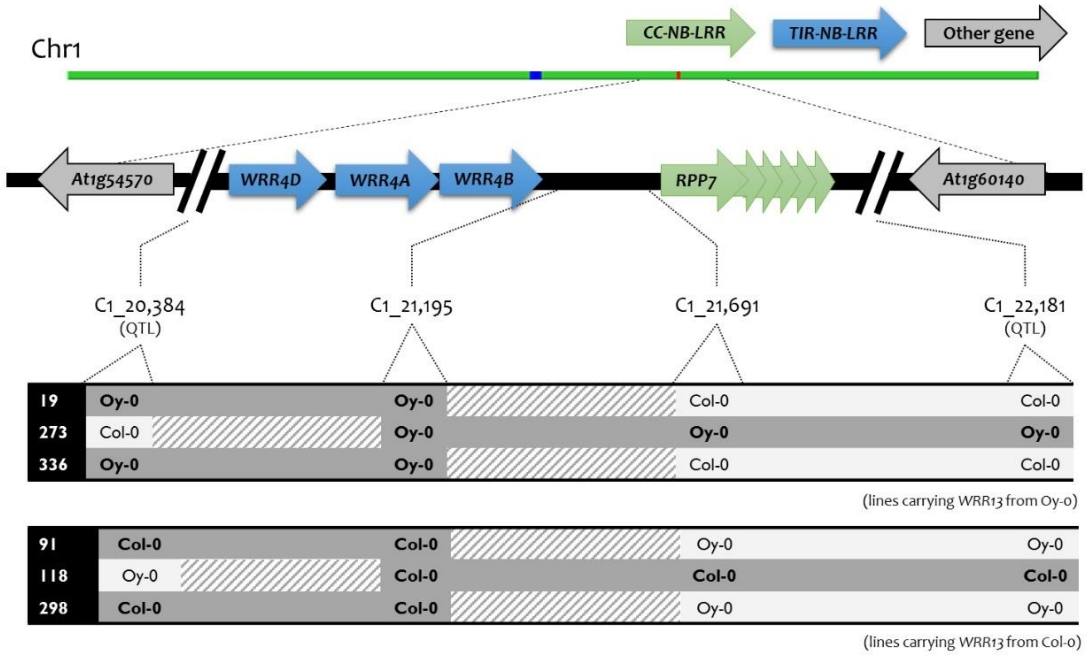

Figure 3-2: The *WRR13* QTL includes the *WRR4* cluster but not the *RPP7* cluster
Six lines were genotyped using two markers within the *WRR13* QTL. Dark grey indicates the presence of the gene underlying *WRR13* resistance, light grey indicates its absence. Dash grey indicates the recombination locus, which can contain the gene underlying *WRR13* resistance. Arrows indicates genes from the Oy-0 resistant genotype. The names of the markers refer to the position in kb on chromosome 1. Figure is not on scale.

3.2.4 Fine mapping of *WRR11*

Eight RILs recombine within the *WRR11* locus. Based on their phenotype and on their genotype at *WRR13* and *WRR15* loci, three have the Col-0 allele of *WRR11*, three have the Oy-0 allele and two were not considered as they could be either **(Table 3-2)**.

Line	*WRR13*	*WRR11*	*WRR15*	Pheno-types	If Col-0	If Oy-0	*WRR11* allele
162	Col-0	recombinant	**Oy-0**	4 – 4 – 4	4 to 5	3 to 4	?
304	Col-0	recombinant	**Oy-0**	3 – 3 – 2	4 to 5	3 to 4	Oy-0
471	**Oy-0**	recombinant	Col-0	4 – 4 – 4	4 to 5	1 to 3	Col-0
472	**Oy-0**	recombinant	Col-0	4 – 4 – 3	4 to 5	1 to 3	Col-0
497	Col-0	recombinant	Col-0	5 – 4 – 4	4 to 5	3	Col-0
155	**Oy-0**	recombinant	**Oy-0**	0 – 0 – 0	1 to 3	0 to 2	Oy-0
367	Col-0	recombinant	Col-0	3 – 3 – 4	4 to 5	3	?
403	Col-0	recombinant	Col-0	3 – 2 - 3	4 to 5	3	Oy-0

Table 3-2: Phenotypes and genotypes of *WRR11* recombinant lines
The phenotype is scored on a scale from 0 (fully resistant) to 5 (as susceptible as Col-0). Lines have been phenotyped three times independently. The "if Col-0" column indicates the phenotypic score range in RILs having the indicated genotype at *WRR13* and *WRR15* loci and being Col-0 at the *WRR11* locus. The "if Oy-0" column indicates the phenotypic score range in RILs having the indicated genotype at *WRR13* and *WRR15* loci and being Oy-0 at the *WRR11* locus. Oy-0 alleles are highlighted in bold. The score range matching the score of each line is underlined.

I identified three RFLP (C3_18,016; C3_18,535; C3_18,850), one CAPS (Cleaved Amplified Polymorphic Sequence; C3_19,122) and one SNP (C3_18,937) markers within *WRR11*. These markers enabled fine mapping (

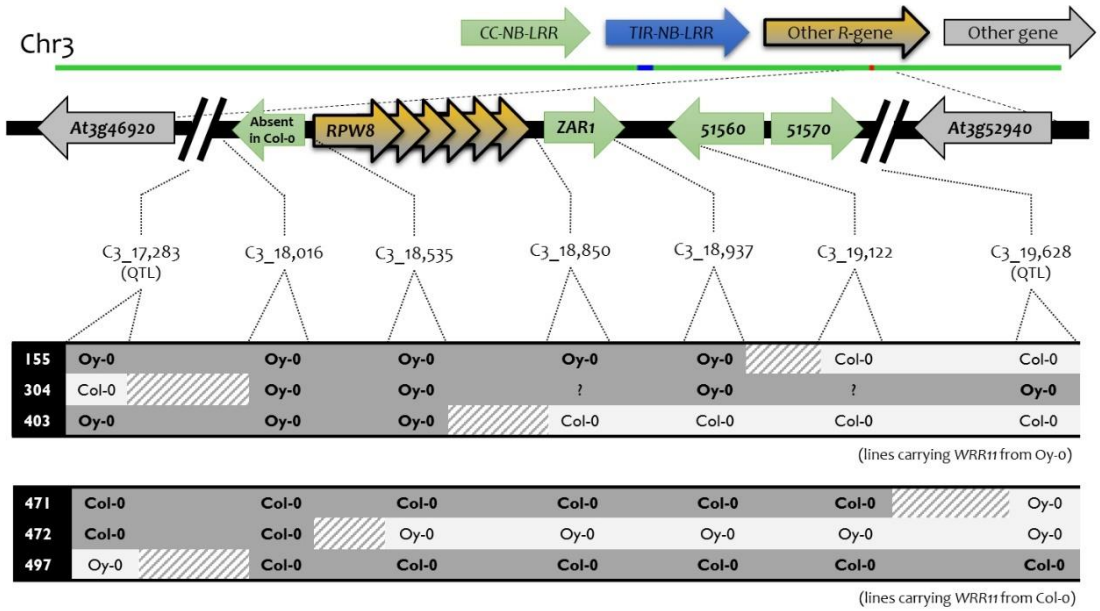

Figure 3-3**)**. Three lines eliminate the TIR-NLR pair, two lines eliminate *ZAR1* and one line eliminates the *RPW8* cluster. It suggests that *WRR11* resistance is mediated by the CC-NLR absent from Col-0 or by a non NLR-encoding gene in its vicinity.

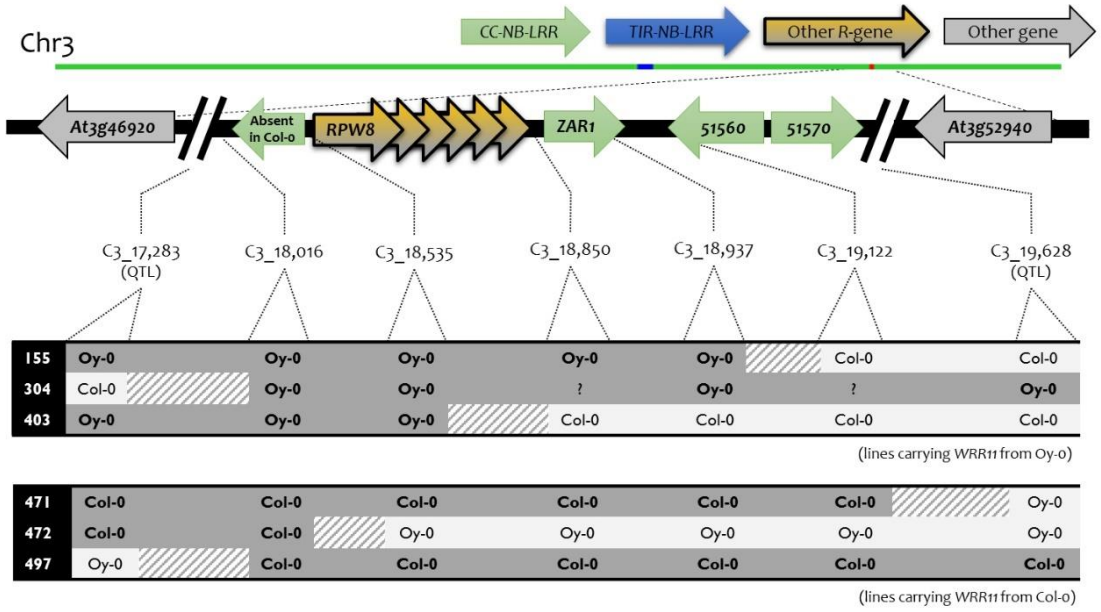

Figure 3-3: The *WRR11* QTL includes a CC-NLR absent from Col-0
Six lines were genotyped using five markers within the *WRR11* QTL. Dark grey indicates the presence of the gene underlying *WRR11* resistance, light grey indicates its absence. Dash grey indicates the recombination locus, which can contain the gene underlying *WRR11* resistance. Arrows indicates genes from the Oy-0 resistant genotype. The names of the markers refer to the position in kb on chromosome 3. Figure is not on scale.

3.2.5 *WRR4A*$^{Oy\text{-}0}$ confers full resistance to AcEx1

In chromosome 1, *WRR4A*, *WRR4B* and *WRR4C* are three TIR-NLRs candidates to be *WRR13*. On chromosome 3, a CC-NLR absent from Col-0 is candidate to be WRR11 (hereafter *CWR11* for *Candidate to be WRR11*). I cloned *WRR4A*, *WRR4B*, *WRR4C* and *CWR11* from Oy-0 with their natural 5' and 3' regulatory sequences by the USER method (Geu-Flores *et al.*, 2007)

and expressed them in the fully susceptible accession Ws-2 (

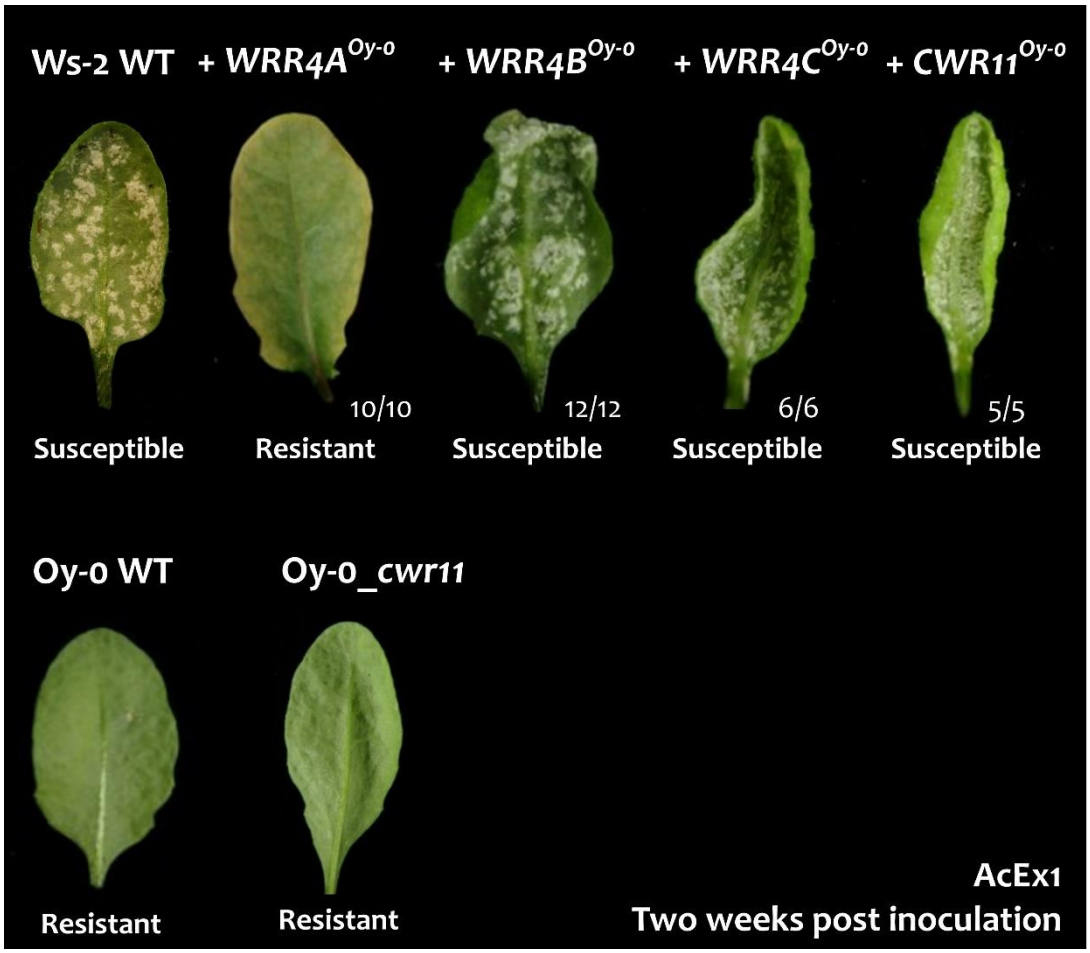

Figure 3-4). Only *WRR4A*$^{Oy-0}$ confers full resistance to AcEx1; all the other genes do not contribute to resistance at all. As *CWR11* is the only NLR candidate at the *WRR11* locus, I used CRISPR to test also its role in AcEx1 resistance by loss-of-function. Briefly, I assembled *Cas9* with the *UBI10* promoter along with two sgRNAs targeting specifically *CWR11* (TGAAGTACTTGCAGCTAAAG**nGG** and AGGAAGATCAAGGTTTGCAG**nGG**) and a FAST-Red selectable marker. The construct was expressed in Oy-0. Three T1 lines out of seven showed somatic activity. I selected eight Cas9-free (*i.e.* selected against FAST-Red) T2 progenies for each of the three lines. Out of these 24 lines, 17 were WT, five were heterozygous and one was homozygous *cwr11* mutant. The homozygous mutation is a c.197del (of 2571 bp total CDS), resulting in an early stop codon in the CC domain encoding

region. This line is fully resistant to AcEx1 (

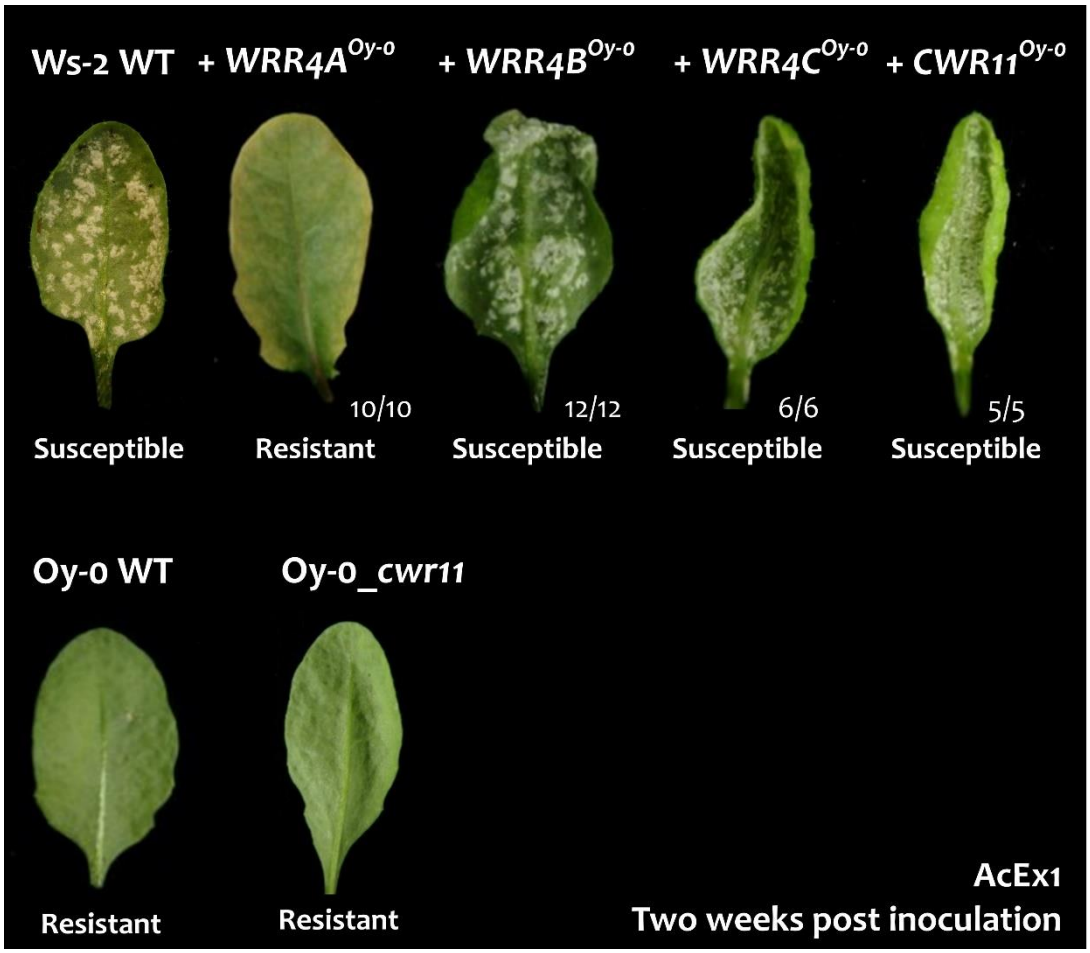

Figure 3-4). Gain-of-function and loss-of-function approaches show that *CWR11* is not sufficient nor required for AcEx1 resistance.

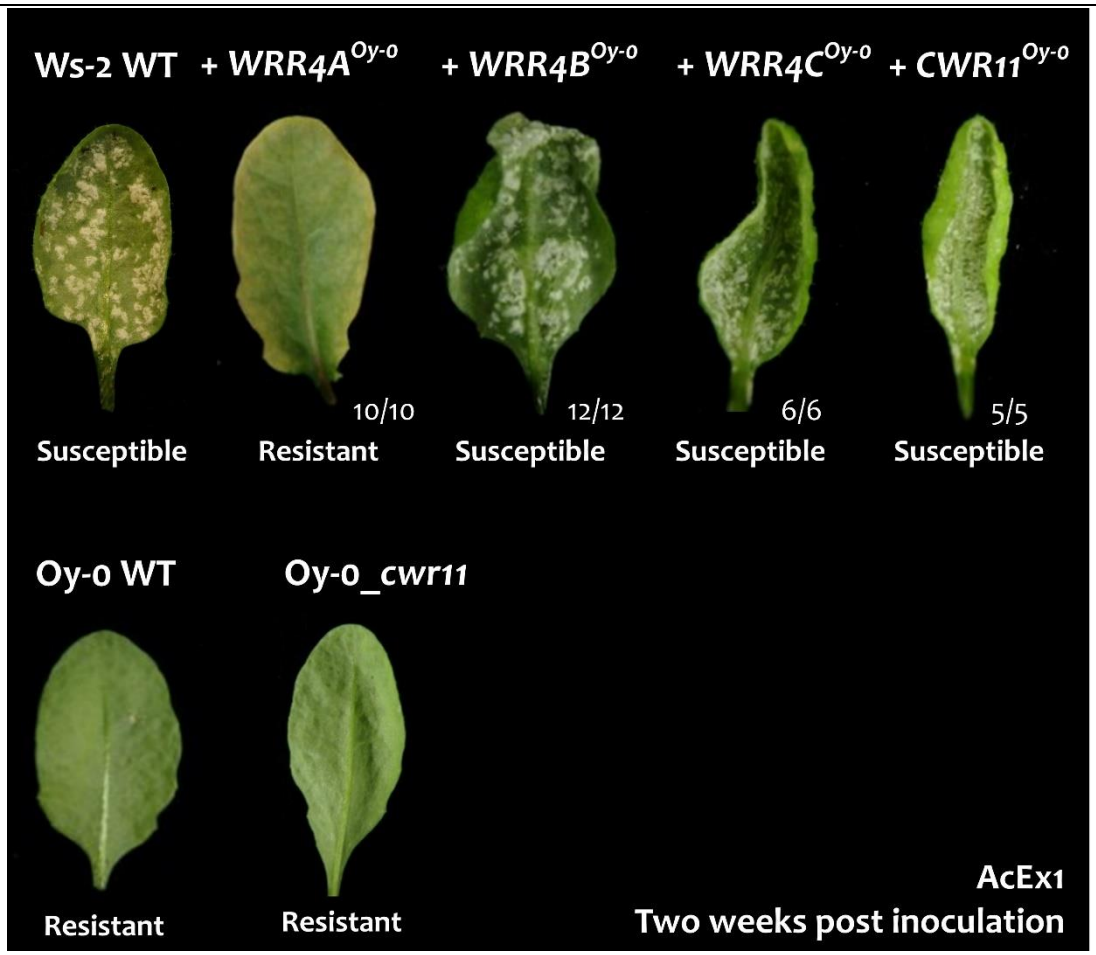

Figure 3-4: *WRR4A*$^{Oy-0}$ confers full resistance to AcEx1
Four genes were cloned from Oy-0 into the AcEx1-susceptible accession Ws-2. *CWR11* was also removed (Oy-0_*cwr11*) from the resistant accession Oy-0. Plants were sprayed inoculated with AcEx1 and pictures were taken two weeks after inoculation. The phenotypes are indicated under each picture. The numbers indicate the number of lines displaying the indicated phenotype out of the number of independent T1 lines transformed with the indicated gene.

3.2.6 An early stop codon in *WRR4A* confers specificity in *Albugo candida* secreted protein recognition

The Col-0 allele of *WRR4A* confers a response to AcEx1 which is not full resistance (

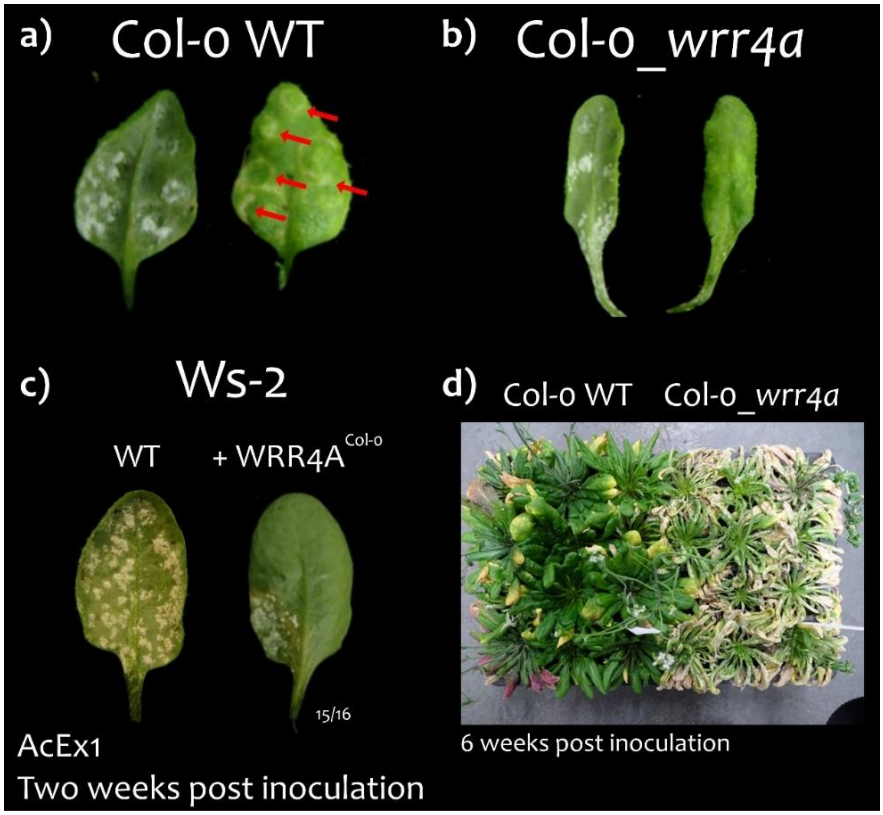

Figure 3-1), while the Oy-0 allele of *WRR4A* confers full resistance to AcEx1 (

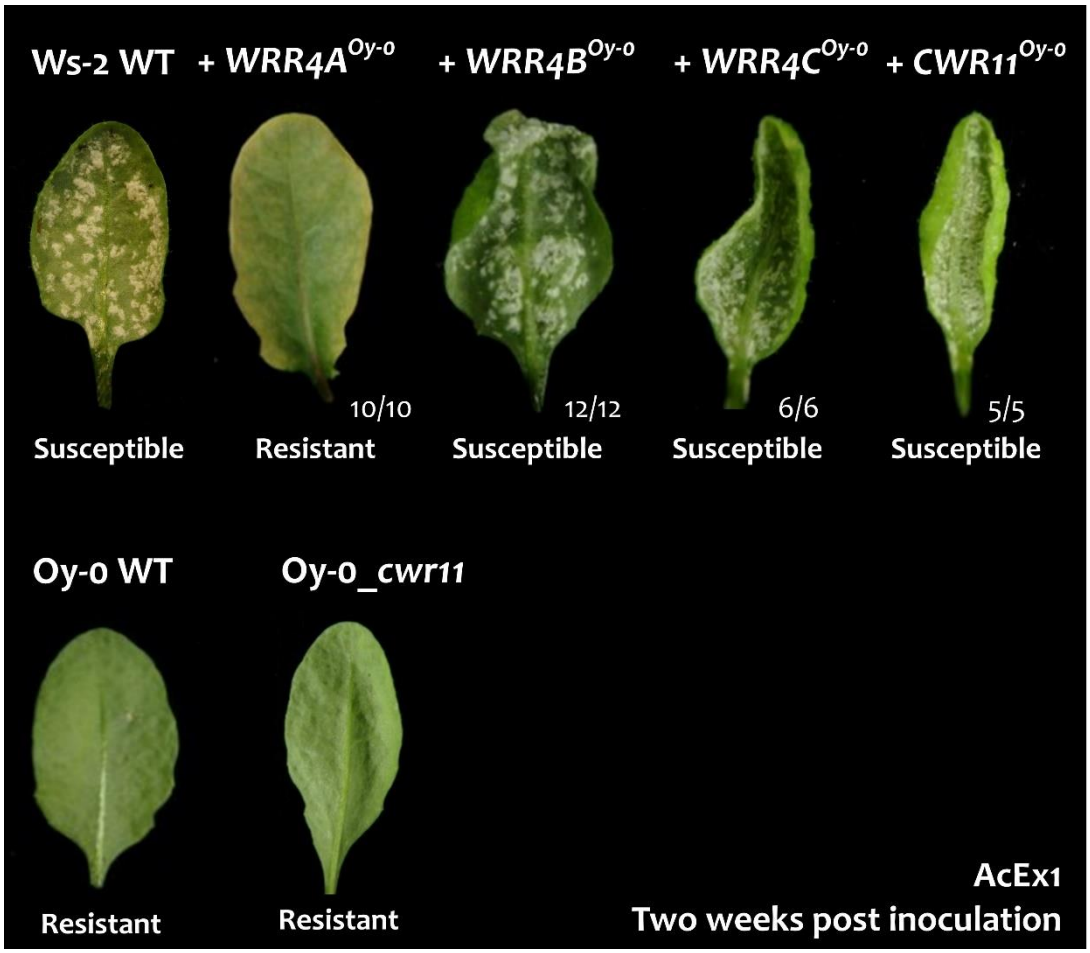

Figure 3-4). I investigated the polymorphism between Oy-0 and Col-0 alleles to explain this dissimilar function. There are 26 non-synonymous SNPs, a 1- and an 8-amino acids

deletion in WRR4A$^{Oy\text{-}0}$ compared to the Col-0 allele (

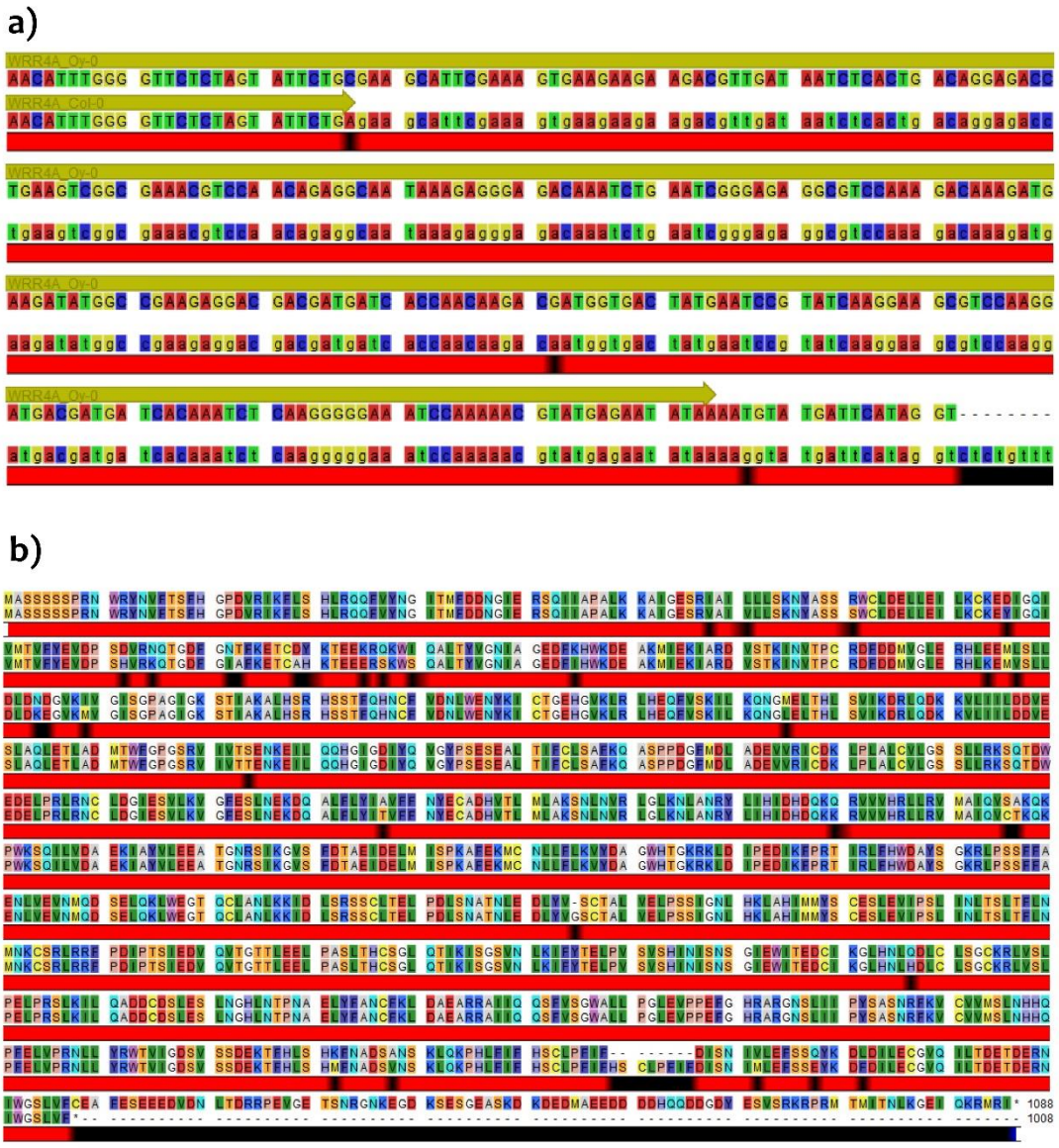

Figure 3-5**).** The most striking difference is an early stop codon in Col-0 that causes an 89-amino acid c-terminal deletion.

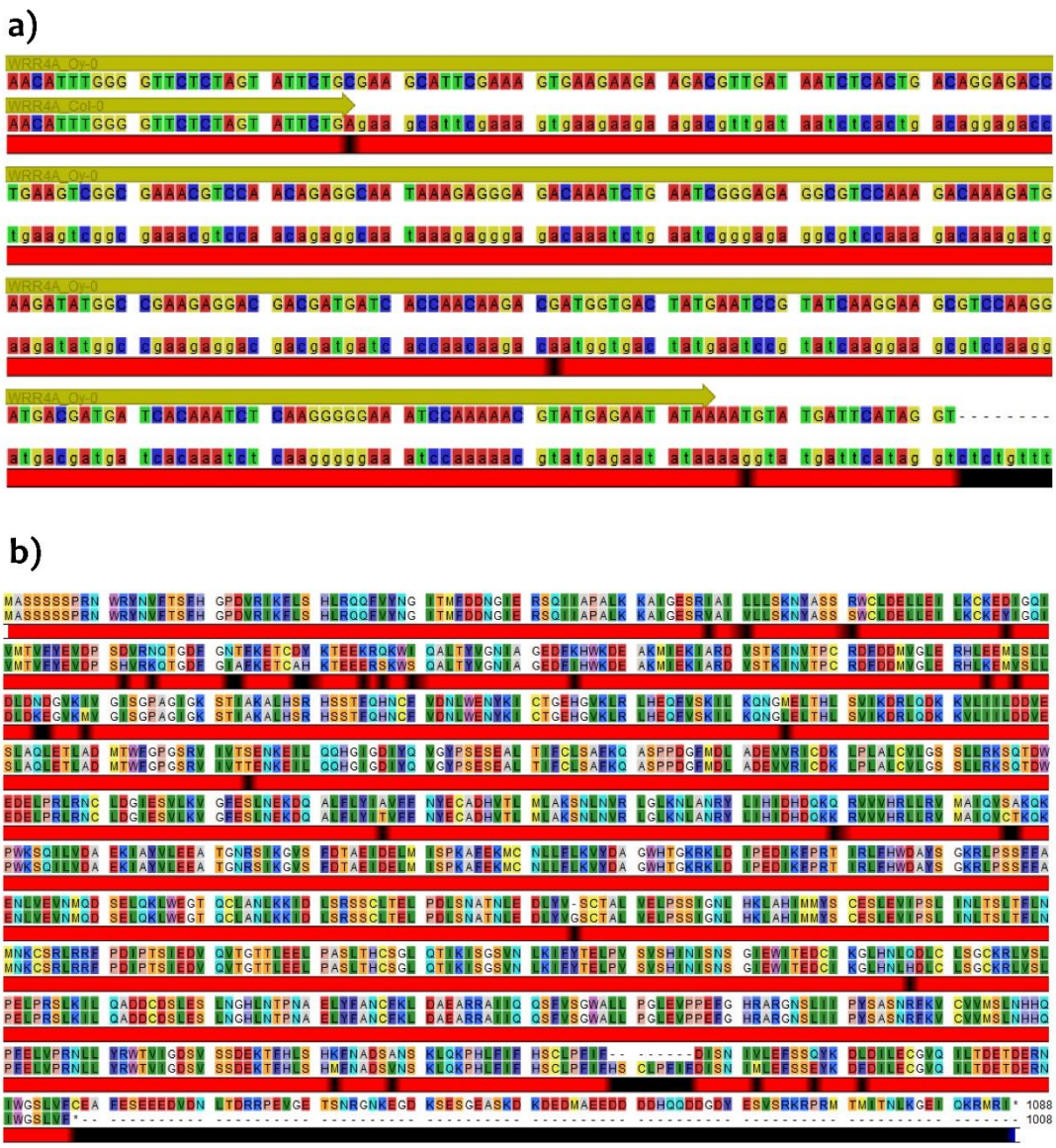

Figure 3-5: Alignment of the Col-0 and the Oy-0 alleles of WRR4A
a. Nucleotide alignment from nucleotide 2998/3024 in Col-0 CDS. Oy-0 is on top, Col-0 is on bottom. Red indicates identity, black indicates polymorphism. **b.** Amino acid alignment of the entire protein sequences. Oy-0 is on top, Col-0 is on bottom. Red indicates identity, black indicates polymorphism.

To test the relevance of this polymorphism, I cloned four alleles of *WRR4A* with the USER method under the control of the *35S* promoter: Col-0 WT, Oy-0 WT, Col-0 without its stop codon and including the following 267 nt (Col-0_ΔSTOP) and Oy-0 with a restored stop codon and lacking the following 267 nt (Oy-0_+STOP). I tested these constructs in transient expression in tobacco leaves for recognition of *Albugo candida* secreted protein

from the CCG family (

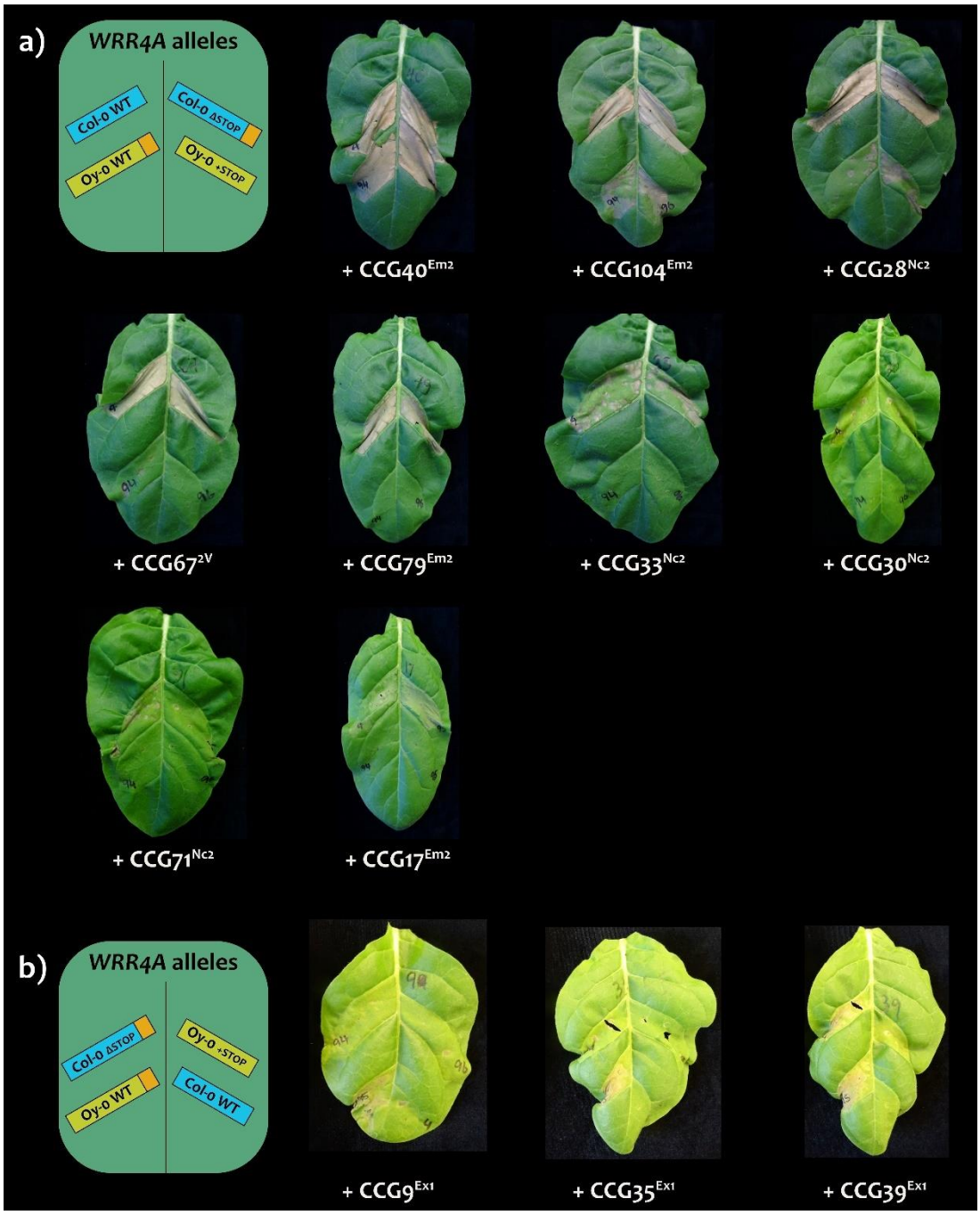

Figure 3-6). HR (hypersensitive response causing macroscopic cell death) was used as a marker of CCG recognition. Amey Redkar and Volkan Cevik previously identified nine CCG proteins recognised by WRR4A$^{Col\text{-}0}$ (Redkar *et al.*, in prep.). These nine CCGs are still recognised by WRR4A$^{Col\text{-}0\Delta STOP}$. Only one is also recognised by WRR4A$^{Oy\text{-}0}$, three are weakly

recognised and five are not recognised at all (

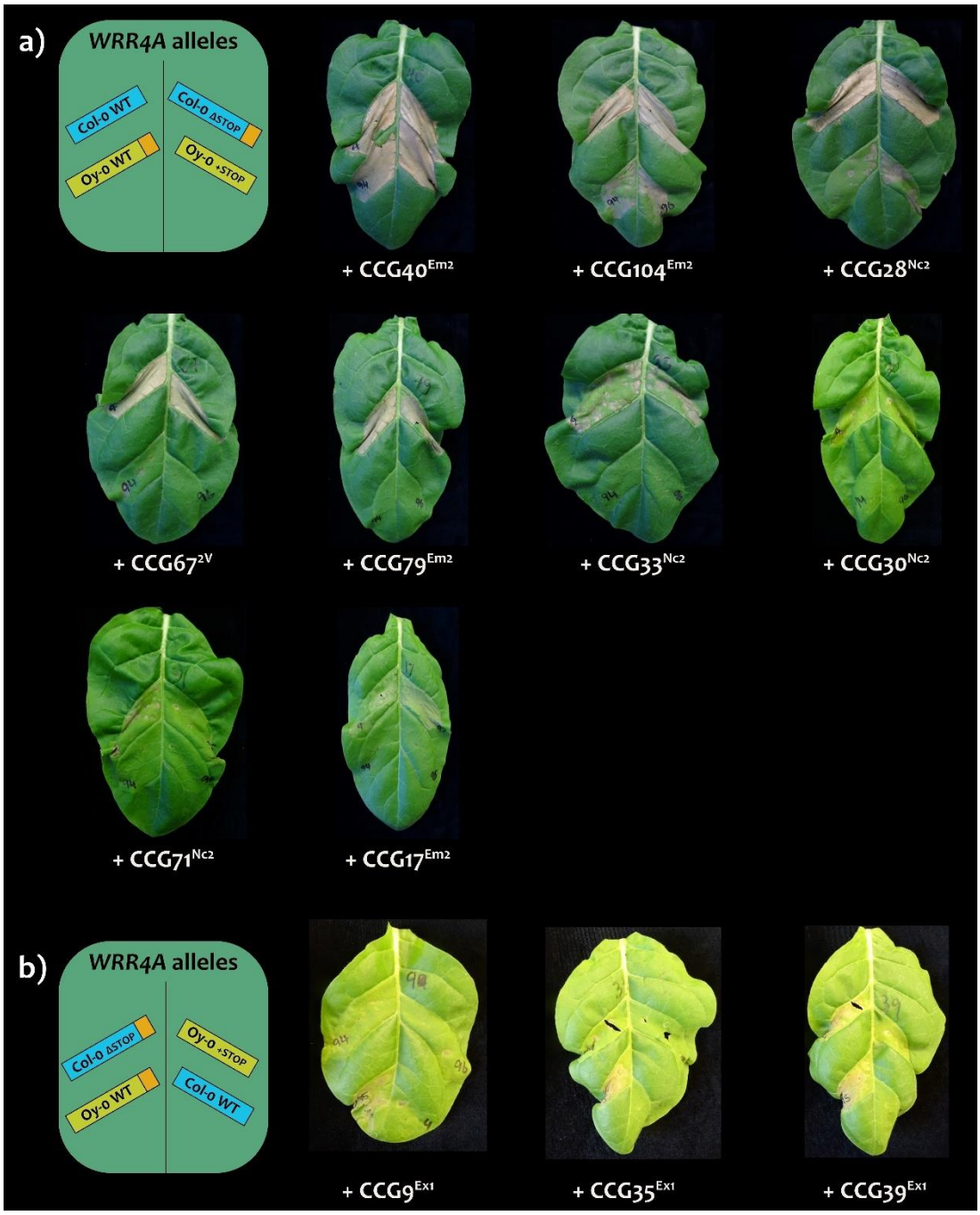

Figure 3-6). It indicates that the recognition of these nine avirulence factors is mediated by the core section of the TIR-NLR. In contrast, three CCGs from AcEx1 are specifically recognised by the Oy-0 allele of WRR4A. They are recognised by WRR4A$^{Col\text{-}0\Delta STOP}$ even

more strongly, but they are not recognised by WRR4A$^{Oy\text{-}0+STOP}$ (

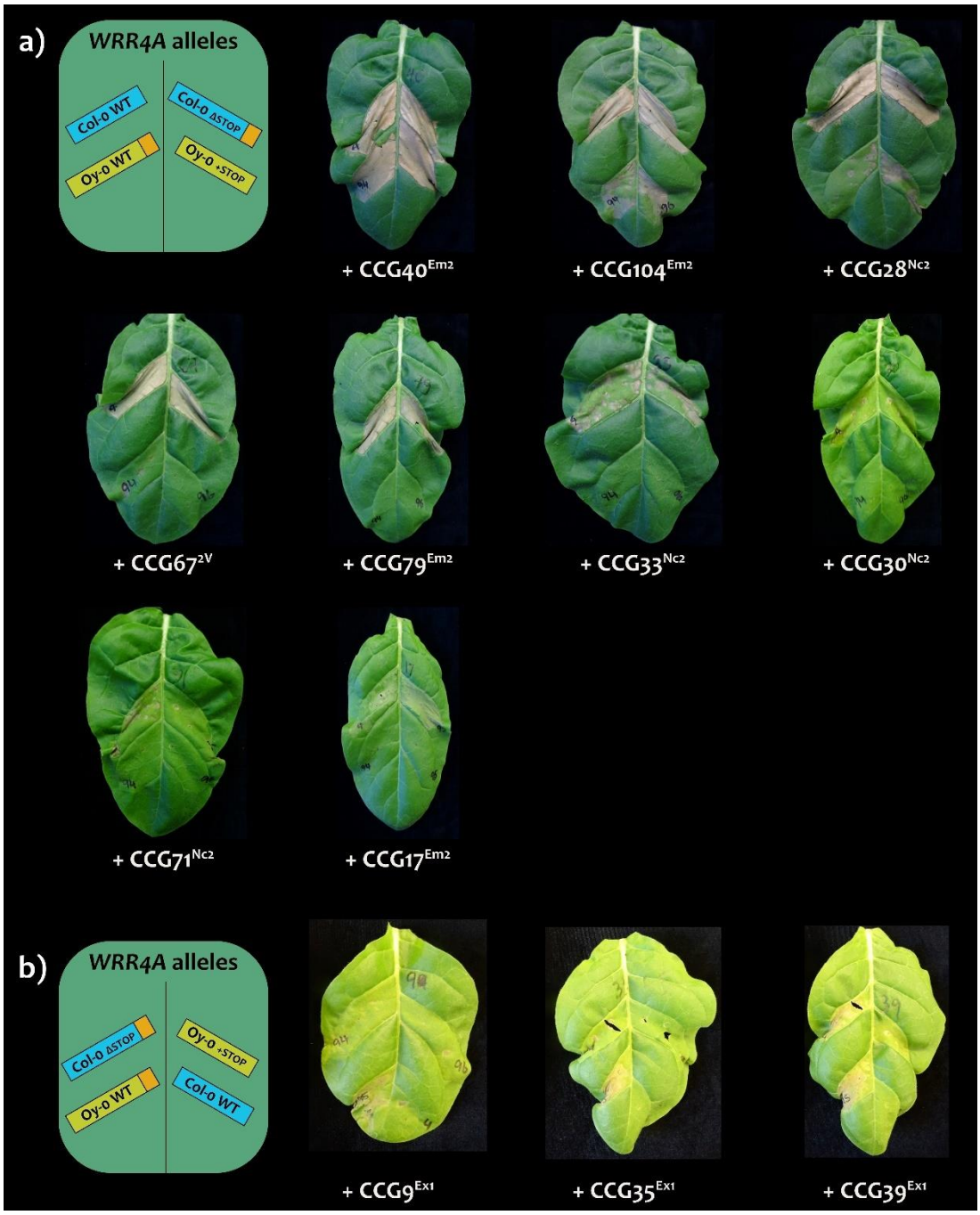

Figure 3-6). It indicates that the c-terminal extension is required for their recognition.

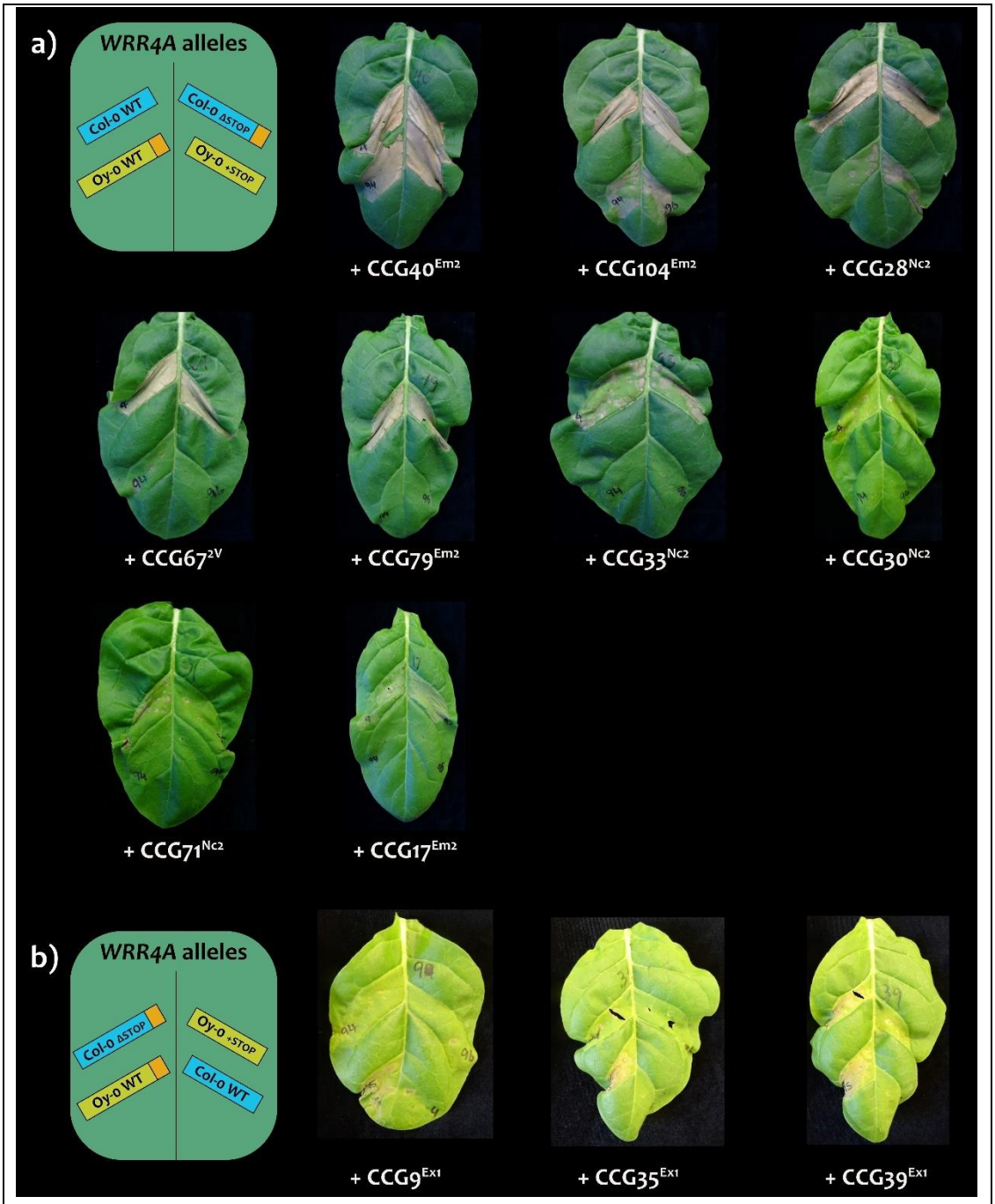

Figure 3-6: An early stop codon in *WRR4A* confers enhanced or loss of recognition of some CCGs
Tobacco leaves (cv Petit Gerard) were infiltrated with *Agrobacterium tumefaciens* delivering denoted constructs via T-DNA somatic integration, at OD_{600} = 0.3. *WRR4A* alleles were infiltrated in the positions indicated in the cartoon on the left. Pictures were taken 3 days after infiltration. CCG alleles are indicated in superscript, according to the *Albugo candida* race they are cloned from. **a.** Test of nine CCGs recognised by $WRR4A^{Col\text{-}0}$. **b.** Test of three CCGs from AcEx1. Data from Amey Redkar.

3.2.7 *WRR4A*$^{Oy\text{-}o}$ resistance can be transferred in the crop *Camelina sativa*

The oil-producing crop *C. sativa* is susceptible to AcEx1 **(Figure 3-7)**. I challenged ten *C. sativa* cv Celine WT plants with AcEx1 and observed disease symptoms two weeks after inoculation. Eight plants displayed white rust on one single leaf; two plants were not infected at all. AcEx1 is not as virulent on *C. sativa* than on Arabidopsis. I transformed *WRR4A*$^{Oy\text{-}o}$ with its natural 5' and 3' regulatory sequences in *C. sativa* cv Celine. I identified independent transformants with WT-like symptoms, reduced symptoms or no symptoms upon AcEx1 inoculation. All the lines with reduced or no symptoms expressed *WRR4A*$^{Oy\text{-}o}$ **(Figure 3-7)**. I tested the transgenic (*i.e.* selected for FAST-Red) T2 progeny of four independent transformants. Lines #1 and #7 segregate 15:1 and lines #5 and #10 segregate 3:1 for FAST-Red, indicative of two and one locus T-DNA insertion respectively. Transgenic (homozygous or heterozygous) progenies of lines #5 and #10 contains 5/9 and 4/10 resistant plants respectively. I harvested seeds from these nine resistant plants for further investigation.

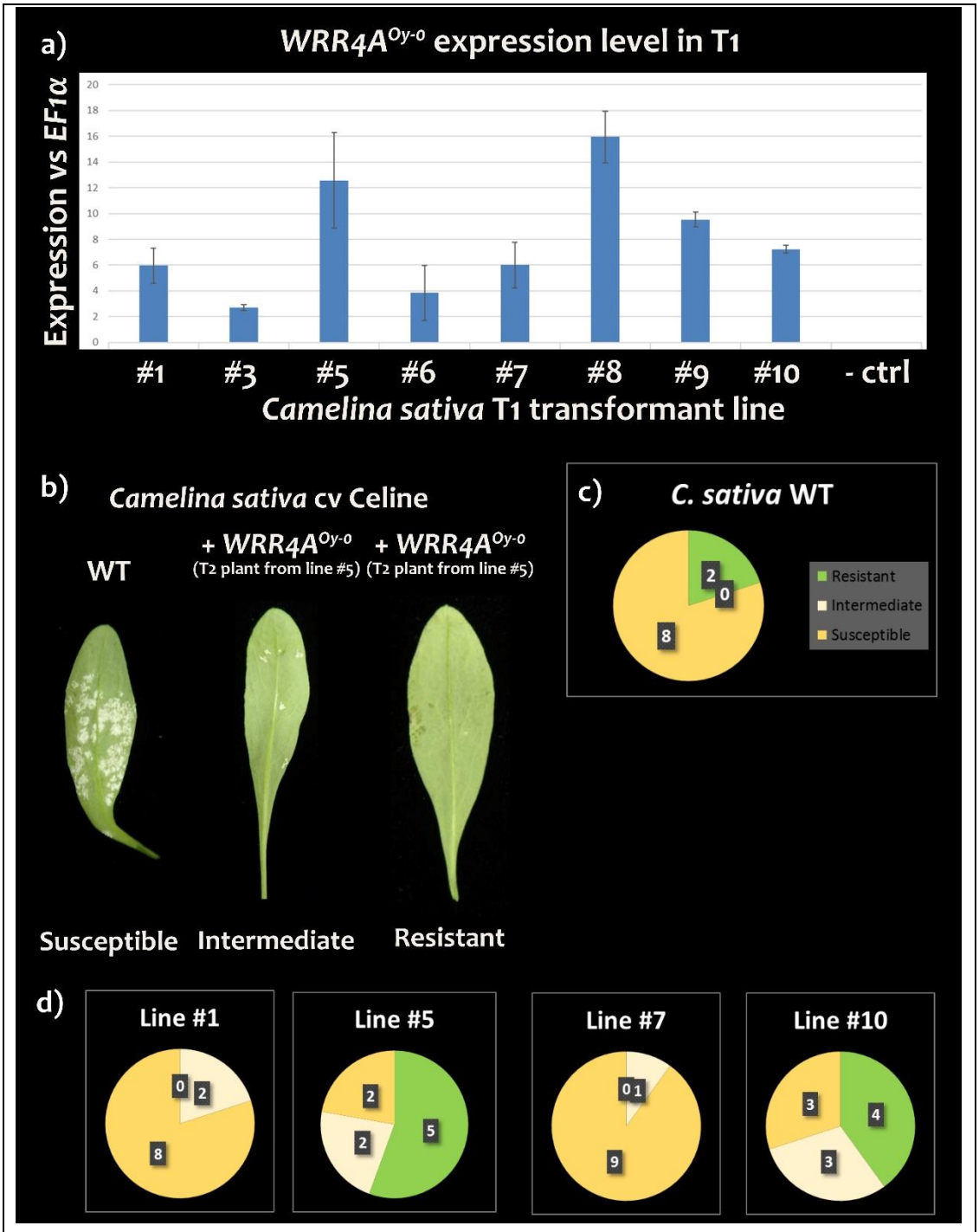

Figure 3-7: Some *C. sativa* expressing *WRR4A*$^{Oy-0}$ display enhanced resistance to AcEx1
a. Expression of *WRR4A*$^{Oy-0}$ in eight *Camelina sativa* lines showing resistance or intermediate phenotype in response to AcEx1. Expression is relative to *EF1α*. RNA was extracted from AcEx1 inoculated plants, 3 weeks post inoculation. – ctrl = negative control, *i.e. C. sativa* line transformed with *CWR11*. *WRR4A*$^{Oy-0}$ is expressed at different levels and is not expressed in a line not transformed with *WRR4A*$^{Oy-0}$. **b.** Examples of AcEx1 symptoms on WT or *WRR4A*$^{Oy-0}$ transgenic *Camelina sativa* cv Celine plants. Pictures were taken at 12 dpi. **c.** Phenotypes of ten *Camelina sativa* cv Celine plants WT, two weeks after AcEx1 inoculation. Some plants do not show symptoms. **d.** Phenotypes of nine or ten *Camelina sativa* cv Celine plants, two weeks after AcEx1 inoculation. Lines are *WRR4A*$^{Oy-0}$ transgenic T2 lines, either homozygous or heterozygous.

3.3 Discussion

3.3.1 *WRR11* QTL on chromosome 3 remains unrevealed

WRR11 is a major QTL involved in AcEx1 resistance to AcEx1 in Oy-0. The only NLR encoding gene associated with the locus is not involved in AcEx1 resistance, as showed by gain-of-function in Ws-2 and loss-of-function in Oy-0 **(Figure 3-4)**. It is possible that that the resistance is mediated by another gene from the locus. Based on the Col-0 genome, there are 645 genes linked to *WRR11*, from At3g46930 to At3G50010. These genes include *SNIPER4*, *RLP44*, *PMEI11*, *EDS1* and many uncharacterised genes. SNIPER4 is involved in signalling of the TIR-NLR SNC1 (Huang *et al.*, 2018). RLP44 interacts with BAK1 and is involved in development (Wolf *et al.*, 2014). PMEI11 is a pectin methylesterase inhibitor involved in resistance against the fungus *Botrytis cinerea* (Lionetti *et al.*, 2017). EDS1 is a lipase-like protein involved in NLR signalling (Parker *et al.*, 1996).

3.3.2 An early stop codon in a TIR-NLR causes loss of recognition of AcEx1

WRR4A$^{Oy\text{-}0}$ provides full resistance to AcEx1, while the Col-0 allele does not **(Figure 3-1 and Figure 3-4)**. The major polymorphism is an early stop codon in Col-0, which causes an 89-amino acid c-terminal deletion. This extension, in Oy-0 or in a mutated Col-0 allele of *WRR4A*, enables recognition of at least three CCGs of AcEx1 **(Figure 3-6)**. They are not recognised by the WT allele of Col-0 or by a mutated allele of Oy-0. Conceivably, the ancestral state of WRR4A had the c-terminal extension. In the absence of AcEx1 selection pressure, an early stop codon mutation occurred in the Col-0 lineage, which also evolved to recognise more CCGs from the races AcEm2, Ac2V and AcNc2. The loss of the extension may confer an advantage in Col-0, such as the recognition of additional avirulence factors or an intramolecular regulation for a balanced immune signalling, but the current data do not demonstrate it.

3.3.3 Crops can be protected using *R*-genes from Arabidopsis

WRR4A$^{Col\text{-}0}$ confers resistance to Ac2V in *B. juncea* and to AcBoT in *B. oleracea* (Borhan *et al.*, 2010; Cevik *et al.*, 2019). As AcEx1 can grow on the crop *C. sativa*, I tested if the *WRR4A*$^{Oy\text{-}0}$ resistance was transferable from Arabidopsis to *C. sativa*. I used the European cultivar Celine because it is the one used to engineer the DHA/EPA-producing line (Petrie *et al.*, 2014). AcEx1 is not particularly virulent in *C. sativa* cv Celine **(Figure 3-7)**. AcEx1 is part of *A.*

candida group II while the *C. sativa* infecting races are part of the group III (Jouet *et al.*, 2018). Groups II and III are very close but distinct. Group III effectors may be more specialised to infect *C. sativa* than the effectors from Group II, explaining the partial compatibility between AcEx1 and *C. sativa*.

I identified two *WRR4A*$^{Oy\text{-}o}$ transgenic *C. sativa* lines with single locus insertion. The progeny of these lines contains slightly more resistant plants than a WT population. The occurrence of susceptible lines in transgenic plants can be explained by lowered expression level. It could also be that *WRR4A*$^{Oy\text{-}o}$ is not functional in *C. sativa*. *WRR8* and *WRR9* are two genes that confers full resistance to Ac2V in Arabidopsis but are not functional in *B. juncea* (Cevik *et al.*, 2019). The progeny of the transgenic resistant plants will be investigated to identify a line with consistent resistance to AcEx1.

Chapter 4 : Optimization of CRISPR-Cas9 method in Arabidopsis

4.1 Introduction

4.1.1 Aspiration

In the previous chapter, I took advantage of natural genetic variation to identify an *R*-gene and investigate the plant immune system. However, genetic variation is not always available. For instance, all the natural Arabidopsis accessions resist the *A. candida* crop-infecting races Ac2V, Ac7V and AcBoT(Cevik *et al.*, 2019). Random mutagenesis can be used to generate polymorphism and characterise genes in a forward genetic approach. In addition, transgressive segregation between 19 resistant Arabidopsis parents was employed to generate Ac2V, Ac7V and AcBoT susceptible lines, enabling the discovery of three novel *White Rust Resistance*(*WRR*)-genes (Cevik *et al.*, 2019). In 2012/2013, CRISPR emerged as a cheap, fast and precise tool to edit genomes and create genetic variation (Gasiunas *et al.*, 2012; Jinek *et al.*, 2012). Conceivably, CRISPR could generate susceptible lines to a given pathogen in a previously non-host species. It appeared that CRISPR-mediated genome editing was not as efficient in Arabidopsis compared to other systems such as human, mouse, tomato and tobacco. Thus, I tried to optimize the method for generation of null alleles in Arabidopsis. The content of this chapter is largely identical to (Castel *et al.*, 2019), a publication under the CC0 license.

4.1.2 Current status of CRISPR in Arabidopsis

Clustered regularly interspaced short palindromic repeat (CRISPR)- CRISPR associated (Cas) site-specific nucleases are components of prokaryotic immunity against viruses and are widely deployed as tools to impose operator-specified nucleotide sequence changes in genomes of interest (Gasiunas *et al.*, 2012; Jinek *et al.*, 2012; Cong *et al.*, 2013; Mali *et al.*, 2013). For instance, the RNA-directed endonuclease Cas9 from the Type II CRISPR system functions in heterologous organisms, enabling applications such as targeted mutagenesis, dynamic imaging of genomic loci, transcriptional regulation and base editing (Barrangou & Horvath, 2017; Dreissig *et al.*, 2017; Shan & Voytas, 2018). Expression of a single-guide RNA (sgRNA, an artificial fusion of the dual endogenous crisprRNA/trans-acting-crisprRNA) with Cas9, causes targeted DNA mutations in animal and plant cells

(Cong *et al.*, 2013; Li *et al.*, 2013; Mali *et al.*, 2013; Nekrasov *et al.*, 2013; Shan *et al.*, 2013). Cas9-sgRNA ribonucleoprotein causes a Double strand break (DSB) on DNA template homologous to the sgRNA spacer sequence. Cleaved DNA strands can be re-ligated by the endogenous Non-Homologous End Joining (NHEJ) system, which can result in insertions or deletions (indels) at the repaired site. Indels in the coding DNA sequence (CDS) can cause a codon reading frame shift resulting in loss-of-function alleles.

Arabidopsis is widely used for plant molecular genetics and lines mutated for a gene of interest are a valuable resource. Expression of CRISPR-Cas9 components can result in loss-of-function alleles of targeted genes in Arabidopsis, with variable efficiency (Jiang *et al.*, 2013; Fauser *et al.*, 2014; Feng *et al.*, 2014). To improve induced mutation rates in Arabidopsis, several groups have evaluated various promoters to drive Cas9 expression (Yan *et al.*, 2015; Wang *et al.*, 2015c; Tsutsui & Higashiyama, 2017). I set out to optimize mutation rates in Arabidopsis. I conducted an extensive comparison of construct architecture, varying promoters, *Cas9* alleles, terminator, sgRNA backbones and transcriptional direction.

There are several methods to deliver Cas9-sgRNA ribonucleoprotein into plant cells. The most common one is the expression of *Cas9* and *sgRNA* by the plant itself after transformation. On the other hand, ribonucleoproteins can be directly delivered by protoplast transformation or particle bombardment (Woo *et al.*, 2015; Wolter & Puchta, 2017; Liang *et al.*, 2018a). In my experiments, *Cas9* and the *sgRNA* were delivered by *Agrobacterium tumefaciens*-mediated transgenesis to avoid the process of regeneration via tissue culture. The method requires three steps: (i) DNA assembly of a binary vector with a selectable marker, a *Cas9* and an *sgRNA* expression cassettes, (ii) transformation of the plasmid via the floral dip method (Clough & Bent, 1998) and (iii) identification of mutants among the transformed lines. I tested multiple T-DNA architectures for their ability to trigger homozygous mutations in the *ADH1* gene. ADH1 converts allyl alcohol into lethal allyl aldehyde. Thus *adh1* mutant lines resist an allyl alcohol treatment, enabling facile measurement of CRISPR-induced mutation rates (Fauser *et al.*, 2014; Tsutsui & Higashiyama, 2017). I defined combinations of CRISPR components that enable high efficiency recovery of stable homozygous mutants in the first generation after transformation.

4.2 Results

4.2.1 T-DNA assembly is facilitated by the Golden Gate cloning method

In Golden Gate modular cloning, the promoter, reading frame and 3' end modules at 'Level 0', are assembled using Type IIS restriction enzymes into 'Level 1' complete transcript unit. Several Level 1 transcript units can then be combined into T-DNAs at 'Level 2'. This enables facile assembly of diverse T-DNA conformations (Weber *et al.*, 2011; Engler *et al.*, 2014). In this project, I used three Level 0 acceptor vectors designed to clone promoter, CDS or terminator fragments. I also used three Level 1 vectors: a glufosinate plant selectable marker in position 1 (pICSL11017, cloned into pICH47732), a *Cas9* expression cassette in position 2 (cloned into pICH47742) and an *sgRNA* expression cassette in position 3 (cloned into pICH47751) **(Figure 3-1)**. Some *Cas9* expression cassettes were cloned into a Level 1 position 2 variant: pICH47811. This vector can be assembled in Level 2 in the same fashion as pICH47742, but it enables Cas9 transcription in the opposite direction as compared to the other Level 1 modules.

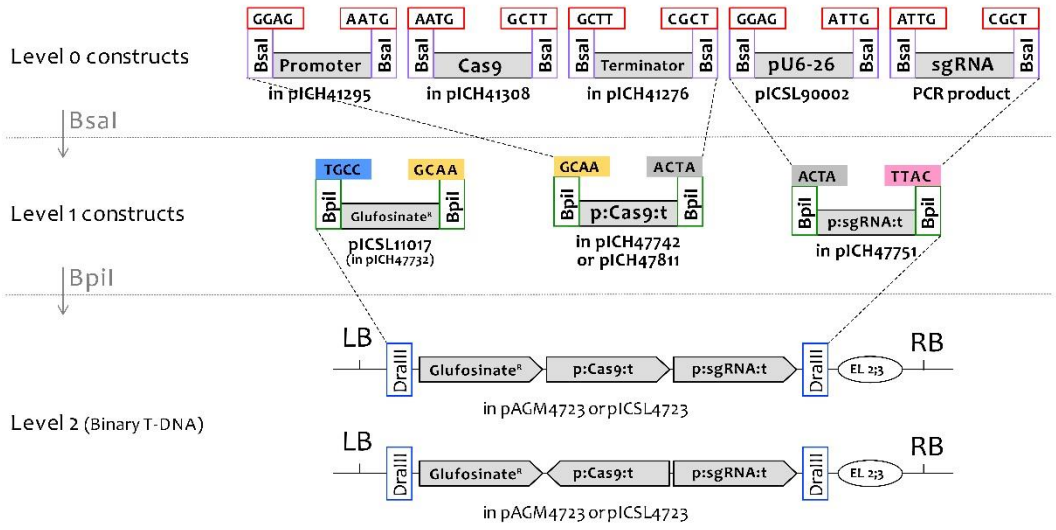

Figure 4-1: Golden Gate-based cloning method to assemble CRISPR constructs
Cas9 alleles, promoters and terminators were cloned into the indicated Level 0 acceptor vectors as described in Materials and Methods and were assembled in Level 1 acceptor vector pICH47742 or pICH47811. An sgRNA targeting *AtADH1* was amplified by PCR and assembled with the *U6-26* promoter vector pICSL90002 in the same manner. Both *Cas9* and *sgRNA* expression units were assembled in Level 2 acceptors pAGM4723 (not containing an overdrive sequence) or pICSL4723 (containing an overdrive) along with a glufosinate resistance plant selectable marker. An end-linker pICH41766 (EL2;3) was used to link the *sgRNA* expression unit to the Level 2 acceptor vector. For a head-to-head orientation of the *sgRNA* and *Cas9* expression cassettes, *Cas9* allele, promoter and terminator were assembled into pICH47811 instead of pICH47742.

With the help of Laurence Tomlinson and Federica Locci, I assembled 25 different Level 1 *Cas9* constructs and four *sgRNA* expression cassettes. The sequence targeted by the sgRNA was CGTATCTTCGGCCATGAAGC***NGG*** (Protospacer Adjacent Motif indicated in bold and italics) which targets specifically *ADH1* in Col-0, enabling selection of CRISPR-induced *adh1* homozygous mutants by selecting with allyl alcohol (Fauser *et al.*, 2014). Assembly of these Level 1 modules resulted in 39 Level 2 T-DNA vectors **(Table 4-1)**.

Cas9 Promoter	Cas9 CDS	Cas9 Term.	Orient.	sgRNA Backbone	sgRNA Term.	Vector	Code
35S	2	Ocs	H2T	EF	7*T	pAGM4723	B
UBI10	2	Ocs	H2T	EF	7*T	pAGM4723	D
UBI10	2	Ocs	H2T	Original	7*T	pAGM4723	E
ICU2	2	Ocs	H2T	EF	7*T	pAGM4723	F
AG	2	Ocs	H2T	EF	7*T	pAGM4723	H
35S	3	Ags	H2T	EF	U6-26_192	pAGM4723	L
ICU2	1	Ocs	H2T	EF	U6-26_192	pAGM4723	M
ICU2	2	Ocs	H2T	EF	U6-26_192	pAGM4723	N
UBI10	2	Ocs	H2T	EF	U6-26_192	pAGM4723	O
UBI10	3	Ags	H2T	EF	U6-26_192	pAGM4723	P
35S	3	Ags	H2T	EF	7*T	pAGM4723	Q
enh. 1.2 + EC1.1	2	Ocs	H2T	EF	7*T	pAGM4723	R
enh. 1.2 + EC1.1	2	Ocs	H2T	EF	U6-26_192	pAGM4723	S
enh. 1.2 + EC1.1	2	E9	H2T	EF	7*T	pAGM4723	T
enh. 1.2 + EC1.1	2	E9	H2T	EF	U6-26_192	pAGM4723	U
EC1.2	2	Ocs	H2T	EF	7*T	pAGM4723	W
EC1.2	2	Ocs	H2T	EF	U6-26_192	pAGM4723	X
EC1.2	2	E9	H2T	EF	7*T	pAGM4723	Y
EC1.2	2	E9	H2T	EF	U6-26_192	pAGM4723	Z
CsVMV	2	Ocs	H2T	EF	7*T	pAGM4723	AA
CsVMV	2	Ocs	H2T	Original	7*T	pAGM4723	AB
CsVMV	1	Ocs	H2T	EF	7*T	pAGM4723	AC
CsVMV	1	Ocs	H2T	Original	7*T	pAGM4723	AD
CsVMV	2	Ocs	H2T	EF	U6-26_192	pAGM4723	AE
CsVMV	1	Ocs	H2T	EF	U6-26_192	pAGM4723	AF
enh. 1.2 + EC1.1	2	E9	H2T	EF	7*T	pICSL4723	AJ
EC1.2	2	E9	H2T	EF	7*T	pICSL4723	AK
MGE1	2	E9	H2T	EF	7*T	pICSL4723	AL
RPS5a	2	Nos	H2T	EF	7*T	pICSL4723	AP
YAO	2	Nos	H2T	EF	7*T	pICSL4723	AQ
enh. 1.2 + EC1.1	3	E9	H2T	EF	U6-26_67	pICSL4723	AS
enh. 1.2 + EC1.1	4	E9	H2T	EF	U6-26_67	pICSL4723	AT
RPS5a	3	E9	H2T	EF	U6-26_67	pICSL4723	AV
UBI10	3	E9	H2T	EF	U6-26_67	pICSL4723	AW
YAO	3	E9	H2T	EF	U6-26_67	pICSL4723	AX
RPS5a	4	E9	H2T	EF	U6-26_67	pICSL4723	AY
YAO	4	E9	H2T	EF	U6-26_67	pICSL4723	AZ
YAO	3	E9	H2H	EF	U6-26_67	pICSL4723	BA
RPS5a	4	E9	H2H	EF	U6-26_67	pICSL4723	BB

Table 4-1: 39 constructs were assembled using Golden Gate
For every construct, the sgRNA targets *ADH1* and is transcribed under the control of the U6-26 promoter. Orientation H2H: head-to-head (with *Cas9* expression expressed in pICH47811), H2T: head-to-tail (with *Cas9* expression expressed in pICH47742). Cas9_1: (Mali *et al.*, 2013); Cas9_2: (Fauser *et al.*, 2014); Cas9_3: (Li *et al.*, 2013); Cas9_4: (Cong *et al.*, 2013). pICSL4723 has an *overdrive*, pAGM4723 does not.

4.2.2 Allyl alcohol enables to select CRISPR-induced Arabidopsis mutations

The 39 Level 2 plasmids were transformed in *A. tumefaciens* strain GV3101 and used to generate Arabidopsis Col-0 transgenic lines. 'T1' refers to independent primary transformants selected from the seeds of the dipped plant; 'T2' refers to the T1 progeny.

For each of the 39 constructs, about 100 T2 progenies from six independent T1 lines were tested for allyl alcohol resistance **(Figure 4-2)**. T2 seeds were selected with 30 mM allyl alcohol for two hours. Six survivors (or all survivors if there were less than six) were screened by PCR amplification and capillary sequencing to confirm the mutation in *ADH1* at the expected target site. This genotyping step enabled to estimate the percentage of non-mutated plants that escape the allyl alcohol selection. Indeed, I identified some lines surviving the allyl alcohol screen that are heterozygous (*ADH1*/*adh1*) or WT (*ADH1*/*ADH1*). CRISPR activity is expressed as [(number of allyl alcohol surviving plants) x (% of homozygous or biallelic mutants confirmed by sequencing among the surviving plants tested) / (number of seeds sown)]. It was measured for four to six independent T2 families, for each of 39 constructs.

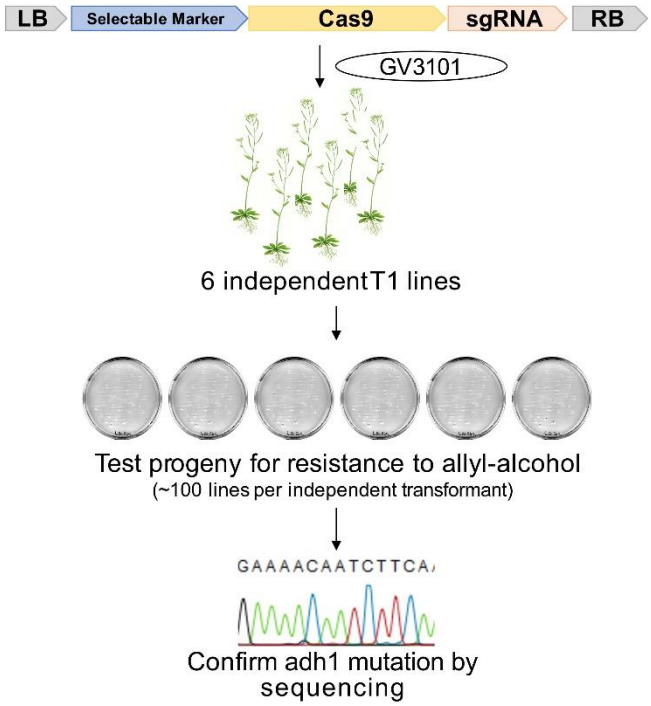

Figure 4-2: Evaluation of mutation rates
Constructs were transformed into Arabidopsis accession Col-0 via *Agrobacterium tumefaciens* strain GV3101. Six independent transformants (T1) were selected using glufosinate. About 100 progeny (T2) of each transformant were selected for allyl alcohol resistance. For each independent T2 family, up to six allyl alcohol resistant plants were genotyped at the *ADH1* locus. For each T2 family, the mutation rate was calculated as [(number of allyl alcohol surviving plants) x (% of homozygous or biallelic mutants confirmed by sequencing among the surviving plants tested) / (number of seeds sown)].

When more than 75% of the lines survived the allyl alcohol treatment and all the lines genotyped are knock-out alleles with the exact same mutation within one T2 family, the T1 parent was assumed to be a homozygous mutant. Such T2 families are indicated in red.

4.2.3 An *overdrive* sequence at the T-DNA right border does not affect the CRISPR activity

First generation of Golden Gate vectors contain a short version of the T-DNA right border, that lacks an *overdrive* sequence. The *overdrive* sequence can increase the integration efficiency (Peraltal *et al.*, 1986). Imperfect integration of the CRISPR T-DNA could explain the low CRISPR efficiency I observed. I assembled the same CRISPR components in pAGM4723, that lacks an *overdrive*, and in pICSL4723, that has an *overdrive* **(Figure 4-3)**. In one comparison the presence of the overdrive resulted in slightly better activity but in another one it did not **(Figure 4-3)**. I concluded that the presence of an overdrive does

not influence the CRISPR efficiency. Thus, I could compare constructs independently of the presence of an *overdrive*.

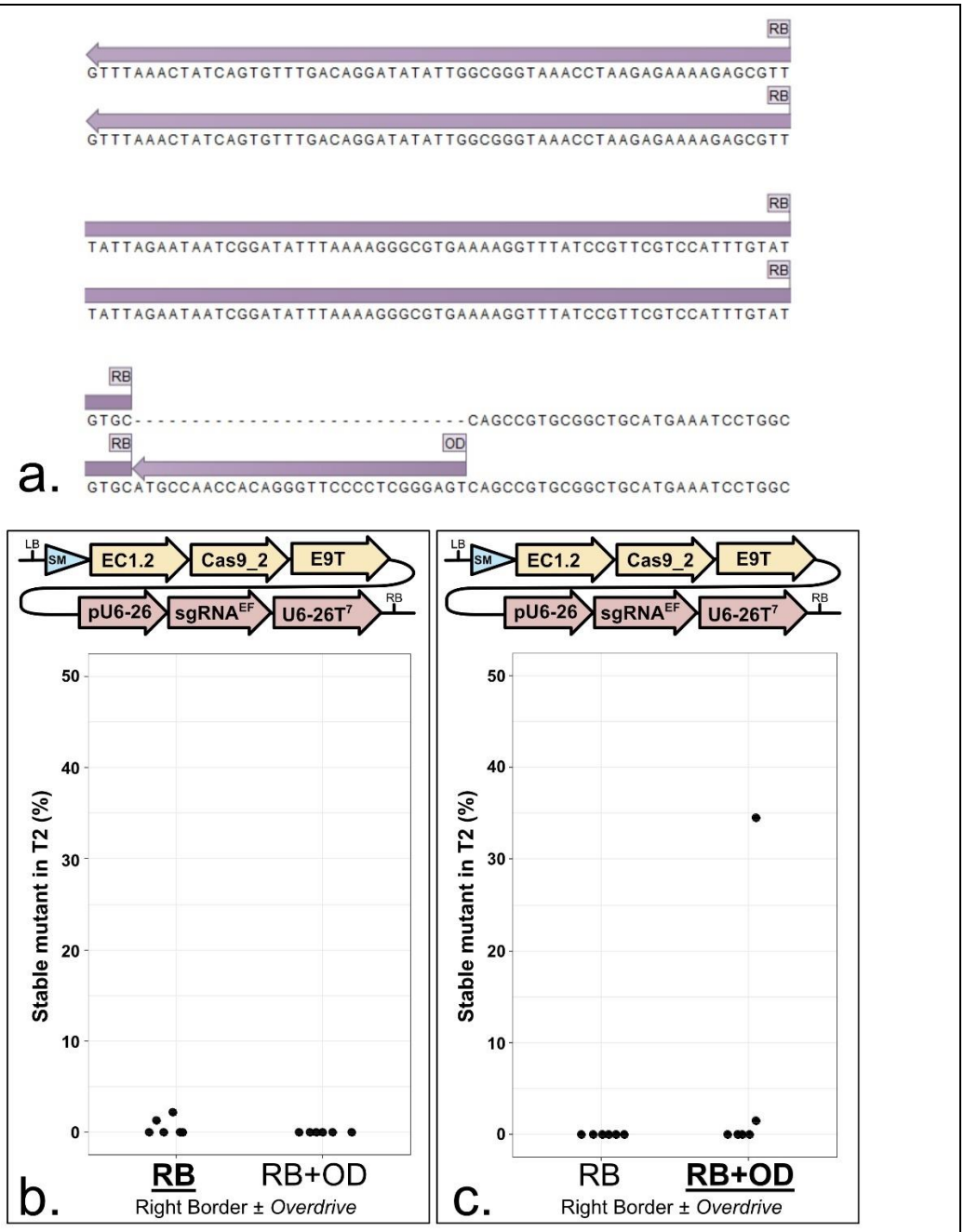

Figure 4-3: The presence of an *overdrive* sequence in the T-DNA right border does not affect the CRISPR efficiency

a. Sequence of the right border with (pICSL4723) or without (pAGM4723) an *overdrive* sequence. **b., c.** Each panel represents a vector comparison in the same context. Vectors can be compared within each panel, not from one panel to another. The modules have been assembled by Golden Gate into pICSL4723 (RB+OD, with an *overdrive*) or pAGM4723 (RB, without an *overdrive*) and transformed into Col-0 via *Agrobacterium tumefaciens* strain GV3101. LB: Left Border. SM: Sel. Marker (Glufosinate resistance gene). *EC1.2*: 1014 bp of the At2g21740 promoter. *EC_enh.*: 752 bp of the At2g21740 promoter fused to 548 bp of the At1g76750 promoter. *Cas9_2*: (Fauser *et al.*, 2014). *E9T*: 631 bp of the *Pisum sativum rbcS E9* terminator. *U6-26p*: 205 bp of the At3g13855 promoter. *sgRNA^EF*: "extension-flip" sgRNA. *U6-26T*: 7 bp of the At3g13855 terminator. RB: Right

Border. The sgRNA targets ADH1. CRISPR activity measured in % of homozygous or biallelic stable mutants in the second generation after transformation (T2). Each dot represents an independent T2 family. Bold and underlined: Most active construct for each panel.

4.2.4 *UBI10*, *YAO* or *RPS5a* promoter-controlled *Cas9* expression enhances mutation rates

CRISPR-mediated DNA sequence changes must occur in the germ-line to be inherited. Ubiquitous promoters are strongly expressed in most tissues, which theoretically include both somatic- and germ-lines. However, the most commonly used ubiquitous promoter, the *35S* promoter from *Cauliflower Mosaic Virus*, is not always expressed at high level in the germ-line (Sunilkumar *et al.*, 2002). I compared *35S* with the Arabidopsis *UBI10*

promoters for CRISPR activity. More mutants were recovered using the *UBI10* promoter, suggesting it is more active than 35S in the germ-line **(Figure 4-4: a, d)**.

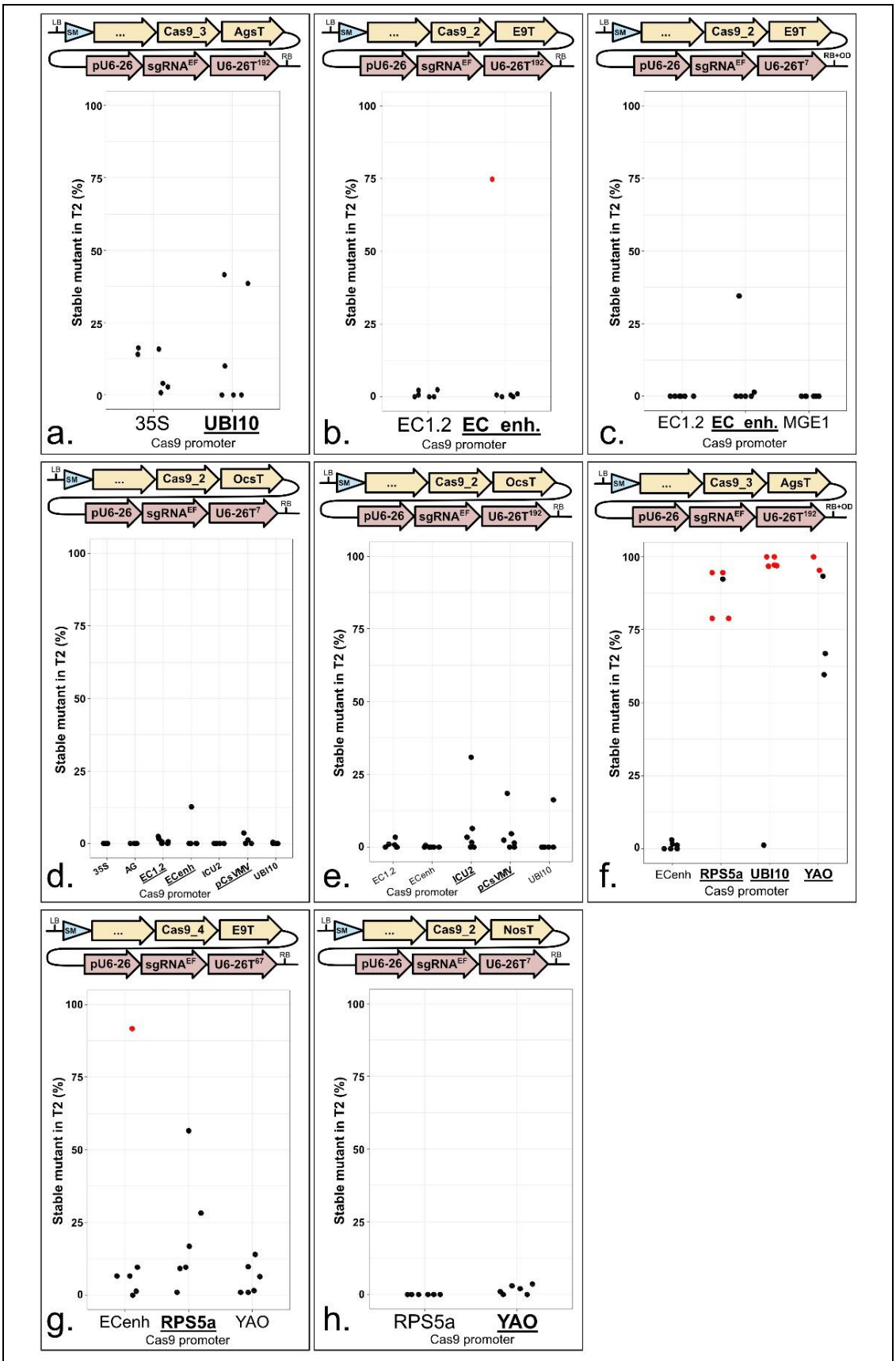

Figure 4-4: UBI10, YAO and RPS5a promoter-regulated Cas9 expression enhances mutation rates
Each panel represents a promoter comparison in the same T-DNA context. Promoters can be compared within each panel, but not from one panel to another. The modules were assembled into pICSL4723 (RB+OD, with an overdrive) or pAGM4723 (RB, without an overdrive) and transformed into Col-0 via *Agrobacterium tumefaciens* strain GV3101. LB: Left Border. SM: Selectable Marker (Glufosinate resistance gene). *35S*: 426 bp of the 35S promoter from *Cauliflower Mosaic Virus*. *UBI10*: 1327 bp of the At4g05320 promoter. *EC1.2*: 1014 bp of the At2g21740 promoter. *EC_enh.*: 752 bp of the At2g21740 promoter fused to 548 bp of the At1g76750 promoter. *MGE1*: 1554 bp of the At5g55200 promoter. *AG*: 3101 bp of the At4g18960 promoter. *ICU2*: 625 bp of the At5g67100 promoter. *CsVMV*: 517 bp of a promoter from *Cassava Vein Mosaic virus*. *RPS5a*: 1688 bp of the At3g11940 promoter. *YAO*: 596 bp of the At4g05410 promoter. *Cas9_1*: (Mali *et al.*, 2013); *Cas9_2*: (Fauser *et al.*, 2014); *Cas9_3*: (Li *et al.*, 2013); *Cas9_4*: (Cong *et al.*, 2013). *E9T*: 631 bp of the *Pisum sativum rbcS E9* terminator. *OcsT*: 714 bp of the *Agrobacterium tumefaciens octopine synthase* terminator. AgsT: 410 bp of the *Agrobacterium tumefaciens agropine synthase* terminator. *NosT*: 267 bp of the *Agrobacterium tumefaciens nopaline synthase* terminator. *pU6-26*: 205 bp of the At3g13855 promoter. $sgRNA^{EF}$: "extension-flip" sgRNA. *U6-26T*: 7, 67 or 192 bp of the At3g13855 terminator. RB: Right Border. **d.** Five lines were tested for *UBI10* and *ICU2* and four lines for *AG* instead of six. **f.** Five lines were tested for *YAO* and *RPS5a* instead of six. The sgRNA targets *ADH1*. CRISPR activity measured in % of homozygous or biallelic stable mutants in the second generation after transformation (T2). Each dot represents an independent T2 family. Red dot: All the T2 lines from this family carry the same mutation, indicating a mutation more likely inherited from the T1 parent rather than being *de novo* from the T2 line. Bold and underlined: Most active construct(s) for each panel.

Other groups have found that some germ-line specific promoters can enhance mutation rates in Arabidopsis (Mao *et al.*, 2015; Yan *et al.*, 2015; Wang *et al.*, 2015c; Eid *et al.*, 2016). Following these observations, I tested more germ-line -expressed promoters.

In the combinations tested, I detected low CRISPR activity using the meiosis I-specific promoter *MGE1* (Eid *et al.*, 2016) **(Figure 4-4: c.)**, the homeotic gene promoter *AG* (Hong *et al.*, 2003) **(Figure 4-4: d.)** and the DNA polymerase subunit-encoding gene promoter *ICU2* (Hyun *et al.*, 2014) **(Figure 4-4: d.)**. They were tested with constructs inducing an overall low activity and I do not exclude that they can perform efficiently in other conditions. In one context specifically, *ICU2* promoter resulted in moderate activity in four of the six T2 families tested, while only one T2 family showed activity with the *UBI10* promoter **(Figure 4-4: e.)**.

EC1.2 and an *EC1.2::EC1.1* fusion (referred as '*EC enhanced*' or '*ECenh*') are specifically expressed in the egg cell and were reported to trigger elevated mutation rates with CRISPR in Arabidopsis (Wang *et al.*, 2015c). In the conditions tested, only *ECenh* induced homozygous mutants in T1 and at low frequency **(Figure 4-4: b., g.)**. In one comparison, *EC1.2* and *ECenh* performed slightly better than *UBI10* **(Figure 4-4: d.)**, but in another, they induced lower activity **(Figure 4-4: e.)**. *EC1.2* and *ECenh* were modified during the Golden

Gate cloning process. Such modifications may have altered some *cis* regulatory elements, rendering them less active.

A promoter from *Cassava Vein Mosaic Virus* (CsVMV) was reported to mediate CRISPR activity in *Brassica oleracea* (Lawrenson *et al.*, 2015). It induced more CRISPR activity than *UBI10* in two combinations tested **(Figure 4-4: d., e.)**.

I also tested the *YAO* and *RPS5a* promoters. Both were reported to boost CRISPR activity in Arabidopsis (Yan *et al.*, 2015; Tsutsui & Higashiyama, 2017). They triggered elevated mutation rates compared with *UBI10* **(Figure 4-4: f.)**. In one comparison, *RPS5a* performed slightly better **(Figure 4-4: g.)**, but in another, *YAO* performed better **(Figure 4-4: h.)**.

As have others, I conclude that the promoter driving *Cas9* expression influences CRISPR-mediated mutation rates (Yan *et al.*, 2015; Wang *et al.*, 2015c; Eid *et al.*, 2016; Tsutsui & Higashiyama, 2017). I observed the best mutation rates using *RPS5a*, *YAO* and *UBI10* promoters.

4.2.5 Codon optimization of Cas9 and presence of an intron elevate mutation rates

The activity of different constructs with the same promoter can be very different. For instance, *RPS5a*- and *YAO*-driven lines were recovered that displayed either high or low activity **(Figure 4-4: f., h.)**. In general, the most active constructs carried *Cas9_3* or *Cas9_4* alleles. I thus compared four *Cas9* alleles side-by-side **(Figure 4-5)**. *Cas9_1* is a human codon-optimized version with a single C-terminal NLS (Nuclear Localization Signal) (Mali *et al.*, 2013). *Cas9_2* is an Arabidopsis codon-optimized version with a single C-terminal NLS (Fauser *et al.*, 2014). *Cas9_3* is a plant codon-optimized version with both N- and C-terminal NLSs, an N-terminal FLAG tag and a potato intron IV (Li *et al.*, 2013). *Cas9_4* is a human

codon-optimized version with both N- and C-terminal NLSs and an N-terminal FLAG tag (Cong *et al.*, 2013).

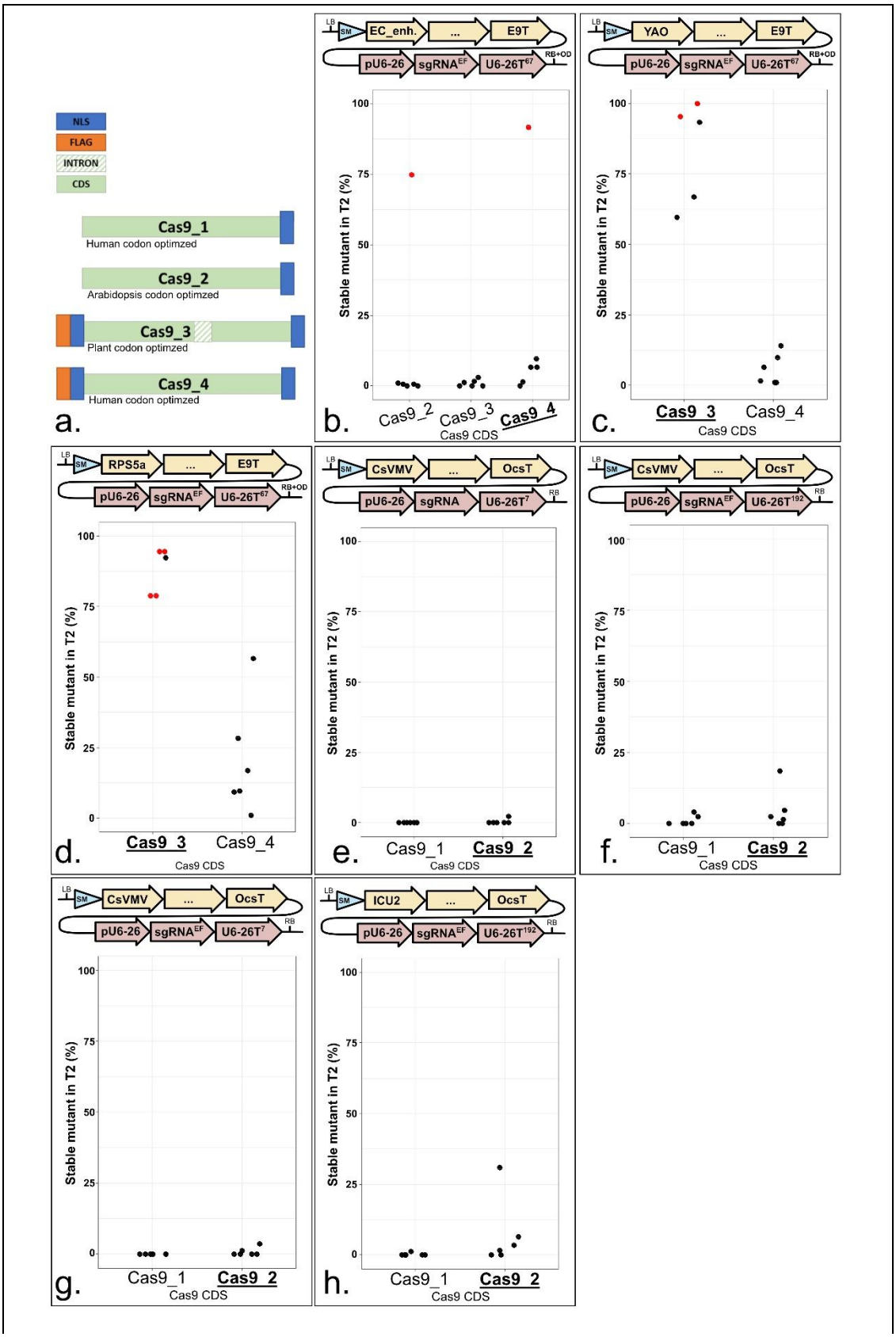

Figure 4-5: An intron-containing allele of Cas9 triggers elevated mutation rates. **a.** *Cas9_1*: (Mali *et al.*, 2013); *Cas9_2*: (Fauser *et al.*, 2014); *Cas9_3*: (Li *et al.*, 2013); *Cas9_4*: (Cong *et al.*, 2013). NLS: Nuclear Localization Signal. FLAG: DYKDDDDK peptide. Apart from FLAG and NLS, the amino acid sequences are identical. The nucleotide sequence (*i.e.* codon optimization) are different. Bars are not in scale. **b.-h.** Each panel represents a CDS comparison in the same context. CDSs can be compared within each panel, not from one panel to another. The modules were assembled into pICSL4723 (RB+OD, with an overdrive) or pAGM4723 (RB, without an overdrive) and transformed into Col-0 via *Agrobacterium tumefaciens* strain GV3101. LB: Left Border. SM: Selectable Marker (Glufosinate resistance gene). *EC_enh.*: 752 bp of the At2g21740 promoter fused to 548 bp of the At1g76750 promoter. *YAO*: 596 bp of the At4g05410 promoter. *RPS5a*: 1688 bp of the At3g11940 promoter. *CsVMV*: 517 bp of a promoter from *Cassava Vein Mosaic virus*. *ICU2*: 625 bp of the At5g67100 promoter. *E9T*: 631 bp of the *Pisum sativum rbcS E9* terminator. *OcsT*: 714 bp of the *Agrobacterium tumefaciens octopine synthase* terminator. *U6-26p*: 205 bp of the At3g13855 promoter. *sgRNA^{EF}*: "extension-flip" sgRNA. *U6-26T*: 7, 67 or 192 bp of the At3g13855 terminator. *RB*: Right Border. **b.** *Cas9_2* is in pAGM4723 (*i.e.* RB) in combination with *U6-26T^{192}*; *Cas9_3* and *Cas9_4* are in pICSL4723 (*i.e.* RB+OD) in combination with *U6-26T^{67}*. **c. and d.** Five lines were tested for *Cas9_3* instead of six. The sgRNA targets *ADH1*. CRISPR activity measured in % of homozygous or biallelic stable mutants in the second generation after transformation (T2). Each dot represents an independent T2 family. Red dot: All the T2 lines from this family carry the same mutation, indicating a mutation more likely inherited from the T1 parent rather than being *de novo* from the T2 line. Bold and underlined: Most active construct(s) for each panel.

I found that in comparable constructs, *Cas9_2* performs better than *Cas9_1* **(Figure 4-5 e., h.)**, consistent with the fact that *Cas9_2* was designed for Arabidopsis codon usage. However, human codon-optimized *Cas9_4* induced more mutants than Arabidopsis optimized *Cas9_2* in one comparison **(Figure 4-5 b.)**. Cas9_4 has an extra N-terminal NLS compared to Cas9_2, which may explain this difference. In this comparison specifically, *Cas9_3* was less efficient than *Cas9_4*. However, by comparing *Cas9_3* and *Cas9_4* in combination with *YAO* or *RPS5a* promoters, *Cas9_3* resulted in high mutation rates **(Figure 4-5 c., d.)**. *Cas9_3* efficiency can be explained by the plant codon optimization, the presence of two NLSs and the inclusion of a plant intron. This intron was originally added to avoid expression in bacteria during cloning and, as side effect, can also increase expression in planta (Callis *et al.*, 1987). In conclusion, I recommend the use of *Cas9_3* for gene editing in Arabidopsis.

4.2.6 A modified sgRNA triggers CRISPR-induced mutations more efficiently

In the endogenous CRISPR immune system, Cas9 binds a crRNA (CRISPR RNA) and a tracrRNA (trans-acting CRISPR RNA) (Wiedenheft *et al.*, 2012). An artificial fusion of both, called sgRNA (single guide RNA), is sufficient for CRISPR-mediated genome editing (Jinek *et al.*, 2012). sgRNA stability was suggested to be a limiting factor in CRISPR system (Jinek *et al.*, 2013). Chen *et al.* proposed an improved sgRNA to tackle this issue (Chen *et al.*, 2013). It carries an A-T transversion to remove a TTTT potential termination signal, and an extended Cas9-binding hairpin structure **(Figure 4-6 a.)**. I compared side-by-side the

'Extended' and 'Flipped' sgRNA (sgRNA^{EF}) with the classic sgRNA **(Figure 4-6 b., c.)**. In two independent comparisons, the efficiency was higher with sgRNA^{EF}. The improvement was not dramatic but sufficient to recommend the use of 'EF'-modified guide RNAs for genome editing in Arabidopsis. Consistently, a comparison of many sgRNA backbone revealed that a flip and an extension significantly increase the overall CRISPR efficiency (Dang *et al.*, 2015).

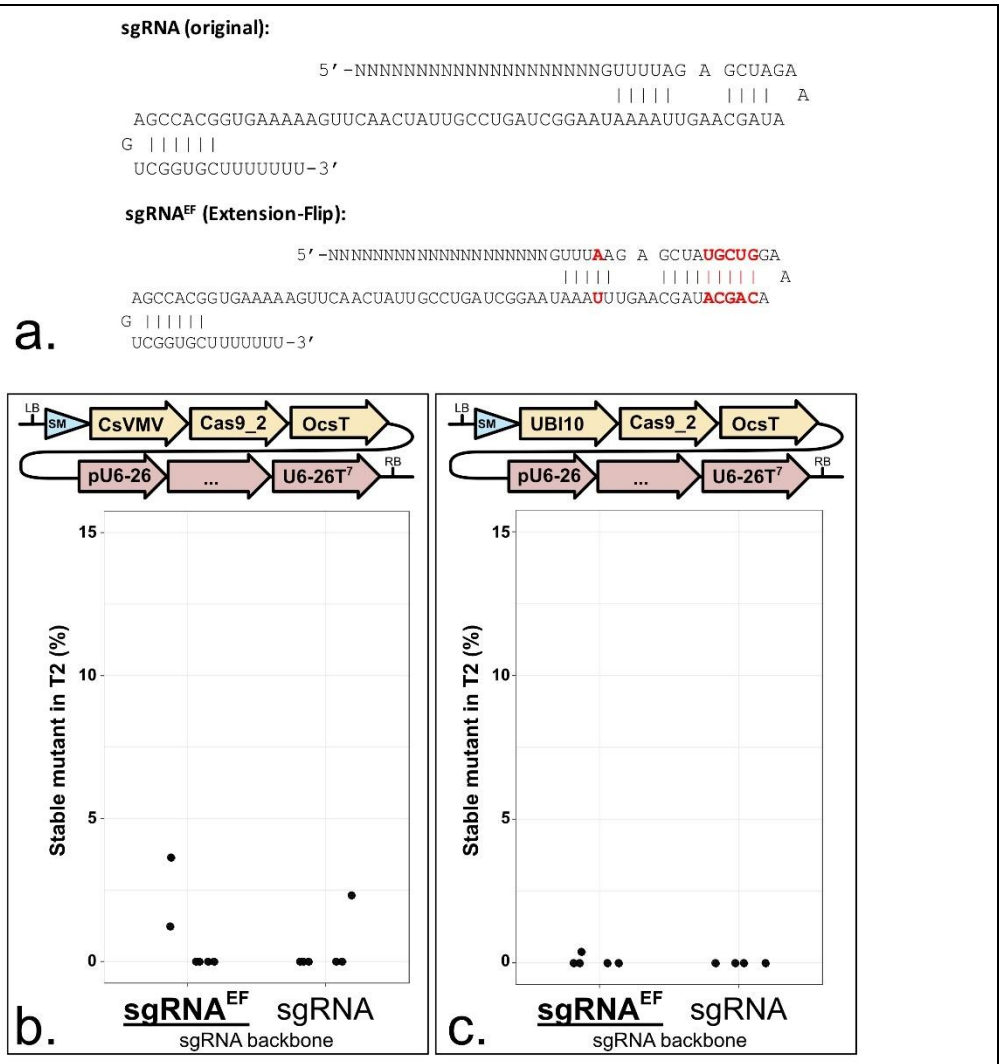

Figure 4-6: A modified sgRNA is slightly more efficient to trigger mutations.
a. Original sgRNA proposed by George Church (Mali *et al.*, 2013). Extension-Flip (EF) sgRNA proposed by Lei Qi and Bo Huang (Chen *et al.*, 2013). **b. and c.** Each panel represents an sgRNA backbone comparison in the same context. sgRNA backbones can be compared within each panel but not from one panel to another. The modules were assembled into pICSL4723 (RB+OD, with an overdrive) or pAGM4723 (RB, without an overdrive) and transformed into Col-0 via *Agrobacterium tumefaciens* strain GV3101. LB: Left Border. SM: Selectable Marker (Glufosinate resistance gene). *CsVMV*: 517 bp of a promoter from *Cassava Vein Mosaic virus*. *UBI10*: 1327 bp of the At4g05320 promoter. *Cas9_2*: (Fauser *et al.*, 2014). *OcsT*: 714 bp of the *Agrobacterium tumefaciens octopine synthase* terminator. *U6-26p*: 205 bp of the At3g13855 promoter. *U6-26T*: 7 bp of the At3g13855 terminator. RB: Right Border. **c.** Five lines were tested for sgRNA^{EF} and four lines for sgRNA instead of six. The sgRNA targets *ADH1*. CRISPR activity measured in % of homozygous or biallelic stable mutants in the second generation after transformation (T2). Each

dot represents an independent T2 family. Bold and underlined: Most active construct(s) for each panel.

4.2.7 The 3' regulatory sequences of *Cas9* and the *sgRNA* influence mutation rates

To avoid post-transcriptional modifications such as capping and polyadenylation, sgRNA must be transcribed by RNA polymerase III (Pol. III). Several approaches involving ribozymes, Csy4 ribonuclease or tRNA-processing systems have been proposed but were not tested here (Gao & Zhao, 2014; Tsai *et al.*, 2014; Xie *et al.*, 2015). *U6-26* is a Pol. III-transcribed gene in Arabidopsis (Li *et al.*, 2007). I used 205 bp of the 5' upstream region of *U6-26* as promoter and compared a synthetic polyT sequence (seven thymines) and 192 bp of the 3' downstream region as terminator. A T-rich stretch has been reported to function as a termination signal for Pol. III (Waibel & Filipowicz, 1990).

In seven out of nine side-by-side comparisons, the authentic 192 bp of *U6-26* terminator directed a higher efficiency of the construct, as compared to a synthetic polyT termination sequence **(Figure 4-7)**. I speculate that a stronger terminator increases the stability of the sgRNA. For multiplex genome editing, the use of 192 bp per sgRNA will result in longer T-DNAs, increasing the risk of recombination and instability. In addition, I generated constructs with only 67 bp of the U6-26 3' downstream sequence. Such constructs were not compared side-by-side with the '192 bp terminator', although they enabled modest to high mutation rates **(*e.g.* Figure 4-4 f., g.)**. With these results in mind, I recommend using 67 bp of the 3' downstream sequence of *U6-26* as terminator for the sgRNA.

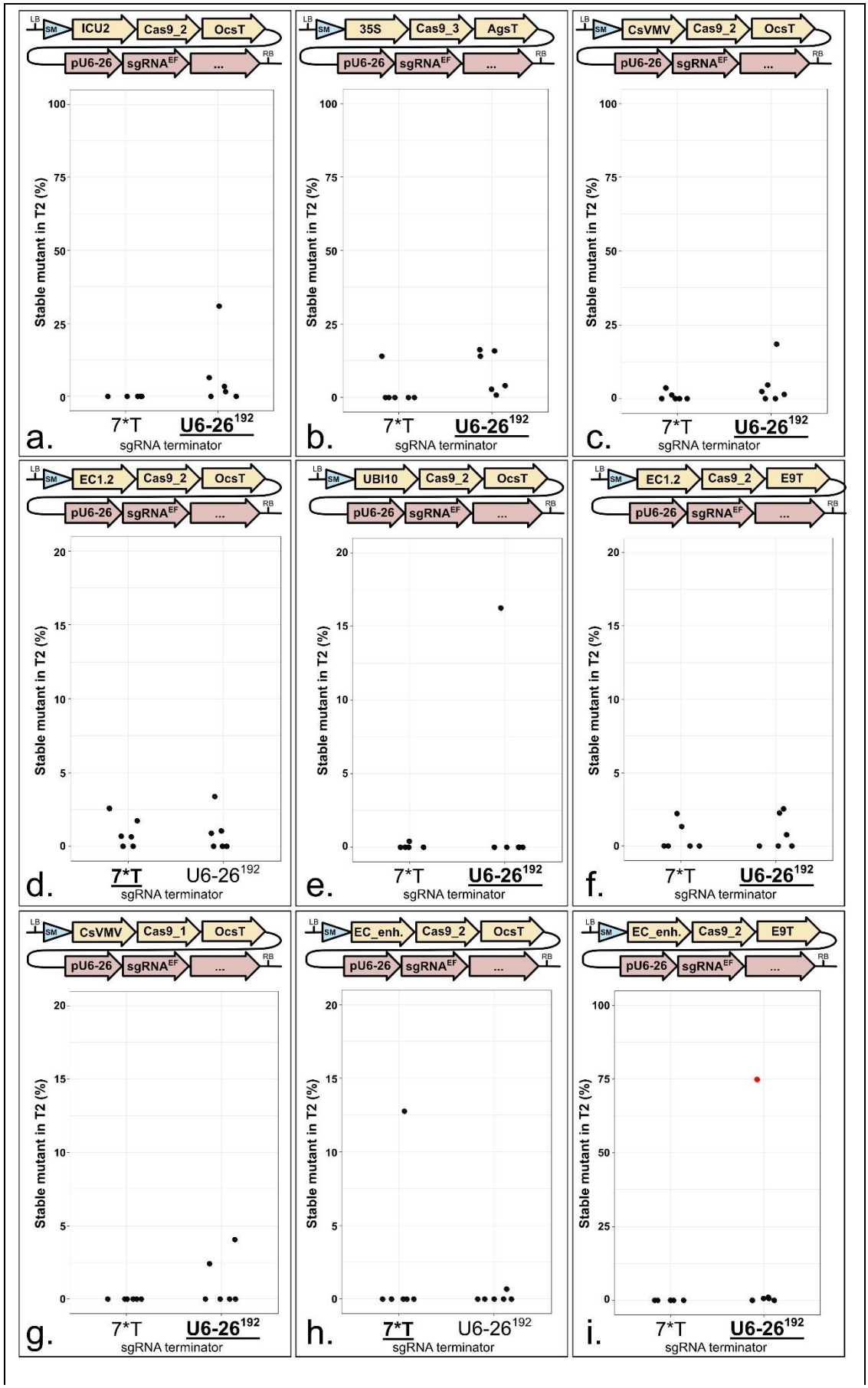
a.
ICU2
Cas9_2
OcsT
b.
35S
Cas9_3
AgsT
c.
CsVMV
Cas9_2
OcsT
d.
EC1.2
Cas9_2
OcsT
e.
UBI10
Cas9_2
OcsT
f.
EC1.2
Cas9_2
E9T
g.
CsVMV
Cas9_1
OcsT
h.
EC_enh.
Cas9_2
OcsT
i.
EC_enh.
Cas9_2
E9T
LB
SM
pU6-26
sgRNA^EF
...
RB
Stable mutant in T2 (%)
7*T
U6-26^192
sgRNA terminator

Figure 4-7: The sgRNA expression regulated by an authentic 3' regulatory sequence of U6-26 produces greater mutation rates.
a. to c. Each panel represents a terminator comparison in the same context. Terminators can be compared within each panel, not from one panel to another. The modules were assembled into pAGM4723 and transformed into Col-0 via *Agrobacterium tumefaciens* strain GV3101. LB: Left Border. SM: Selectable Marker (Glufosinate resistance gene). *ICU2*: 625 bp of the At5g67100 promoter. 35S: 426 bp of the 35S promoter from *Cauliflower Mosaic Virus*. *CsVMV*: 517 bp of a promoter from *Cassava Vein Mosaic virus*. *Cas9_2*: (Fauser *et al.*, 2014). *Cas9_3*: (Li *et al.*, 2013). *OcsT*: 714 bp of the *Agrobacterium tumefaciens octopine synthase* terminator. *AgsT*: 410 bp of the *Agrobacterium tumefaciens agropine synthase* terminator. U6-26p: 205 bp of the At3g13855 promoter. $sgRNA^{EF}$: "extension-flip" sgRNA. U6-26T: 7 or 192 bp of the At3g13855 terminator. RB: Right Border. **a.** Five lines were tested for $U6\text{-}2T^{67}$ instead of six. The sgRNA targets *ADH1*. CRISPR activity measured in % of homozygous or biallelic stable mutants in the second generation after transformation (T2). Each dot represents an independent T2 family. Bold and underlined: Most active construct(s) for each panel.

Since 3' regulatory sequences can influence sgRNA stability, I tested if the same was true for Cas9. I compared the *Pisum sativum rbcS E9* with two *A. tumefaciens* terminators commonly used in Arabidopsis: *Ocs* and *Ags* **(Figure 4-8)**. I did not observe consistent differences between *E9* and *Ocs* **(Figure 4-8)**. However, in one comparison, *E9* outperformed *Ags* tremendously **(Figure 4-8)**. This is consistent with previous observations that RNA Polymerase II (Pol. II) terminators quantitatively control gene expression and influence CRISPR efficiency in Arabidopsis (Nagaya *et al.*, 2010; Wang *et al.*, 2015c). I propose that a weak terminator after *Cas9* enables Pol. II readthrough that could interfere with Pol. III transcription of *sgRNAs* in some T-DNA construct architectures. This limiting factor can be corrected by divergent transcription of *Cas9* and *sgRNAs*.

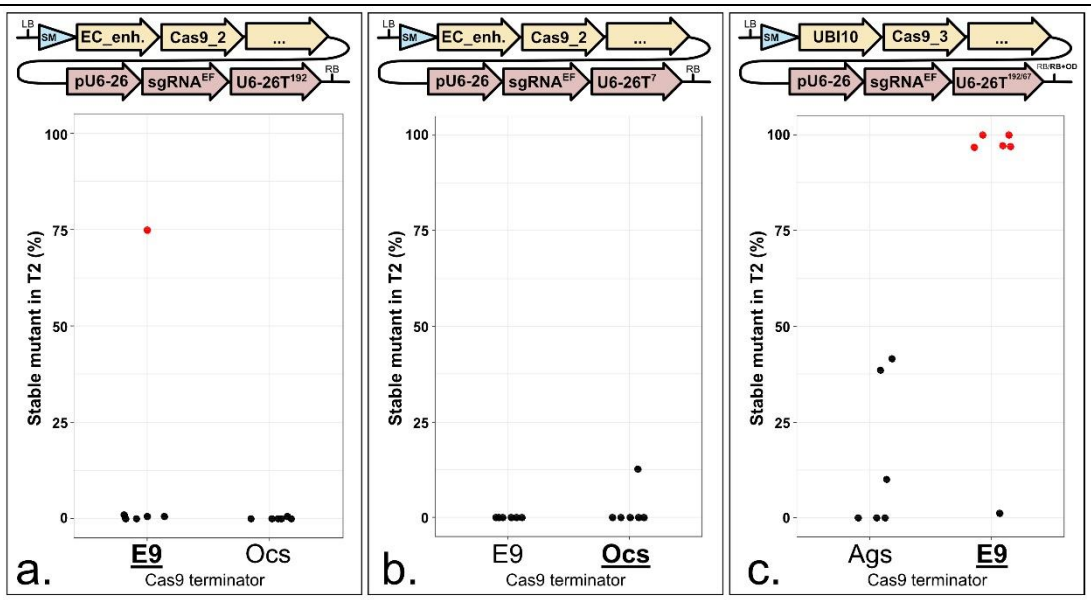

Figure 4-8: A weak 3' regulatory sequence reduces the CRISPR-induced mutation rate.
a. to c. Each panel represents a terminator comparison in the same context. Terminators can be compared within each panel, not from one panel to another. The modules were assembled into

pAGM4723 and transformed into Col-0 via Agrobacterium tumefaciens strain GV3101. LB: Left Border. SM: Selectable Marker (Glufosinate resistance gene). *EC_enh.*: 752 bp of the At2g21740 promoter fused to 548 bp of the At1g76750 promoter. *UBI10*: 1327 bp of the At4g05320 promoter. *Cas9_2*: (Fauser *et al.*, 2014). *Cas9_3*: (Li *et al.*, 2013). *E9T*: 631 bp of the *Pisum sativum rbcS E9* terminator. *OcsT*: 714 bp of the *Agrobacterium tumefaciens octopine synthase* terminator. AgsT: 410 bp of the *Agrobacterium tumefaciens agropine synthase* terminator. *pU6-26*: 205 bp of the At3g13855 promoter. *sgRNA^{EF}*: "extension-flip" sgRNA. *U6-26T*: 7, 67 or 192 bp of the At3g13855 terminator. RB: Right Border. For the comparison using the *UBI10* promoter, the *AgsT* is in combination with *U6-26T^{192}*; *OcsT* is in combination with *U6-26T^{67}*. The sgRNA targets ADH1. CRISPR activity measured in % of homozygous or biallelic stable mutants in the second generation after transformation (T2). Each dot represents an independent T2 family. Red dot: All the T2 lines from this family carry the same mutation, indicating a mutation more likely inherited from the T1 parent rather than being *de novo* from the T2 line. Bold and underlined: Most active construct(s) for each panel.

4.2.8 Divergent transcription of *Cas9* and *sgRNA* can elevate mutation rates

The Golden Gate Level 1 acceptor vector collection contains seven 'forward' expression cassettes and seven 'reverse' expression cassettes, which are interchangeable (Engler *et al.*, 2014). I assembled '*RPS5a:Cas9_4:E9*' and '*YAO:Cas9_3:E9*' in both the Level 1 vector position 2 forward (pICH47742) and reverse (pICH47811) (Figure 4-1). In one case, CRISPR activity was moderate when *Cas9* and *sgRNA* are expressed in the same direction and high when they are expressed in opposite direction **(Figure 4-9: a.)**. In another configuration, CRISPR activity was very high in both cases **(Figure 4-9: b.)**.

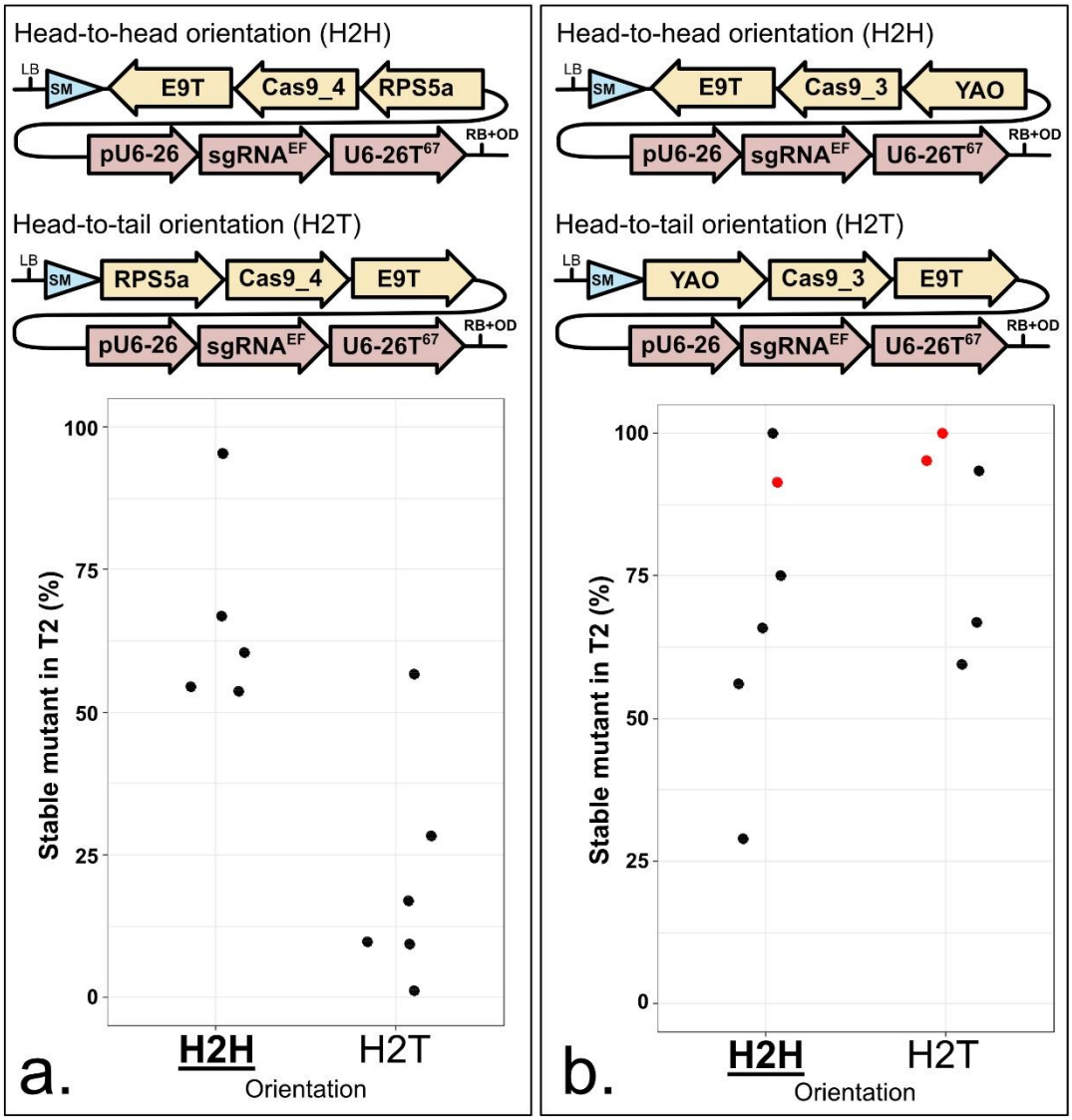

Figure 4-9: CRISPR activity is similar or higher when the sgRNA and the Cas9 expression cassettes are in a head-to-head orientation

a. and b. Each panel represents an orientation comparison in the same context. Orientations can be compared within each panel, not from one panel to another. The modules have been assembled by Golden Gate into pICSL4723 (RB+OD, with an *overdrive*) and transformed into Col-0 via *Agrobacterium tumefaciens* strain GV3101. LB: Left Border. SM: Selectable Marker (Glufosinate resistance gene. *RPS5a*: 1688 bp of the At3g11940 promoter. *YAO*: 596 bp of the At4g05410 promoter. *Cas9_3*: (Li *et al.*, 2013). *Cas9_4*: (Cong *et al.*, 2013). *E9T*: 631 bp of the *Pisum sativum rbcS E9* terminator. *U6-26p*: 205 bp of the At3g13855 promoter. *sgRNA^EF*: "extension-flip" sgRNA. *U6-26T*: 67 bp of the At3g13855 terminator. RB: Right Border. **a.** Five lines were tested for H2H instead of six. **b.** Five lines were tested for H2T instead of six. The sgRNA targets *ADH1*. CRISPR activity measured in % of homozygous or biallelic stable mutants in the second generation after transformation (T2). Each dot represents an independent T2 family. Red dot: All the T2 lines from this family carry the same mutation, indicating a mutation more likely inherited from the T1 parent rather than being de novo from the T2 line. Bold and underlined: Most active construct(s) for each panel.

These data support the use a strong terminator after Cas9 (*e.g. E9* or *Ocs*) and express *Cas9* and *sgRNA* in opposite directions.

4.2.9 Most of the stable double events are homozygous rather than biallelic

From the mutant screen, 315 allyl alcohol resistant lines were confirmed by capillary sequencing. 59% were homozygous (single sequencing signal, different than ADH1 WT), 11% were heterozygous (dual sequencing signal, one matching ADH1 WT) and 10% were biallelic (dual sequencing signal, none matching ADH1 WT), while 20% were difficult to assign (unclear sequencing signals, either biallelic or due to somatic mutations, but clearly different than WT, heterozygous or homozygous genotypes) **(Figure 4-10)**. The recovery of heterozygous (*ADH1/adh1*) lines indicates that the loss of a single copy of *ADH1* can enable plants to escape the allyl alcohol selection.

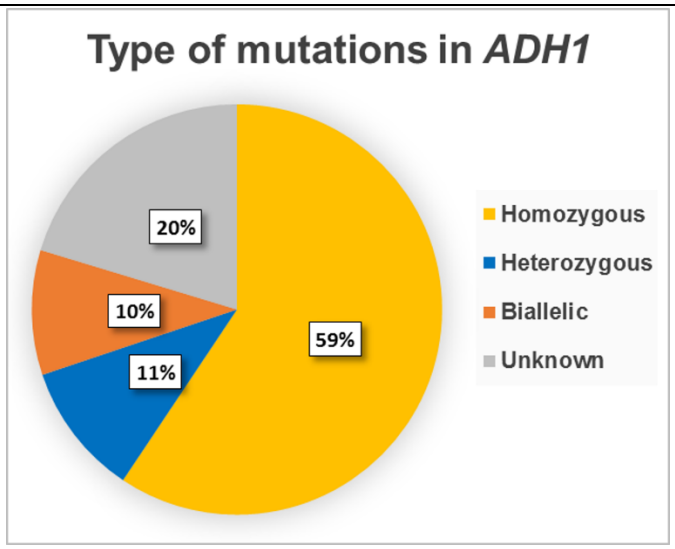

Figure 4-10: Genotype at ADH1 locus confirmed by capillary sequencing
For each T2 family tested, up to six allyl alcohol resistant plants were genotyped by capillary sequencing of an sgRNA target (ADH1) PCR amplicon. I retrieved a total of 315 sequences with a mutation. 59% (187) showed a single sequencing signal, different than ADH1 WT and were classified as "Homozygous". 11% (33) showed an overlap of two sequencing signals, one matching ADH1 WT and one different; and were classified as "Heterozygous". 10% (31) showed an overlap of two sequencing signals, none matching ADH1 WT; and were classified as "Biallelic". 64 (20%) showed an overlap of signals different than WT but not clear enough to distinguish; and were classified as "Unknown". The "Unknown" sequences can be biallelic or due to somatic mutations but are different than WT, heterozygous or homozygous genotypes.

4.3 Discussion

4.3.1 Identification of a CRISPR T-DNA leading to elevated mutation rates

CRISPR emerged in 2012/2013 as a useful tool for targeted mutagenesis in many organisms including plants (Gasiunas *et al.*, 2012; Jinek *et al.*, 2012; Nekrasov *et al.*, 2013). In Arabidopsis, the transgenic expression of CRISPR components can be straightforward, avoiding tedious tissue culture steps. However, the mutation rates were variable. Often many lines have to be genotyped before identifying a mutant (Hyun *et al.*, 2014). Many strategies to enhance the overall CRISPR-induced mutation rate have been proposed (Fauser *et al.*, 2014; Yan *et al.*, 2015; Wang *et al.*, 2015c; Peterson *et al.*, 2016; Tsutsui & Higashiyama, 2017). I conducted a systematic comparison of putative limiting factors including promoters, terminators, codon optimization, sgRNA improvement and T-DNA architecture.

I found that the best promoters to control *Cas9* expression are *UBI10*, *YAO* and *RPS5a*. The best terminators were *Ocs* from *A. tumefaciens* and *rbcS E9* from *P. sativum*. A plant codon-optimized, intron-containing *Cas9* allele outperformed the other alleles tested. A modified sgRNA with a hairpin Extension and a nucleotide Flip, called sgRNA^{EF}, triggered slightly elevated mutation rates. The *sgRNA* transcription regulation by the authentic 3' regulatory sequence of *AtU6-26* results in better CRISPR activity. I get high mutation rates with either 67 bp or 192 bp of terminator and recommend using the shortest (67 bp). I hypothesise that a weak terminator after Cas9 enables RNA-polymerase II readthrough within the *sgRNA* expression cassette, preventing optimal expression of the *sgRNA*. Indeed, I recorded an elevated CRISPR-Cas9 efficiency by expressing *Cas9* and *sgRNA* in opposite directions.

Considering the combinations of Cas9 and sgRNA genes tested in this comparison, I recommend using a '*YAO:Cas9_3:E9*' and a '*pU6-26:sgRNAEF:U6-26T*^{67}' cassettes in head-to-head orientation. This combination is included in the constructs tested here **(Figure 4-9: b.)** and enabled us to recover one homozygous mutant in five T1 plants tested. I also noted useful rates with other constructs **(*e.g.* Figure 4-4: f.)**, indicating that the CRISPR components do not entirely explain the final CRISPR activity. It was recently reported that heat stress increases the efficiency of CRISPR in Arabidopsis (Le Blanc *et al.*, 2017). Environmental conditions may explain fluctuation of the CRISPR activity, independently of the T-DNA architecture.

4.3.2 DSB-induced allelic recombination results in more homozygous than biallelic lines

I was surprised to recover more homozygous than biallelic events. Stable double mutations are the result of two CRISPR events, on the male and female inherited chromosome respectively. In this scenario, lines can be recovered with two different mutations, resulting in a biallelic (*e.g. adh1-2*/*adh1-3*) genotype, rather than having the same mutation on both chromosomes (*e.g. adh1-1*/*adh1-1*). DSB-induced homologous recombination occurs between allelic sequences (Gisler *et al.*, 2002). It has been reported that double strand breaks caused by CRISPR-Cas9 can increase this phenomenon (Hayut *et al.*, 2017). Allelic recombination can explain our observation of the same mutation on both copies of *ADH1*. The prevalence of homozygous over biallelic genotypes facilitates the genotyping and is an advantage for targeted mutagenesis using CRISPR-Cas9.

4.3.3 Non-lethal selectable markers to obtain T-DNA-free mutants

I used a glufosinate resistance selectable marker which enables easy selection of transgenic lines in T1. It can be important to segregate away the T-DNA in the CRISPR mutant line for multiple reasons. For instance, a loss-of-function phenotype must be confirmed by complementation of the CRISPR-induced mutation. A CRISPR construct still present in the mutant can target the complementation transgene and interfere with the resulting phenotypes. Selection of non-transgenic lines is possible but complicated with classic selectable markers such as kanamycin or glufosinate resistance, since a selective treatment kills the non-transgenic plants. FAST-Green and FAST-Red provide a rapid non-destructive selectable marker and involve expression of a GFP- or RFP-tagged protein in the seed (Shimada *et al.*, 2010). Transgenic and non-transgenic seeds can be distinguished under fluorescence microscopy (Morineau *et al.*, 2017; Tsutsui & Higashiyama, 2017; Wu *et al.*, 2018c). This facilitates recovery of mutant seeds lacking the T-DNA **(Figure 4-11)**. Homozygous mutants can be identified among the independent T1 lines. Non-fluorescent seeds can be selected from the T1 progeny seeds. The resulting T2 plants are homozygous mutant and non-transgenic.

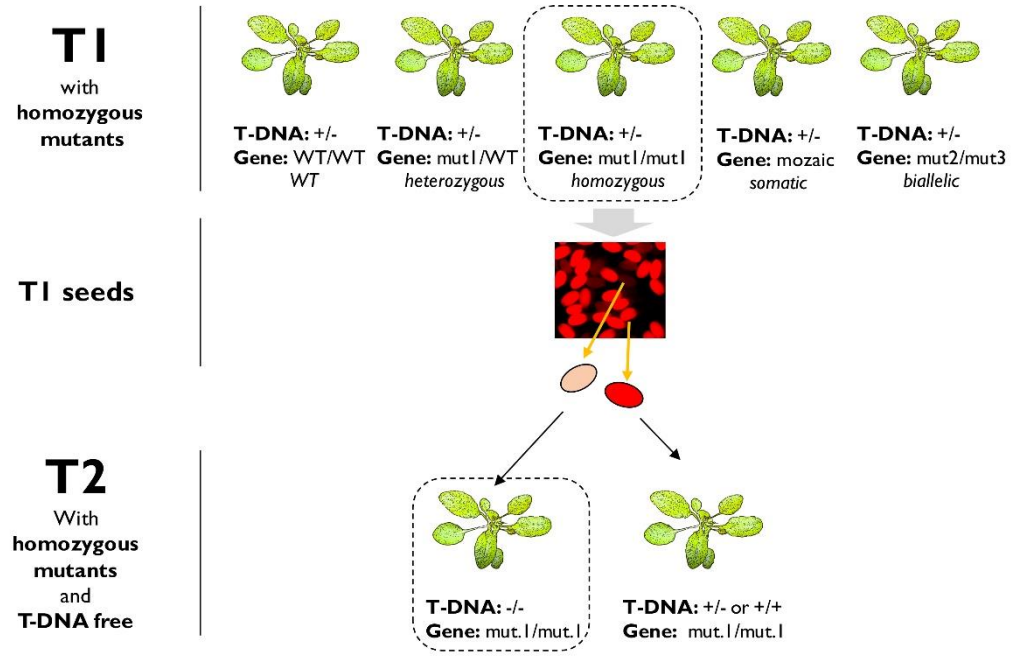

Figure 4-11: FAST-Red combined with CRISPR to generate T-DNA free mutants
The five T1 lines are independent transformants. They are all hemizygous for the T-DNA. At the sgRNA target site, they can be WT, or display somatic, heterozygous, biallelic of homozygous mutations. All the possibilities are represented here. "Somatic" describes events happening in somatic cells, not inherited in the next generation. As somatic events can happen independently in each cell, they often result in mosaic pattern of mutations across the leaf. One line has homozygous mutation (*mut1/mut1*). It produces seeds segregating for the T-DNA, visible under microscope if using FAST-Red. The seeds will segregate 3:1 (Red : Non-red) if there is one locus insertion, 15:1 (Red : Non-red) if there are two loci insertion, etc. The T2 progeny of (*mut1/mut1*) is 100% homozygous for the mutation. The non-red seeds are also T-DNA free.

By comparing diverse combinations of CRISPR components, I identified a CRISPR- and Golden Gate-based method to generate stable Arabidopsis mutant lines in one generation. By trying to elevate mutation rates in Arabidopsis, I found several limiting factors mostly related to *Cas9* and *sgRNA* transcription. Some of these findings can be tested for other plant species and for knock-in breeding. The generation of null alleles via CRISPR is today quick and simple, facilitating the investigation of gene function. For instance, many components of the plant immune system remain uncharacterised likely due to redundancy (Eulgem & Somssich, 2007; Zipfel, 2009). CRISPR enables to target several gene family members at the same time to test for their redundancy.

Chapter 5 : NLR immune receptors signal via the RPW8-NLR NRG1

This chapter is largely identical to (Castel *et al.*, 2018), a publication under the CC-BY license.

5.1 Introduction

The plant immune system involves both cell-surface receptors that detect extracellular pathogen-associated molecular patterns (PAMPs) and intracellular receptors that detect pathogen 'effector' proteins that if not detected, usually contribute to pathogen virulence (Jones & Dangl, 2006). Most *R* (*Resistance*)-genes cloned encode nucleotide-binding, leucine-rich repeat (NLR) immune receptors (Kourelis & Van Der Hoorn, 2018). These receptors are widely deployed during breeding for crop disease resistance (Borhan *et al.*, 2010; Jones *et al.*, 2014; Witek *et al.*, 2016). A better understanding of NLR-mediated immunity could facilitate their deployment to safeguard crops from pathogens, reducing the need for chemical applications.

Most NLRs comprise an N-terminal domain, a central NB-ARC (NB (nucleotide-binding) domain shared by APAF-1 (apoptotic protease activating factor 1), plant R-proteins and CED-4 (cell death protein 4) domain and C-terminal LRRs (Leucine-rich Repeats). At their N-termini, they usually carry a TIR (Toll/Interleukin-1 receptor/Resistance protein) domain or non-TIR N-terminus, often with CCs (Coiled-Coils). A phylogenetically distinct NLR subset carries an N-terminal RPW8 (Resistance to Powdery Mildew 8) domain. The corresponding TIR-NLR, CC-NLR and RPW8-NLR proteins, upon activation, trigger a complex network of responses including gene induction, production of reactive oxygen species and SA (salicylic acid), transcriptional reprogramming and a form of cell death called the HR (hypersensitive response), resulting in resistance (Jones & Dangl, 2006).

The RPW8-NLR NbNRG1 was first identified in *Nicotiana benthamiana* as required for resistance to *Tobacco Mosaic Virus* (TMV) mediated by the *N* gene (Peart et al., 2005). *N* encodes a TIR-NLR that activates resistance upon recognition of the TMV replicase component p50. *NRG1* is widespread in angiosperms suggesting an important role in immunity (Collier *et al.*, 2011; Shao *et al.*, 2014).

Two additional 'helpers' have been described in plants. ADR1 is part of a conserved clade within angiosperms and contributes to function of RPP2, RPP4, RPS2, SNC1, CHS3 and

RRS1 in Arabidopsis (Bonardi *et al.*, 2011; Dong *et al.*, 2016). Interestingly, ADR1s are also RPW8-NLRs, phylogenetically close to the NRG1 clade (Collier *et al.*, 2011; Shao *et al.*, 2014). The NRC helper NLRs in Solanaceae are required for the sensor NLRs Rpi-blb2, Mi2-5, Sw5b, R8, R1, Prf, Rx, Bs2 and CNL-119900, amongst others (Wu *et al.*, 2017). In both cases, the helper clade is relatively conserved and partially redundant, while their associated sensors are expanded and diversified. Phylogenetic analyses revealed that the conserved NRG1 clade and TIR-NLRs co-occur in angiosperm genomes: all clades that lack NRG1 also lack TIR-NLRs (Collier *et al.*, 2011; Shao *et al.*, 2016). Conceivably, all RPW8-NLRs are helper NLRs, with ADR1 signalling downstream of CC-NLRs and TIR-NLRs and NRG1s signalling downstream of TIR-NLRs only.

I set out to test if NRG1 is a helper for other TIR-NLRs. I generated *nrg1a-nrg1b* loss-of-function double mutants in Arabidopsis and a mutant of the single *NRG1* copy in *N. benthamiana* using CRISPR/Cas9 and tested for loss of TIR-NLR activities. I found that NRG1 is at least partially required for the signalling of the TIR-NLRs WRR4A, WRR4B, RPP1, RPP2, RPP4 and the NLR pairs CHS1/SOC3, CHS3/CSA1 and RRS1/RPS4. In contrast, *nrg1* loss-of-function does not compromise the CC-NLR R proteins RPS5 and MLA. RPM1 and RPS2 (CC-NLRs) function is slightly compromised in an *nrg1* mutant. Thus, NRG1 is required for full TIR-NLR function and contributes to the signalling of some CC-NLRs. Recent studies also suggested a requirement of NRG1 for RPP1-mediated signalling and identified Roq1, an additional NRG1-dependent TIR-NLR (Brendolise *et al.*, 2018; Qi *et al.*, 2018). Surprisingly, I found that NRG1 is required the HR but not for the bacterial disease resistance conferred by RRS1/RPS4. I discuss the potentially complementary roles of NRG1 and its sister clade ADR1. I propose that some NLRs signal via NRG1 only (*e.g.* CSA1/CHS3), some via ADR1 only (*e.g.* RPS2) and some via both (*e.g.* RRS1/RPS4).

5.2 Results

5.2.1 Identification of ADR1 in *N. benthamiana* genome

I used the NB-ARC amino acid sequence of *NbNRG1* (D L P L Q E L K V K L L E E K E K V V V L S A P A G C G K T T L A A M L C Q E D D I K D K Y R D I F FV T V S K K A N I K R I V G E I F E M K G Y K G P D F AS E H A AV C Q L N N L L R R S T S Q P V L L V L D D V W S E S D F V I E S F I F Q I P G F K I L V T S RS V FP K F D T Y K L N L L S E K D AK A LF Y S S A F KD S I P Y V Q L D L V H KA V R S C C G F P L A L K VV G R S LC G Q P E L I W F N R V M L Q S K R Q I L F PT E N D L L R T L R A S I D A L D E I D L Y S S E A T T L R D CY LD LG S F P E D H R I H A A A I L

D M W V E RY N L D E D) as a tblastn query sequence on the 'N. benthamiana Genome v1.0.1 predicted cDNA' database from Sol Genomic Network (Fernandez-Pozo *et al.*, 2015). I identified three transcripts: *Niben101Scf02118g00018.1* (*NbNRG1*), *Niben101Scf03844g01015.1* (*NbNRG2*, pseudogene) and *Niben101Scf02422g02015.1* (uncharacterised). The other results were not considered due to low coverage or low identity. *Niben101Scf02422g02015.1* predicted transcript does not start with a START codon and does not finish with a STOP codon so could be incomplete. *Niben101Scf02422g02015.1* was used as blastn query on 'N. benthamiana Genome v1.0.1 Contigs' to identify the gene in its genomic context. I retrieved *Niben101Scf02422g02015.1* genomic sequence on contig *Niben101Scf02422Ctg032* and identified a START codon 23 bp upstream and a STOP codon 564 bp downstream of *Niben101Scf02422g02015.1*, framing a 2487 bp gene including exons and introns **(Figure 5-1).** The resulting protein was analysed using SMART protein domain annotation resource (Letunic *et al.*, 2012). It contains an N-terminal RPW8 domain, a central NB-ARC domain followed by LRRs. A phylogenetic reconstruction of Niben101Scf02422g02015.1 NB-ARC domain along with the NB-ARC domains of AtADR1, AtADR1-L1, AtADR1-L3, AtADR1-L3, AtNRG1A, AtNRG1B, AtDAR5, NbNRG1 and AtZAR1 as outer group places Niben101Scf02422g02015.1 in the ADR1 clade **(Figure 5-1)**.

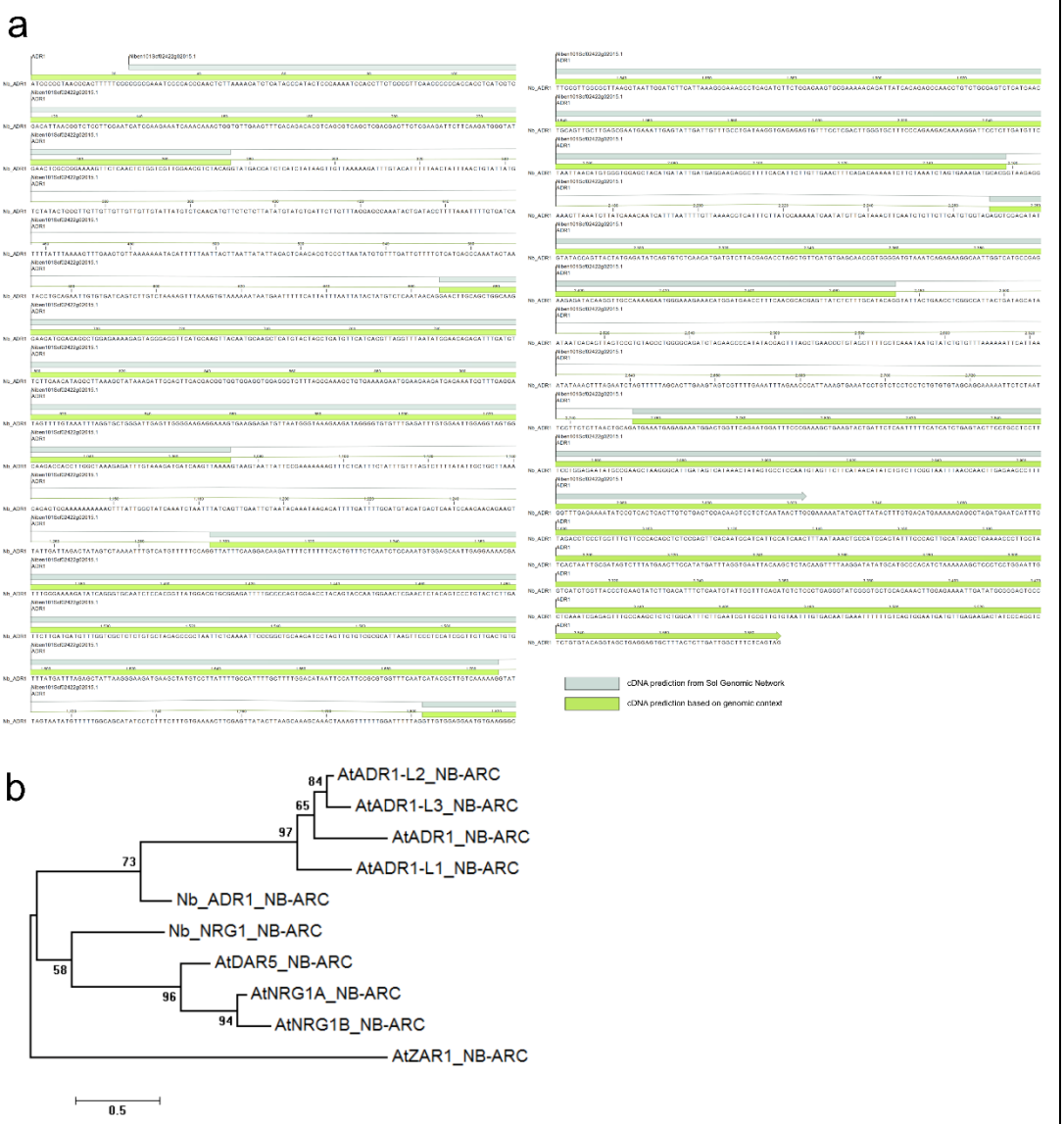

Figure 5-1: Phylogenetic tree of RPW8-NLRs (NB-ARC domain) from Arabidopsis and *Nicotiana benthamiana*

The sequences used here are from TAIR10 for Arabidopsis and SolGenomicsNetwork for *N. benthamiana*. The CC-NLR AtZAR1 was used an outer group. NB-ARC domain amino acid sequences were aligned using 'MUSCLE'. The phylogenetic reconstruction was made using the Maximum Likelihood method. The robustness of the tree was tested by Bootstraps (100 replicates). The tree is drawn to scale, with branch lengths measured in the number of substitutions per site. The analysis involved 10 amino acid sequences. All positions with less than 95% site coverage were eliminated. That is, fewer than 5% alignment gaps, missing data, and ambiguous bases were allowed at any position. There was a total of 57 positions in the final dataset. Evolutionary analyses were conducted with the software MEGA7. b. Sequence of NbADR1 in genomic context from contig Niben101Scf02422Ctg032. Blue: cDNA of the annotated Niben101Scf03844g01015.1 gene from Sol Genomic Network. Green: Putative ADR1 CDS framed with ha START and STOP codon. The figure was made using CLC Main Workbench Version 8.0.1. MUSCLE was used to generate phylogenetic trees using the Maximum Likelihood methods with 100 bootstraps. This analysis was carried out using the MEGA7 software.

5.2.2 CRISPR enables recovery of *nrg1* mutants in Arabidopsis and *N. benthamiana* and a *wrr4b* mutant in Arabidopsis

Four CRISPR constructs (CRISPR-1, CRISPR-2, CRISPR-3 and CRISPR-4) were assembled using Golden Gate cloning method and expressed via *Agrobacterium tumefaciens* strain GV3101 in Arabidopsis Ws-2, Col-0 or *N. benthamiana* **(Figure 5-2)**.

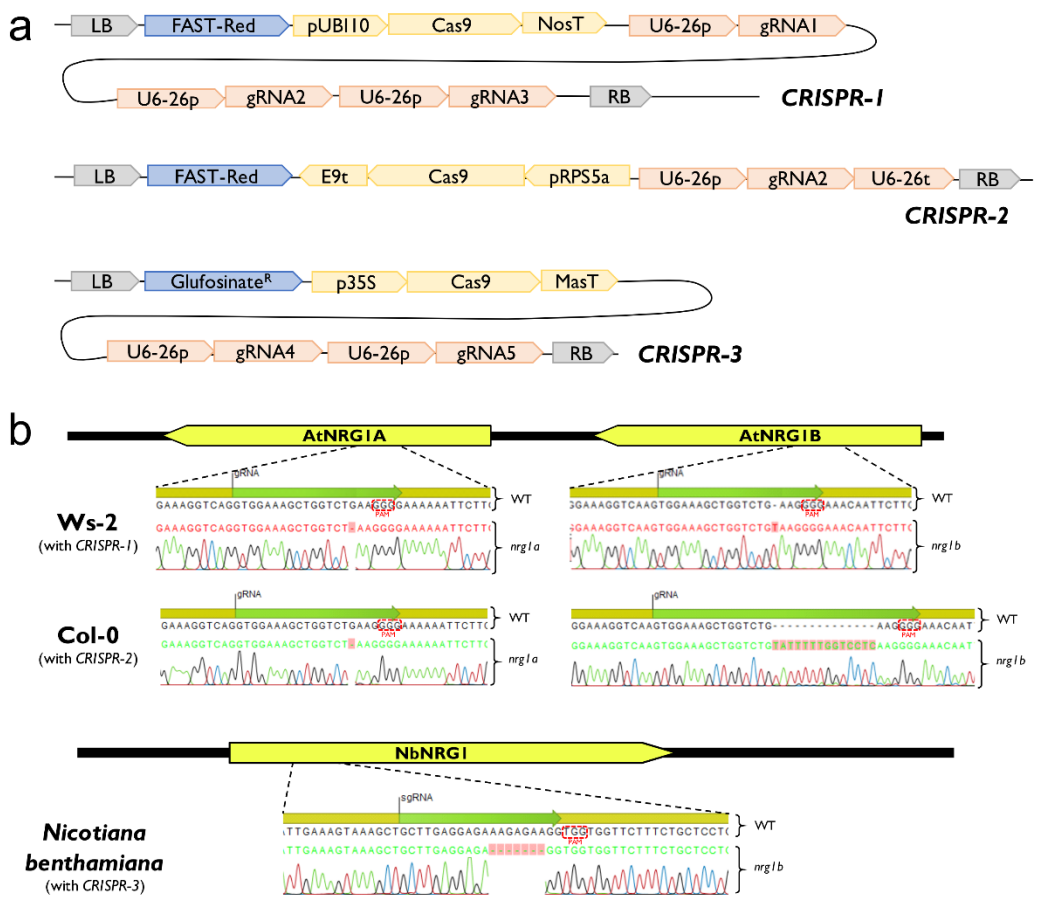

Figure 5-2: CRISPR enables to generate nrg1 mutants in plants
a. Schematic representation of the T-DNA containing a plant selectable marker (blue), a *Cas9* (yellow) and a *gRNA* (orange) expression cassettes. The modules were assembled using the Golden Gate cloning method. **b.** Constructs were expressed in plants via *Agrobacterium tumefaciens* strain GV3101. In Ws-2, one progeny carries a T deletion in *NRG1A* and a T insertion in *NRG1B*. In Col-0, one progeny carries a T deletion in *NRG1A* and a G deletion in *NRG1B*. In *Nicotiana benthamiana*, one progeny carries an AAGAGAA deletion in *NRG1*. These mutations cause a codon reading frame shift resulting in an early stop codon in the NB-ARC domains. The sequences were analysed using CLC Main Workbench Version 7.7.1. Red Square: PAM (Protospacer Adjacent Motif). LB: Left Border, *pUBI10*: 1327 bp of the At4g05320 promoter. *pRPS5a*: 1688 bp of the At3g11940 promoter. *35S*: 426 bp of the 35S promoter from *Cauliflower Mosaic Virus*. *E9T*: 631 bp of the *Pisum sativum rbcS E9* terminator. *U6-26p*: 205 bp of the At3g13855 promoter. *U6-26t*: 67 bp of the At3g13855 terminator. RB: Right border.

For CRISPR-1, three sgRNAs targeting both AtNRG1A and AtNRG1B (GCTCATTACCAAACCTGAAA[nGG], GTGGAAAGCTGGTCTGAAG[nGG] and

GATGATTTGTTCTCATCGAAA[nGG]) were designed and assembled by PCR to a sgRNA backbone in a Golden Gate compatible fashion (Methods S1) (Castel *et al.*, 2019). sgRNAs were assembled with *AtU6-26* promoter in the Golden Gate Level 1 vectors pICH47751, pICH47761, pICH47772 respectively. A human codon optimized allele of *Cas9* was assembled with the *AtUBI10* promoter and Nos terminator in Golden Gate compatible Level 1 vector pICH47742. These four level 1 vectors, along with a FAST-Red selectable marker in Level 1 vector pICH47732, were assembled in the binary vector pAGM4723, resulting in CRISPR-1 final vector.

For CRISPR-2, only one sgRNA targeting both *AtNRG1A* and *AtNRG1B* (GTGGAAAGCTGGTCTGAAG[nGG]) was used. A plant codon-optimized allele of *Cas9* containing a potato IV2 intron was assembled with *AtRPS5a* promoter and *Pisum sativum rbcS E9* terminator in pICH47811. There were cloned in binary vector pICSL4723 in a similar fashion as CRISPR-1, resulting in CRISPR-2 final vector.

For CRISPR-3, one sgRNA targeting *NbNRG1* (CAGTATTCGATGACATCGAG[nGG]) was used. A human codon-optimized allele of *Cas9* was assembled with *35S* promoter and *Mas* terminator in Golden Gate Level 1 vector pICH47742. The two vectors, along with a glufosinate resistance plant selectable marker in Level 1 vector pICH47732, were assembled in pICSL4723, resulting in CRISPR-3 final vector.

For CRISPR-4, two sgRNAs targeting *WRR4B* in Arabidopsis Ws-2 (AATCGCTTCCGTGAGAGCTG[nGG] and TACATAGTGTACTATCTAAA[nGG]) were used. A plant codon optimized allele of *Cas9* was assembled with *AtUBI10* promoter and *Ocs* terminator in Golden Gate Level 1 vector pICH47742. The two vectors, along with a FAST-Red selectable marker in Level 1 vector pICH47732, were assembled in pAGM4723, resulting in CRISPR-4 final vector.

For CRISPR-2 sgRNA specifically, 67 bp of the *AtU6-26* terminator was included by PCR at the sgRNA 3' end. Expression of CRISPR-1 in Arabidopsis Ws-2 resulted in a c.1153delG mutation in *NRG1A* and a c.1159_1160insT mutation in *NRG1B*. Expression of CRISPR-2 in Arabidopsis Col-0 resulted in a c.1153delG mutation in *NRG1A* and a c.1159_1160insTATTTTTGGTCCTC mutation *NRG1B*. Expression of CRISPR-3 in *N. benthamiana* resulted in a c.638_644delAAGAGAA mutation in *NbNRG1*. Expression of CRISPR-4 in Arabidopsis Ws-2 resulted in a c.181_182insA mutation in *WRR4B*. All these mutations cause a codon reading frame shift and early stop codons in of before the NB-ARC domain encoding region. Progenies of the mutants were analysed and I selected lines

without T-DNA and *nrg1* or *wrr4b* mutation at homozygous state. I refer to these lines as Ws-2_*nrg1a-nrg1b*, Col-0_*nrg1a-nrg1b*, *N. benthamiana*_*nrg1* and Ws-2_*wrr4b*.

5.2.3 NRG1 is required for RRS1/RPS4-mediated HR but not bacterial resistance in Ws-2

In Arabidopsis Ws-2, RRS1-R and RPS4 comprise a TIR-NLR pair that recognises the effectors PopP2 from *Ralstonia solanacearum* and AvrRps4 from *Pseudomonas syringae*. Their paralogs RRS1B and RPS4B also recognise AvrRps4 but not PopP2. RRS1/RPS4 and RRS1B/RPS4B activation results in HR, defence gene induction and bacterial resistance (Narusaka *et al.*, 2009; Saucet *et al.*, 2015). I tested if these responses require NRG1. I delivered the effector AvrRps4 using *Pseudomonas syringae* pv. tomato strain DC3000 and assessed cell death **(Figure 5-3)**. I observed fewer leaves displaying cell death in Ws-2_*nrg1a-nrg1b* than in Ws-2 WT. Cell death was not completely abolished in Ws-2_*nrg1a-nrg1b*. However, some combinations indicate that DC3000 can induce AvrRps4-independent cell death, such as DC3000 with empty vector in wild type, or with AvrRps4 in an *rrs1-rps4-rps4b* mutant. DC3000 carries a diverse set of effectors that influence immunity and could mask the AvrRps4-induced HR.

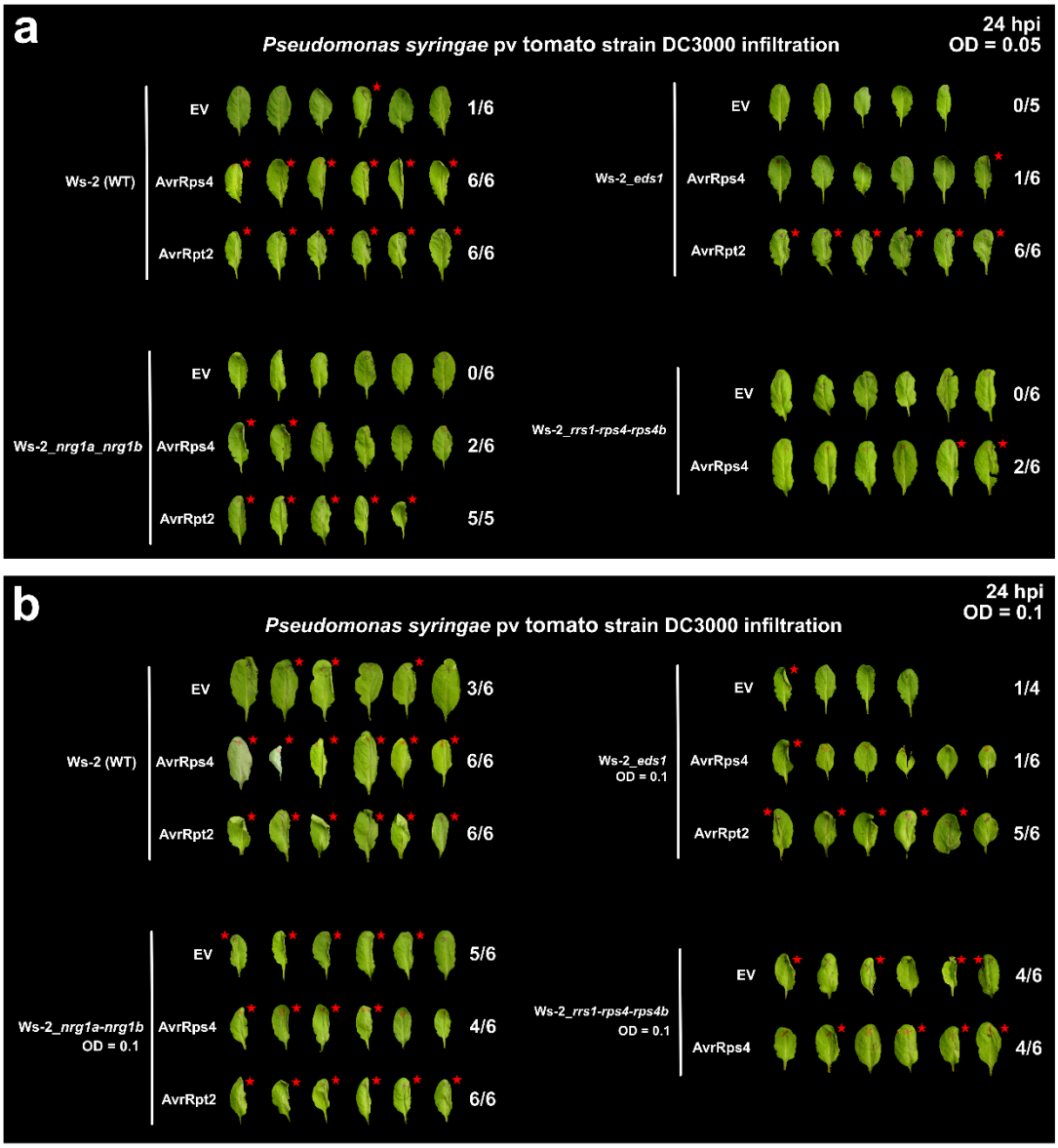

Figure 5-3: Cell death assay using *Pseudomonas syringae* strain DC3000
Arabidopsis leaves were infiltrated with *Pseudomonas syringae* pv tomato strain DC3000 expressing indicated effectors, OD600 = 0.05 **(a.)** or 0.1 **(b.)**. Half-leaf was infiltrated. Pictures were taken 24 hours post infiltration. The red stars show a host tissue collapse. The numbers indicate the number of plants displaying cell death out of the total number of plants tested. OD: optical density at 600 nm. hpi: hour(s) post-inoculation.

To test for HR after delivery of a single effector, I used the *Pseudomonas fluorescens* strain Pfo-1 carrying a type III secretion system (Pfo-1 EtHAn) (Thomas *et al.*, 2009). With the Pfo-1 system, AvrRps4 induces a specific HR in Ws-2 and Col-0, due to the activation of RRS1/RPS4 and RRS1B/RPS4B (Saucet *et al.*, 2015). The RRS1/RPS4 and RRS1B/RPS4B-mediated HR is completely lost in both Col-0_*nrg1a-nrg1b* and Ws-2_*nrg1a-nrg1b* backgrounds **(Figure 5-4)**. This observation confirms that the cell death observed with

DC3000_AvrRps4 in Ws-2_*nrg1a-nrg1b*, Ws-2_*eds1* and Ws-2_WT is independent of AvrRps4 **(Figure 5-3)**. However, AvrRpt2, AvrRpm1 and AvrPphB, which activate the CC-NLRs RPS2, RPM1 and RPS5 respectively (Debener *et al.*, 1991; Kunkel *et al.*, 1993; Simonich & Innes, 1995), induce HR after delivery from Pfo-1 even in an *nrg1a-nrg1b* mutant background. Both AtNRG1A and AtNRG1B can complement Ws-2_*nrg1a-nrg1b* loss of TIR-NLR-mediated HR, indicating that they are redundant for this function **(Figure 5-3)**.

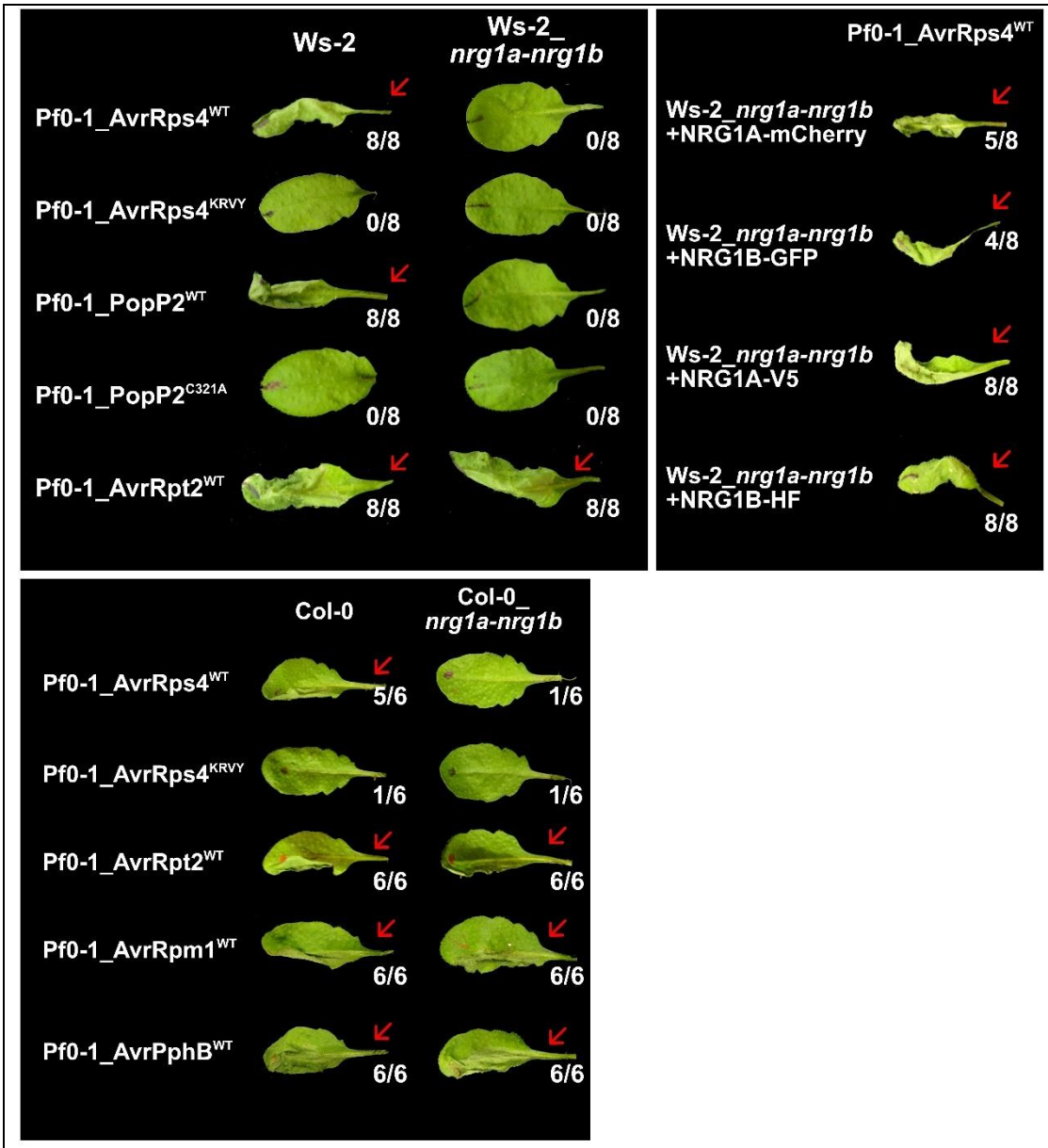

Figure 5-4: NRG1 is required for RRS1/RPS4 mediated HR
a. Arabidopsis leaves were infiltrated with *Pseudomonas fluorescens* strain Pfo-1 expressing indicated effectors, OD600 = 0.2. For Ws-2, the whole leaf was infiltrated. For Col-0, half-leaf was infiltrated. Pictures were taken 24 hours post inoculation. The red arrow shows a hypersensitive response (HR), indicating NLR activation by cognate effector. The numbers indicate the number of plants displaying HR out of the total number of plants tested. PopP2- and AvrRps4-mediated HR is lost in Ws-2_*nrg1a-nrg1b* and Col-0_*nrg1a-nrg1b*. AvrRps4^{KRVY} (AvrRps4$^{KRVY-AAAA}$) and PopP2^{C321A} are mutant alleles unable to trigger HR in WT plants, used as negative control for HR in

WT. They did not trigger HR indeed. AvrRpt2, AvrRpm1 and AvrPphB are CC-NLR-activating effectors used as positive control for HR in *nrg1*. They all trigger HR in both WT and *nrg1* mutant lines. HR is recovered in lines complemented with either *NRG1A* or *NRG1B*, tagged with mCherry, GFP, V5 of HF.

I conducted an electrolyte leakage assay to test whether the HR caused by the CC-NLRs RPS2, RPM1 and RPS5 was quantitatively reduced in Col-0_*nrg1a-nrg1b* **(Figure 5-5)**. Indeed, RPS2- and RPM1-, but not RPS5-mediated HR, as assayed by ion leakage assay, are also partially reduced at an early time point. This reduction is not seen at later time points for RPM1. These data indicate that NRG1 is fully required for the HR mediated by the TIR-NLRs RRS1/RPS4 and RRS1B/RPS4B, partially required for the HR mediated by the CC-NLRs RPM1 and RPS2, and not required for the HR mediated by the CC-NLR RPS5.

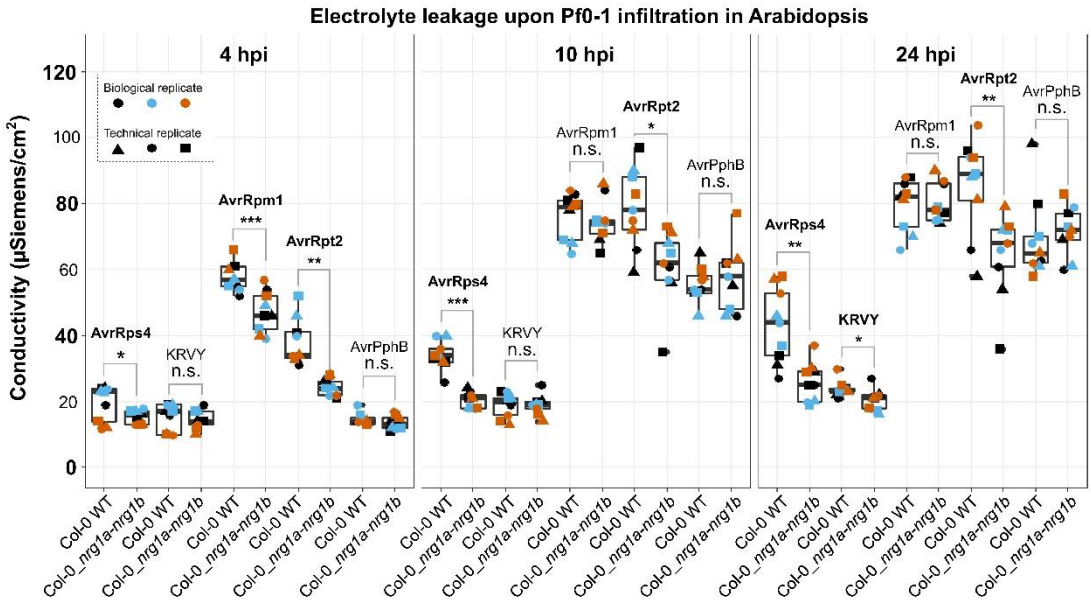

Figure 5-5: NRG1 is partially required for RPS2- and RPM1- mediated ion leakage
HR was quantified by the electrolyte leakage assay. Col-0 WT or Col-0_*nrg1a-nrg1b* plants were infiltrated in the same conditions as for the pictures. 16 discs were collected, rinsed and immersed in 10 ml of water. The electroconductivity was measure at 4, 10 and 24 hpi. Boxplots represent nine data points (three biological replicates x three technical replicates). Colours indicates biological replicates (plants grown at different times); shapes indicate technical replicates (different plants inoculated with the same inoculum). Significance was calculated with t-tests and the p-value is indicate by n.s. (non-significant, > 0.05), * (<0.05), ** (<0.01) or *** (<0.001). WT: wild type. HR: hypersensitive response. hpi: hour(s) post inoculation.

I used the *Pseudomonas syringae* pv. tomato strain DC3000 to test for bacterial resistance (Xin & He, 2013). Bacterial growth on Ws-2 is reduced for DC3000 expressing *AvrRps4*, due to recognition by RRS1/RPS4 and RRS1B/RPS4B. Surprisingly, this AvrRps4-dependent reduced growth is unaltered in an *nrg1a-nrg1b* double mutant **(Figure 5-6)**. Although DC3000 can trigger AvrRps4-independent cell death, the AvrRps4-dependent HR is lost in *nrg1a-nrg1b* **(Figure 5-3, Figure 5-4, Figure 5-5)**. Thus, loss of NRG1 function abolishes HR

from activation of RRS1/RPS4 and RRS1B/RPS4B but does not compromise activation of disease resistance to bacteria in Arabidopsis. The maintenance of RPS2-mediated HR in the absence of NRG1 correlates with resistance to DC3000 expressing AvrRpt2 in Col-0_*nrg1a-nrg1b* **(Figure 5-6)**.

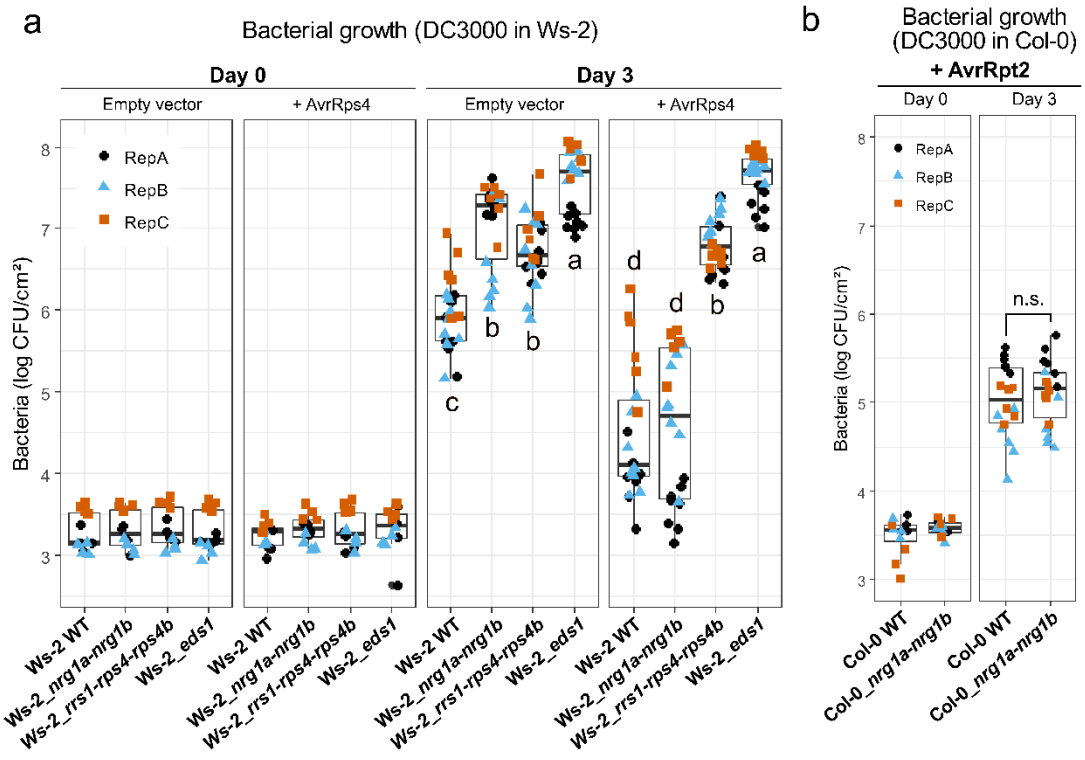

Figure 5-6: NRG1 is not required for bacterial resistance
Bacterial growth assay in Arabidopsis using *Pseudomonas syringae* pv tomato strain DC3000 (DC3000). One leaf per plant was infiltrated with DC3000 expressing or not **(a)** AvrRps4 or **(b)** AvrRpt2 at OD600 = 0.001. Bacteria quantification was done just after infiltration (0 dpi) and 3 days post inoculation (3 dpi). Each dot represents one individual plant. Colours and shapes represent three biological replicates. **a.** Letters above the bars indicate significant differences (P<0.05) as determined by a one-way ANOVA followed by post hoc Tukey HSD analysis. **b.** The growth of DC3000_AvrRpt2 was not different in Col-0 WT and Col-0_*nrg1a-nrg1b*, as indicated by a non-significant (n.s) t-test (p-value = 0.418). Rep: Biological replicate. CFU: colony forming unit.

Activation of RRS1/RPS4 also results in induction of salicylic acid (SA)-related genes such as *ICS1* and *PR1* (Sohn *et al.*, 2014). SA plays a crucial role as a signalling molecule that activates plant immunity (Durner *et al.*, 1997). I measured changes in SA levels, the expression of SA-responsive *PR1* and SA-biosynthetic gene *ICS1* in response to Pfo-1_AvrRps4, and as a control, to Pfo-1_AvrRps4^{KRVY}, a Pfo-1 strain carrying non-recognized allele of AvrRps4 (Sohn *et al.*, 2012). *PR1* and *ICS1* both show RPS4/RRS1/AvrRps4-dependent gene induction even in the absence of NRG1 **(Figure 5-7a and c)**. SA is weakly induced by Pfo-1_AvrRps4^{KRVY}, likely due to PTI, and strongly induced by Pfo-1_AvrRps4

(Figure 5-7b). SA induction is not reduced in Ws-2_*nrg1a-nrg1b*. Thus, NRG1 is not required for RRS1/RPS4-mediated elevation of SA levels and induction of defence genes.

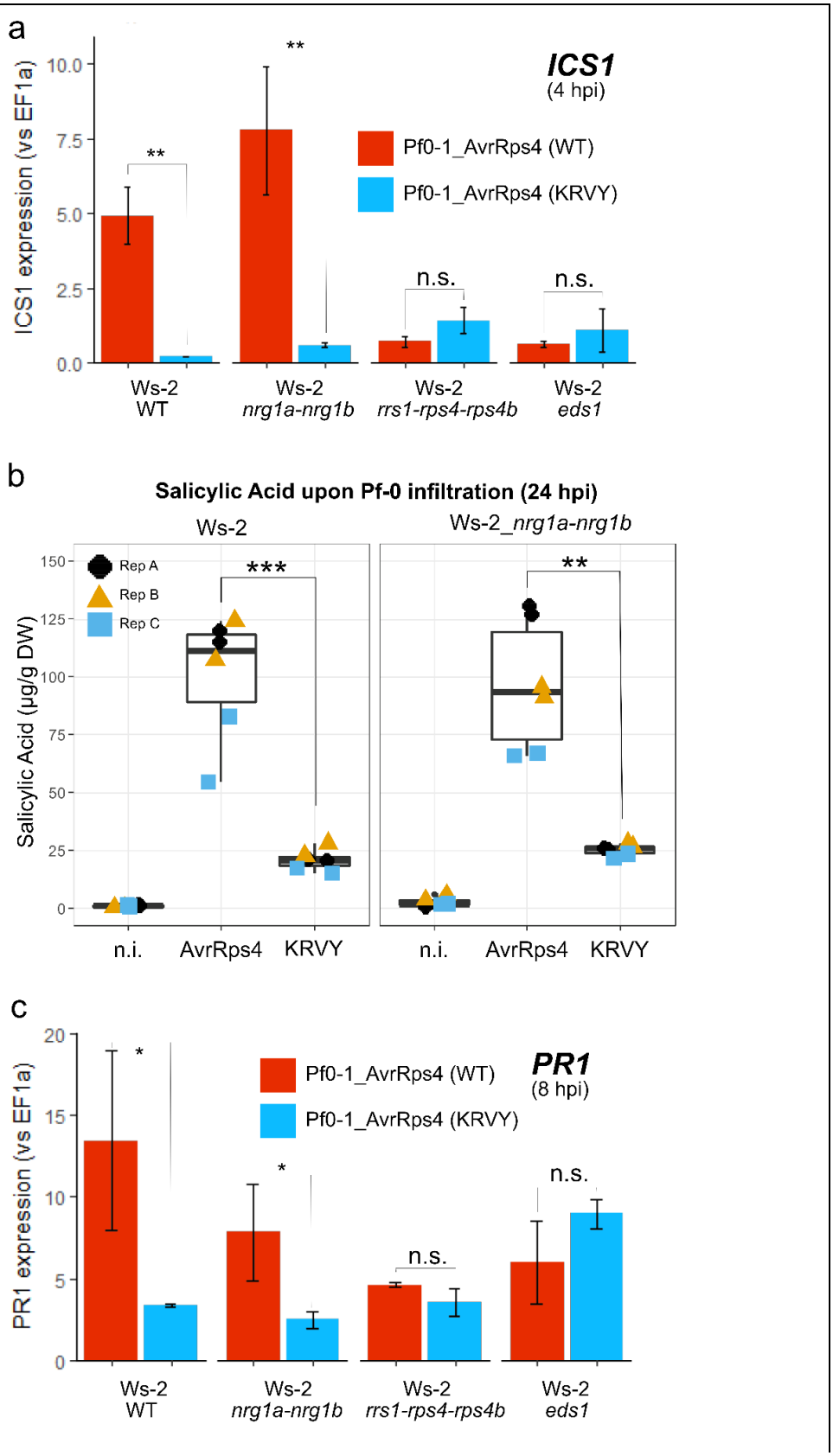

Figure 5-7: NRG1 is not required for salicylic acid pathway activation
a. and c. Induction of *ICS1* and *PR1* upon Pf0-1 strain infiltration. Arabidopsis leaves were infiltrated with bacteria at OD600 = 0.2. Samples were collected 4 hpi for *ICS1* expression and 8 hpi for *PR1* expression. Values represent the expression level as compared to *EF1α*, using the 'double delta Ct' method. Three lines were used and bulked for each treatment. Error bars represent standard error of three technical replicates. Three biological replicates all showed induction of *ICS1* and *PR1* by AvrRps4 in both WT and Ws-2_*nrg1a-nrg1b*. **b.** Induction of salicylic acid upon Pf0-1 strain infiltration. Arabidopsis leaves were infiltrated with bacteria at OD600 = 0.05. Samples were collected 24 hpi. SA was extracted from 10 mg of dry weight and SA was quantified by Ultra high-pressure liquid chromatography. Colours and shapes represent three biological replicates, each represented by two independent extractions from the same set of infiltrated leaves. Significance was calculated with t-tests and the p-value is indicate by n.s. (> 0.05), * (<0.05), ** (<0.01) or *** (<0.001). hpi: hour(s) post inoculation. n.i.: non-infiltrated

5.2.4 Arabidopsis *nrg1* mutants show impaired TIR-NLR-dependent resistance to oomycete pathogens

Arabidopsis accession Col-0 resists *Hyaloperonospora arabidopsidis* (downy mildew or Hpa) races Emoy2 and Cala2 via the TIR-NLRs RPP2 and RPP4 respectively (Van Der Biezen *et al.*, 2002; Sinapidou *et al.*, 2004). In Ws-2, Hpa race Cala2 is resisted via the TIR-NLR RPP1_WsA (Botella *et al.*, 1998). I tested whether Cala2 and Emoy2 resistance requires NRG1. I found that Cala2 hyphal growth in cotyledons was more extensive in Ws-2_*nrg1a-nrg1b* than in Ws-2 WT for Cala2 **(Figure 5-8)**.

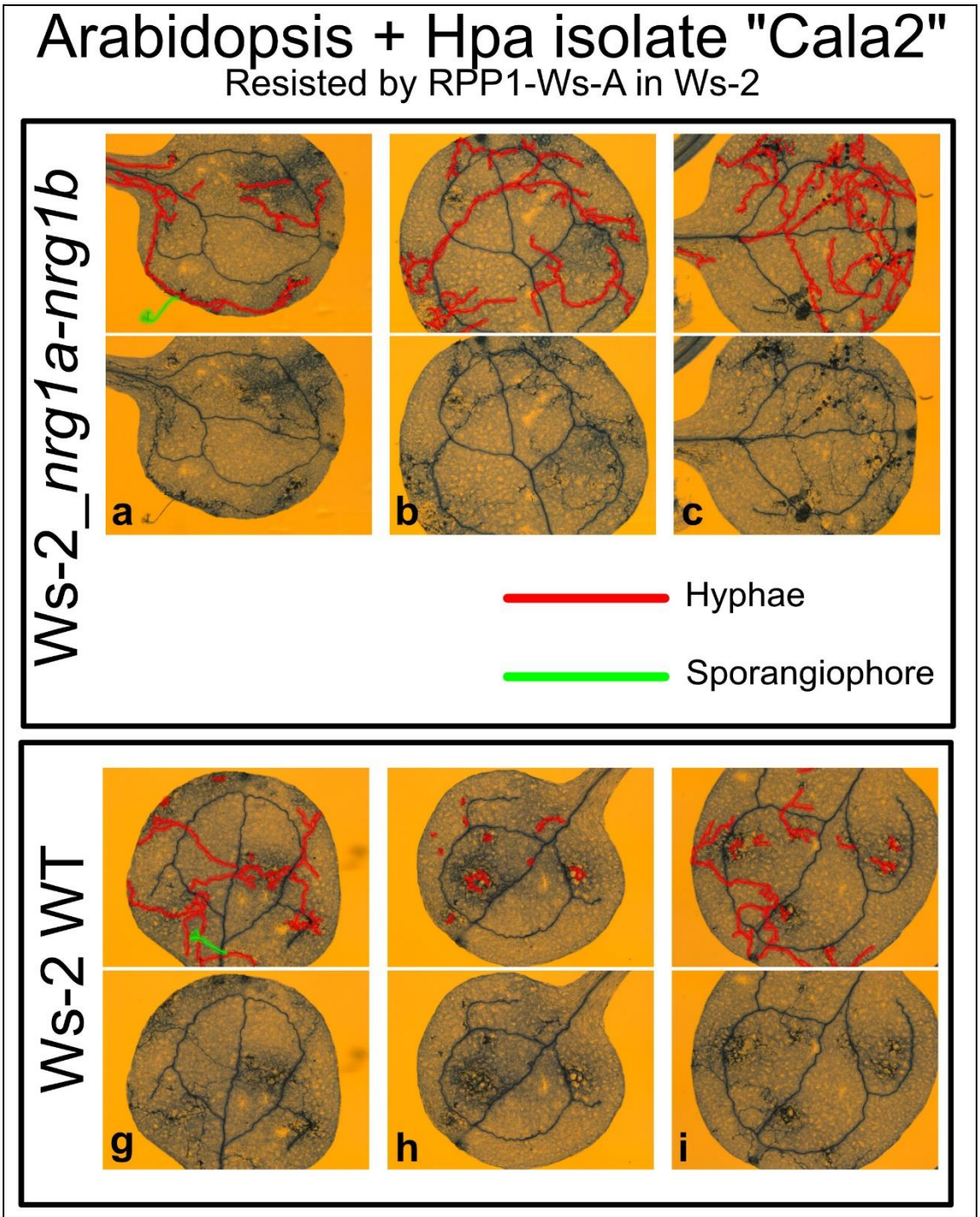

Figure 5-8: Ws-2_*nrg1a-nrg1b* mutant is partially compromised in resistance to RPP1-mediated resistance to Cala2

7-day old plants were sprayed inoculated with *Hyaloperonospora arabidopsidis* Cala2, resisted by RPP1-Ws-1A in Ws-2. Plants were phenotyped 7 days after inoculation. Plants were stained with trypan blue to visualise hyphae growth. Six cotyledons for each genotype were examined under microscope. **a.-f.** Six cotyledons from Ws-2_*nrg1a-nrg1b* inoculated plants. **g.-h.** Six cotyledons from Ws-2 WT inoculated plants. Images were annotated using the software Affinity Photo. Hyphae and sporangiophores are coloured in red and green. The original pictures are showed on the bottom.

Moreover, more spores were produced on *nrg1a-nrg1b* infected plants, but not to the level of *eds1* (*enhanced disease resistance 1*, an Arabidopsis mutant strongly affected in resistance mediated by TIR-NLRs (Parker *et al.*, 1996)) (Figure 5-9). Some spores were observed in the resistant WT plant; these could either be spores that persist from the inoculation or fresh spores from rare sporangiophores sometimes observed in cotyledons of WT plant (**Figure 5-8g**). I conclude that RPP1- and RPP2-mediated resistance to Cala2 and RPP4-mediated resistance to Emoy2 partially requires NRG1.

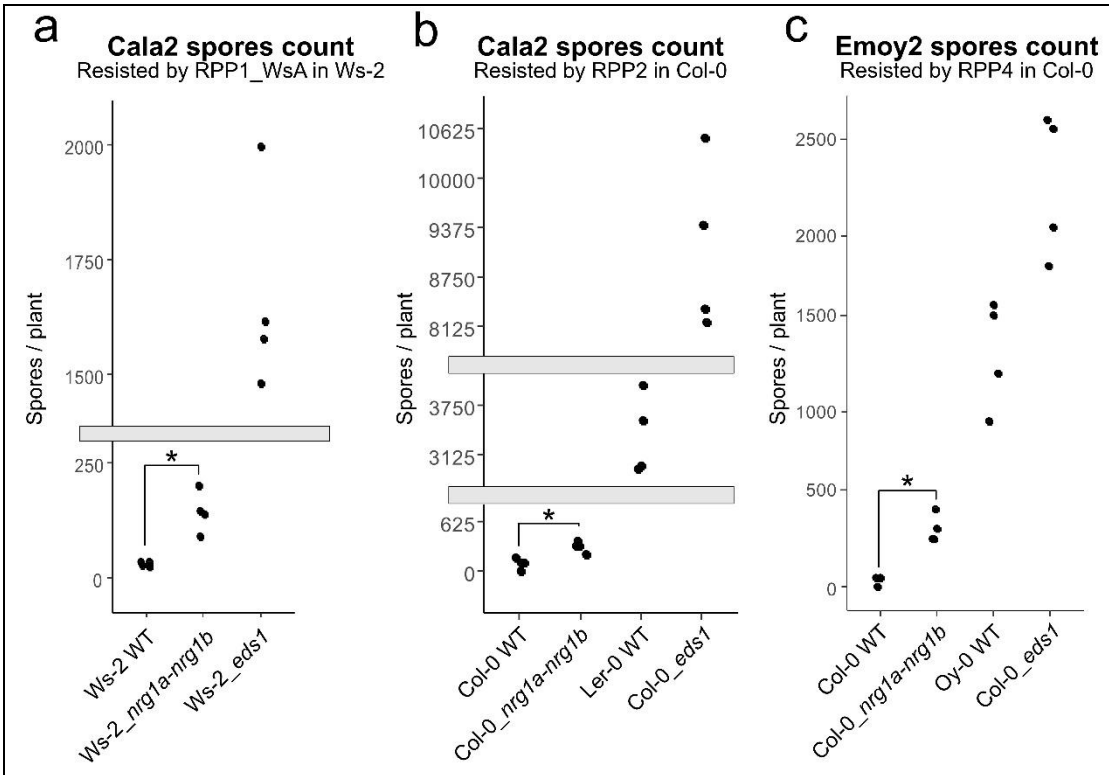

Figure 5-9: *nrg1* mutants are partially compromised in resistance to downy mildew
7-day old plants were sprayed inoculated with *Hyaloperonospora arabidopsidis* race Emoy2 or Cala2. Plants were phenotyped 7 days after inoculation. **a. b. c.** Full resistance was observed in Col-0 and Ws-2 WT, full susceptibility was observed in Col-0_*eds1* (*eds1-2*) and Ws-2_*eds1* (*eds1-1*) and intermediated phenotype in Col-0_*nrg1a-nrg1b* and Ws-2_*nrg1a-nrg1b*. Ler-0 and Oy-0 were used as susceptible controls for Cala2 and Emoy2 infections respectively. (*) stars indicate significant differences (t-test at 0.05 significance) between WT and nrg1 mutant plants. Data are expressed in spores per plant.

Arabidopsis Col-0 and Ws-2 also contain TIR-NLRs that confer resistance to the oomycete *Albugo candida* (Ac), the cause of white rust. For instance, the TIR-NLR WRR4A confers resistance to the white rust race AcEm2 (Borhan *et al.*, 2008). I expressed an allele of *WRR4A* from Arabidopsis accession Oy-0 in the AcEm2-compatible accession Ws-2 and observed full resistance indeed **(Figure 5-10)**. However, Ws-2_*nrg1a-nrg1b* transformed with *WRR4A* was partially susceptible, showing that *WRR4A* requires NRG1 to activate full resistance to white rust. All transgenic lines expressed WRR4A, at different levels within

the same range **(Figure 5-10)**. Thus, the partial loss of resistance in Ws-2_*nrg1a-nrg1b_WRR4A* is not due to low expression of *WRR4A* but rather to the loss of NRG1.

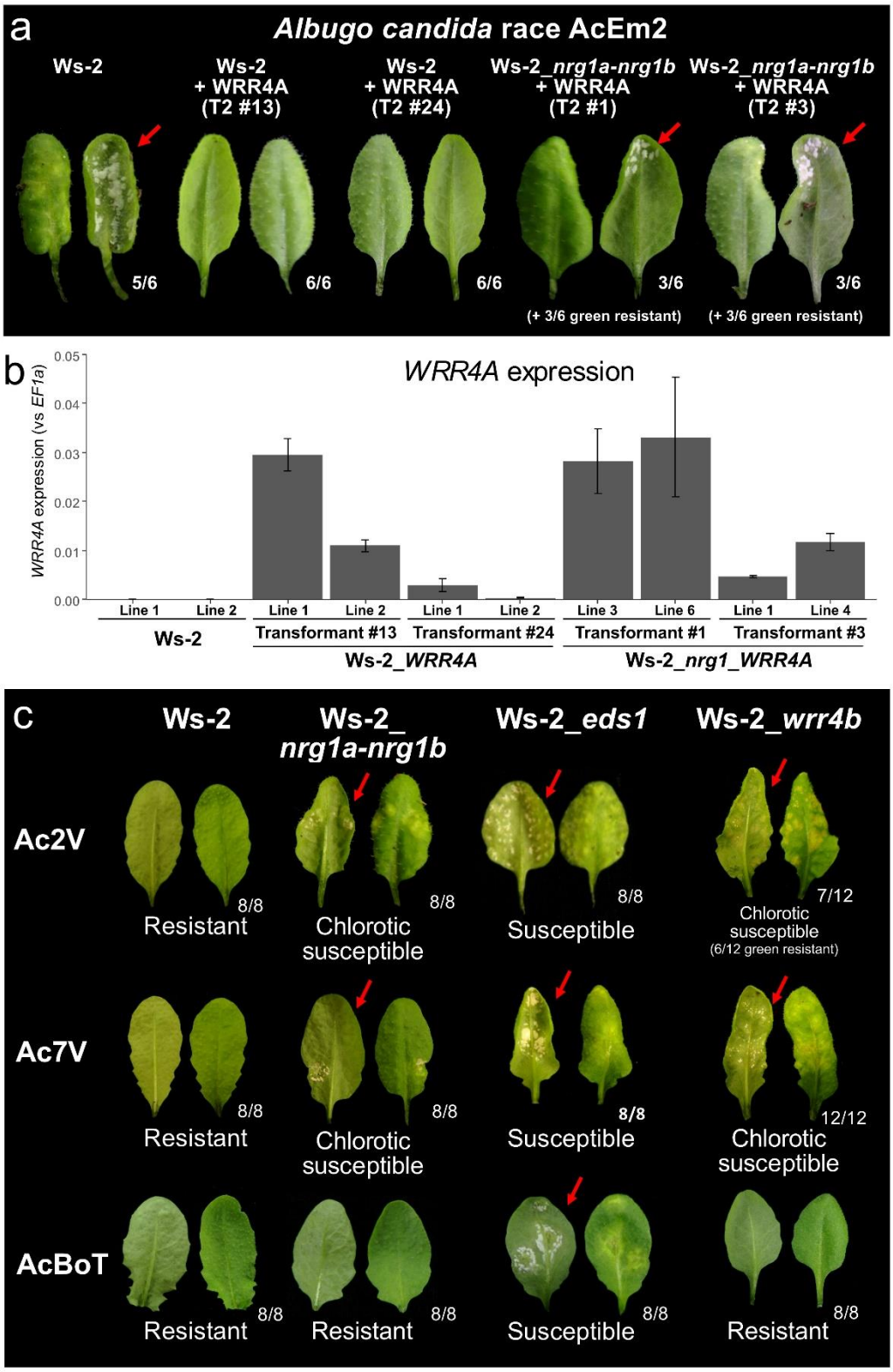

Figure 5-10: nrg1 mutants are partially compromised in resistance to white rust
3- to 5-week old plants were sprayed inoculated with *Albugo candida*. Plants were phenotyped 12 days after inoculation. Abaxial and adaxial picture of the same leaf are showed. Numbers indicate

the number of individual plants showing similar phenotype out of the number of plants tested. **a.** Two independent lines for Ws-2 WT and two independent lines for Ws-2_*nrg1a-nrg1b* were tested for *Albugo candida* race AcEm2 resistance. 6 plants were tested for each line. Ws-2 is susceptible, while *WRR4A* transgenic lines are resistant. Ws-2_*nrg1a-nrg1b* expressing *WRR4A* are still partially susceptible to AcEm2. Oy-0 allele of *WRR4A* was used here. **b.** RT-qPCR was conducted in *WRR4A* transgenic lines. Two lines were tested for each independent transformants. Error bars indicate standard error of three technical replicates. *WRR4A* is expressed in those lines at a higher level than in the fully resistant Col-0 WT. **c.** Eight or twelve plants for each genotype were tested with *Albugo candida* races Ac2V, Ac7V and AcBoT. Ws-2_*eds1* (*eds1-1*) are fully susceptible to *Albugo candida* races Ac2V and Ac7V, while Ws-2_WT are resistant. Ws-2_*nrg1a-nrg1b* and Ws-2_*wrr4b* are partially susceptible to Ac2V and Ac7V. AcBoT resistance is not affected in Ws-2_*nrg1a-nrg1b* and Ws-2_*wrr4b* mutants, while Ws-2_*eds1* is partially susceptible. Red arrows indicate presence of white pustules, resulting from production of zoospores. T2: line from the second generation after transformation. #: reference number of the independent transformant line.

Ws-2 lacks *WRR4A* but contains a paralog, called *WRR4B*, which confers resistance to the white rust races Ac2V, Ac7V and AcBoT (Cevik *et al.*, 2019). I expressed a Cas9 construct targeting *WRR4B* with two sgRNAs and recovered a homozygous mutant line. This line is partially susceptible to Ac2V and Ac7V, but still resists AcBoT **(Figure 5-10)**. Similarly, Ac2V and Ac7V, but not AcBoT can complete their life cycle on Ws-2_*nrg1a-nrg1b*. Thus, both WRR4B and NRG1 are required for full Ac2V and Ac7V resistance, and the phenotypes of both loss-of-function mutants are similar, suggesting that WRR4B also requires NRG1 to confer white rust resistance.

5.2.5 NRG1 is required for SOC3/CHS1- and CSA1/CHS3-induced HR in *Nicotiana benthamiana*

CSA1 and *CHS3* are two adjacent TIR-NLR-encoding genes from Arabidopsis. CHS3 carries an integrated C-terminal LIM domain. *chs3-2D* is a gain-of-function allele that confers a CSA1-dependent autoimmune phenotype in Arabidopsis (Xu *et al.*, 2015). Similarly, SOC3 and CHS1 are a TIR-NLR/TIR-NB (TIR, NB-ARC but no LRR) pair encoded by two adjacent genes in Arabidopsis. They interact to modulate immunity (Zhang *et al.*, 2016c). I transiently expressed *CSA1* and *chs3-2D* or *SOC3* and *CHS1* in leaves of *N. benthamiana* and in the Nb_*nrg1* mutant. I found that CSA1 and chs3-2D can induce HR in *N. benthamiana* but not in Nb_*nrg1* **(Figure 5-11)**.

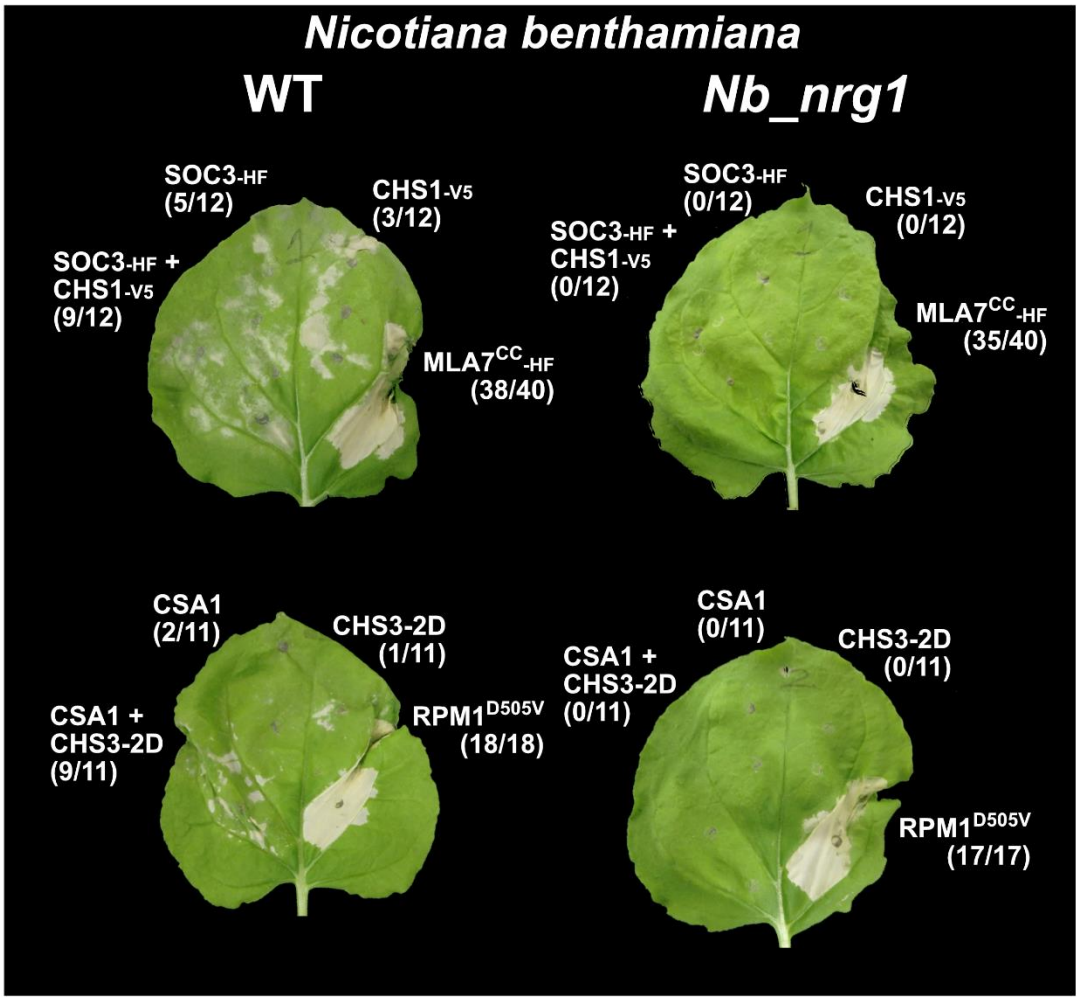

Figure 5-11: CSA1/CHS3 and SOC3/CHS1 induce an NRG1-dependent HR *in N. benthamiana*
4-week old *N. benthamiana* plants were infiltrated with *Agrobacterium tumefaciens* strain GV3101 at OD600 = 0.4. Genes are expressed under the control of the 35S promoter and the *Ocs* terminator. Pictures were taken 5 dpi. Both SOC3/CHS1 and CSA1/CHS3 pairs induce Hypersensitive Response (HR) in WT but not in *nrg1* mutant. SOC3, CHS1, CSA1, CHS3-2D give sometime an HR on their own. The CC domain of MLA7 from barley and RPM1^{D505V} auto-active allele were used as non TIR-NLR controls. Numbers indicate the number of HR observed out of the number of infiltrations for a given combination. Even weak HRs were considered. For instance, on WT plants from this figure, SOC3, CHS1, SOC3+CHS1, CSA1+CHS3-2D and CHS3-2D were considered as positive for HR, while CSA1 was considered as negative.

I also observed an HR triggered by SOC3 and CHS1 alone or in combination, which is lost in the absence of NRG1. Although the CHS1/SOC3 and CHS3/CSA1 phenotypes are weak in WT, they never induce HR in Nb_*nrg1*. The CC domain of the CC-NLR MLA from barley and the D505V 'autoimmune' allele of the CC-NLR RPM1 from Arabidopsis activates HR in *N. benthamiana* (Gaoa *et al.*, 2011; Maekawa *et al.*, 2011). Transient expression of these alleles results in HR in both *N. benthamiana* and Nb_*nrg1*. I tested the expression of CHS1 and SOC3 and found that the proteins are still expressed in Nb_*nrg1* **(Figure 5-12)**. As CHS3-2D

and CSA1 are not tagged, I tested the expression of their mRNA and found that there were also expressed in Nb_*nrg1*.

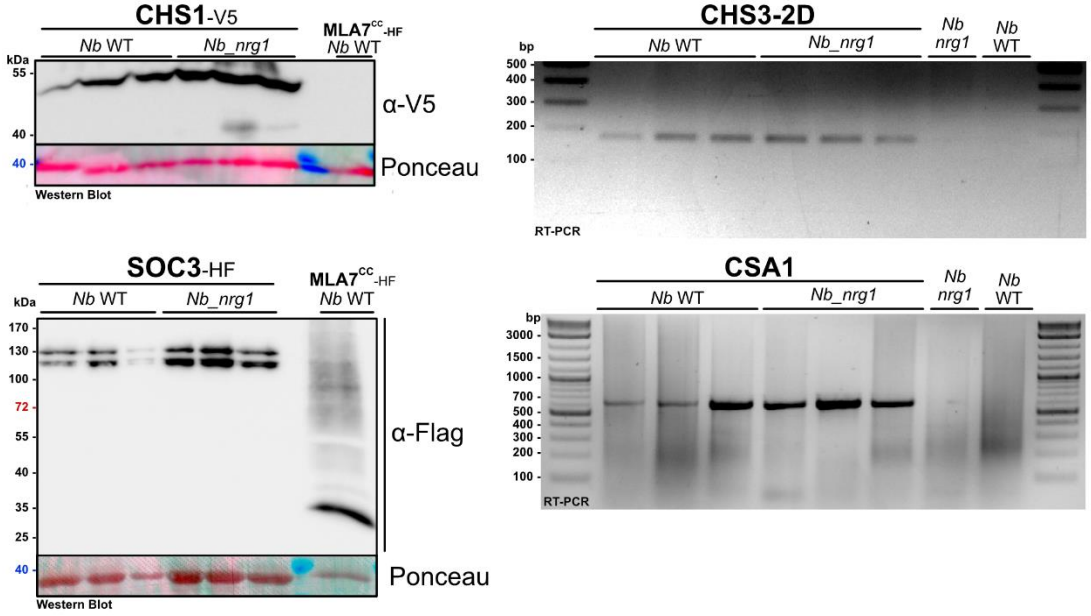

Figure 5-12: Expression of CHS1/SOC3 and CHS3/CSA1 in *Nicotiana benthamiana*
CHS1-V5, SOC3-HF, CHS3-2D and CSA1 were transiently expressed in *Nicotiana benthamiana*. For CHS1-V5 and SOC3-HF, proteins were extracted 3 dpi and revealed by Western Blot. Both are detected at their expected size, i.e. 50.39 kDa for CHS1-V5 and 124.66 kDa for SOC3-HF. Two bands are observed for SOC3-HF. CHS3-2D and CSA1 are not tagged and cannot be revealed by immunoblot. Their expression was measured by RT-PCR. RNA was extracted 3 dpi. RT-PCR was conducted to amplify a 176 bp fragment in *CHS3-2D* and a 643 bp fragment in *CSA1*. They were both expressed in *N. benthamiana* WT and *nrg1* mutant after infiltration.

I conclude that NRG1 is required for the HR initiated by the TIR-NLR pair CSA1-CHS3 and the TIR-NLR/TIR-NB pair SOC3-CHS1 but not by the CC-NLRs MLA7 and RPM1 in *N. benthamiana*.

5.3 Discussion

5.3.1 NRG1 is a conserved clade of RPW8-NLR that contributes to TIR-NLR signalling

NRG1 was originally identified in *N. benthamiana* as required for resistance mediated by the TIR-NLR N (Peart *et al.*, 2005). *NRG1* is broadly conserved within angiosperms, forming the so-called *NRG1* clade (Collier *et al.*, 2011). NRG1 could be a helper clade for many NLR sensors. Interestingly, there is a correlation of NRG1 and TIR-NLR occurrence within plant genomes; the *NRG1* lineage is missing in monocots and Lamiales, which also lack TIR-NLRs (Collier *et al.*, 2011). On the other hand, the NLRome of *Amborella trichopoda*, an early

diverging lineage among angiosperms, contains both TIR-NLRs and NRG1 (Shao *et al.*, 2016). This observation suggests that NRG1 could be specifically required for all TIR-NLR-mediated immunity. To test this hypothesis, I mutated *NRG1* from *N. benthamiana* and Arabidopsis and tested for loss or reduction of TIR-NLR function. *N. benthamiana* and Arabidopsis carry one and two copies of *NRG1* respectively (*NbNRG1* and *AtNRG1A*/*AtNRG1B*). I found that NbNRG1 is required for the HR triggered by the TIR-NLR pairs *SOC3*/*CHS1* and *CSA1*/*CHS3-2D* **(Figure 5-11)**. Signalling of the CC-NLRs MLA7 and RPM1 still results in an HR in *Nb_nrg1* that is indistinguishable from WT. In Arabidopsis, CHS3 signals via NRG1 but not CHS1, which signals via ADR1 (Wu *et al.*, 2018b). It is possible that NbADR1 is too diverged from the three Arabidopsis ADR1 alleles to support CHS1 function and complement the loss of NRG1.

In Arabidopsis accession Ws-2, transgenic expression of *WRR4A* confers NRG1-dependent resistance to the *A. candida* race AcEm2 **(Figure 5-10)**. Moreover, resistance to *A. candida* races Ac2V and Ac7V is strongly reduced in an *nrg1a-nrg1b* double mutant **(Figure 5-10)**. This resistance is mediated in part by the TIR-NLR WRR4B, suggesting that the WRR4B paralog of WRR4A can also signal via NRG1. I also found that resistance mediated by the TIR-NLRs RPP1, RPP2 and RPP4 is partially dependent on NRG1 in Arabidopsis **(Figure 5-9)**. However, the requirement of NRG1 by RPP1, RPP2 and RPP4 for downy mildew resistance, although significant, was weak. In addition, RPP4 function was not affected in an independent experiment (Wu *et al.*, 2018b). Thus, other helpers, such as ADR1, already reported to contribute to RPP4 function (Bonardi *et al.*, 2011), likely also contribute to RPP1, RPP2 and RPP4 function.

Using the Pfo-1 system, I found that the HR induced by RRS1/RPS4 and RRS1B/RPS4B is fully dependent on NRG1 in Arabidopsis **(Figure 5-4)**. Surprisingly, I observed a weak reduction of the HR induced by AvrRpt2 (via CC-NLR RPS2) and AvrRpm1 (via CC-NLR RPM1) **(Figure 5-5)**. The HR induced by AvrPphB (via CC-NLR RPS5) is unaltered in Col-0_*nrg1a-nrg1b*. It was previously reported that another CC-NLR, Rx2 from potato, also requires NRG1 redundantly with ADR1 to confer resistance to *Potato Virus X* (Collier et al., 2011).

NRG1 is indeed required for full function of all tested TIR-NLRs. However, the function of some CC-NLRs is also compromised in the absence of NRG1.

Arabidopsis genomes contains two *NRG1* copies in tandem while *N. benthamiana* has only one copy. This tandem duplication must have a biological relevance. The HR mediated by

RRS1-RPS4 is NRG1-dependent and both alleles are sufficient **(Figure 5-4)**. It indicates that NRG1A and NRG1B are redundant for this function. However, NRG1A and NRG1B share less than 72% amino acid identity. It could be that NRG1A and NRG1B are not redundant for recognition of other NLRs. In addition, the polymorphism can enable to avoid targeting of both copies by the same effector. In both cases, the duplication event resulted in one more node in the NRG1 helper network, making it more robust.

5.3.2 Disease resistance is possible without HR

Despite the absence of AvrRps4-induced HR, RRS1/RPS4 still confers bacterial resistance in a Ws-2_*nrg1a-nrg1b* background **(Figure 5-4, Figure 5-6)**. The HR is a form of cell death associated with plant resistance, and is strongly correlated with activation of a host R protein by a pathogen avirulence factor (Morel & Dangl, 1997). For instance, the recognized effectors AvrRpm1 and AvrRpt2 trigger both HR and bacterial resistance in Arabidopsis, due to recognition by the R proteins RPM1 and RPS2 (Mackey *et al.*, 2002). However, not all avirulence factors induce HR. For example, the effectors HopZ5 and HopPsyA from *P. syringae* pv *actinidiae* and *P. syringae* pv syringae induce an HR-independent resistance in Arabidopsis accession Col-0 (Gassmann, 2005; Jayaraman et al., 2017). Similarly, the HR-induction by the CC-NLR Rx is not required to confer extreme resistance against *potato virus X* (Bendahmane *et al.*, 1999). Here I found that NRG1 is required for HR but not resistance mediated by the TIR-NLR pair RRS1/RPS4. It was previously reported that AvrRps4 activates cell death from the cytoplasm and resistance from the nucleus, and that these two functions are independent (Heidrich *et al.*, 2011). Whether NRG1 plays a specific role in this cytoplasmic cell death pathway is unknown. Moreover, RPP1-mediated HR in *N. benthamiana* fully requires *NbNRG1* (Brendolise *et al.*, 2018; Qi *et al.*, 2018), while RPP1 function is partially retained in Ws-2_*nrg1a-nrg1b* **(Figure 5-9)**. The uncoupling of HR and resistance highlights the ambiguous relationship between these two defence outputs.

In contrast, NRG1 is required for Roq1-mediated HR and Roq1-dependent bacterial resistance in *N. benthamiana* (Qi *et al.*, 2018). I speculate that ADR1 proteins, from the sister clade of NRG1, might partially complement the loss of NRG1s for some TIR-NLRs, *e.g.* RRS1/RPS4 and RPP1 but not Roq1.

5.3.3 TIR-NLRs activate in parallel an SA-dependent pathway and an NRG1-dependent pathway that results in HR

ADR1 proteins are required for RPS2/AvrRpt2-induced SA production in Arabidopsis (Bonardi *et al.*, 2011). I tested if the same is true for NRG1 proteins. I measured the induction of SA and the expression of the SA-biosynthetic gene *ICS1* (*Isochorismate Synthase 1*) and the SA-responsive gene *PR1* (*Pathogenesis-Related1*) in Ws-2_*nrg1a-nrg1b* (Dong, 2004). In this assay, I compared induction after infiltration of Pfo-1_AvrRps4^{WT} (inducing both PTI and ETI via RRS1/RPS4 and RRS1B/RPS4B) and infiltration of a Pfo-1_AvrRps4^{KRVY} (inducing PTI only) **(Figure 5-7)**. In Ws-2_*rrs1-rps4-rps4b* and Ws-2_*eds1*, *ICS1* and *PR1* expression are not induced by AvrRps4 or its inactive allele AvrRps4KRKY. However, AvrRps4 specifically enhances *ICS1* and *PR1* expression in both WT and *nrg1a-nrg1b* mutant lines. This is consistent with the production of SA, which is maintained at similar levels after induction in both WT and *nrg1a-nrg1b*. Although NRG1 is required for RRS1/RPS4 mediated HR, it is dispensable for the SA pathway activation. In contrast, ADR1 is required for SA induction during ETI (Bonardi *et al.*, 2011). Retention of SA production upon RRS1/RPS4 activation could explain the wild-type-like bacterial resistance in Ws-2_*nrg1a-nrg1b*, despite the loss of HR. These results indicate that SA-dependent pathway and NRG1-dependent pathway (resulting in HR) can be activated in parallel by TIR-NLRs. Of the genes differentially regulated during XopQ-induced ETI (via the NRG1-dependent TIR-NLR Roq1), 80% depend on NRG1 (Qi *et al.*, 2018). Some of these genes are involved in photosynthesis, RNA processing and protein degradation. Thus, it is likely that NRG1 regulates response pathways in addition to HR. In contrast, as ~20% of the ETI genes are still normally regulated in *nrg1*, SA-signalling is likely not the only immune response still active in *nrg1* mutants.

5.3.4 Some TIR-NLRs signal via NRG1 only, some signal via both ADR1 and NRG1

RPW8-NLRs are a monophyletic anciently diverged clade. They do not show extensive diversification or expansion, and are conserved in angiosperms, gymnosperms and bryophytes (Zhong & Cheng, 2016). RPW8-NLRs diverged into ADR1 and NRG1 sub-clades before the monocot/dicot separation (Collier *et al.*, 2011). ADR1s have been characterised in Arabidopsis as helpers for the R proteins RPP2, RPP4 and RPS2 (Bonardi *et al.*, 2011). Additionally, an *adr1-triple* (*adr1-adr1-l1-adr-l2*) mutant can partially suppress the autoimmune phenotype of *slh1-9*, which is an Arabidopsis line with an auto-active allele of *RRS1* (Dong *et al.*, 2016). Thus, RPS2, RPP2, RPP4 and RRS1/RPS4 can signal via ADR1s. Here

I found that full RPP2-, RPP4- and RRS1/RPS4-mediated immune responses require NRG1s. Therefore, these three immune receptors signal via both ADR1s and NRG1s.

Unlike *slh1-9*, the *chs3-1* autoimmune phenotype is totally independent of ADR1 (Dong *et al.*, 2016). Here I found that CHS3-induced HR requires NbNRG1. Moreover, the *chs3-2D* autoimmune phenotype is completely lost in an *nrg1a-nrg1b-nrg1c* mutant of Arabidopsis (Wu *et al.*, 2018b). Thus, CHS3 signals only via NRG1s.

Conversely, RPS2-mediated macroscopic HR does not require NRG1 **(Figure 5-5)**, while it requires ADR1 (Bonardi *et al.*, 2011). Thus, RPS2 mainly signals via ADR1. It also partially requires NRG1 as indicated by a reduction of ion leakage in the absence of NRG1 **(Figure 5-5)**.

AvrRpm1-induced macroscopic HR in Arabidopsis is still active in the *adr1-triple* mutant (Bonardi *et al.*, 2011) and in the *nrg1a-nrg1b* mutant backgrounds **(Figure 5-4)**. RPM1 either signals independently of ADR1 and NRG1 or can achieve full function dependent on either ADR1 or NRG1, like the CC-NLR Rx2 (Collier *et al.*, 2011).

In conclusion, some R proteins signal via NRG1 only (e.g. CHS3) and some via both ADR1 and NRG1 (e.g. RRS1/RPS4, RPP2, RPP4, RPS2, Rx2, CHS1, SNC1) **(Figure 5-13)**. Some others may signal via ADR1 only. A recently generated *adr1-adr1-L1-adr1-L2-nrg1a-nrg1b-nrg1c* sextuple mutant showed redundancy between NRG1s and ADR1s for TIR-NLR function.

The requirement of RPW8-NLRs by multiple sensor NLRs suggest that they form an NLR signalling network similar to the NRC signalling network (Wu *et al.*, 2017, 2018a). In the NRC model, sensors and helpers evolved from a single pair. Through duplication events, the sensor clade expanded massively to enable effector recognition diversification. The helper clade underwent limited diversification (Wu *et al.*, 2018a). Similarly, RPW8-NLR encoding genes are conserved and in low copy number in plant genomes (Shao *et al.*, 2016, 2018). But in contrast to the NRC-sensor clade, the RPW8-NLR-dependent sensors does not fall in a defined phylogenetic clade. A more comprehensive definition of the sensor NLRs from the RPW8-NLR network will help to propose an evolutionary model for this network. In addition, RPW8-NLR and NRC co-exist in Asterids. It will be interesting to test if they form hermetic networks or if some sensor NLRs could signal via both NRC and RPW8-NLRs, adding another level of complexity, thus of robustness, in NLR signalling network.

As there are multiple copy of RPW8-NLRs in plant genomes, their characterisation was difficult with classic genetic tools. CRISPR method enabled to generate variation in RPW8-NLRs and confirm the hypothesis that they are required for multiple NLR functions (Qi *et al.*, 2018; Wu *et al.*, 2018b). In the future, unravelling the mechanism of RPW8 (Xiao *et al.*, 2005; Chae *et al.*, 2014) and RPW8-containing NLRs will push forward our understanding of the plant immune system and may ultimately be applied to deploy wisely genetic resistance in crops.

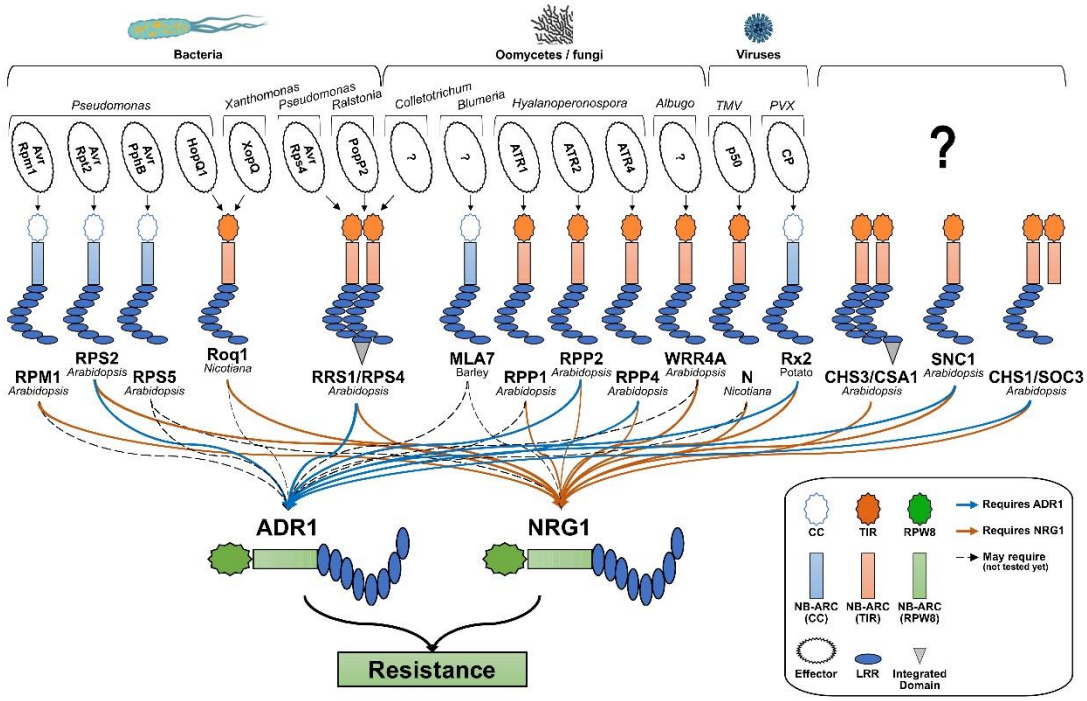

Figure 5-13: CC-NLRs and TIR-NLRs can signal via NRG1 and/or ADR1
NLRs are immune surveillance devices. Specific activation by pathogen effectors triggers resistance. For full response, they require RPW8-containing proteins NRG1 and ADR1. All the TIR-NLRs can signal via NRG1 and some can also signal via ADR1. CC-NLRs Signal via ADR1 and partially via NRG1. Some NLR may signal independently of ADR1 and NRG1. ADR1 and NRG1 are conserved within Angiosperms, suggesting that this model can be applied for all the flowering plants. RPM1, RPS2, RRS1/RPS4, RPP1, RPP2, RPP4, WRR4A, CSA1/CHS3 and SOC3/CHS1 signal via NRG1 (this thesis). RPS2, RPP2 and RPP4 signal via ADR1 (Bonardi *et al.*, 2011). RPP4, RRS1 but not CHS3, signal via ADR1 (Dong *et al.*, 2016). Roq1 signal via NRG1 (Brendolise *et al.*, 2018). Roq1 and RPP1 signal via NRG1 (Qi *et al.*, 2018). N signal via NRG1 (Peart *et al.*, 2005). Rx2 signal via both NRG1 and ADR1 (Collier *et al.*, 2011). SNC1 signals via both ADR1 and NRG1, CHS3 signals specifically via NRG1 (Wu *et al.*, 2018b). TMV: *tobacco mosaic virus*. PVX: *potato virus X*.

Chapter 6 : General discussion

6.1 History of plant-microbe interaction genetics

Pioneering work by Gregor Mendel revealed the inheritance of genetic factors from both parents, resulting in predictable ratios for heritable phenotypes in their progenies (Mendel, 1865). These factors are encoded on the chromosomes (Morgan *et al.*, 1915). Later, Harold Flor studied the genetic basis of the resistance to and avirulence in the flax rust fungus *Melampsora lini* (Flor, 1955, 1971). He was particularly interested in the genetics of avirulence in the pathogen. By crossing two races of rust, he determined that avirulence factors are inherited following the Mendel model. More importantly, he observed that the recognition of a single avirulence factor by flax is monogenic and proposed the gene-for-gene model. For each of the *R*-genes in flax, *e.g. K*, *L6*, *M*, *N*, *P*, there is a cognate avirulence factor in rust, *e.g.* AvrK, AvrL6, AvrM, AvrN, AvrP. Later, the diversity in compatibility within other pathosystems was used to identify more gene-for-gene pairs: RPS2-AvrRpt2 (Kunkel *et al.*, 1993), RPM1-AvrRpm1 (Debener *et al.*, 1991), RRS1-AvrRps4 (Hinsch & Staskawicz, 1995), RPS5-AvrPphB (Simonich & Innes, 1995) using the Arabidopsis-*P. syringae* pathosystem and RPP1-ATR1 (Rehmany *et al.*, 2005), RPP2-ATR2 (Sinapidou *et al.*, 2004), RPP4-ATR4 (Asai *et al.*, 2018), RPP5-ATR5 (Bailey *et al.*, 2011), RPP13-ATR13 (Allen *et al.*, 2004) using the Arabidopsis-*Hpa* pathosystem.

The gene-for-gene terminology suggests that a single R-protein recognises a single effector. However, there are several examples of R-proteins that recognise many effectors, sometimes from highly diverged pathogens. WRR4A from Arabidopsis recognises nine avirulence factors from the oomycete *Albugo candida* (A. Redkar *et al.*, in prep). RRS1 recognises three avirulence factors from the bacteria *Pseudomonas* and *Ralstonia* and the fungus *Colletotrichum* (Narusaka *et al.*, 2009). Also, the same effector can be recognized by multiple different *R*-genes. For instance, the effector Avr2 from *P. infestans* is recognised by R2 in the Mexican *Solanum* species and by Rpi-mcq1 in Peruvian *Solanum* species (Aguilera-Galvez *et al.*, 2018). The hunt for gene-for-gene pairs initiated by Flor has led to the discovery of many components of the plant immune system, unravelling many aspects of its mechanisms.

6.2 Limit to *R*-gene discovery

Any genetic study relies on phenotypic diversity. In the case of plant-microbe interactions, mapping of resistance loci requires a susceptible and a resistant parent that can produce a fertile progeny. This condition is not fulfilled for several crop-infecting races of *A. candida* in Arabidopsis: all the accessions tested are resistant to the brown mustard-infecting race Ac2V, the *Brassica rapa*-infecting race Ac7V and the cabbage-infecting race AcBoT. Thus, natural accessions cannot be used to identify the underlying *R*-genes.

6.3 Meeting the challenge of lack of natural diversity

6.3.1 Successful approaches

When susceptible parents are not available in the wild, susceptibility can be induced by mutagenesis. For instance, Col-0 seeds have been randomly mutagenized with EMS (ethyl methanesulfonate). A line that lacks recognition of AvrRpt2, called *rps2-201*, was identified from this mutant collection (Kunkel *et al.*, 1993). A backcross of *rps2-201* with the No-0 resistant parent enabled to map and clone *RPS2*.

Transgressive segregation in MAGIC Arabidopsis (Kover *et al.*, 2009) enabled the identification of two lines susceptible to Ac2V and Ac7V, and subsequently one line susceptible to AcBoT. They were used to map and clone novel *R*-genes to Ac2V, Ac7V and AcBoT (Cevik *et al.*, 2019).

6.3.2 Unsuccessful approach

While the "transgressive segregation" project (Cevik *et al.*, 2019) was ongoing in the Jones' laboratory, several groups reported that CRISPR could be used to generate targeted mutations *in vivo* (Cong *et al.*, 2013; Mali *et al.*, 2013; Nekrasov *et al.*, 2013). At that time, no MAGIC line susceptible to AcBoT was identified. I thus tried to tackle this project by using genome editing rather than transgressive segregation. As Col-0_*eds1* is susceptible to AcBoT, I speculated that the gene(s) involved in AcBoT resistance encode(s) TIR-NLR(s). I assembled 25 sgRNAs supposedly targeting all the 96 TIR-NLR encoding genes in Col-0, with a Cas9 expression cassette. This construct did not show any CRISPR activity at the loci tested in Arabidopsis. For this reason, I investigated different parameters of the construct and by a process of hypothesis-testing combined with trial-and error, developed an optimized system for CRISPR in Arabidopsis **(Chapter 4)**. In the

meantime, an AcBoT-compatible MAGIC line was identified so I stopped trying to knock-out all the TIR-NLR encoding genes in Col-0.

6.4 Beyond *R*-gene discovery: characterization of NLR signalling components

6.4.1 A black box between plant NLR and actual resistance

Hundreds of *R*-genes have been mapped and cloned in the last decades (Kourelis & Van Der Hoorn, 2018). However, little is known about the way they get activated and the signalling they trigger. In animals, it is well described that some NLRs form an oligomeric inflammasome upon activation (Lamkanfi & Dixit, 2017). The inflammasome imposes oligomerisation of the NLR N-terminal domain, recruiting and activating caspases 4, 5 and 11 upstream of caspase 1 activation, finally resulting in gasdermin D cleavage, membrane permeabilization and pyroptosis (a form of cell death). Plant NLRs can activate cell death but it is not known if they oligomerise, nor how they signal to fulfil this function. Random mutagenesis enabled identification of some general components of the plant immune system, such as EDS1, ICS1 and NDR1 (Century *et al.*, 1995; Parker *et al.*, 1996; Wildermuth *et al.*, 2001). Conceivably, the most important regulators of immunity are encoded by redundant genes, thus unlikely to be revealed by EMS mutagenesis. This is the case for *EDS1*, which exists in two copies in Col-0 and many other accessions but was found in EMS screens in Ler-0 and Ws-2, that only have one copy. Similarly, the *NRC* genes encode for helper NLRs redundantly required for signalling of many CC-NLRs in Asterids (Wu *et al.*, 2017).

6.4.2 RPW8-NLRs are candidates to be major ETI components

RPW8-NLRs are a characteristic sub-class of plant NLRs (Shao *et al.*, 2016). Angiosperms carry two types of RPW8-NLRs: ADR1 and NRG1. In *N. benthamiana*, the single copy of NRG1 is required for the TIR-NLR sensor N function (Peart *et al.*, 2005). As RPW8-NLRs are conserved and not expanded, they were proposed to be helper NLRs by Peter Moffett's laboratory (Collier *et al.*, 2011). The group tested and proved its hypothesis for the CC-NLR Rx2 (Collier *et al.*, 2011).

In Arabidopsis, there are three copies of ADR1. They are genetically unlinked, so a triple mutant could be obtained from crosses using the single mutants. Such *adr1-triple* mutant

is at least partially impaired in signalling of many NLRs including RPS2, RPP4, RRS1 and UNI-1D (Bonardi *et al.*, 2011; Dong *et al.*, 2016).

There are two copies of NRG1 in Arabidopsis but they are in tandem in the genome, rendering it very difficult to get a double mutant from a cross between two single mutants. Although the hypothesis that NRG1s are helpers for TIR-NLRs was formulated in 2011, it was difficult to address that question before the availability of CRISPR-based targeted mutagenesis.

6.4.3 RPW8-NLRs are indeed major ETI regulators, as proven using CRISPR

In 2018/2019, three groups reported that they could use CRISPR to knock-out *NRG1* in Arabidopsis and in *N. benthamiana* (Qi *et al.*, 2018; Wu *et al.*, 2018b) **(Chapter 5)**.They found that, in addition to N, NRG1 is also a helper for many more TIR-NLRs: RPP1, Roq1, SNC1 and CHS3. Furthermore, I found that the TIR-NLRs RRS1/RPS4, RPP2, RPP4, WRR4A, CHS1 partially require NRG1. Although NRG1s and TIR-NLRs have co-evolved, NRG1 can also be a helper for CC-NLRs, as showed for Rx2 (Collier *et al.*, 2011), RPS2 and RPM1 **(Chapter 5)**.

NRG1 and ADR1 have mostly been studied independently. The only two studies inactivating NRG1 and ADR1 at the same time showed that they are redundantly required for full function of the CC-NLR Rx2 (Collier *et al.*, 2011) and the TIR-NLR pair RRS1/RPS4 (Wu *et al.*, 2018b). Conceivably, RPW8-NLRs are major ETI regulators, fully required in all angiosperms for function of many, if not all, other NLRs.

6.5 How do RPW8-NLRs regulate ETI?

6.5.1 What can we learn from RPW8-NLR homologues in fungi and animals?

There is a similarity in cell death induced by the mammalian NLR NLRP3 and the fungal NLR NWD2 in fungi (Cai *et al.*, 2014). Upon activation, NLRP3 interacts via its N-terminal domain with the protein ASC, inducing its active toxic prion form. Activation of cell death in fungus by NWD2 is similar. The active form of NWD2 recruits and converts the protein HET-S into its prion form. PNT1/HELPP is a pair homologous to NWD2/HET-S in the fungus *Chaetomium globosum* (NWD2/HET-S is described in the fungus *Podospora anserina*), which is thought to also cause cell death via prionisation (Daskalov *et al.*, 2016).

Similar mechanisms have not been observed with plant NLRs. However, there is homology between NWD2, PNT1 and NRG1. All three are NLRs with a glycine zipper motif

at their N-termini (Daskalov *et al.*, 2016). Whether RPW8-NLRs recruit or form a prion forming protein via their N-terminal domain to trigger cell death is not known.

6.5.2 What do we currently know about RPW8-induced immunity?

The two hypotheses proposed based on knowledge about animal and fungal NLR are (i) NLR activation induces oligomerisation of an RPW8-NLR and (ii) an N-terminal glycine zipper in RPW8-NLRs is involved in recruitment and activation of a cell death executor.

The evidence of self-association of NRG1 are contradictory. The Staskawicz laboratory observed self-interaction of NbNRG1 in the absence of activation (Qi *et al.*, 2018). Xin Li's laboratory could not see self-association of NRG1A or association between NRG1A and NRG1B even after activation (Wu *et al.*, 2018b). Moreover, NRG1 does not interact with its sensor NLR N (Peart *et al.*, 2005). Those data do not support an oligomerization model involving RPW8-NLRs.

To investigate the function of NRG1, I complemented a Ws-2_*nrg1a-nrg1b* mutant with NRG1A-mCherry and NRG1B-GFP (**Figure 5-4**). I could detect fluorescence under a confocal microscope upon activation (eight hours after infiltration of Pf0-1 carrying AvrRps4) of both NRG1A-mCherry and NRG1B-GFP. However, the resolution was too low to determine the sub-cellular localisation of the signal. Transient expression of these fluorescent-tagged Arabidopsis alleles of NRG1 in *N. benthamiana* suggest a cytoplasmic and endoplasmic reticulum localisation. Since these Arabidopsis alleles do not complement the loss of HR in an *N. benthamiana_nrg1* mutant, I did not interpret those data any further. Consistently, Xin Li's laboratory found that NRG1 primarily localises in the cytosol and at the ER (endoplasmic reticulum) in Arabidopsis and *N. benthamiana* (Wu *et al.*, 2018b). The sub-cellular localisation and re-localisation upon activation will give clues about the NRG1 mechanism and I am planning to investigate this question.

RPW8.2, involved in powdery mildew resistance, is specifically targeted to the extra-haustorial membrane (EHM) during infection (Zhang *et al.*, 2015). Surprisingly, a predicted trans-membrane domain (TMD) is not required for the EHM targeting (Wang *et al.*, 2013b). It is possible that this domain is sufficient for EHM targeting but not required, if RPW8.2 forms a complex with other RPW8 or RPW8-NLR proteins having a functional TMD. Indeed, RPW8.2 N-terminal domain (that contains the predicted TMD) is conserved between other RPW8 alleles and also with NRG1 and the fungal cell death activators HET-S and HELPP (Daskalov *et al.*, 2016). Particularly, this region contains a highly conserved

glycine zipper motif, required for plasma-membrane targeting and cell death activation for HELPP. I expressed two glycine zipper motif mutants of NRG1A (G8I and G10I) in Ws-2_*nrg1a-nrg1b*. These alleles did not complement the loss of AvrRps4-triggered HR, unlike the WT allele of NRG1A. However, I do not know if the mutated proteins were expressed. If those preliminary data get confirmed, it will indicate that the N-terminal predicted TMD of NRG1A is required for function.

6.5.3 Can we formulate a unifying hypothesis for RPW8-NLR function?

NLRs emerged independently as cell death activator in animals, fungi and plants. It is tempting to speculate that RPW8-NLRs regulate cell death in a similar fashion as do fungal and animal NLRs. But the current data suggest that it is not the case, and RPW8-NLRs cause cell death via a different mechanism. Previous data indicate that overexpression of the RPW8 domains of NRG1 and ADR1 causes cell death in tobacco and *N. benthamiana* leaves. One hypothesis is that ADR1 and NRG1 activate a cell death executor via their N-terminal RPW8 domain. The best candidate to be this cell death executor is the small protein RPW8 itself.

The relevance of RPW8-NLRs in ETI has recently been emphasized using genetics. The next step is now the investigation of their mechanism of action. Unravelling the mode of action of RPW8 and RPW8-NLRs will contribute to our knowledge in the plant immune system, for wise deployment of genetics to protect crop plants from pests.

6.6 What to expect from CRISPR?

6.6.1 A powerful genetic tool for biology

In this thesis, I exemplify the usefulness of CRISPR to interrogate a 7-year-old hypothesis. Peter Moffett's laboratory proposed that NRG1s are helpers for many TIR-NLRs in plants. The two copies of *NRG1* are in tandem in the genome of the model plant Arabidopsis. Thus, CRISPR was indeed the best technology to investigate Peter Moffett's hypothesis by loss-of-function. CRISPR has been used to describe other gene families than NRG1, such as the *yellow* genes involved in pigmentation of the butterfly *Agrotis ipsilon* (Chen *et al.*, 2018), or the *CDR* genes that confers antifungal drug resistance in *Candida albicans* (Vyas *et al.*, 2015). Genome engineering is not limited to biological investigations: it can be used in biotechnology for production of biofuel, improved food or biomaterials; and in medicine to develop drugs or gene surgery (Hsu *et al.*, 2014).

6.6.2 Deployment of knock-in breeding

Alteration of targeted genomic sequence is the most probable outcome of CRISPR-mediated DNA cleavage, from imprecise repair by NHEJ. Such alteration often affects the codon reading frame of a gene, resulting in a loss-of-function allele. Double-strand breaks induced by CRISPR can also stimulate HDR. Co-delivery of a CRISPR nuclease with an operator-specified sequence, homologous to the target site, can result in replacement of the target by the delivered sequence. This can be applied for *in-vivo* gene tagging for fundamental research or replacement of a gene by an allele of interest for breeders. Introgression of an allele of interest, *e.g.* an *R*-gene, into a selected crop can be achieved by classic crossing. This method is effective but slow, involving successive back-crossing and genotyping. Gene replacement mediated by CRISPR, also called knock-in breeding (KIB), can be achieved in one generation and requires only one back-cross to eliminate transgenic sequences used during the process. Conditional excision of the transgene or transgene-free delivery (*e.g.* bombardment of pre-assembled ribonucleoprotein complexes into plant cells) are alternative methods to circumvent a back-cross step. KIB presents several advantages compared to classic breeding. The resulting product will conserve all its genetic information, while products from classic breeding are likely to contain linked fragments of the donor genome. KIB also enables breeders to introgress genes from wild relative species that are sexually incompatible with the selected crop.

The optimization of KIB is currently ongoing. Substantial progresses have recently been reported (Čermák *et al.*, 2015; Dahan-Meir *et al.*, 2018; Huang & Puchta, 2019; Vu *et al.*, 2019).

6.6.3 Deployment of base editing

The nuclease function of CRISPR nucleases can be inactivated. Delivery of an inactive protein at a target site is not valuable *per se*, unless implemented with a novel function. The base editors are one remarkable example of engineering an innovative re-purpose of Cas9, by targeting specific nucleotides using deaminase enzymes. The cytidine deaminase APOBEC1 (apolipoprotein B mRNA editing enzyme, catalytic polypeptide-like 1) and a modified adenosine deaminase TadA can excise the amine group of cytosine or adenosine, converting them to uracil or inosine respectively. Uracil and inosine are processed as thymine and guanine during replication, causing targeted C->T and A->G mutation. Fusions of Cas9 with APOBEC or TadA, called base editors, have been applied

in rice to generate semi-dwarf plants, by inducing a SNP mutation in the *SLR1* gene (Lu & Zhu, 2017).

CRISPR-Cas9 was successfully used to reconstruct the domestication of tomato using NHEJ-mediated repair (Li *et al.*, 2018; Zsögön *et al.*, 2018). Domestication of wild species can be further enhanced with base editors. Indeed, some traits relative to crop domestication are explained by single amino acid substitution, such as the naked kernel in maize caused by a Lys->Asn mutation in the transcription factor *TGA1*. Conceivably, base editors could be used to generate novel traits in existing crops.

6.6.4 Perspective for agriculture

Inactivation of deleterious genes, KIB and base editors are novel tools available for breeders to face the current and future agricultural challenges. Blast resistant rice, powdery mildew resistant wheat and tomato, virus resistant cucumbers and many others improved crops have been already generated using CRISPR (Langner *et al.*, 2018; Ramasamy *et al.*, 2018). As the final products are identical to similar products that would have been obtain with classic breeding or mutagenesis, they would be expected to be under the same regulation. In fact, the regulation of CRISPR engineered crops was discussed by policy makers of the European Union. Their conclusion was that CRISPR plants should be considered as GM (genetically modified). Thus, they are subjected to the same regulation as GM crops. It is understandable that public may perceive CRISPR plants as less "natural". However, CRISPR-induced mutations are indistinguishable from naturally occurring mutations. Moreover, CRIPSR plants including plants resisting pathogen with reduced need for chemical sprays. This can be highly valuable for farmers and customers. Further discussions involving breeders, farmers, customers, policy makers and scientists are required to adopt smarter regulations for engineering, farming and commercialisation of CRISPR crops, so that the promise of this innovative new technology can be realized.

References

Abudayyeh OO, Gootenberg JS, Essletzbichler P, Han S, Joung J, Belanto JJ, Verdine V, Cox DBT, Kellner MJ, Regev A, *et al.* 2017. RNA targeting with CRISPR–Cas13. *Nature* **550**: 280–284.

Abudayyeh OO, Gootenberg JS, Konermann S, Joung J, Slaymaker IM, Cox DB, Shmakov S, Makarova KS, Semenova E, Minakhin L, *et al.* 2016. C2c2 is a single-component programmable RNA-guided RNA-targeting CRISPR effector. *Science* **353**: aaf5573.

Acevedo-Garcia J, Kusch S, Panstruga R. 2014. Magical mystery tour: MLO proteins in plant immunity and beyond. *Journal of Physiology* **204**: 273–281.

Ade J, DeYoung BJ, Golstein C, Innes RW. 2007. Indirect activation of a plant nucleotide binding site-leucine-rich repeat protein by a bacterial protease. *Proceedings of the National Academy of Sciences* **104**: 2531–2536.

Aguilera-Galvez C, Champouret N, Rietman H, Lin X, Wouters D, Chu Z, Jones JDG, Vossen JH, Visser RGF, Wolters PJ, *et al.* 2018. Two different *R* gene loci co-evolved with Avr2 of *Phytophthora infestans* and confer distinct resistance specificities in potato. *Studies in Mycology* **89**: 105–115.

Akira S, Takeda K. 2004. Toll-like receptor signalling. *Nature Reviews Immunology* **4**: 499–511.

Albert I, Böhm H, Albert M, Feiler CE, Imkampe J, Wallmeroth N, Brancato C, Raaymakers TM, Oome S, Zhang H, *et al.* 2015. An RLP23-SOBIR1-BAK1 complex mediates NLP-triggered immunity. *Nature Plants* **1**: 15140.

Allen RL, Bittner-Eddy PD, Grenvitte-Briggs LJ, Meitz JC, Rehmany AP, Rose LE, Beynon JL. 2004. Host-parasite coevolutionary conflict between Arabidopsis and downy mildew. *Science* **306**: 1957–1960.

Aman R, Ali Z, Butt H, Mahas A, Aljedaani F, Khan MZ, Ding S, Mahfouz M. 2018. RNA virus interference via CRISPR/Cas13a system in plants. *Genome Biology* **19**: 10.1186/s13059-017-1381-1.

Andolfo G, Jupe F, Witek K, Etherington GJ, Ercolano MR, Jones JDG. 2014. Defining the full tomato NB-LRR resistance gene repertoire using genomic and cDNA RenSeq. *BMC Plant Biology* **14**: 120.

Arora H, Padmaja KL, Paritosh K, Mukhi N, Tewari AK, Mukhopadhyay A, Gupta V, Pradhan AK, Pental D. 2019. *BjuWRR1*, a CC-NB-LRR gene identified in *Brassica juncea*, confers resistance to white rust caused by *Albugo candida*. *bioRxiv*: 10.1101/509851.

Asai S, Furzer OJ, Cevik V, Kim DS, Ishaque N, Goritschnig S, Staskawicz BJ, Shirasu K, Jones JDG. 2018. A downy mildew effector evades recognition by polymorphism of expression and subcellular localization. *Nature Communications* **9**: 5192.

Ausubel FM. 2005. Are innate immune signaling pathways in plants and animals conserved? *Nature Immunology* **6**: 973–979.

Axtell MJ, Staskawicz BJ. 2003. Initiation of RPS2-specified disease resistance in Arabidopsis is coupled to the AvrRpt2-directed elimination of RIN4. *Cell* **112**: 369–377.

Bai S, Liu J, Chang C, Zhang L, Maekawa T, Wang Q, Xiao W, Liu Y, Chai J, Takken FLW, *et al.* 2012. Structure-function analysis of barley NLR immune receptor MLA10 reveals its cell compartment specific activity in cell death and disease resistance. *PLoS Pathogens* **8**: e1002752.

Bailey K, Cevik V, Holton N, Byrne-Richardson J, Sohn KH, Coates M, Woods-Tor A, Aksoy HM, Hughes L, Baxter L, *et al.* 2011. Molecular cloning of ATR5^{Emoy2} from *Hyaloperonospora arabidopsidis*, an avirulence determinant that triggers RPP5-mediated defense in Arabidopsis. *Molecular Plant-Microbe Interactions* **24**: 827–838.

Bari R, Jones JDG. 2009. Role of plant hormones in plant defence responses. *Plant molecular biology* **69**: 473–488.

Barrangou R, Horvath P. 2017. A decade of discovery: CRISPR functions and applications. *Nature Microbiology* **2**: 17092.

Bartsch M, Gobbato E, Bednarek P, Debey S, Schultze JL, Bautor J, Parker J. 2006. Salicylic Acid-Independent ENHANCED DISEASE SUSCEPTIBILITY1 Signaling in Arabidopsis Immunity and Cell Death Is Regulated by the Monooxygenase FMO1 and the Nudix Hydrolase NUDT7. *The Plant Cell* **18**: 1038–1051.

Baudin M, Hassan JA, Schreiber KJ, Lewis JD. 2017. Analysis of the ZAR1 Immune Complex Reveals Determinants for Immunity and Molecular Interactions. *Plant Physiology* **174**: 2038–2053.

Beakes GW, Glockling SL, Sekimoto S. 2012. The evolutionary phylogeny of the oomycete "fungi". *Protoplasma* **249**: 3–19.

Beakes GW, Sekimoto S. 2008. The Evolutionary Phylogeny of Oomycetes-Insights Gained from Studies of Holocarpic Parasites of Algae and Invertebrates. In: Oomycete Genetics and Genomics: Diversity, Interactions, and Research Tools. 1–24.

Belhaj K, Cano LM, Prince DC, Kemen A, Yoshida K, Dagdas YF, Etherington GJ, Schoonbeek HJ, van Esse HP, Jones JDG, *et al.* 2017. Arabidopsis late blight: infection of a nonhost plant by *Albugo laibachii* enables full colonization by *Phytophthora infestans*. *Cellular Microbiology* **19:** 10.1111/cmi.12628.

Berkey R, Zhang Y, Ma X, King H, Zhang Q, Wang W, Xiao S. 2017. Homologues of the RPW8 Resistance Protein Are Localized to the Extrahaustorial Membrane that Is Likely Synthesized *De Novo*. *Plant Physiology* **173:** 600–613.

Bernoux M, Ve T, Williams S, Warren C, Hatters D, Valkov E, Zhang X, Ellis JG, Kobe B, Dodds PN. 2011. Structural and functional analysis of a plant resistance protein TIR domain reveals interfaces for self-association, signaling, and autoregulation. *Cell Host and Microbe* **9:** 200–211.

Betancor MB, Sprague M, Usher S, Sayanova O, Campbell PJ, Napier JA, Tocher DR. 2015. A nutritionally-enhanced oil from transgenic *Camelina sativa* effectively replaces fish oil as a source of eicosapentaenoic acid for fish. *Scientific Reports* **5:** 8104.

Van Der Biezen E, Freddie CT, Kahn K, Parker JE, Jones JDG. 2002. Arabidopsis *RPP4* is a member of the *RPP5* multigene family of TIR-NB-LRR genes and confers downy mildew resistance through multiple signalling components. *Plant Journal* **29:** 439–451.

Van Der Biezen EA, Jones JDG. 1998a. The NB-ARC domain: a novel signalling motif shared by plant resistance gene products and regulators of cell death in animals. *Current biology* **8:** R226–R227.

Van Der Biezen EA, Jones JDG. 1998b. Plant disease-resistance proteins and the gene-for-gene concept. *Trends in Biochemical Sciences* **23:** 454–456.

Le Blanc C, Zhang F, Mendez J, Lozano Y, Chatpar K, Irish V, Jacob Y. 2017. Increased efficiency of targeted mutagenesis by CRISPR/Cas9 in plants using heat stress. *Plant Journal* **9:** 377–386.

Bendahmane A, Kanyuka K, Baulcombe D. 1999. The *Rx* Gene from Potato Controls Separate Virus Resistance and Cell Death Responses. The Plant Cell **11:** 781-792.

Bonardi V, Cherkis K, Nishimura MT, Dangl JL. 2012. A new eye on NLR proteins: Focused

on clarity or diffused by complexity? *Current Opinion in Immunology* **24**: 41–50.

Bonardi V, Tang S, Stallmann A, Roberts M, Cherkis KA, Dangl JL. 2011. Expanded functions for a family of plant intracellular immune receptors beyond specific recognition of pathogen effectors. *Proceedings of the National Academy of Sciences* **108**: 16463–16468.

Borhan MH, Gunn N, Cooper A, Gulden S, Tör M, Rimmer SR, Holub EB. 2008. *WRR4* encodes a TIR-NB-LRR protein that confers broad-spectrum white rust resistance in *Arabidopsis thaliana* to four physiological races of *Albugo candida*. *Molecular Plant-Microbe Interactions* **21**: 757–768.

Borhan MH, Holub EB, Kindrachuk C, Omidi M, Bozorgmanesh-Frad G, Rimmer SR. 2010. *WRR4*, a broad-spectrum TIR-NB-LRR gene from Arabidopsis thaliana that confers white rust resistance in transgenic oilseed brassica crops. *Molecular Plant Pathology* **11**: 283–291.

Botella MA, Parker JE, Frost LN, Bittner-Eddy PD, Beynon JL, Daniels MJ, Holub EB, Jones JDG. 1998. Three genes of the Arabidopsis RPP1 complex resistance locus recognize distinct *Peronospora parasitica* avirulence determinants. *The Plant Cell* **10**: 1847–1860.

Boutrot F, Zipfel C. 2017. Function, Discovery, and Exploitation of Plant Pattern Recognition Receptors for Broad-Spectrum Disease Resistance. *Annual Review of Phytopathology* **55**: 257–286.

Brendolise C, Martinez-Sanchez M, Morel A, Chen R, Dinis R, Deroles S, Peeters N, Rikkerink EHA, Montefiori M. 2018. NRG1-mediated recognition of HopQ1 reveals a link between PAMP- and Effector-triggered Immunity. *bioRxiv*: 10.1101/293050.

Broz P, Dixit VM. 2016. Inflammasomes: mechanism of assembly, regulation and signalling. *Nature Reviews Immunology* **16**: 407–420.

Burch-Smith TM, Schiff M, Caplan JL, Tsao J, Czymmek K, Dinesh-Kumar SP. 2007. A novel role for the TIR domain in association with pathogen-derived elicitors. *PLoS Biology* **5**: e68.

Buscaill P, Rivas S. 2014. Transcriptional control of plant defence responses. *Current Opinion in Plant Biology* **20**: 35–46.

Cai X, Chen J, Xu H, Liu S, Jiang QX, Halfmann R, Chen ZJ. 2014. Prion-like polymerization underlies signal transduction in antiviral immune defense and inflammasome activation. *Cell* **156**: 1207–1222.

Callis J, Fromm M, Walbot V. 1987. Introns increase gene expression in cultured maize

cells. *Genes & development* **1**: 1183–1200.

Campos ML, Kang J-H, Howe G a. 2014. Jasmonate-Triggered Plant Immunity. *Journal of Chemical Ecology* **40**: 657–675.

Castel B, Ngou PM, Cevik V, Kim DS, Yang Y, Ding P, Jones JDG. 2018. Diverse NLR immune receptors activate defence via the RPW8-NLR NRG1. *New Phytologist*: 10.1111/nph.15659.

Castel B, Tomlinson L, Locci F, Yang Y, Jones JDG. 2019. Optimization of T-DNA architecture for Cas9-mediated mutagenesis in Arabidopsis. *PLoS ONE* **14**: e0204778.

Century KS, Holubt EB, Staskawiczt BJ. 1995. *NDR1*, a locus of *Arabidopsis thaliana* that is required for disease resistance to both a bacterial and a fungal pathogen. *Proceedings of the National Academy of Sciences* **92**: 6597–6601.

Čermák Tomáš, Baltes Nicholas J., Čegan Radim, Zhang Yong, Voytas Daniel F. 2015. High-frequency, precise modification of the tomato genome. Genome Biology **16**:232

Čermák T, Curtin SJ, Gil-Humanes J, Čegan R, Kono TJY, Konečná E, Belanto JJ, Starker CG, Mathre JW, Greenstein RL, *et al.* 2017. A multi-purpose toolkit to enable advanced genome engineering in plants. *The Plant Cell* **29**: 1196–1217.

Cesari S, Thilliez G, Ribot C, Chalvon V, Michel C, Jauneau A, Rivas S, Alaux L, Kanzaki H, Okuyama Y, *et al.* 2013. The Rice Resistance Protein Pair RGA4/RGA5 Recognizes the Magnaporthe oryzae Effectors AVR-Pia and AVR1-CO39 by Direct Binding. *The Plant Cell* **25**: 1463–1481.

Cevik V, Boutrot F, Apel W, Robert-Seilaniantz A, Furzer O, Redkar A, Castel B, Kover P, Prince D, Holub E, *et al.* 2019. Transgressive segregation reveals mechanisms of Arabidopsis immunity to Brassica-infecting races of white rust (*Albugo candida*). *Proceedings of the National Academy of Sciences* **116**: 2767-2773.

Chae E, Bomblies K, Kim ST, Karelina D, Zaidem M, Ossowski S, Martín-Pizarro C, Laitinen RAE, Rowan BA, Tenenboim H, *et al.* 2014. Species-wide genetic incompatibility analysis identifies immune genes as hot spots of deleterious epistasis. *Cell* **159**: 1341–1351.

Chen X, Cao Y, Zhan S, Zhang Y, Tan A, Huang Y. 2018. Identification of yellow gene family in *Agrotis ipsilon* and functional analysis of *Aiyellow-y* by CRISPR/Cas9. *Insect Biochemistry and Molecular Biology* **94**: 1–9.

Chen B, Gilbert LA, Cimini BA, Schnitzbauer J, Zhang W, Li G-W, Park J, Blackburn EH,

Weissman JS, Qi LS, *et al.* 2013. Dynamic imaging of genomic loci in living human cells by an optimized CRISPR/Cas system. *Cell* **155**: 1479–1491.

Chen LQ, Hou BH, Lalonde S, Takanaga H, Hartung ML, Qu XQ, Guo WJ, Kim JG, Underwood W, Chaudhuri B, *et al.* 2010. Sugar transporters for intercellular exchange and nutrition of pathogens. *Nature* **468**: 527–532.

Cheng TC, Hong C, Akey I V, Yuan S, Akey CW. 2016. A near atomic structure of the active human apoptosome. *eLife* **5**: e17755.

Chern M, Fitzgerald HA, Canlas PE, Navarre DA, Ronald PC. 2005. Overexpression of a Rice *NPR1* Homolog Leads to Constitutive Activation of Defense Response and Hypersensitivity to Light. *Molecular Plant-Microbe Interactions* **18**: 511–520.

Choi Y-J, Shin H-D, Thines M. 2009. The host range of *Albugo candida* extends from Brassicaceae through Cleomaceae to Capparaceae. *Mycological Progress* **8**: 329–335.

Choudhury SR, Cui Y, Lubecka K, Stefanska B, Irudayaraj J. 2016. CRISPR-dCas9 mediated TET1 targeting for selective DNA demethylation at *BRCA1* promoter. *Oncotarget* **7**: 46545–46556.

Clough SJ, Bent AF. 1998. Floral dip: A simplified method for Agrobacterium-mediated transformation of *Arabidopsis thaliana*. *Plant Journal* **16**: 735–743.

Clough SJ, Fengler KA, Yu I, Lippok B, Smith RK, Bent AF. 2000. The Arabidopsis *dnd1* '*defense, no death*' gene encodes a mutated cyclic nucleotide-gated ion channel. *Proceedings of the National Academy of Sciences* **97**: 9323–9328.

Collier SM, Hamel L-P, Moffett P. 2011. Cell death mediated by the N-terminal domains of a unique and highly conserved class of NB-LRR protein. *Molecular Plant-Microbe Interactions* **24**: 918–931.

Collier SM, Moffett P. 2009. NB-LRRs work a 'bait and switch' on pathogens. *Trends in Plant Science* **14**: 521–529.

Cong L, Ran F, Cox D, Lin S, Barretto R, Habib N, Hsu P, Wu X, Jiang W, Marraffini L, *et al.* 2013. Multiplex Genome Engineering Using CRISPR/Cas Systems. *Science* **339**: 819–822.

Conrath U, Beckers GJM, Langenbach CJG, Jaskiewicz MR. 2015. Priming for Enhanced Defense. *Annual Review of Phytopathology* **53**: 97–119.

Cook DE, Mesarich CH, Thomma BPHJ. 2015. Understanding Plant Immunity as a

Surveillance System to Detect Invasion. *Annual Review of Phytopathology* **53**: 541–563.

Cooper AJ, Latunde-Dada AO, Woods-Tör A, Lynn J, Lucas JA, Crute IR, Holub EB. 2008. Basic compatibility of *Albugo candida* in *Arabidopsis thaliana* and *Brassica juncea* causes broad-spectrum suppression of innate immunity. *Molecular Plant-Microbe Interactions* **21**: 745–756.

Cornelis GR. 2006. The type III secretion injectisome. *Nature Reviews Microbiology* **4**: 811–825.

Cornelis GR, Van Gijsegem F. 2000. Assembly and Function of Type III Secretory Systems. *Annual Review of Microbiology* **54**: 735–774.

Couto D, Zipfel C. 2016. Regulation of pattern recognition receptor signalling in plants. *Nature Reviews Immunology* **16**: 537–552.

Cui H, Gobbato E, Kracher B, Qiu J, Bautor J, Parker JE. 2017. A core function of EDS1 with PAD4 is to protect the salicylic acid defense sector in Arabidopsis immunity. *New Phytologist* **213**: 1802–1817.

Cui H, Qiu J, Zhou Y, Stuttmann J, Bhandari D, Bautor J, Parker JE. 2018. Antagonism of transcription factor MYC2 by EDS1/PAD4 complexes bolsters salicylic acid defense in Arabidopsis effector-triggered immunity. *Molecular Plant* **11**: 1053–1066.

Dahan-Meir T, Filler-Hayut S, Melamed-Bessudo C, Bocobza S, Czosnek H, Aharoni A, Levy AA. 2018. Efficient *in planta* gene targeting in tomato using geminiviral replicons and the CRISPR/Cas9 system. *Plant Journal* **95**: 5–16.

Dang Y, Jia G, Choi J, Ma H, Anaya E, Ye C, Shankar P, Wu H. 2015. Optimizing sgRNA structure to improve CRISPR-Cas9 knockout efficiency. *Genome Biology* **16**: 280.

Dangl JL, Jones JDG. 2001. Defence Responses To Infection. *Nature* **411**: 826–833.

Daskalov A, Habenstein B, Sabaté R, Berbon M, Martinez D, Chaignepain S, Coulary-Salin B, Hofmann K, Loquet A, Saupe SJ. 2016. Identification of a novel cell death-inducing domain reveals that fungal amyloid-controlled programmed cell death is related to necroptosis. *Proceedings of the National Academy of Sciences* **113**: 201522361.

Daskalov A, Saupe SJ. 2015. As a toxin dies a prion comes to life: A tentative natural history of the [Het-s] prion. *Prion* **9**: 184–189.

Debener T, Lehnackers H, Arnold M, Dangl JL. 1991. Identification and molecular mapping

of a single *Arabidopsis thaliana* locus determining resistance to a phytopathogenic *Pseudomonas syringae* isolate. *Plant Journal* **1:** 289–302.

Deltcheva E, Chylinski K, Sharma CM, Gonzales K, Chao Y, Pirzada ZA, Eckert MR, Vogel J, Charpentier E. 2011. CRISPR RNA maturation by trans-encoded small RNA and host factor RNase III. *Nature* **471:** 602–607.

Ding Y, Sun T, Ao K, Peng Y, Zhang Y, Li X, Zhang Y, Xu F, Li Y, Zhu Z, *et al.* 2018. Opposite Roles of Salicylic Acid Receptors NPR1 and NPR3/NPR4 in Transcriptional Regulation of Plant Immunity. *Cell* **13:** 191–202.

Doench JG, Hartenian E, Graham DB, Tothova Z, Hegde M, Smith I, Sullender M, Ebert BL, Xavier RJ, Root DE. 2014. Rational design of highly active sgRNAs for CRISPR-Cas9–mediated gene inactivation. *Nature Biotechnology* **32:** 1262–7.

Dong X. 2004. NPR1, all things considered. *Current Opinion in Plant Biology* **7:** 547–552.

Dong OX, Tong M, Bonardi V, El Kasmi F, Woloshen V, Wünsch LK, Dangl JL, Li X. 2016. TNL-mediated immunity in Arabidopsis requires complex regulation of the redundant *ADR1* gene family. *New Phytologist* **210:** 960–973.

Dreissig S, Schiml S, Schindele P, Weiss O, Rutten T, Schubert V, Gladilin E, Mette MF, Puchta H, Houben A. 2017. Live-cell CRISPR imaging in plants reveals dynamic telomere movements. *Plant Journal* **91:** 565–573.

Du L, Ali GS, Simons KA, Hou J, Yang T, Reddy ASN, Poovaiah BW. 2009. Ca^{2+}/calmodulin regulates salicylic-acid-mediated plant immunity. *Nature* **457:** 1154–1158.

Durner J, Shah J, Klessig DF. 1997. Salicylic acid and disease resistance in plants. *Trends in Plant Science* **2:** 266–274.

Durrant WE, Dong X. 2004. Systemic Acquired Resistance. *Annual Review of Phytopathology* **42:** 185–209.

Duxbury Z, Ma Y, Furzer OJ, Huh SU, Cevik V, Jones JDG, Sarris PF. 2016. Pathogen perception by NLRs in plants and animals: Parallel worlds. *Bioessays*: **38:** 769–781.

Dyrka W, Lamacchia M, Durrens P, Kobe B, Daskalov A, Paoletti M, Sherman DJ, Saupe SJ. 2014. Diversity and variability of NOD-like receptors in fungi. *Genome Biology and Evolution* **6:** 3137–3158.

Eckardt NA. 2002. Plant Disease Susceptibility Genes? *The Plant Cell* **14:** 1983–1986.

Eid A, Ali Z, Mahfouz MM. 2016. High efficiency of targeted mutagenesis in arabidopsis via meiotic promoter-driven expression of Cas9 endonuclease. *Plant Cell Reports* **35:** 1555–1558.

Endo A, Masafumi M, Kaya H, Toki S. 2016. Efficient targeted mutagenesis of rice and tobacco genomes using Cpf1 from *Francisella novicida*. *Scientific Reports* **6:** 38169.

Engler C, Gruetzner R, Kandzia R, Marillonnet S. 2009. Golden gate shuffling: A one-pot DNA shuffling method based on type IIs restriction enzymes. *PLoS ONE* **4:** e5553.

Engler C, Youles M, Gruetzner R, Ehnert TM, Werner S, Jones JDG, Patron NJ, Marillonnet S. 2014. A Golden Gate modular cloning toolbox for plants. *ACS Synthetic Biology* **3:** 839–843.

Essuman K, Summers DW, Sasaki Y, Mao X, DiAntonio A, Milbrandt J. 2017. The SARM1 Toll/Interleukin-1 Receptor Domain Possesses Intrinsic NAD+ Cleavage Activity that Promotes Pathological Axonal Degeneration. *Neuron* **93:** 1334–1343.e5.

Essuman K, Summers DW, Sasaki Y, Mao X, Yim AKY, DiAntonio A, Milbrandt J. 2018. TIR Domain Proteins Are an Ancient Family of NAD^+-Consuming Enzymes. *Current Biology* **28:** 421-430.

Eulgem T, Somssich IE. 2007. Networks of WRKY transcription factors in defense signaling. *Current Opinion in Plant Biology* **10:** 366–371.

Falk A, Feys BJ, Frost LN, Jones JDG, Daniels MJ, Parker JE. 1999. EDS1, an essential component of *R* gene-mediated disease resistance in Arabidopsis has homology to eukaryotic lipases. *Proceedings of the National Academy of Sciences* **96:** 3292–3297.

Fauser F, Schiml S, Puchta H. 2014. Both CRISPR/Cas-based nucleases and nickases can be used efficiently for genome engineering in *Arabidopsis thaliana*. *Plant Journal* **79:** 348–359.

Feng Z, Mao Y, Xu N, Zhang B, Wei P, Yang D-L, Wang Z, Zhang Z, Zheng R, Yang L, *et al.* 2014. Multigeneration analysis reveals the inheritance, specificity, and patterns of CRISPR/Cas-induced gene modifications in Arabidopsis. *Proceedings of the National Academy of Sciences* **111:** 4632–4637.

Fernandez-Pozo N, Menda N, Edwards JD, Saha S, Tecle IY, Strickler SR, Bombarely A, Fisher-York T, Pujar A, Foerster H, *et al.* 2015. The Sol Genomics Network (SGN)-from genotype to phenotype to breeding. *Nucleic Acids Research* **43:** D1036–D1041.

Flor HH. 1955. Host-parasite interactions in flax rust - its genetics and other implications. *Phytopathology* **45:** 680–685.

Flor HH. 1971. Current status of the gene-for-gene concept. *Annual Review Phytopathology* **9:** 275–296.

Galon Y, Nave R, Boyce JM, Nachmias D, Knight MR, Fromm H. 2008. Calmodulin-binding transcription activator (CAMTA) 3 mediates biotic defense responses in Arabidopsis. *FEBS Letters* **582:** 943–948.

Gao Y, Wang W, Zhang T, Gong Z, Zhao H, Han G-Z. 2018. Out of Water: The Origin and Early Diversification of Plant *R*-Genes. *Plant Physiology* **177:** 82-89.

Gao Y, Zhao Y. 2014. Self-processing of ribozyme-flanked RNAs into guide RNAs in vitro and in vivo for CRISPR-mediated genome editing. *Journal of Integrative Plant Biology* **56:** 343–349.

Gaoa Z, Chunga E-H, Eitasa TK, Dangl JL. 2011. Plant intracellular innate immune receptor Resistance to Pseudomonas syringae pv. maculicola 1 (RPM1) is activated at, and functions on, the plasma membrane. *Proceedings of the National Academy of Sciences* **108:** 8914–8914.

Gasiunas G, Barrangou R, Horvath P, Siksnys V. 2012. Cas9-crRNA ribonucleoprotein complex mediates specific DNA cleavage for adaptive immunity in bacteria. *Proceedings of the National Academy of Sciences* **109:** E2579–E2586.

Gaudelli NM, Komor AC, Rees HA, Packer MS, Badran AH, Bryson DI, Liu DR. 2017. Programmable base editing of A•T to G•C in genomic DNA without DNA cleavage. *Nature* **551:** 464–471.

Geu-Flores F, Nour-Eldin HH, Nielsen MT, Halkier BA. 2007. USER fusion: A rapid and efficient method for simultaneous fusion and cloning of multiple PCR products. *Nucleic Acids Research* **35:** e55.

Gibson DG, Young L, Chuang R-Y, Venter JC, Hutchison CA, Smith HO. 2009. Enzymatic assembly of DNA molecules up to several hundred kilobases. *Nature Methods* **6:** 343–345.

Gisler B, Salomon S, Puchta H. 2002. The role of double-strand break-induced allelic homologous recombination in somatic plant cells. *Plant Journal* **32:** 277–284.

Glazebrook J, Rogers EE, Ausubel FM. 1997. Use of Arabidopsis for genetic dissection of

plant defense responses. *Annual review of genetics* **31**: 547–569.

Gootenberg JS, Abudayyeh OO, Lee JW, Essletzbichler P, Dy AJ, Joung J, Verdine V, Donghia N, Daringer NM, Freije CA, *et al.* 2017. Nucleic acid detection with CRISPR-Cas13a/C2c2. *Science* **356**: 438–442.

Han G-Z. 2018. Origin and evolution of the plant immune system. *New Phytologist*: 10.1111/nph.15596.

Hayut SF, Bessudo CM, Levy AA. 2017. Targeted recombination between homologous chromosomes for precise breeding in tomato. *Nature Communications* **8**: 15605.

Heidrich K, Wirthmueller L, Tasset C, Pouzet C, Deslandes L, Parker JE. 2011. Arabidopsis EDS1 Connects Pathogen Effector Recognition to Cell Compartment-Specific Immune Responses. *Science* **334**: 1401–1404.

Heller J, Clavé C, Gladieux P, Saupe SJ, Glass NL. 2018. NLR surveillance of essential SEC-9 SNARE proteins induces programmed cell death upon allorecognition in filamentous fungi. *Proceedings of the National Academy of Sciences* **115**: E2292–E2301.

Hilton IB, D'Ippolito AM, Vockley CM, Thakore PI, Crawford GE, Reddy TE, Gersbach CA. 2015. Epigenome editing by a CRISPR-Cas9-based acetyltransferase activates genes from promoters and enhancers. *Nature Biotechnology* **33**: 510–517.

Hinsch M, Staskawicz B. 1995. Identification of a New Arabidopsis Disease Resistance Locus, *RPS4*, and Cloning of the Corresponding Avirulence Gene, *avrRps4*, from *Pseudomonas syringae* pv. *pisi*. *Molecular Plant-Microbe Interactions* **9**: 55–61.

Hodges LD, Cuperus J, Ream W. 2004. *Agrobacterium rhizogenes* GALLS Protein Substitutes for Agrobacterium tumefaciens Single-Stranded DNA-Binding Protein VirE2. *Journal of Bacteriology* **186**: 3065–3077.

Holub EB, Brose E, Tör M, Clay C, Crute IR, Beynon JL. 1995. Phenotypic and genotypic variation in the interaction between *Arabidopsis thaliana* and *Albugo candida*. *Molecular plant-microbe interactions* **8**: 916–928.

Hong RLRL, Hamaguchi L, Busch MA, Weigel D. 2003. Regulatory elements of the floral homeotic gene *AGAMOUS* identified by phylogenetic footprinting and shadowing. *The Plant Cell* **15**: 1296–1309.

van der Hoorn R a L, Kamoun S. 2008. From Guard to Decoy: a new model for perception

of plant pathogen effectors. *The Plant Cell* **20:** 2009–2017.

Horvath P, Barrangou R. 2010. CRISPR/Cas, the immune system of bacteria and archaea. *Science* **327:** 167–170.

Hsu PD, Lander ES, Zhang F. 2014. Development and applications of CRISPR-Cas9 for genome engineering. *Cell* **157:** 1262–1278.

Hu JH, Miller SM, Geurts MH, Tang W, Chen L, Sun N, Zeina CM, Gao X, Rees HA, Lin Z, *et al.* 2018. Evolved Cas9 variants with broad PAM compatibility and high DNA specificity. *Nature* **556:** 57–63.

Hu X, Wang C, Liu Q, Fu Y, Wang K. 2016. Targeted mutagenesis in rice using CRISPR-Cpf1 system. *Journal of Genetics and Genomics* **44:** 71-73.

Huang X, Li J, Bao F, Zhang X, Yang S. 2010. A Gain-of-Function Mutation in the Arabidopsis Disease Resistance Gene *RPP4* Confers Sensitivity to Low Temperature. *Plant Physiology* **154:** 796–809.

Huang T-K, Puchta H. 2019. CRISPR/Cas-mediated gene targeting in plants: finally a turn for the better for homologous recombination. Plant Cell Reports 10.1007/s00299-019-02379-0.

Huang J, Zhu C, Li X. 2018. $SCF^{SNIPER4}$ controls the turnover of two redundant TRAF proteins in plant immunity. *Plant Journal* **95:** 504–515.

Hyun Y, Kim J, Cho SW, Choi Y, Kim J-S, Coupland G. 2014. Site-directed mutagenesis in *Arabidopsis thaliana* using dividing tissue-targeted RGEN of the CRISPR/Cas system to generate heritable null alleles. *Planta* **241:** 271–284.

Jiang W, Zhou H, Bi H, Fromm M, Yang B, Weeks DP. 2013. Demonstration of CRISPR/Cas9/sgRNA-mediated targeted gene modification in Arabidopsis, tobacco, sorghum and rice. *Nucleic acids research* **41:** e188.

Jinek M, Chylinski K, Fonfara I, Hauer M, Doudna JA, Charpentier E. 2012. A Programmable Dual-RNA-Guided DNA Endonuclease in Adaptive Bacterial Immunity. *Science* **337:** 816–821.

Jinek M, East A, Cheng A, Lin S, Ma E, Doudna J. 2013. RNA-programmed genome editing in human cells. *eLife* **2013:** e00471.

Johal GS, Briggs SP. 1992. Reductase activity encoded by the HM1 disease resistance gene

in maize. *Science* **258:** 985–987.

Jones JDG, Dangl JL. 2006. The plant immune system. *Nature* **444:** 323–329.

Jones JDG, Vance RE, Dangl JL. 2016. Intracellular innate immune surveillance devices in plants and animals. *Science* **354.**

Jones JDG, Witek K, Verweij W, Jupe F, Cooke D, Dorling S, Tomlinson L, Smoker M, Perkins S, Foster S. 2014. Elevating crop disease resistance with cloned genes. *Philosophical Transactions of the Royal Society B* **369:** 20130087.

Jouet A, Saunders DGO, McMullan M, Ward B, Furzer O, Jupe F, Cevik V, Hein I, Thilliez GJA, Holub E, *et al.* 2018. *Albugo candida* race diversity, ploidy and host-associated microbes revealed using DNA sequence capture on diseased plants in the field. *New Phytologist* **221:** 1529-1543.

Jupe F, Witek K, Verweij W, Śliwka J, Pritchard L, Etherington GJ, Maclean D, Cock PJ, Leggett RM, Bryan GJ, *et al.* 2013. Resistance gene enrichment sequencing (RenSeq) enables reannotation of the NB-LRR gene family from sequenced plant genomes and rapid mapping of resistance loci in segregating populations. *Plant Journal* **76:** 530–544.

Kamoun S. 2006. A Catalogue of the Effector Secretome of Plant Pathogenic Oomycetes. *Annual Review of Phytopathology* **44:** 41–60.

Kamoun S, Furzer O, Jones JDG, Judelson HS, Ali GS, Dalio RJD, Roy SG, Schena L, Zambounis A, Panabières F, *et al.* 2015. The Top 10 oomycete pathogens in molecular plant pathology. *Molecular Plant Pathology* **16:** 413–434.

Kang B, Yun J, Kim S, Shin Y, Ryu J, Choi M, Woo JW, Kim J. 2018. Precision genome engineering through adenine base editing in plants. *Nature Plants* **4:** 427–431.

Kanzaki H, Yoshida K, Saitoh H, Fujisaki K, Hirabuchi A, Alaux L, Fournier E, Tharreau D, Terauchi R. 2012. Arms race co-evolution of *Magnaporthe oryzae AVR-Pik* and rice *Pik* genes driven by their physical interactions. *Plant Journal* **72:** 894–907.

Karvelis T, Gasiunas G, Miksys A, Barrangou R, Horvath P, Siksnys V. 2013. crRNA and tracrRNA guide Cas9-mediated DNA interference in *Streptococcus thermophilus*. *RNA Biology* **10:** 841–851.

Kemen E, Gardiner A, Schultz-Larsen T, Kemen AC, Balmuth AL, Robert-Seilaniantz A, Bailey K, Holub EB, Studholme DJ, MacLean D, *et al.* 2011. Gene Gain and Loss during

Evolution of Obligate Parasitism in the White Rust Pathogen of *Arabidopsis thaliana*. *PLoS Biology* **9**: e1001094.

Kleinstiver BP, Prew MS, Tsai SQ, Topkar V V., Nguyen NT, Zheng Z, Gonzales APW, Li Z, Peterson RT, Yeh J-RJ, *et al.* 2015. Engineered CRISPR-Cas9 nucleases with altered PAM specificities. *Nature* **523**: 481–5.

Knepper C, Savory E a., Day B. 2011. Arabidopsis NDR1 Is an Integrin-Like Protein with a Role in Fluid Loss and Plasma Membrane-Cell Wall Adhesion. *Plant Physiology* **156**: 286–300.

Kobe B, Kajava A. 2001. The leucine-rich repeat as a protein recognition motif. *Current opinion in structural biology* **11**: 725–732.

Komor AC, Kim YB, Packer MS, Zuris JA, Liu DR. 2016. Programmable editing of a target base in genomic DNA without double-stranded DNA cleavage. *Nature* **533**: 420–424.

Kourelis J, Van Der Hoorn RAL. 2018. Defended to the Nines: 25 years of Resistance Gene Cloning Identifies Nine Mechanisms for R Protein Function. *The Plant Cell* **30**: 285–299.

Kover PX, Valdar W, Trakalo J, Scarcelli N, Ehrenreich IM, Purugganan MD, Durrant C, Mott R. 2009. A Multiparent Advanced Generation Inter-Cross to Fine-Map Quantitative Traits in *Arabidopsis thaliana*. *PLoS Genetics* **5**: e1000551.

Krasileva K V., Dahlbeck D, Staskawicz BJ. 2010. Activation of an Arabidopsis resistance protein is specified by the *in planta* association of its leucine-rich repeat domain with the cognate oomycete effector. *The Plant Cell* **22**: 2444–2458.

Kunkel BN, Bent AF, Dahlbeck D, Innes RW, Staskawicz BJ. 1993. *RPS2*, an Arabidopsis disease resistance locus specifying recognition of *Pseudomonas syringae* strains expressing the avirulence gene *avrRpt2*. *The Plant Cell* **5**: 865–875.

Lamkanfi M, Dixit VM. 2017. The inflammasome turns 15. *Nature* **548**: 534-535.

Langner T, Kamoun S, Belhaj K. 2018. CRISPR Crops: Plant Genome Editing Toward Disease Resistance. *Annual Review of Phytopathology* **56**: 22.1-22.34.

Lawrenson T, Shorinola O, Stacey N, Li C, Østergaard L, Patron NJ, Uauy C, Harwood W. 2015. Induction of targeted, heritable mutations in barley and *Brassica oleracea* using RNA-guided Cas9 nuclease. *Genome biology* **16**: 258.

Lechtenberg BC, Mace PD, Riedl SJ. 2014. Structural mechanisms in NLR inflammasome

assembly and signaling. *Current Opinion in Structural Biology* **29:** 17–25.

Leipe DD, Koonin E V., Aravind L. 2004. STAND, a class of P-loop NTPases including animal and plant regulators of programmed cell death: Multiple, complex domain architectures, unusual phyletic patterns, and evolution by horizontal gene transfer. *Journal of Molecular Biology* **343:** 1–28.

Lenarčič T, Albert I, Böhm H, Hodnik V, Pirc K, Zavec AB, Podobnik M, Pahovnik D, Žagar E, Pruitt R, *et al.* 2017. Eudicot plant-specific sphingolipids determine host selectivity of microbial NLP cytolysins. *Science* **358:** 1431–1434.

Letunic I, Doerks T, Bork P. 2012. SMART 7: Recent updates to the protein domain annotation resource. *Nucleic Acids Research* **40:** 302–305.

Lewis JD, Lee AH-Y, Hassan J a, Wan J, Hurley B, Jhingree JR, Wang PW, Lo T, Youn J-Y, Guttman DS, *et al.* 2013. The Arabidopsis ZED1 pseudokinase is required for ZAR1-mediated immunity induced by the Pseudomonas syringae type III effector HopZ1a. *Proceedings of the National Academy of Sciences* **110:** 18722–18727.

Li X, Clarke JD, Zhang Y, Dong X. 2001. Activation of an EDS1-mediated R-gene pathway in the snc1 mutant leads to constitutive, NPR1-independent pathogen resistance. *Molecular plant-microbe interactions* **14:** 1131–1139.

Li X, Jiang DH, Yong K, Zhang DB. 2007. Varied transcriptional efficiencies of multiple Arabidopsis *U6* small nuclear RNA genes. *Journal of Integrative Plant Biology* **49:** 222–229.

Li J-F, Norville JE, Aach J, McCormack M, Zhang D, Bush J, Church GM, Sheen J. 2013. Multiplex and homologous recombination–mediated genome editing in Arabidopsis and *Nicotiana benthamiana* using guide RNA and Cas9. *Nature Biotechnology* **31:** 686–688.

Li T, Yang X, Yu Y, Si X, Zhai X, Zhang H, Dong W, Gao C, Xu C. 2018. Domestication of wild tomato is accelerated by genome editing. *Nature Biotechnology* **36:** 1160–1163.

Liang Z, Chen K, Zhang Y, Liu J, Yin K, Qiu J-L, Gao C. 2018a. Genome editing of bread wheat using biolistic delivery of CRISPR/Cas9 *in vitro* transcripts or ribonucleoproteins. *Nature Protocols* **13:** 413–430.

Liang W, van Wersch S, Tong M, Li X. 2018b. TIR-NB-LRR immune receptor SOC3 pairs with truncated TIR-NB protein CHS1 or TN2 to monitor the homeostasis of E3 ligase SAUL1. *New Phytologist* **221:** 2054-2066.

Lieber MR. 2008. The mechanism of human nonhomologous DNA End joining. *Journal of Biological Chemistry* **283:** 1–5.

Links MG, Holub EB, Jiang RHY, Sharpe AG, Hegedus D, Beynon E, Sillito D, Clarke WE, Uzuhashi S, Borhan MH. 2011. *De novo* sequence assembly of *Albugo candida* reveals a small genome relative to other biotrophic oomycetes. *BMC Genomics* **12:** 503.

Lionetti V, Fabri E, De Caroli M, Hansen AR, Willats WGT, Piro G, Bellincampi D. 2017. Three Pectin Methylesterase Inhibitors Protect Cell Wall Integrity for Arabidopsis Immunity to *Botrytis*. *Plant Physiology* **173:** 1844–1863.

Liu JQ, Rimmer SR. 1993. Production and germination of oospores of *Albugo Candida*. *Canadian Journal of Plant Pathology* **15:** 265–271.

Liu L, Sonbol F-M, Huot B, Gu Y, Withers J, Mwimba M, Yao J, He SY, Dong X. 2016a. Salicylic acid receptors activate jasmonic acid signalling through a non-canonical pathway to promote effector-triggered immunity. *Nature Communications* **7:** 13099.

Liu X, Zhang Z, Ruan J, Pan Y, Magupalli VG, Wu H, Lieberman J. 2016b. Inflammasome-activated gasdermin D causes pyroptosis by forming membrane pores. *Nature* **535:** 153–158.

Livak K and Schmittgen T. Analysis of Relative Gene Expression Data Using Real-Time Quantitative PCR and the $2^{-\Delta\Delta CT}$ Method. Methods **25:** 402-408.

Lolle S, Greeff C, Petersen K, Roux M, Jensen MK, Bressendorff S, Rodriguez E, Sømark K, Mundy J, Petersen M. 2017. Matching NLR Immune Receptors to Autoimmunity in *camta3* Mutants Using Antimorphic NLR Alleles. *Cell Host and Microbe* **21:** 518–529.

Lorenzo G De, Brutus A, Savatin DV, Sicilia F, Cervone F. 2011. Engineering plant resistance by constructing chimeric receptors that recognize damage-associated molecular patterns (DAMPs). *FEBS Letters* **585:** 1521–1528.

Loutre C, Wicker T, Travella S, Galli P, Scofield S, Fahima T, Feuillet C, Keller B. 2009. Two different CC-NBS-LRR genes are required for Lr10-mediated leaf rust resistance in tetraploid and hexaploid wheat. *Plant Journal* **60:** 1043–1054.

Lu Y and Zhu J-K. 2017. Precise Editing of a Target Base in the Rice Genome Using a Modified CRISPR/Cas9 System. *Molecular Plant* **10:** 523-525.

Lupas A. 1996. Coiled coils: New structures and new functions. *Trends in Biochemical*

Sciences **21:** 375–382.

Ma Y, Guo H, Hu L, Pons P, Moschou PN, Cevik V, Ding P. 2018. Distinct modes of derepression of an Arabidopsis immune receptor complex by two different bacterial effectors. *Proceedings of the National Academy of Sciences* **115:** 10218–10227.

Ma H, Marti-Gutierrez N, Park SW, Wu J, Lee Y, Suzuki K, Koski A, Ji D, Hayama T, Ahmed R, *et al.* 2017. Correction of a pathogenic gene mutation in human embryos. *Nature* **548:** 413–419.

Mackey D, Holt BF, Wiig A, Dangl JL. 2002. RIN4 interacts with *Pseudomonas syringae* type III effector molecules and is required for RPM1-mediated resistance in *Arabidopsis*. *Cell* **108:** 743–754.

Maekawa T, Cheng W, Spiridon LN, Töller A, Lukasik E, Saijo Y, Liu P, Shen QH, Micluta MA, Somssich IE, *et al.* 2011. Coiled-coil domain-dependent homodimerization of intracellular barley immune receptors defines a minimal functional module for triggering cell death. *Cell Host and Microbe* **9:** 187–199.

Makarova KS, Zhang F, Koonin E V. 2017a. SnapShot: Class 1 CRISPR-Cas Systems. *Cell* **168:** 946.

Makarova KS, Zhang F, Koonin E V. 2017b. SnapShot: Class 2 CRISPR-Cas Systems. *Cell* **168:** 328.

Mali P, Yang L, Esvelt KM, Aach J, Guell M, DiCarlo JE, Norville JE, Church GM. 2013. RNA-guided human genome engineering via Cas9. *Science* **339:** 823–8266.

Mao Y, Zhang Z, Feng Z, Wei P, Zhang H, Botella JR, Zhu J-K. 2015. Development of germ-line-specific CRISPR-Cas9 systems to improve the production of heritable gene modifications in *Arabidopsis*. *Plant Biotechnology Journal* **14:** 519-532.

Marquenet E, Richet E. 2007. How Integration of Positive and Negative Regulatory Signals by a STAND Signaling Protein Depends on ATP Hydrolysis. *Molecular Cell* **28:** 187–199.

Mauch-Mani B, Baccelli I, Luna E, Flors V. 2017. Defense Priming: An Adaptive Part of Induced Resistance. *Annual Review of Plant Biology* **68:** 485–512.

McMullan M, Gardiner A, Bailey K, Holub EB, Ward BJ, Cevik V, Robert-Seilaniantz A, Schultz-Larsen T, Balmuth AL, van Oosterhout C, *et al.* 2015. Evidence for suppression of immunity as a driver for genomic introgressions and host range expansion in races of

Albugo candida, a generalist parasite. *eLife* **4**: 0.7554/eLife.04550.

Mendel G. 1865. Experiments in plant hybridization. *Verhandlungen des naturforschenden Vereines in Brünn* **4**: 3–47.

Morel J-B, Dangl JL. 1997. The hypersensitive response and the induction of cell death in plants. *Cell Death and Differentiation* **4**: 671–683.

Morgan W, Kamoun S. 2007. RXLR effectors of plant pathogenic oomycetes. *Current Opinion in Microbiology* **10**: 332–338.

Morgan T, Sturtevant AH, Muller HJ, Bridges CB. 1915. *The mechanisms of Mendelian heredity*.

Morineau C, Bellec Y, Tellier F, Gissot L, Kelemen Z, Nogué F, Faure JD. 2017. Selective gene dosage by CRISPR-Cas9 genome editing in hexaploid *Camelina sativa*. *Plant Biotechnology Journal* **15**: 729–739.

Murugan K, Babu K, Sundaresan R, Rajan R, Sashital DG. 2017. The Revolution Continues: Newly Discovered Systems Expand the CRISPR-Cas Toolkit. *Molecular Cell* **68**: 15–25.

Nagaya S, Kawamura K, Shinmyo A, Kato K. 2010. The HSP terminator of *Arabidopsis thaliana* increases gene expression in plant cells. *Plant and Cell Physiology* **51**: 328–332.

Narusaka M, Shirasu K, Noutoshi Y, Kubo Y, Shiraishi T, Iwabuchi M, Narusaka Y. 2009. *RRS1* and *RPS4* provide a dual *Resistance*-gene system against fungal and bacterial pathogens. *Plant Journal* **60**: 218–226.

Nekrasov V, Staskawicz BJ, Weigel D, Jones JDG, Kamoun S. 2013. Targeted mutagenesis in the model plant *Nicotiana benthamiana* using Cas9 RNA-guided endonuclease. *Nature Biotechnology* **31**: 691–693.

Nekrasov V, Wang C, Win J, Lanz C, Weigel D, Kamoun S. 2017. Rapid generation of a transgene-free powdery mildew resistant tomato by genome deletion. *Scientific Reports* **7**: 1–6.

Nimma S, Ve T, Williams SJ, Kobe B. 2017. Towards the structure of the TIR-domain signalosome. *Current Opinion in Structural Biology* **43**: 122–130.

Nishida K, Arazoe T, Yachie N, Banno S, Kakimoto M, Tabata M, Mochizuki M, Miyabe A, Araki M, Hara KY, *et al.* 2016. Targeted nucleotide editing using hybrid prokaryotic and vertebrate adaptive immune systems. *Science* **353**: aaf8729

Nishimasu H, Ran FA, Hsu PD, Konermann S, Shehata SI, Dohmae N, Ishitani R, Zhang F, Nureki O. 2014. Crystal structure of Cas9 in complex with guide RNA and target DNA. *Cell* **156**: 935–949.

Nishimasu H, Shi X, Ishiguro S, Gao L, Hirano S, Okazaki S, Noda T, Abudayyeh OO, Gootenberg JS, Mori H, *et al.* 2018. Engineered CRISPR-Cas9 nuclease with expanded targeting space. *Science* **361**: 1259–1262.

Nishimura MT, Anderson RG, Cherkis KA, Law TF, Liu QL, Machius M. 2016. TIR-only protein RBA1 recognizes a pathogen effector to regulate cell death in Arabidopsis. *Proceedings of the National Academy of Sciences* **114**: E2053-E2062.

Oldroyd GED. 2013. Speak, friend, and enter: Signalling systems that promote beneficial symbiotic associations in plants. *Nature Reviews Microbiology* **11**: 252–263.

van Ooijen G, Mayr G, Kasiem MM a, Albrecht M, Cornelissen BJC, Takken FLW. 2008. Structure-function analysis of the NB-ARC domain of plant disease resistance proteins. *Journal of experimental botany* **59**: 1383–1397.

Ordon J, Gantner J, Kemna J, Schwalgun L, Reschke M, Streubel J, Boch J, Stuttmann J. 2017. Generation of chromosomal deletions in dicotyledonous plants employing a user-friendly genome editing toolkit. *Plant Journal* **89**: 155–168.

Paoletti M, Saupe SJ. 2009. Fungal incompatibility: Evolutionary origin in pathogen defense? *Bioessays* **31**: 1201–1210.

Parker JE, Holub EB, Frost LN, Falk A, Gunn ND, Daniels MJ. 1996. Characterization of *eds1*, a mutation in Arabidopsis suppressing resistance to *Peronospora parasitica* specified by several different *RPP* genes. *The Plant Cell* **8**: 2033–2046.

Peart JR, Mestre P, Lu R, Malcuit I, Baulcombe DC. 2005. NRG1, a CC-NB-LRR protein, together with N, a TIR-NB-LRR protein, mediates resistance against *tobacco mosaic virus*. *Current Biology* **15**: 968–973.

Peng J, Zhou Y, Zhu S, Wei W. 2015. High-throughput screens in mammalian cells using the CRISPR-Cas9 system. *FEBS Journal* **282**: 2089–2096.

Peraltal EG, Hellmiss R, Ream W. 1986. Overdrive, a T-DNA transmission enhancer on the *A. tumefaciens* tumour-inducing plasmid. *The EMBO Journal* **5**: 1137–1142.

Peterson BA, Haak DC, Nishimura MT, Teixeira PJPL, James SR, Dangl JL, Nimchuk ZL.

2016. Genome-Wide Assessment of Efficiency and Specificity in CRISPR/Cas9 Mediated Multiple Site Targeting in Arabidopsis. *PLoS ONE* **11:** e0162169.

Petrie JR, Shrestha P, Belide S, Kennedy Y, Lester G, Liu Q, Divi UK, Mulder RJ, Mansour MP, Nichols PD, *et al.* 2014. Metabolic engineering *Camelina sativa* with fish oil-like levels of DHA. *PLoS ONE* **9**: 1–8.

Pidskalny RS, Rimmer SR. **1985**. Virulence of *Albugo Candida* from turnip rape (*Brassica campestris*) and mustard (*Brassica juncea*) on various crucifers. *Canadian Journal of Plant Pathology* **7**: 283–286.

Pieterse CMJ, Van der Does D, Zamioudis C, Leon-Reyes A, Van Wees SCM. **2012**. Hormonal Modulation of Plant Immunity. *Annual Review of Cell and Developmental Biology* **28**: 489–521.

Prasad KVSK, Abdel-Hameed AAE, Xing D, Reddy ASN. **2016**. Global gene expression analysis using RNA-seq uncovered a new role for SR1/CAMTA3 transcription factor in salt stress. *Scientific Reports* **6**: 27021.

Prince DC, Rallapalli G, Xu D, Schoonbeek H, Cevik V, Asai S, Kemen E, Cruz-Mireles N, Kemen A, Belhaj K, *et al.* 2017. Albugo-imposed changes to tryptophan-derived antimicrobial metabolite biosynthesis may contribute to suppression of non-host resistance to *Phytophthora infestans* in *Arabidopsis thaliana*. *BMC Biology* **15**: 20.

Puchta H. **2005**. The repair of double-strand breaks in plants: Mechanisms and consequences for genome evolution. *Journal of Experimental Botany* **56**: 1–14.

Puchta H, Fauser F. **2013**. Gene targeting in plants: 25 years later. *International Journal of Developmental Biology* **57**: 629–637.

Qi T, Seong K, Thomazella DPT, Kim JR, Pham J, Seo E, Cho M-J, Schultink A, Staskawicz BJ. **2018**. NRG1 functions downstream of EDS1 to regulate TIR-NLR-mediated plant immunity in *Nicotiana benthamiana*. *Proceedings of the National Academy of Sciences* **115:** E10979-E10987.

Rairdan GJ, Collier SM, Sacco M a, Baldwin TT, Boettrich T, Moffett P. **2008**. The coiled-coil and nucleotide binding domains of the Potato Rx disease resistance protein function in pathogen recognition and signaling. *The Plant Cell* **20**: 739–751.

Raitskin O, Schudoma C, West A, Patron NJ. **2018**. Comparison of efficiency and specificity of CRISPR-associated (Cas) nucleases in plants: An expanded toolkit for precision genome

engineering. *bioRxiv* 10.1101/422766.

Ramasamy K, Jayabalan S, Sellamuthu G, Jayabalan S and Gayatri V. 2018. CRISPR for crop improvement: an update review. *Frontiers in Plant Science* **9**:985.**Rehmany AP, Gordon A, Rose LE, Allen RL, Armstrong MR, Whisson SC, Kamoun S, Tyler BM, Birch PRJ, Beynon JL. 2005**. Differential recognition of highly divergent downy mildew avirulence gene alleles by *RPP1* resistance genes from two Arabidopsis lines. *The Plant Cell* **17:** 1839–1850.

Riek R, Saupe SJ. 2016. The HET-S / s Prion Motif in the Control of Programmed Cell Death. *Cold Spring Harb Perspectives in Biology* **8:** a013515.

Römer P, Hahn S, Jordan T, Strauß T, Bonas U, Lahaye T. 2013. Plant Pathogen Recognition Mediated by Promoter Activation of the Pepper *Bs3* Resistance Gene. *Science* **339:** 1095–1099.

Rose JKC, Ham K-S, Darvill AG, Albersheim P. 2002. Molecular Cloning and Characterization of Glucanase Inhibitor Proteins: Coevolution of a Counterdefense Mechanism by Plant Pathogens. *The Plant Cell* **14:** 1329–1345.

Saharan GS, Verma PR, Meena PD, Kumar A. 2014. *White Rust Of Crucifers: Biology, Ecology and Management*.

Sander JD, Joung JK. 2014. CRISPR-Cas systems for editing, regulating and targeting genomes. *Nature biotechnology* **32:** 347–55.

Saucet SB, Ma Y, Sarris PF, Furzer OJ, Sohn KH, Jones JDG. 2015. Two linked pairs of *Arabidopsis TNL* resistance genes independently confer recognition of bacterial effector AvrRps4. *Nature Communications* **6:** 6338.

Schindele P, Wolter F, Puchta H. 2018. Transforming plant biology and breeding with CRISPR/Cas9, Cas12 and Cas13. *FEBS Letters* **592:** 1954–1967.

Schmidt C, Pacher M, Puchta H. 2019. DNA Break Repair in Plants and Its Application for Genome Engineering. In: Transgenic Plants. 237–266.

Schneider JC, Suzanne H, Somerville CR. 1995. Chilling-sensitive mutants of Arabidopsis. *Plant Molecular Biology Reporter* **13:** 11–17.

Seto D, Koulena N, Lo T, Menna A, Guttman DS, Desveaux D. 2017. Expanded type III effector recognition by the ZAR1 NLR protein using ZED1-related kinases. *Nature Plants* **3:** 17027.

Shan Q, Voytas DF. 2018. Editing plant genes one base at a time. *Nature Plants* **4:** 412-413.

Shan Q, Wang Y, Li J, Zhang Y, Chen K, Liang Z, Zhang K, Liu J, Xi JJ, Qiu J-L, *et al.* 2013. Targeted genome modification of crop plants using a CRISPR-Cas system. *Nature Biotechnology* **31:** 684–686.

Shao Z-Q, Xue J-Y, Wu P, Zhang Y-M, Wu Y, Hang Y-Y, Wang B, Chen J-Q. 2016. Large-scale analyses of angiosperm nucleotide-binding site-leucine-rich repeat genes reveal three anciently diverged classes with distinct evolutionary patterns. *Plant Physiology* **170:** 2095–2109.

Shao Z-Q, Zhang Y-M, Hang Y-Y, Xue J-Y, Zhou G-C, Wu P, Wu X-Y, Wu X-Z, Wang Q, Wang B, *et al.* 2014. Long-Term Evolution of Nucleotide-Binding Site-Leucine-Rich Repeat Genes: Understanding Gained from and beyond the Legume Family. *Plant Physiology* **166:** 217–234.

Shen Q-H, Saijo Y, Mauch S, Biskup C, Bieri S, Keller B, Seki H, Ulker B, Somssich IE, Schulze-Lefert P. 2007. Nuclear Activity of MLA Immune Receptors Links Isolate-Specific and Basal Disease-Resistance Responses. *Science* **315:** 1098–1103.

Shimada TL, Shimada T, Hara-Nishimura I. 2010. A rapid and non-destructive screenable marker, FAST, for identifying transformed seeds of *Arabidopsis thaliana*. *Plant Journal* **61:** 519–528.

Shirano Y, Kachroo P, Shah J, Klessig DF. 2002. A gain-of-function mutation in an Arabidopsis Toll Interleukin-1 Receptor-Nucleotide Binding Site-Leucine-Rich Repeat type *R* gene triggers defense responses and results in enhanced disease resistance. *The Plant Cell* **14:** 3149–3162.

Shmakov S, Abudayyeh OO, Makarova KS, Wolf YI, Gootenberg JS, Semenova E, Minakhin L, Joung J, Konermann S, Severinov K, *et al.* 2015. Discovery and Functional Characterization of Diverse Class 2 CRISPR-Cas Systems. *Molecular Cell* **60:** 385–397.

Sidhu KS. 2003. Health benefits and potential risks related to consumption of fish or fish oil. *Regulatory Toxicology and Pharmacology* **38:** 336–344.

Simonich MT, Innes RW. 1995. A disease resistance gene in Arabidopsis with specificity for the *avrPph3* gene of *Pseudomonas syringae* pv. *phaseolicola*. *Molecular Plant-Microbe Interactions* **8:** 637–640.

Sinapidou E, Williams K, Nott L, Bahkt S, Tör M, Crute I, Bittner-Eddy P, Beynon J. 2004.

Two *TIR:NB:LRR* genes are required to specify resistance to *Peronospora parasitica* isolate Cala2 in Arabidopsis. *Plant Journal* **38**: 898–909.

Smargon AA, Cox DBT, Pyzocha NK, Zheng K, Slaymaker IM, Gootenberg JS, Abudayyeh OA, Essletzbichler P, Shmakov S, Makarova KS, *et al.* 2017. Cas13b Is a Type VI-B CRISPR-Associated RNA-Guided RNase Differentially Regulated by Accessory Proteins Csx27 and Csx28. *Molecular Cell* **65**: 618–630.e7.

Sohn KH, Hughes RK, Piquerez SJ, Jones JDG, Banfield MJ. 2012. Distinct regions of the *Pseudomonas syringae* coiled-coil effector AvrRps4 are required for activation of immunity. *Proceedings of the National Academy of Sciences* **109**: 16371–16376.

Sohn KH, Lei R, Nemri A, Jones JDG. 2007. The Downy Mildew Effector Proteins ATR1 and ATR13 Promote Disease Susceptibility in *Arabidopsis thaliana*. *The Plant Cell* **19**: 4077–4090.

Sohn KH, Segonzac C, Rallapalli G, Sarris PF, Woo JY, Williams SJ, Newman TE, Paek KH, Kobe B, Jones JDG. 2014. The nuclear immune receptor RPS4 is required for *RRS1^{SLH1}*-dependent constitutive defense activation in *Arabidopsis thaliana*. *PLoS Genetics* **10**: e1004655.

Sohn KH, Zhang Y, Jones JDG. 2009. The *Pseudomonas syringae* effector protein, AvrRPS4, requires in planta processing and the KRVY domain to function. *Plant Journal* **57**: 1079–1091.

Steinert J, Schiml S, Fauser F, Puchta H. 2015. Highly efficient heritable plant genome engineering using Cas9 orthologues from *Streptococcus thermophilus* and *Staphylococcus aureus*. *Plant Journal* **84**: 1295–1305.

Steinert J, Schiml S, Puchta H. 2016. Homology-based double-strand break-induced genome engineering in plants. *Plant Cell Reports* **35**: 1429–1438.

Sunilkumar G, Mohr L, Lopata-Finch E, Emani C, Rathore KS. 2002. Developmental and tissue-specific expression of CaMV 35S promoter in cotton as revealed by GFP. *Plant Molecular Biology* **50**: 463–474.

Swiderski MR, Birker D, Jones JDG. 2009. The TIR domain of TIR-NB-LRR resistance proteins is a signaling domain involved in cell death induction. *Molecular plant-microbe interactions* **22**: 157–165.

Takken FLW, Albrecht M, Tameling WIL. 2006. Resistance proteins: molecular switches of plant defence. *Current Opinion in Plant Biology* **9**: 383–390.

Takken FLW, Goverse A. 2012. How to build a pathogen detector: Structural basis of NB-LRR function. *Current Opinion in Plant Biology* **15:** 375–384.

Tameling WIL, Vossen JH, Albrecht M, Lengauer T, Berden JA, Haring MA, Cornelissen BJC, Takken FLW. 2006. Mutations in the NB-ARC domain of I-2 that impair ATP hydrolysis cause autoactivation. *Plant physiology* **140:** 1233–45.

Tang X, Lowder LG, Zhang T, Malzahn AA, Zheng X, Voytas DF, Zhong Z, Chen Y, Ren Q, Li Q, *et al.* 2017. A CRISPR–Cpf1 system for efficient genome editing and transcriptional repression in plants. *Nature Plants* **3:** 17018.

Thakore PI, D'Ippolito AM, Song L, Safi A, Shivakumar NK, Kabadi AM, Reddy TE, Crawford GE, Gersbac CA. 2015. Highly specific epigenome editing by CRISPR-Cas9 repressors for silencing of distal regulatory elements. *Nature methods* **12:** 1143–1149.

Thines M. 2014. Phylogeny and evolution of plant pathogenic oomycetes—a global overview. *European Journal of Plant Pathology* **138:** 431–447.

Thines M, Choi YJ, Kemen E, Ploch S, Holub EB, Shin HD, Jones JDG. 2009. A new species of Albugo parasitic to *Arabidopsis thaliana* reveals new evolutionary patterns in white blister rusts (Albuginaceae). *Persoonia* **22:** 123–128.

Thomas WJ, Thireault CA, Kimbrel JA, Chang JH. 2009. Recombineering and stable integration of the *Pseudomonas syringae* pv. *syringae* 61 *hrp/hrc* cluster into the genome of the soil bacterium *Pseudomonas fluorescens* Pf0-1. *Plant Journal* **60:** 919–928.

Thomma BPHJ, Nürnberger T, Joosten MHAJ. 2011. Of PAMPs and Effectors: The Blurred PTI-ETI Dichotomy. *The Plant Cell* **23:** 4–15.

Tocher DR. 2015. Omega-3 long-chain polyunsaturated fatty acids and aquaculture in perspective. *Aquaculture* **449:** 94–107.

Tong M, Kotur T, Liang W, Vogelmann K, Kleine T, Leister D, Brieske C, Yang S, Zhang Y, Lüdke D, *et al.* 2017. E3 ligase SAUL1 serves as a positive regulator of PAMP-triggered immunity and its homeostasis is monitored by TNL SOC3. *New Phytologist* **215:** 1516-1532.

Tran DTN, Chung EH, Habring-Müller A, Demar M, Schwab R, Dangl JL, Weigel D, Chae E. 2017. Activation of a Plant NLR Complex through Heteromeric Association with an Autoimmune Risk Variant of Another NLR. *Current Biology* **27:** 1148–1160.

Tsai SQ, Wyvekens N, Khayter C, Foden JA, Thapar V, Reyon D, Goodwin MJ, Aryee MJ,

Joung JK. 2014. Dimeric CRISPR RNA-guided FokI nucleases for highly specific genome editing. *Nature Biotechnology* **32:** 569–576.

Tsutsui H, Higashiyama T. 2017. pKAMA-ITACHI vectors for highly efficient CRISPR/Cas9-mediated gene knockout in *Arabidopsis thaliana*. *Plant & Cell physiology* **58:** 46–56.

Venugopal SC, Jeong R-D, Mandal MK, Zhu S, Chandra-Shekara a. C, Xia Y, Hersh M, Stromberg AJ, Navarre D, Kachroo A, *et al.* 2009. Enhanced Disease Susceptibility 1 and Salicylic Acid Act Redundantly to Regulate Resistance Gene-Mediated Signaling. *PLoS Genetics* **5:** e1000545.

Vojta A, Dobrinic P, Tadic V, Bockor L, Korac P, Julg B, Klasic M, Zoldos V. 2016. Repurposing the CRISPR-Cas9 system for targeted DNA methylation. *Nucleic Acids Research* **44:** 5615–5628.

Volpi e Silva N, Patron NJ. 2017. CRISPR-based tools for plant genome engineering. *Emerging Topics in Life Sciences* **11:** 961-972.

Vu T Van, Sivankalyani V, Kim E-J, Tran MT, Kim J, Sung YW, Doan DTH, Kim J-Y. 2019. Homology-directed repair using transient CRISPR/Cpf1-geminiviral replicon in tomato. bioRxiv 10.1101/521419

Vyas VK, Barrasa MI, Fink GR. 2015. A *Candida albicans* CRISPR system permits genetic engineering of essential genes and gene families. *Science Advances* **1:** e1500248.

Wagner S, Stuttmann J, Rietz S, Guerois R, Brunstein E, Bautor J, Niefind K, Parker JE. 2013. Structural Basis for Signaling by Exclusive EDS1 Heteromeric Complexes with SAG101 or PAD4 in Plant Innate Immunity. *Cell Host & Microbe* **14:** 619–630.

Waibel F, Filipowicz W. 1990. U6 snRNA genes of Arabidopsis are transcribed by RNA polymerase III but contain the same two upstream promoter elements as RNA polymerase II-transcribed U-snRNA genes. *Nucleic acids research* **18:** 3451–3458.

Vande Walle L, Lamkanfi M. 2016. Pyroptosis. *Current Biology* **26:** R568–R572.

Wang Y, Cheng X, Shan Q, Zhang Y, Liu J, Gao C, Qiu JL. 2014. Simultaneous editing of three homoeoalleles in hexaploid bread wheat confers heritable resistance to powdery mildew. *Nature Biotechnology* **32:** 947–951.

Wang GF, Ji J, El-Kasmi F, Dangl JL, Johal G, Balint-Kurti PJ. 2015a. Molecular and Functional Analyses of a Maize Autoactive NB-LRR Protein Identify Precise Structural

Requirements for Activity. *PLoS Pathogens* **11:** 1–33.

Wang G, Roux B, Feng F, Guy E, Li L, Li N, Zhang X, Lautier M, Jardinaud M-F, Chabannes M, *et al.* 2015b. The Decoy Substrate of a Pathogen Effector and a Pseudokinase Specify Pathogen-Induced Modified-Self Recognition and Immunity in Plants. *Cell Host & Microbe* **18:** 285–295.

Wang W, Wen Y, Berkey R, Xiao S. 2009. Specific Targeting of the Arabidopsis Resistance Protein RPW8.2 to the Interfacial Membrane Encasing the Fungal Haustorium Renders Broad-Spectrum Resistance to Powdery Mildew. *The Plant Cell* **21:** 2898–2913.

Wang Z-P, Xing H-L, Dong L, Zhang H-Y, Han C-Y, Wang X-C, Chen Q-J. 2015c. Egg cell-specific promoter-controlled CRISPR/Cas9 efficiently generates homozygous mutants for multiple target genes in Arabidopsis in a single generation. *Genome Biology* **16:** 10.1186/s13059-015-0715-0.

Wang Y, Zhang Y, Wang Z, Zhang X, Yang S. 2013a. A missense mutation in CHS1, a TIR-NB protein, induces chilling sensitivity in Arabidopsis. *Plant Journal* **75:** 553–565.

Wang W, Zhang Y, Wen Y, Berkey R, Ma X, Pan Z, Bendigeri D, King H, Zhang Q, Xiao S. 2013b. A comprehensive mutational analysis of the Arabidopsis resistance protein RPW8.2 reveals key amino acids for defense activation and protein targeting. *The Plant Cell* **25:** 4242–4261.

Ward JD. 2014. Rapid and Precise Engineering of the *Caenorhabditis elegans* Genome with Lethal Mutation Co-conversion and Inactivation of NHEJ Repair. *Genetics* **199:** 363–77.

Weber E, Engler C, Gruetzner R, Werner S, Marillonnet S. 2011. A modular cloning system for standardized assembly of multigene constructs. *PLoS ONE* **6:** e16765.

Wiedenheft B, Sternberg SH, Doudna JA. 2012. RNA-guided genetic silencing systems in bacteria and archaea. *Nature* **482:** 331–338.

Wiermer M, Feys BJ, Parker JE. 2005. Plant immunity: the EDS1 regulatory node. *Current Opinion in Plant Biology* **8:** 383–389.

Wildermuth MC, Dewdney J, Wu G, Ausubel FM. 2001. Isochorismate synthase is required to synthesize salicylic acid for plant defence. *Nature* **414:** 562–565.

Williams SB, Sohn KH, Wan L, Bernoux M, Sarris PF, Segonzac C, Ve T, Ma Y, Saucet S, Ericsson D, *et al.* 2014. Structural Basis for Assembly and Function of a Heterodimeric Plant

Immune Receptor. *Science* **344**: 299–304.

Witek K, Jupe F, Witek AI, Baker D, Clark MD, Jones JDG. 2016. Accelerated cloning of a potato late blight-resistance gene using RenSeq and SMRT sequencing. *Nature Biotechnology* **34**: 656–660.

Wolf S, van der Does D, Ladwig F, Sticht C, Kolbeck A, Schürholz A-K, Augustin S, Keinath N, Rausch T, Greiner S, *et al.* 2014. A receptor-like protein mediates the response to pectin modification by activating brassinosteroid signaling. *Proceedings of the National Academy of Sciences* **111**: 15261–15266.

Wolter F, Klemm J, Puchta H. 2018. Efficient *in planta* gene targeting in Arabidopsis using egg cell-specific expression of the Cas9 nuclease of *Staphylococcus aureus*. *Plant Journal* **94**: 735–746.

Wolter F, Puchta H. 2017. Knocking out consumer concerns and regulator's rules: Efficient use of CRISPR/Cas ribonucleoprotein complexes for genome editing in cereals. *Genome Biology* **18**: 17–19.

Wolter F, Puchta H. 2018. The CRISPR/Cas revolution reaches the RNA world: Cas13, a new Swiss Army knife for plant biologists. *Plant Journal* **94**: 767–775.

Woo JW, Kim J, Kwon S Il, Corvalán C, Cho SW, Kim H, Kim S-G, Kim S-T, Choe S, Kim J-S. 2015. DNA-free genome editing in plants with preassembled CRISPR-Cas9 ribonucleoproteins. *Nature Biotechnology* **33**: 1162-1164.

Wu C-H, Abd-El-Haliem A, Bozkurt TO, Belhaj K, Terauchi R, Vossen JH, Kamoun S. 2017. NLR signaling network mediates immunity to diverse plant pathogens. *Proceedings of the National Academy of Sciences* **114**: 8113–8118.

Wu C-H, Belhaj K, Bozkurt TO, Kamoun S. 2016. The NLR helper protein NRC3 but not NRC1 is required for Pto-mediated cell death in *Nicotiana benthamiana*. *New Phytologist* **209**: 1344–1352.

Wu C-H, Derevnina L, Kamoun S. 2018. Receptor networks underpin plant immunity. *Science* **360**: 1300-1301.

Wu Z, Li M, Dong OX, Xia S, Liang W, Bao Y, Wasteneys G, Li X. 2018b. Differential regulation of TNL-mediated immune signaling by redundant helper CNLs. *New Phytologist* 10.1111/nph.15665.

Wu R, Lucke M, Jang Y, Zhu W, Symeonidi E, Wang C, Fitz J, Xi W, Schwab R, Weigel D. 2018b. An efficient CRISPR vector toolbox for engineering large deletions in *Arabidopsis thaliana*. *Plant Methods* **14:** 65.

Xiao S, Brown S, Patrick E, Brearley C, Turner JG. 2003. Enhanced Transcription of the Arabidopsis Disease Resistance Genes *RPW8.1* and *RPW8.2* via a Salicylic Acid–Dependent Amplification Circuit Is Required for Hypersensitive Cell Death. *The Plant Cell* **15:** 33–45.

Xiao S, Calis O, Patrick E, Zhang G, Charoenwattana P, Muskett P, Parker JE, Turner JG. 2005. The atypical resistance gene, *RPW8*, recruits components of basal defence for powdery mildew resistance in Arabidopsis. *Plant Journal* **42:** 95–110.

Xiao S, Ellwood S, Calis O, Patrick E, Li T, Coleman M, Turner JG. 2001. Broad-spectrum mildew resistance in *Arabidopsis thaliana* mediated by *RPW8*. *Science* **291:** 118–120.

Xie K, Minkenberg B, Yang Y. 2015. Boosting CRISPR/Cas9 multiplex editing capability with the endogenous tRNA-processing system. *Proceedings of the National Academy of Sciences* **112:** 3570–3575.

Xie C, Zhang Y-P, Song L, Luo J, Qi W, Hu J, Lu D, Yang Z, Zhang J, Xiao J, *et al.* 2016. Genome editing with CRISPR/Cas9 in postnatal mice corrects PRKAG2 cardiac syndrome. *Cell Research* **26:** 1099–1111.

Xin X-F, He SY. 2013. *Pseudomonas syringae* pv. *tomato* DC3000: A Model Pathogen for Probing Disease Susceptibility and Hormone Signaling in Plants. *Annual Review of Phytopathology* **51:** 473–498.

Xing H-L, Dong L, Wang Z-P, Zhang H-Y, Han C-Y, Liu B, Wang X-C, Chen Q-J. 2014. A CRISPR/Cas9 toolkit for multiplex genome editing in plants. *BMC plant biology* **14:** 327.

Xu F, Zhu C, Cevik V, Johnson K, Liu Y, Sohn KH, Jones JDG, Holub EB, Li X. 2015. Autoimmunity conferred by *chs3-2D* relies on *CSA1*, its adjacent TNL-encoding neighbour. *Scientific reports* **5:** 8792.

Yan S, Dong X. 2014. Perception of the plant immune signal salicylic acid. *Current Opinion in Plant Biology* **20:** 64–68.

Yan L, Wei S, Wu Y, Hu R, Li H, Yang W, Xie Q. 2015. High efficiency genome editing in Arabidopsis using *YAO* promoter-driven CRISPR/Cas9 system. *Molecular Plant* **8:** 1820–1823.

Yang H, Shi Y, Liu J, Guo L, Zhang X, Yang S. 2010. A mutant CHS3 protein with TIR-NB-LRR-LIM domains modulates growth, cell death and freezing tolerance in a temperature-dependent manner in Arabidopsis. *Plant Journal* **63:** 283–296.

Yoshida S, Cui S, Ichihashi Y, Shirasu K. 2016. The Haustorium, a Specialized Invasive Organ in Parasitic Plants. *Annual review of plant biology* **67:** 643–667.

Yu IC, Parker J, Bent AF. 1998. Gene-for-gene disease resistance without the hypersensitive response in Arabidopsis *dnd1* mutant. *Proceedings of the National Academy of Sciences* **95:** 7819–7824.

Zaidi SS e. A, Mukhtar MS, Mansoor S. 2018. Genome Editing: Targeting Susceptibility Genes for Plant Disease Resistance. *Trends in Biotechnology* **36:** 898–906.

Zelensky AN, Schimmel J, Kool H, Kanaar R, Tijsterman M. 2017. Inactivation of Pol θ and C-NHEJ eliminates off-target integration of exogenous DNA. *Nature Communications* **8:** 66.

Zetsche B, Gootenberg JS, Abudayyeh OO, Slaymaker IM, Makarova KS, Essletzbichler P, Volz SE, Joung J, van der Oost J, Regev A, *et al.* 2015. Cpf1 Is a Single RNA-Guided Endonuclease of a Class 2 CRISPR-Cas System. *Cell* **163:** 759-771.

Zhang Q, Berkey R, Pan Z, Wang W, Zhang Y, Ma X, King H, Xiao S. 2015. Dominant negative RPW8.2 fusion proteins reveal the importance of haustorium-oriented protein trafficking for resistance against powdery mildew in Arabidopsis. *Plant Signaling & Behavior* **10:** e989766.

Zhang X, Bernoux M, Bentham AR, Newman TE, Ve T, Casey LW. 2016a. Multiple functional self-association interfaces in plant TIR domains. *Proceedings of the National Academy of Sciences* **114:** E2046-E2052.

Zhang X, Dodds PN, Bernoux M. 2017. What Do We Know About NOD-Like Receptors in Plant Immunity? *Annual Review of Phytopathology.* **55:** 205-229.

Zhang J, Li W, Xiang T, Liu Z, Laluk K, Ding X, Zou Y, Gao M, Zhang X, Chen S, *et al.* 2010. Receptor-like cytoplasmic kinases integrate signaling from multiple plant immune receptors and are targeted by a *Pseudomonas syringae* effector. *Cell Host and Microbe* **7:** 290–301.

Zhang YM, Shao ZQ, Wang Q, Hang YY, Xue J-Y, Wang B, Chen JQ. 2016b. Uncovering the dynamic evolution of nucleotide-binding site-leucine-rich repeat (NBS-LRR) genes in

Brassicaceae. *Journal of Integrative Plant Biology* **58**: 165–177.

Zhang Y, Wang Y, Liu J, Ding Y, Wang S, Zhang X, Liu Y, Yang S. 2016c. Temperature-dependent autoimmunity mediated by *chs1* requires its neighboring TNL gene *SOC3*. *New Phytologist* **213**: 1330–1345.

Zhao Y, Thilmony R, Bender CL, Schaller A, He SY, Howe GA. 2003. Virulence systems of *Pseudomonas syringae* pv. *tomato* promote bacterial speck disease in tomato by targeting the jasmonate signaling pathway. *Plant Journal* **36**: 485–499.

Zhong Y, Cheng Z-M (Max). 2016. A unique RPW8-encoding class of genes that originated in early land plants and evolved through domain fission, fusion, and duplication. *Scientific Reports* **6**: 32923.

Zhou M, Li Y, Hu Q, Bai XC, Huang W, Yan C, Scheres SHW, Shi Y. 2015. Atomic structure of the apoptosome: Mechanism of cytochrome c- and dATP-mediated activation of Apaf-1. *Genes and Development* **29**: 2349–2361.

Zipfel C. 2008. Pattern-recognition receptors in plant innate immunity. *Current Opinion in Immunology* **20**: 10–16.

Zipfel C. 2009. Early molecular events in PAMP-triggered immunity. *Current Opinion in Plant Biology* **12**: 414–420.

Zong Y, Wang Y, Li C, Zhang R, Chen K, Ran Y, Qiu J, Wang D, Gao C. 2017. Precise base editing in rice, wheat and maize with a Cas9-cytidine deaminase fusion. **35**: 438-440.

Zsögön A, Čermák T, Naves ER, Notini MM, Edel KH, Weinl S, Freschi L, Voytas DF, Kudla J, Peres LEP. 2018. *De novo* domestication of wild tomato using genome editing. *Nature Biotechnology* 10.1038/nbt.4272.